UNIVERSITY OF BIRMINGHAM

Treatment of Endocrine Disrupting Chemicals Using the Downflow Gas Contactor Reactor

By

Faisal S Althafiri

A thesis submitted to

The University of Birmingham

for the degree of

DOCTOR OF PHILOSOPHY

School of Chemical Engineering
College of Engineering and Physical Science
University of Birmingham
February 2016

ABSTRACT

The photodegradation of the selected female steroid hormones, 17β-Estradiol (17β-E2), 17α-Estradiol (17α-E2), Estrone (E1) and Progesterone (PG) in aqueous solutions has been studied using the Downflow Gas Contactor Reactor (DGCR). The performance evaluation of the DGCR as providing an efficient and economical advanced oxidation process (AOP) demonstrated that it can be considered a promising AOP capable of total degradation in a short period of time. All studies on the pilot-scale DGCR were conducted as batch modes with a recycle loop employing the absorption of oxygen into water as the model system. A fast and reliable chromatographic method was developed and validated to study the performance of the DGCR down to the ng L^{-1} level. The analytical method was based on offline Oasis HLB solid phase extraction (SPE) followed by instrumental analysis using a high performance liquid chromatograph equipped with a diode array detector (HPLC–DAD). A total run time of 12 minutes was sufficient to allow for the quantification of selected female hormones in different water matrices. Compound purity and identity confirmation were evaluated using liquid chromatography time-of-flight mass spectrometry (LC–TOF–MS). The approach enabled hormone recoveries greater than 88.2%. The limit of detection (LOD) was determined for the selected hormones and ranged from 0.80 ± 0.57 ng L^{-1} for 17β-estradiol to 3.97 ± 0.40 ng L^{-1} for progesterone.

Hydrodynamic and mass transfer characteristics of the DGCR were examined extensively, and the optimum operating conditions were identified. Gas hold-up values up to 50–60% were achieved. The performance of the DGCR in approaching gas/liquid equilibrium in a short time with 100% of gas utilization results in high values of the volumetric gas-liquid mass transfer coefficient ($K_L a$) and values for the mixed flow model were higher than the plug flow model (Boyes et al., 1995a).

The photodegradation process fit well with pseudo-first order kinetics with $R^2 \geq 99\%$. UV irradiation (photolysis) is the main factor affecting the whole degradation process with two regions: fast degradation in the first 6 min followed by a slow degradation process. The effect of the initial concentration, initial pH, different O_2 flowrates, hydrogen peroxide and different combinations of UV systems with the DGCR were all explored to evaluate the photodegradation performance and the removal efficiency. E1 has the fastest degradation rate while PG has the slowest. 17β-E2 and 17α-E2 were similar in photodegradation behaviour. The results indicate that the photodegradation rate was optimum in the pH range of 5–7. A total degradation was achieved using 20 mg L^{-1} of H_2O_2 for 17β-E2 and 17α-E, at 10 min, E1 at 8 min and PG at 16 min. The use of O_2 and H_2O_2 oxidizers enhanced and accelerated the photodegradation process. The total cost for a total degradation of the selected female steroid hormones is <30 pence per run. These results show great promise for the DGCR that it can be considered a promising AOP at the industrial scale applications.

بِسْمِ اللَّهِ الرَّحْمَٰنِ الرَّحِيمِ

وَجَعَلْنَا مِنَ الْمَاءِ كُلَّ شَيْءٍ حَيٍّ ۖ أَفَلَا يُؤْمِنُونَ

“In the name of Allah, Most Gracious, Most Merciful”

" We made from water every living thing. Will they not then believe?"

Chapter 17: Surat Al-Anbiyaa / The Prophets

Holly Quran

This work is dedicated to

my parents and my family

AKNOWLEDGEMENTS

I would like to thank my supervisor Dr. Gary Leeke for his scientific guidance; moral support and encouragement throughout my PhD. Thanks are due to Dr. Regina Santos, my Co-Supervisor for the advice and support throughout my PhD.

I would also like to thank my colleagues and friends who were always there for guidance and advice.

I would also like to thank departmental staff especially Lynn Draper and David from the workshop for providing all the essential assistance.

Finally, I would like to thank my family for all the support and encouragement throughout my PhD.

TABLE OF CONTENTS

LIST OF FIGURES

LIST OF TABLES

LIST OF ABBREVIATIONS

APE	Alkylphenol Ethoxylate
AOPs	Advanced Oxidation Processes
ASE	Accelerated Solvent Extraction
BAC	Benzalkonium Chloride
BOC	British Oxygen Company
BPA	Bisphenol A
BSD	Bubble Size Distribution
CARPT	Computer Automated Radioactive Particle Tracking
DAD	Diode Array Detector
DGCR	Downflow Gas Contactor Reactor
DHE	Dynamic Headspace Extraction
EDCs	Endocrine Disrupting Chemicals
EO	Electrochemical Oxidation
EU	European Union
FID	Flame Ionization Detector
GAC	Granular Activated Carbon
GC	Gas Chromatography
GC-MS	Gas Chromatography – Mass Spectrometry
GLP	Good Laboratory Practice

HBCD	Hexabromocyclodecane
HPHTSE	High-Pressure, High-Temperature Solvent Extraction
HPLC	High Performance Liquid Chromatography
HPSE	High-Pressure Solvent Extraction
HSAS	Headspace Auto Sampler
IPCS	International Programme On Chemical Safety
LAS	Linear Alkylbenzene Sulfonic Acid
LC	Liquid Chromatography
LLE	Liquid–Liquid Extraction
LOD	Limit of Detection
LOQ	Limit of Quantitation
LR	Linear range
MAE	Microwave-Assisted Extraction
MS	Mass Spectrometry
MS/MS	Tandem Mass Spectrometry
MTBE	tert-Butyl Methyl Ether
OF	Objective function
PAC	Powdered Activated Carbon
PBDE	Polybrominated Diphenyl Ether
PFE	Pressurized Fluid Extraction
PFR	Plug Flow Reactor
PHSE	Pressurized Hot Solvent Extraction
PHWE	Pressurized Hot Water Extraction
PLE	Pressurized Liquid Extraction

PPCPs	Personal Care Products
PSE	Pressurized Solvent Extraction
QC	Quality Control
R	Recovery, %
RO	Reverse Osmosis
RSD	Relative Standard Deviation
RTD	Residence Time Measurements
SBSE	Stir Bar Sorptive Extraction
SCWO	Supercritical Water Oxidations
SD	standard deviation
SFE	Supercritical Fluid Extraction
SHE	Static Headspace Extraction
SLS	Sodium Lauryl Sulfate
SPE	Solid-Phase Extraction
SPME	Solid-Phase Microextraction
SSE	Subcritical Solvent Extraction
TBBPA	Tetrabromobisphenol A
TOF	Time of Flight
UNEP	United Nations Environment Programme
UV	Ultra-Violet
WHO	World Health Organization
WWTPs	Wastewater Treatment Plants

NOMENCLATURE

a	Gas-Liquid Interfacial Area, $m^2\ m^{-3}$
C	Tracer Concentration, mg L^{-1} or ng L^{-1}
C^*:	Equilibrium Concentration of Gas in the Liquid Phase, mg L^{-1}
C^{calc}	Calculated Concentrations at Time T (Min), ng L^{-1}
C^{exp}	Experimental Concentrations at Time T (Min), ng L^{-1}
C_i	Concentration of Gas in Liquid Phase at Dispersion Inlet, mg L^{-1}
C_o	Concentration of Gas in Liquid Phase at Dispersion Outlet, mg L^{-1}
C_r	Reference Standard, ng L^{-1}
C_s	Spiked Sample, ng L^{-1}
D	Diameter of tube, m
D_c	Column diameter, m
d_b	Bubble Diameter, m
d_o	Orifice Diameter, m
DO	Dissolved Oxygen, mg L^{-1}
d_s	Mean Surface to Volume Diameter
D_T	Column Diameter
E	Longitudinal or Axial Dispersion Coefficient
F_L	volumetric Liquid Flowrate, $m^3\ s^{-1}$
G_i	Gas Inlet
G_o	Gas Outlet
H	Henrys Low Coefficient, $Pa.m^3\ kg^{-1}\ mol^{-1}$

h_d	Dispersion Height, m
i.d	Internal diameter of, m
k	Rate Constant (min^{-1})
k_La	Volumetric Mass Transfer Coefficient, s^{-1}
L	Length, m
L_c	Characteristic Length, m
L_i	Liquid Inlet
L_o	Liquid Outlet
o.d	Out diameter of pipe, m
P	Pressure, MPa
P_{col}	Reactor Column Pressure, barg
Pe	Peclet Number, uL E_{ZL}^{-1}
P_k	Kinetic Jet Power, Watt (W)
Re	Reynolds Number, Dimensionless Quantity
t	Time (min)
T	Temperature (K or ºC)
t_o	Reactor Operating Time, min
t_R	Retention Time, min
t_I	Irradiation Time, min
U_G	Superficial Gas Velocity, m s^{-1}
u_i	Dispersion-Initiating Velocity, m s^{-1}
V_d	Gas-Liquid Dispersion Volume, L or m^3
V_g	Gas-Phase Volume in The Dispersion, L or m^3
V_j	Liquid Inlet Velocity at Nozzle, m s^{-1}

V_L	Liquid-Phase Volume In The Dispersion, L or m^3
$V_Г$	Reaction Zone Volume, L or m^3
V_s	Reactor Total Volume, L or m^3
v_L	Kinematic Liquid Viscosity, $m^2\ s^{-1}$
ε_g	Gas Hold-Up, Dimensionless Numbers
ρ_L	Liquid Density, kg m^{-3}
ρ_g	Gas Density, kg m^{-3}
σ	Standard Deviation

CHAPTER 1

1 INTRODUCTION

1.1 Background

Endocrine disrupting chemicals (EDCs) have been acknowledged as one of the main concerns related to emerging chemicals over the last two decades in the environment (Kavlock et al., 1996; Kolpin et al., 2002). In 2012, a document entitled State of the Science of Endocrine Disrupting Chemicals - 2012 was published by the United Nations Environment Programme (UNEP) and the World Health Organization (WHO). This document is an update of a previous document that was published in 2002 entitled Global Assessment of the State-of-the-Science of Endocrine Disruptors (IPCS, 2002) by the International Programme on Chemical Safety (IPCS), a joint programme of the WHO, the UNEP, and the International Labour Organization. This document provides the global status of scientific knowledge on exposure to EDCs and its effects on humans and wildlife. EDCs have been defined as "an exogenous substance or mixture that alters the function of the endocrine system and can eventually cause adverse effects in an organism, its progeny or within its (sub) population" (Damstra, 2002). European statistics (Eurostat) published in 2015 on the production of the environmentally harmful chemicals in millions of tonnes based on 28 EU countries which were then broken down into five environmental impact classes as shown in Figure 1.1 (EUROSTAT, 2015).

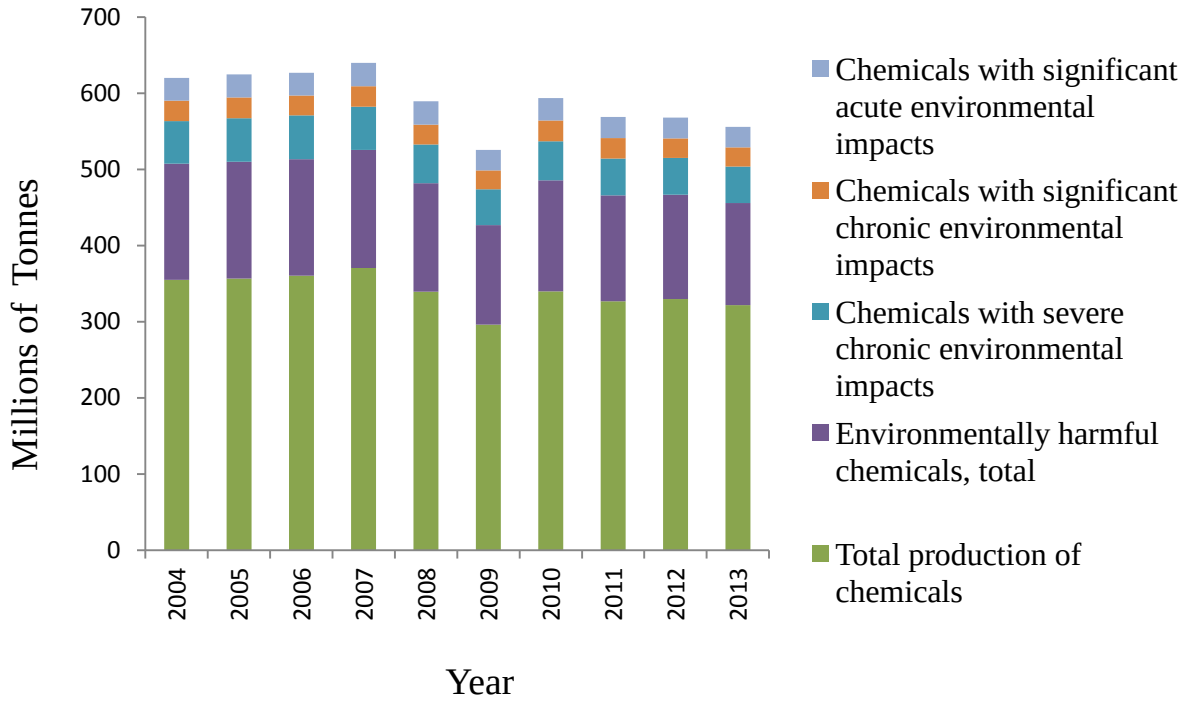

Figure 1-1 Production of environmentally harmful chemicals, by environmental impact class in millions of tonnes based on 28 of EU countries

EDCs can be classified in to a wide range of substances and can be natural or man-made such as pharmaceuticals, synthetic and natural hormones, personal care products (PCPs), heavy metals, pesticides, plasticizers and dioxin and dioxin-like compounds. The adverse effects of EDCs can arise at the ng L^{-1} level. Those adverse effects include feminization in wild fish (intersex) in some lakes and rivers, lowered populations, reduced reproduction and increased cancer rates (Dzieweczynski and Hebert, 2013; Filby et al., 2010; Liu et al., 2012). The accumulation of EDCs in the environment as a result of the continuous release of chemicals having the ability to interfere with the endocrine systems of humans and wildlife will lead to adverse long-term effects. The release of EDCs in the aquatic environment has raised awareness about the central role of wastewater treatment plants (WWTPs) and their ability to remove wastewater contaminants, especially those that have an estrogenic activity, such as natural and

synthetic hormones, and to control the water quality (Geary, 2005; Lishman et al., 2006; Scandura and Sobsey, 1997). The continuous development of powerful analytical methods able to quantify extremely low concentrations (ng L^{-1} level) of EDCs in a complex matrix can enrich the knowledge of EDCs, their impact on the aquatic environment, and the evaluation of various treatment methods. These analytical methods include the use of LC-UV, LC–MS, LC–MS/MS, GC–MS and GC–MS/MS for routine analyses. The presence of such powerful analytical methods can improve the evaluation of a variety of current EDCs treatment processes and lead to the development of new methods that are able to remove EDCs at trace level in more efficient and economical ways and ensure the quality of the aquatic environment. EDCs treatment processes, such as advanced oxidation processes (AOPs), which are considered promising technologies, can be divided into two main categories: non-photochemical treatment methods such as Fenton reactions, electrochemical oxidation, hydrodynamic/ultrasonic cavitation and sub/supercritical water, and photochemical treatment methods such as photo-Fenton reaction, heterogeneous photocatalysis, UV/H_2O_2 and UV/O_3. Bubble column reactors are considered a promising technology and characterized with the ability of combining most of the above mentioned technologies and can work as a photochemical or non-photochemical reactor.

1.2 Thesis Aim and Objectives

The aim of this study was to evaluate the performance of a downflow gas contactor reactor (DGCR) as an efficient and economical promising technology for the photodegradation of selected female steroid hormones, 17β-estradiol (17β-E2), 17α-estradiol (17α-E2), Estrone (E1) and Progesterone (PG) as model pollutants in aqueous solution. To achieve this aim, the following objectives were examined in sequence:

1. The adverse effects of EDCs can take place at the ng L^{-1} level; therefore, development of a new analysis method is considered essential in the evaluation of DGCR performance with reliable and accurate results for the detection of four selected female steroid hormones at the ng L^{-1} level.
2. Outstanding performance is always linked to economy; therefore, optimizing the DGCR performance is the next step to evaluate its hydrodynamic and mass transfer characteristics to identify the optimum operating conditions required for the removal of the EDCs present in aqueous solution.
3. Finally, degradation studies were performed to explore different experimental conditions and factors on the removal efficiency of selected female steroid hormones in their mixtures in aqueous solution.

1.3 Thesis Layout

This thesis consists of seven chapters that present extensive experimental work to evaluate the downflow gas contactor reactor (DGCR) performance for the removal of the endocrine disrupting compounds (EDCs) present in water samples. In Chapter 1, a brief introduction describes the EDCs as emerging chemicals that can produce adverse effects in both humans and wildlife, followed by the thesis objectives and layout. Chapter 2 provides an extensive and detailed literature survey that is up-to-date on the main research undertaken with respect to EDCs, bubble column reactors in general, and the downflow gas contactor reactor (DGCR), in particular investigation of the latter the main objective of this thesis. This reactor is used to achieve a total degradation of the selected EDCs in aqueous samples. Chapter 3 describes the experimental apparatus, materials, and methods developed and used. Experimental set-up of mass transfer and degradation studies with the start-up and shut-down procedures are described in detail. Also, the general analytical procedures used throughout this work are provided in order to achieve satisfactory results at the ng L^{-1} level. Good Laboratory Practice (GLP) when dealing with EDCs of high acute toxicity, which is considered the most important assurance for health and safety for both humans and the environment and is described in detail. In Chapter 4, the results and discussion of the optimization and validation for the analyses of selected female steroid hormones, 17β-Estradiol (17β-E2), 17α-Estradiol (17α-E2), Estrone (E1) and Progesterone (PG) in aqueous samples are presented. A new analytical method was developed that is capable of detection down to the ng L^{-1} level using Liquid Chromatography–Mass Spectrometry (LC/MS), thus allowing the evaluation of the performance of the DGCR as an effective wastewater treatment technology. Chapter 5 describes the results and discussion of the hydrodynamic characteristics and mass transfer studies of the DGCR. In this chapter,

optimization of the operating conditions is described with characterization of flow patterns, dispersion process, bubble size characteristics, gas holdup (ε_g) and interfacial area (a) which led to the assessment of the volumetric gas-liquid mass transfer coefficient ($k_L a$). The content of this chapter were important to be fully understood, as optimizing the DGCR is considered a necessary step for the photodegradation of 17β-E2, 17α-E2, E1 and PG. Chapter 6 describes the results and discussion of the photodegradation of 17β-E2, 17α-E2, E1 and PG as model pollutants in aqueous solution. A degradation kinetics model using different experimental conditions was proposed. The effects of initial concentration, initial pH, different O_2 flowrates, different H_2O_2 dosages and different combinations of UV systems were studied to evaluate the best combination of these systems on the photodegradation performance and the removal efficiency. Chapter 7 presents the main findings and achievements of the present study and recommendations for the future that will help to further extend the current research accomplishments.

CHAPTER 2

2 LITERATURE SURVEY

Chapter Overview

In this chapter, an extensive and detailed up-to-date literature survey will cover five principal areas of research: endocrine disrupting chemicals (EDCs) classification and sources, current analytical methods for EDCs at trace level and the challenges of sample preparation with the most common methods for the analysis of hormones in particular , the main current technologies of EDCs treatment, bubble column reactors in general and finally the downflow gas contactor reactor (DGCR) in particular

2.1 Endocrine Disrupting Chemicals (EDCs)

2.1.1 Introduction

Human and environmental health is considered the most important criteria when dealing with any industrial activity, including the treatment of domestic wastewater. UK and European water authorities regularly update regulations to ensure water resources such as rivers, lakes and groundwater remain safe for humans, wildlife and agriculture and prevent exposure to any chemicals that can cause serious health effects (Kavlock et al., 1996). New instrumental capabilities and the development of analysis and sample preparation technologies increase the ability of researchers to observe a more complicated matrix of new chemicals with greater sensitivity (Chang et al., 2008; Viglino et al., 2008).

Over the last two decades, there has been increased concern by scientists and local authorities about exposure to a group of chemicals called endocrine disrupting chemicals (EDCs) (Belfroid et al., 1998; Blackburn and Waldock, 1995; Desbrow et al., 1998). EDCs have been defined as "an exogenous substance or mixture that alters the function of the endocrine system and can eventually cause adverse effects in an organism, its progeny or within its (sub) population" (Damstra, 2002). The first meeting recognizing a need for action on EDCs was organized by Theo Colborn and co-workers in Racine, Wisconsin in July, 1991 (Colborn and Clement, 1992). The European Union (EU) first recognized a need for action on EDCs at a workshop entitled "The impact of endocrine disrupters on human health and wildlife" in Weybridge, UK, 2-4 December 1996 (Commission of the European Communities, 1997). International organizations continue to develop and evaluate monitoring systems as well as update documentation about EDCs, which are reviewed by scientists and researchers.

2.1.2 EDC Classification

Putative and confirmed endocrine disrupting functions have been found or suspected in many industrial and as well as household chemicals, such as cleaning agents and pesticides, as well as chemicals found in consumer goods such as plastic additives. Endocrine organ functions can be disturbed or altered by endocrine chemicals. They can also interact with cell receptors, change hormone metabolism either directly in an endocrine organ (for example, inhibiting steroid development) or peripherally (for example, increasing hepatic metabolism and clearance) (EDSTAC, 1998).

Researchers have categorized EDCs in many different ways, due to the fact that many different kinds of chemicals can function as EDCs. Diamanti-Kandarakis and co-workers classified EDCs into two groups: naturally occurring substances such as phytoestrogens and synthesized substances such as plasticizers, pesticides and fungicides, etc (Diamanti-Kandarakis et al., 2009). Other researchers have classified EDCs into groups according to their origins: natural hormones and artificial hormones, industrial chemicals and side products of industrial processes (Caliman and Gavrilescu, 2009). In a similar manner, EDCs have been classified into three groups according to the occurrence in the environment: pesticides such DDT and chloropyrifos, chemicals present in products used by humans in daily life that have the possibility to be released to the environment such as pharmaceuticals and personal care products (PCPs), and food contact material such as food plastic containers and epoxides used in canned food (Gore, 2014). Table 2.1 provides some examples of common EDCs found in the environment, their sources and their main effects on humans and environment. The EDCs are listed in six groups: as follows; pharmaceuticals, pesticides, plasticizers, surfactants, hormones and flame retardants.

Table 2-1 Common EDCs found in humans and wildlife

Emerging contaminant	category	Sources	Known effects to organisms	References
Acetaminophen Ibuprofen Fibrates Tetracyclines Sulphonamides	Pharmaceuticals	Pharmaceutical industry waste, hospital waste effluents, animal manure, sewage sludge and WWTP	Long-term exposure leads to microbial and bacterial resistance. Also, increased toxicity to the receptor organism in humans and aquatic biota	(Collier, 2007; Gadipelly et al., 2014; Kolpin et al., 2002)
DDT Chloropyrifos Atrazine Terbuthylazine Diazinon	Pesticides	Agriculture and forestry, horticulture, or amenities and WWTP	Toxic to the aquatic ecosystem and increased rate of thyroid cancer, kidney failure and liver problems.	(Hernando et al., 2011; Moreno-Gonzalez et al., 2013; van Wezel and van Vlaardingen, 2004)
Bisphenol A (BPA) Phthalates	Plasticizers	Plastic manufacture process such as food contact materials and WWTP	Known disturbances to the humans and animals hormonal system and increased risk of birth defects.	(Bang et al., 2012; Hauser and Calafat, 2005; Nagel and Bromfield, 2013; Rosenfeld, 2015)
Linear alkylbenzene Sulfonic acid (LAS) Sodium lauryl sulfate (SLS) Benzalkonium chloride (BAC) Alkylphenol ethoxylate (APE)	Surfactants	Household cleaning detergents, personal care products, paints, polymers, paper industries and WWTP	Toxic to organisms and can effect and modify DNA. Also, the intermediates of the biodegradation process being more harmful to the environment than the parent compound.	(Haigh, 1996; Ivankovic and Hrenovic, 2010; Ying, 2006)

Estradiol (E2) Estrone (E1) Progesterone (PG) 17α-ethynylestradiol (EE2) Testosterone Phytoestrogens	Hormones	Pharmaceutical industry waste, hospital waste effluents, animal manure, sewage sludge and WWTP	Disturbance to the male and female reproductive organs, immunity system, increased rate of cancers. Also, there was feminization of some fish in some lakes	(Caldwell et al., 2010; Kavlock et al., 1996; Liu et al., 2012; Schubert et al., 2014)
Tetrabromobisphenol A (TBBPA) Hexabromocyclodecane (HBCD) Polybrominated diphenyl ether (PBDE)	Flame retardants	Flame retardants manufacture process such as food contact materials and WWTP	Toxic to organisms and can effect and modify DNA. Known disturbances to the humans and animals hormonal system and increased risk of cancer rate.	(Birnbaum and Staskal, 2004; Hale et al., 2001)

WWTP: Wastewater Treatment Plant

2.1.3 Hormone Classifications

Hormones are acknowledged as one of the most important endocrine disruptors (Filby et al., 2007). Hormones can be classified as:

a) Natural hormones (for example):

- Oestrogen (female sexual development)
- Progesterone and testosterone (male sexual development)
- Phytoestrogens, (substances contained in some plants, such as soya beans, displaying oestrogen-like action in body).

b) Synthetic hormones:

Synthetic hormones or hormone-equivalent, such as oral contraceptives, hormone-alternative treatments and some animal feed additives.

2.1.4 EDCs Sources

Endocrine disruptor chemicals can be found in the water, air, food and soil. The discovery of EDCs in the aquatic environment has raised the awareness of the central role of sewage treatment plants and their ability to remove wastewater contaminants, especially chemicals that have an estrogenic effect (Conn et al., 2006; Gabet et al., 2007; Geary, 2005; Rudel et al., 1998; Scandura & Sobsey, 1997). Often EDCs sources entering a wastewater treatment facility are actually naturally produced from plants and animals. Plants and plant by-products are the primary sources of these compounds: for example, soy-based products can contain hormonally active agents. In addition humans and other animals excrete compounds that are hormonally active and

can be EDCs; these compounds can be internally produced or be derived from the milk, meat or vegetables we eat (Courant et al., 2007; Hartmann et al., 1998; Malekinejad et al., 2006; Poelmans et al., 2005). Industrial products (or their by-products), found in wastewater can also contain EDCs. EDCs are used in pharmaceutical products such as birth control pills. The production of plastics can release compounds called plasticizers, some of which are EDCs. Some pesticides can be hormonally active. Detergents contain compounds called surfactants that enhance their cleaning power; some of these surfactants can be hormonally active, Only moderate removal of steroid oestrogens was observed through five wastewater treatment systems (Stanford and Weinberg, 2010).

2.1.5 Regulating Steroids Levels for Humans and Wild-life

Arguments over steroids and their impact on human health focus on the maximum allowable concentrations that can be discharged from wastewater treatment plants (WWTP) into the aquatic environment. Several unique features and characteristics, such as low-dose effects and long-time exposure consequences require further investigation. According to an EPA survey, 115 chemicals are known to have serious EDC effects, but more than 87,000 chemicals have yet to be tested for EDC effects. Many researchers agree that low traces of steroids may affect the endocrine system after exposure for long periods (Regal et al., 2010).

Different research approaches have detected phenolic compounds and oestrogens in surface and drinking water at ng L^{-1} levels (Desbrow et al., 1998; Lagana et al., 2004; Mol et al., 2000), and some researchers have detected pg L^{-1} levels (Kuch and Ballschmiter, 2001). Steroid

hormones remain challenging because their discharge is neither constant nor can be monitored and controlled easily.

2.2 Analysis of Endocrine Disrupting Chemicals (EDCs)

2.2.1 Introduction

The adverse effects of EDCs on the environment and humans alerted the scientific community to update and develop new, fast and efficient test methods able to identify and quantify these emerging contaminants at trace level (ng L^{-1} – pg L^{-1}) (Azzouz and Ballesteros, 2014; Kuch & Ballschmiter, 2001). The need for accurate detection methods at that level of sensitivity is challenging due to the complexity and diversity of different environmental matrices. In addition, the physical properties of the targeted EDCs can put some limitations on some analytical methods such as derivatisation steps (Vega-Morales et al., 2012). Therefore, the evolution of analytical methods improves knowledge about environmental contamination, which leads to taking more precautions for the quality of water, food, air and everything that is used on a daily basis. It was reported that many countries, including the UK, the US, Germany, France, Spain, Canada, Finland and Japan were able to detect EDCs such as pharmaceuticals and hormones in wastewater treatment plants' effluents and rivers (Jiang et al., 2013). Another study states that high levels of natural and synthetic oestrogens in milk and milk derivatives were detected (Socas-Rodriguez et al., 2013). The sequence of analytical methods is important to achieve satisfactory results with trace levels down to ng L^{-1}. These include sample collection and

preparation, sample clean up and extraction and sample analysis (identification and quantification).

2.2.2 Sample Collection and Preparation

EDCs are normally at trace levels in the environment. Therefore, any losses during the analytical procedure will lead to results that do not represent the precise contamination level. The first step in sample collection is the prevention of sample contaminants binding to the container walls by using a chemical coating process called silanization with dimethyldichlorosilane solution for all glassware before any contact with EDCs (Ahrer et al., 2001; Suri et al., 2012). In addition, amber glass is preferred by many researchers to avoid any light effects on the targeted collected EDCs in aqueous samples (Suri et al., 2012). Sample containers are recommended to be rinsed in the field many times after filtration using a proper filter (≤0.45 um), glass-fibre filters are common in EDC filters and filled after that with the filtered sample (Ferrer and Thurman, 2012). The samples pH is normally adjusted immediately (pH = 2) with acid as a sample preservative to prevent biodegradation processes (Vanderford et al., 2003). Storage of samples at 4°C until extraction and subsequent analyses, which should be within 24 h of collection, is highly recommended.

2.2.3 Sample Clean Up and Extraction

Amongst the analysis procedure steps, the extraction method is considered the most crucial step for reliable results. Unknown samples can be very challenging due to their unknown composition and the complication of sample matrices that can contain hundreds to thousands of

chemical components. This diversity of different physical properties of different chemical components can make successful analytical methods able to identify and quantify unknown contaminants at trace level a state of the art practice. Therefore, samples must be prepared for chromatographic analysis using filtration to remove any impurities to avoid any plugging problems and to extend the life of the chromatography instruments. After this step, an extraction step is necessary for the following advantages;

- Any interference in the sample will make the analysis and quantification difficult, leading to confusion between peaks, loss of resolution, tailing peaks, broad peaks, ghost peaks and peak height problems.
- At trace level, the analyte concentration needs enrichment so that it can be easily detected. This is undertaken using large sample volumes through the extraction phase and to have more of the desired analyte.

Sample-extraction techniques used in analytical methods are diverse due to the diversity of the targeted analyte's physical and chemical properties. The targeted analytes can be included in different complex matrices, such as soil, liquid, food or a mixture of more than one phase. In addition, the degree of volatility, solubility and hydrophobicity are very important in selecting the appropriate analysis methods. Therefore, to achieve a satisfactory accuracy, precision, cost, time and other relevant constraints, it is important to take these steps into account carefully. The main extraction techniques used for organic compounds are summarized in Figure 2.1.

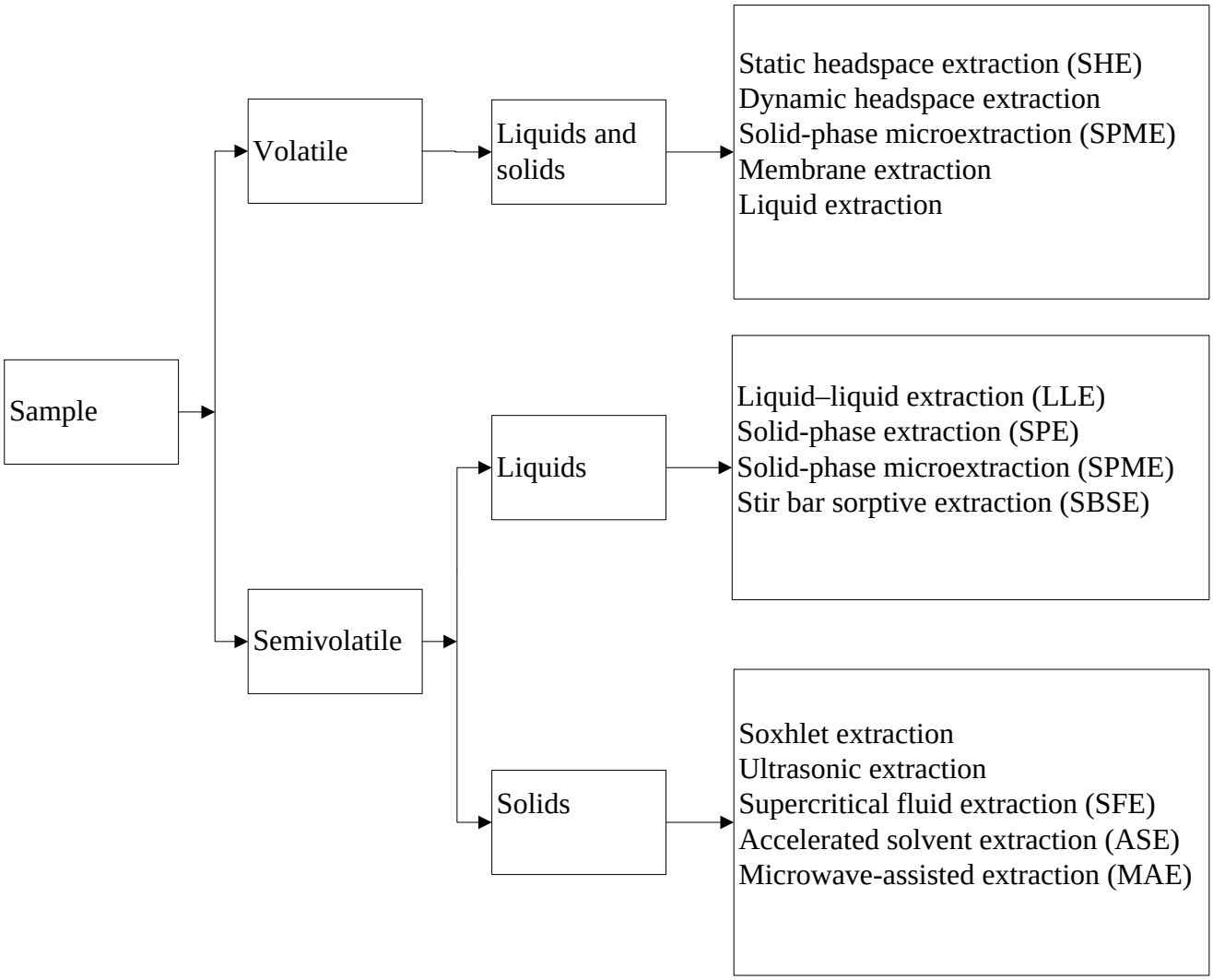

Figure 2-1 Organic compounds extraction techniques reproduced from (Somenath Mitra, 2003)

2.2.3.1 Extraction Methods of Semivolatile Organics from Liquid Samples

Liquid–liquid extraction (LLE) is used to extract the analytes from an aqueous sample solution using solvents based on solubility difference (immiscible solvent extraction). In general, less polar or nonpolar organic solvents are used, such as ethyl acetate, isopropanol and hexane

(Xie et al., 2011). LLE can be automated with a continuous extraction process, but the difficulties of using LLE are that it can be time consuming, expensive glassware is required and large amounts of organic solvents are used. Liquid–solid phase extraction methods such as solid-phase extraction (SPE), solid-phase microextraction (SPME) and stir bar sorptive extraction (SBSE) are used to extract the analytes from an aqueous sample solution using solid–phase media. In general, it is used as a batch system. SPE compared with LLE is more cost effective due to the time needed being shorter and the use of less solvents. In addition, the solid–phase extraction media used, normally disposable cartridges are safer for the technician with less cross-contamination and it can be easily automated, thus it is widely used for polar and nonpolar interactions such as pharmaceutical and environmental applications (Poole, 2003). In addition, SPE is considered the most commonly successful method used for hormones extraction in environmental samples (Guo et al., 2013; Kuster et al., 2009; Miege et al., 2009). Selecting SPE sorbents is critical to having a high recovery of the target analytes from the aqueous sample. There are several kinds of sorbents depending on the physical and chemical properties of the analytes and sample, such as polar sorbents, bonded silica sorbents, ion-exchange sorbents and mixed-mode sorbents. SPE is considered very sensitive to suspended particles in aqueous samples that can block the SPE cartridge; therefore, prefiltering the sample is essential with this extraction process. SPME is a straightforward solvent free extraction method used widely in pharmaceutical and environmental analysis (Lord et al., 2006; Vas and Vekey, 2004). Preconcentration of the analytes from gas or liquid samples in SPME uses a fibre surface coated with appropriate sorbents or capillary tube internal surface (exhaustive extraction procedure). Thus, it can be easily automated to the analytical instruments due to the procedure including only sorption and desorption processes. SPME extracts ≤20 % of analyte and the entire sample is injected, while SPE extracts ≥90 % of

analyte and 1-2 % of the sample is injected. SPME can be highly affected by the degree of matrix of purity, which can affect the equilibration process between the sorbents and the analytes, which is considered a disadvantage of this method. SBSE method is similar to SPME and used for larger quantitative extraction samples compared with the SPME method (Serodio and Nogueira, 2006). Normally, sorbents are coated on a stir bar immersed in aqueous samples. Therefore, time and stirr bar speed are important in achieving an equilibrium state between analytes and sorbent media. The analytes are then desorbed thermally and injected into the gas chromatograph. The SBSE method can be applied easily, but the availability of selective sorbents for different aqueous samples is still a difficulty that needs to be overcome.

2.2.3.2 Extraction Methods of Semivolatile Organics from Solids Samples

Extraction of semivolatile organics from solids is done by a desorption process followed by dissolving with an appropriate selective solvent. This process is influenced by mass transfer, matrix effects and solubility. Normally, these factors are highly affected by physical properties such as temperature, pressure, particle size and the degree of solubility between the analytes and the solvent. The efficiency of extraction can be enhanced by a sample pre-extraction process such as smaller particle size or fine powders and drying, but it is not recommended for volatile analytes. One of the main problems in this kind of extraction is the difficulty of desorption of analytes from the matrix due to the strong interactions between the extracted analytes and the matrix. In addition, the large volume of solvents after the extraction process needs a cleaning step prior to chromatographic analysis. Soxhlet extraction was the most widely used extraction method for semivolatile organics from solids. This extraction method can be automated, and

typically the analytes are extracted with a low boiling point solvent and then cooled and condensed with a cycle process that leads to higher amounts of analytes extracted. The drawbacks of this kind of extraction method are the long time needed for extraction (6 to 48 h), fresh solvents in each cycle leads to a large solvent consumption. Ultrasonic extraction is another extraction method with limited applications. The extraction method normally consists of an ultrasonic probe immersed in the sample mixed with the selected solvent. A clean-up step is necessary after the extraction process prior to chromatographic analysis. It was reported that extraction of oestrogens in human urine was enhanced (Zou et al., 2012). Although sonication is a fast extraction method, these methods are uncommon at a low trace level due to the low extraction efficiency and the possibility of analyte decomposition that can occur with ultrasonic irradiation (Kotronarou et al., 1992). Supercritical fluid extraction (SFE), considered a sophisticated extraction method, utilizes the properties of supercritical fluids for the extraction of analytes from solids. It was reported that SFE was effectively used for the extraction of carotenoids, pesticides, herbicides and other pharmaceutical substances (Kagliwal et al., 2011; Mendes et al., 2003; Sun and Temelli, 2006). This method can be run offline or online coupled with a gas chromatograph, but offline is considered more flexible than online offering more choices of different analytical methods besides the extraction method used. SFE is fast, minimum solvent used per sample, uses a non-toxic, non-flammable solvent (CO_2) and no filtration is required due to the frits included in the extraction cell. The selectivity can be controlled by manipulating the operating conditions. SFE instruments are considered expensive, matrix dependent, require addition of organic modifiers and cannot handle large sample sizes. Accelerated solvent extraction (ASE) evolved initially from SFE and is used for the extraction of organic analytes from solids (Giergielewicz-Mozajska et al., 2001). ASE is known by different

names, such as pressurized fluid extraction (PFE), pressurized solvent extraction (PSE), pressurized liquid extraction (PLE), pressurized hot solvent extraction (PHSE) , pressurized hot water extraction (PHWE), subcritical solvent extraction (SSE), high-pressure, high-temperature solvent extraction (HPHTSE) and high-pressure solvent extraction (HPSE) (Carabias-Martinez et al., 2000). ASE can be run up to 180ºC and 13.79 MPa. ASE is considered a faster and more complete extraction method than SFE. The wide diversity of ASE applications was reported extensively in research fields such as environmental, food and biological solid samples (Carabias-Martinez et al., 2005; Nieto et al., 2008; Nieto et al., 2010; Smith, 2002). ASE can be fully automated, is a very fast extraction method (15 min), simple method development, using a wide range of solvents and has built-in filtration. The only negative thing is the high initial equipment cost. Microwave-assisted extraction (MAE) is considered an efficient extraction method due to its shorter extraction time and low use of organic solvent (Tan et al., 2011; Teo et al., 2013; Teo et al., 2008). In the last two decades, there has been a steady improvement of MAE towards environmental and food analysis; pure water (green extraction solvent) was used successfully as an extraction solvent for nonpolar organic compounds in food analysis at optimized conditions (Fang et al., 2009; Rodriguez-Rojo et al., 2012). The MAE principle is using the microwave energy (electromagnetic radiation) in the range of 300 MHz (radio radiation) to 300 GHz (infrared radiation) leading to heating the sample by ionic conduction and dipole rotation with no effect on the molecular structure (Gabriel et al., 1998; Lidstrom et al., 2001). MAE advantages are fast extraction (20–30 min), can handle samples up to 20 g with high sample throughput and low use of solvents. However, expensive equipment is needed, filtration is required as a clean-up step, solvents must be polar and there is a possibility of chemical reactions and degradation.

2.2.3.3 Extraction of Volatile Organics from Solid and Liquid Samples

Static headspace extraction (SHE) is normally coupled with gas chromatography (GC) and also known as headspace or equilibrium headspace extraction. The method is straightforward and it can be used for the quantitative and qualitative analysis of volatile samples with reliable results. The SHE method in brief is as follows: a liquid or solid sample is placed in the headspace auto sampler (HSAS) vial, which is heated until the equilibrium state is reached between the vapour phase and the sample, a fraction of the vapour then collected and injected directly by the auto sampler into the GC for analysis. The SHE method was improved by adding a trapping step (headspace trap) using a solid-phase trap to improve the GC response; it was reported that the response was increased by 55 fold in a beverage application (Schulz et al., 2007). A derivatization step and ionic liquids as solvents can be used to enhance SHE performance (Alzaga et al., 2007; Liu and Jiang, 2007). SHE can be automated easily with simple, cheap and fast optional sample preparation, but it can be highly affected by the sample matrix and the solubility and volatility of the analytes in aqueous samples. Dynamic headspace extraction (DHE) or the purge and trap extraction method relies mainly on the analytes volatility. Analytes are removed continuously by using a flowing gas without the need for the equilibrium state to be reached; thus, this method is preferred over SHE. This method was successfully used in environmental, biological and food samples (Beltran et al., 2006; Cervera, I et al., 2011). DHE can be an exhaustive extraction by controlling the concentration gradient, which is controlled by the flowing gas. The role of the trap is crucial in selectivity and eliminating impurities, therefore, selecting the trap materials is considered very important, especially for trace level analysis. The limitation of DHE is that water accumulation from the gas-purging process can reduce GC column efficiency, which implies adding proper water management methods such as a dry purge

step or a condenser consisting of inert material. SPME and LLE have already been described previously in Section 2.2.3.1. The additional discussion for volatile organic samples is selecting the appropriate coated fibre surface with the direct or headspace sample collecting method. LLE coupled with GC analysis due to the improvement of injection systems has recently improved handling of large liquid volumes up to 2 mL, but this method experiences a common problem with sensitivity in particular with dirty samples. Membrane extraction is considered a promising one-step extraction method consisting of a sample diluted (in general) in water passing through a thin layer of semi-permeable substance using an external driving force (Minioti et al., 2007). The most common uses of the membrane extraction method are in food beverage samples and it can be easily be used in continuous online analysis attached to detection devices such as a GC or mass spectrometer, which are useful at trace level detection limits.

2.2.4 Overview of Current Analytical Methods

The final step following sample collection, preparation and extraction is analysis using an instrument of choice that is able to identify and quantify unknown contaminants. The variety of analysis instruments is due to the different analysis methods required for different samples that have different chemical and physical properties. Chromatography is the common method of analysis for organic analytes, while atomic spectroscopy is used for metal analysis and capillary electrophoresis used for DNA. The great diversity of the analysis methods needs comprehensive exploration in the literature survey. Therefore, the following discussion will focus on the analysis methods involved for the determination of various classes of selected oestrogens. The most extensively published information on hormones can be found related to water resources such as

rivers, lakes, drinking water and wastewater treatment plants, which have a high impact on humans, wildlife and agriculture with adverse serious health effects. The most common methods for the analysis of hormones are liquid chromatography (LC) coupled with ultraviolet (UV), mass spectrometry (MS) or tandem mass spectrometry (MS/MS) detection. Gas chromatography (GC) also is used widely, but a derivatization step is required, which adds extra time and cost for the analytical procedure. GC can be coupled with flame ionization detector (FID), MS or MS/MS detection. A summary of common analytical methods used for the determination of hormones is given in Table 2.2.

Table 2-2 Summary of common analytical methods used for the determination of hormones

Analyte	Matrix	Sample preparation	Instrument	LOD / LOQ	Reference
17β-estradiol, Estrone 17α-ethynylestradiol	STW effluents, UK	SPE C_{18} (IST, Hengoed) LLE	HPLC GC-MS.	1 -80 ng L^{-1}	(Desbrow et al., 1998)
17β-estradiol, Estrone 17α-ethynylestradiol 16α-hydroxyestrone	STW effluents, River and ground water Germany and Canada	SPE RP C_{18} (Lichrolut -EN) Derivatization	GC-MS/MS	1 -70 ng L^{-1}	(Ternes et al., 1999)
17β-estradiol and 17α-ethynylestradiol 4-octylphenol, 2,4-dichlorophenol, Pentachlorophenol, Bisphenol-A	Surface water Netherlands	SPE (PS-DVB) (styrene–di-vinylbenzene) Derivatization LLE	GC-MS	4 - 6 ng L^{-1} LOD	(Mol et al., 2000)
Estradiol Estrone Estriol 17α-ethynylestradiol Mestranol	STW sediment UK	LLE	GC-MS	5 ng L^{-1} LOD	(Lai et al., 2000)
17β-estradiol estriol estrone ethynylestradiol mestranol diethylstilbestrol progesterone levonorgestrel Norethindrone	STW influents and effluents surface water drinking water	Automated SPE (Villiers-leBel)	LC-DAD-MS	2 - 500 ng L^{-1} LOD	(de Alda and Barcelo, 2000)

phenol 4-nonylphenol 17β-estradiol 17α-estradiol 17α-ethinylestradiol	surface drinking water	SPE LiChrolut EN	HRGC-(NCI)-MS	20-200 pg L^{-1} LOD	(Kuch & Ballschmiter, 2001)
Estriol Estradiol Ethynyl estradiol Estrone Levonogestrel Progesterone	water and river sediment Spain	SPE RP-18 Oasis HLB HySphere PLRP-S	LC-DAD-MS	0.5 - 20 ng L^{-1} LOD	(de Alda and Barcelo, 2001)
Progesterone Ethynylestradiol Estradiol Testosterone	surface water USA	SPE Oasis HLB	LC- ESI – MS LC- API – MS	7.5 - 50 ng L^{-1} LOD	(Vanderford et al., 2003)
Estriol Estradiol Ethynyl Estradiol Estrone Diethylstilbestrol Mestranol	surface water Spain	SPE C_{18} (Octadecyl) derivatization BSTFA	LC-ESI-MS/MS GC-MS	0.1–10 ng L^{-1} LOD	(Diaz-Cruz et al., 2003)
Estrone 17a-Estradiol 17b-Estradiol Estriol Ethynyl estradiol	River Lake STP effluent Japan	SPE Autoprep EDS-1 Oasis HLB	LC- ESI – MS	0.1 ng L^{-1} LOD	(Isobe et al., 2003)
17-estradiol Estrone estriol 17-ethynylestradiol	STP influents and effluents Italy	SPE Oasis HLB	LC–MS–MS	30 ng L^{-1} LOD	(Lagana et al., 2004)

Estriol Estradiol Estrone	river water industrial effluents WWTP effluents Belgium	SPE Oasis HLB	LC-ESI-MS/MS	0.1 -20 ng L^{-1} LOD	(Benijts et al., 2004)
Diethylstilbestrol Estrone 17-estradiol Mestranol 17-ethinylestradiol estriol	river water STP influents and effluents Spain	SPE Oasis HLB derivatization N-methyl-N-(trimethylsilyl)trifluoroacetamide	GC–MS GC–MS–MS	1 -20.0 ng L^{-1} LOD	(Quintana et al., 2004)
17α-ethynylestradiol 17β-estradiol estrone	Purified sewage surface, ground, and drinking water Germany	SPE RP-C18	LC-MS/MS	0.1 -2 ng L^{-1} LOQ	(Zuehlke et al., 2005)
Bisphenol A 17α-ethinylestradiol	lake water landfill water China	SPME Zylon fiber packed PEEK	HPLC	0.12 ng L^{-1} LOD	(Fan et al., 2005)
estrone 17β-estradiol estriol 17α-ethynylestradiol	WWTP effluents China	SPE ENVI-CARB	LC-MS/MS	0.5 -2 ng L^{-1} LOQ	(Cui et al., 2006)
17 α-estradiol 17 β-estradiol 17 α-dihydroequilin 17 α-ethinyl estradiol Estriol Estrone Equilin Medrogestone Levonorgestrel Gestodene	WWTP effluents USA	SPE Varian C-18 Derivatization	GC-MS	1.2 - 259 ng L^{-1} LOD	(Chimchirian et al., 2007)

Estriol Cholesterol Desmosterol Estrone Ergosterol Equilin Campesterol 17-Estradiol Testosterone	WWTP influents and effluents Bleached kraft mill effluent (BKME) Canada	Derivatization	GC-HRMS	1- 529 ng L^{-1} LOD	(Ikonomou et al., 2008)
Estrone 17 -estradiol 17 -ethynylestradiol 16 -hydroxyestrone Nonylphenol Nonylphenol carboxylate Octylphenol Octylphenol carboxylate Bisphenol A	WWTP effluents France	SPE Oasis HLB	LC-MS/MS	0.21 ng L^{-1} LOD	(Stavrakakis et al., 2008)
Estrone 17α-estradiol 17β-estradiol 17α-ethynylestradiol Estriol	WWTP influents and effluents Rivers France	SPE Oasis HLB	LC-MS/MS	0.4 -3 ng L^{-1} LOQ	(Miege et al., 2009)
Cortisol Dexamethasone Flumethasone Prednisolone Methyltestosterone Nortestosterone Progesterone	river drinking water Hungary	SPE Oasis HLB Oasis MAX	LC-MS/MS	0.21 ng L^{-1} LOD	(Tolgyesi et al., 2010)

17α-estradiol 17β-estradiol 17α-dihydroequilin 17α-ethinyl estradiol Estriol Estrone Equilin Medrogestone Levonorgestrel Norgestrel Gestodene	STW influent and effluent USA	SPE Spec C-18 (Spec) Varian Bond Elut C-18 (Varian) Waters Sep-pack C-18 (Waters) Phenomenex Strata-X 33 µm Supelco DSC-18 (DSC-18) Supelco DSC- 18LT (DSC-18LT) Derivatization	GC-MS	30 to 870 ng L^{-1} LOD	(Suri et al., 2012)
Bisphenol A Estriol Estrone 17-estradiol 17-ethynilestradiol Testosterone Diethylstilbestrol Norgestrel	WWTP effluents Spain	SPE Oasis HLB	UHPLC–MS/MS	0.3–2.1 ng L^{-1} LOD	(Vega-Morales et al., 2012)
17α-estradiol 17β-estradiol 17α-ethinyl estradiol	WWTP influent and effluent USA	SPE Oasis HLB	LC-MS/MS	0.6-0.9 ng L^{-1} LOQ	(Gunatilake et al., 2013)
17β-estradiol Estrone Estriol 17α-ethinyloestradiol Bisphenol A	Island cost Portugal	SPE Oasis HLB	GC-MS	2.8-18.1 ng L^{-1} LOQ	(Rocha et al., 2013)

Bisphenol A 17α-ethinyloestradiol	Surface and supply water Brazil	SPE Strata C18	HPLC-fluorescence	1.5-2.1 ng L^{-1} LOQ	(Melo and Brito, 2014)
Estrone 17β-estradiol Diethylstilbestrol	Milk samples	Magnetic –SPE	HPLC-DAD	0.26-0.61 ng L^{-1} LOD	(Wang et al., 2015)
17β-estradiol Estrone Estriol Progesterone	WWTP effluents Spain	SPE Oasis HLB	UHPLC-MS/MS	3.1-52.8 ng L^{-1} LOD	(Guedes-Alonso et al., 2015)

Abbreviations: Sewage-treatment works (STW), WWTP: Wastewater Treatment Plant, solid phase extraction (SPE), Limit of Detection (LOD), N-methyl-N-(tert.-butyldimethyltrifluoroacetamide), Liquid–liquid extraction (LLE), high-resolution gas chromatography with negative chemical ionization mass spectrometric detection (HRGC-(NCI)-MS), mass spectrometry (MS), tandem mass spectrometry (MS/MS) detection. Gas chromatography (GC), liquid chromatography–diode array detection–mass spectrometry (LC-DAD-MS), LiChrolut RP-18 (RP-18), HySphere-Resin-GP cartridge (HySphere), Sep-Pak C Plus cartridges (PLRP-S), hydrophilic-lipophilic balance, Waters (Oasis HLB), electrospray ionization (ESI), atmospheric pressure (API), bis(trimethylsilyl)trifluoroacetamide (BSTFA), sewage treatment plants (STP), Limits of quantification (LOQ), Oasis MAX (Mixed mode Anion exchange)

2.3 Endocrine Disruptor Chemicals Treatment Processes

Despite the fact that water is considered the most abundant resource for human consumption, less than 1% of water can be used in a safe manner (Grey et al., 2013). In addition, increased contamination of water resources has been reported by the scientific community (WHO, 2012). Therefore, the need for developing efficient and cost-effective water-treatment techniques able to remove emerging contaminants is considered essential to the environment and wildlife. The evaluation of different water-treatment techniques depends on performance, cost and environmental impacts. The main current technologies include coagulation/precipitation, filtration, biological treatment, oxidation, photocatalysis, Fenton/photo-Fenton and adsorption.

2.3.1 Coagulation/precipitation

Coagulation or chemical precipitation is considered to be a simple process and is commonly used for the removal of heavy metals. The contaminants removal is done by a reaction between heavy metal ions and an appropriate chemical precipitant followed by a separation process using either sedimentation or filtration (Fu and Wang, 2011; Srivastava and Majumder, 2008). The performance of the coagulation process is considered ineffective with hormones contaminants. It was noticed that the removals of estradiol, estrone, progesterone and testosterone were <20 % (Snyder et al., 2007). The main problem with this kind of treatment method is considered to be the cost due to the large quantity of chemical reagents required. In addition, a pH adjustment for the effluent is needed and the large amount of hazardous sludge that is produced from the treatment process, which adds extra cost for the hazardous sludge

management related to the environmental regulations that require additional treatment (Adeleye et al., 2016; Kartinen and Martin, 1995; Shi et al., 2007).

2.3.2 Filtration

Filtration is a process where contaminants are separated from water using a filtration medium. The performance of filtration is highly affected by particle size, charge and hydrophobicity. Filtration techniques can be straightforward, such as sand filtration to more complicated and effective techniques for most wastewater contaminants such as reverse osmosis (RO) and membrane filtration (Campos et al., 2002). The performance of RO in removing steroid hormones from wastewater was greater than 90%, while membrane filtration (microfiltration and ultrafiltration) was ineffective for steroid hormone elimination in a full-scale wastewater treatment plant (Huang and Sedlak, 2001). The downside of using such a kind of treatment is the high operating and maintenance cost. Membrane filtration and RO require high pressure, which will raise the operating cost. In addition, common problems are fouling, clogging, pH adjustments and backwashing is required to maintain the performance of the processes.

2.3.3 Biological treatment

Biological treatment systems such as bioreactors and biofilters include both aerobic and anaerobic treatment methods and are dependent on microorganisms for the contaminants degradation. Biological treatment can be used for the removal of organic and inorganic non-metals from wastewater. However, biological treatment was found to be ineffective for the removal of EDCs at the trace level (Quintero et al., 2005; Rosal et al., 2010). It was found that

when the biological treatment was combined with filtration treatment it was more effective for the removal of heavy metals from wastewater (Srivastava & Majumder, 2008). Many factors can affect the efficiency of biological treatments, such as wastewater matrix composition, loading rate, temperature and the degree of aeration. The common problems are fouling, filter clogging and slow process (Adeleye et al., 2016).

2.3.4 Oxidation

Chemical oxidation processes can be used to degrade difficult organic substances that cannot be degraded using conventional treatment methods such as coagulation, filtration and/or biological methods (Esplugas et al., 2007; Malik and Saha, 2003; Wert et al., 2009). Chemical oxidation processes will affect the chemical properties of the organic pollutants which will break into smaller fragments and degrade more easily than the original organic pollutants. Common oxidation methods include the use of chlorine, hydrogen peroxide, ozone, wet oxidation, supercritical water oxidation treatment and electrochemical oxidation.

Chlorine disinfection is a common inexpensive treatment process used in the water industry. The chlorination process is carried out by using either chlorine gas or concentrated hypochlorite solution to form aqueous chlorine, whose oxidative power is highly dependent on pH. The reported effectiveness of chlorine disinfection for the removal of organic pollutants in a full scale wastewater treatment was very low (EPA, 2010). The highly toxic and corrosive properties of chlorine gas are considered the downside of this process. In addition, the byproducts of the chlorination process, such as chloroform, are potentially harmful, which requires additional treatment.

Ozone (O_3), considered a strong oxidizing and disinfecting agent is used in both drinking and wastewater processes. The decomposition of O_3 occurs rapidly within minutes of addition to water and can be used as direct reactions or indirect to generate highly reactive hydroxyl radicals. O_3 oxidation can be enhanced by using ultraviolet (UV) light and/or hydrogen peroxide. In addition, O_3 can be generated and used on-site but it is very difficult to store the gas; therefore all of the generated gas must be used directly. The downside of O_3 is the high cost required related to the on-site production.

Hydrogen peroxide (H_2O_2) is used for the production of hydroxyl radicals ($HO^{\bullet}$) which be used in wastewater treatment processes for the removal of organic contaminants. The global demand on H_2O_2 has increased and 55% of H_2O_2 production was consumed by Europe alone (Asghar et al., 2015). H_2O_2 is commonly combined with UV as an effective advanced oxidation process (AOPs). The downside of using H_2O_2 relates to the safety issues with storage and transportation and the high cost of H_2O_2, which is considered an economic challenge.

Wet and supercritical water oxidations (SCWO) both are considered hydrothermal oxidation processes used for the removal of organic contaminants in wastewater treatment processes. High temperature and pressure are required in the presence of oxygen or air as an oxidizing agent in these systems. The wet oxidation process in general has operating conditions in the range 180–320ºC and 7–18 MPa, while the SCWO range is 400–650ºC and 20–30 MPa (Serikawa et al., 2000). The resulting products of the organic contaminants treatment are innocuous compounds such as water and CO_2, which are safe for the environment. Wet and supercritical water oxidations are available for the commercial use, but the downside of these systems is the high cost for the significant energy input and equipment (Vince et al., 2008).

Electrochemical oxidation (EO) is a process where the oxidation can be directly achieved by hydroxyl radicals produced from the anode's surface or by indirect oxidation using oxidizing agents such as chlorine, ozone and hydrogen peroxide on the electrodes. EO operating conditions in general are atmospheric pressure and temperatures up to 80ºC (Serikawa et al., 2000). It was reported that complete oxidation of some organic contaminants was not achieved (Savall, 1995). In addition, at low temperature the reaction is slow due to its kinetics limitations (Comninellis, 1994). The disadvantages of EO are the significant energy input and electrode corrosion (Martinez-Huitle and Ferro, 2006).

2.3.5 Photolysis or photocatalysis

UV radiation is considered a promising treatment technology compared with conventional treatment technologies for the removal of EDCs from wastewater. UV can be used directly without the use of catalysing material (photolysis degradation) or combined with catalysing material such as TiO_2 to accelerate the reaction rate (photocatalytic degradation). Photolysis or photocatalytic degradation treatment technologies were able successfully to remove various EDCs (Kim and Tanaka, 2009; Nasuhoglu et al., 2012; Rosenfeldt and Linden, 2004; Rosenfeldt et al., 2007; Souza et al., 2014). UV radiation can be divided into three parts as shown in Figure 2.2 based on the wavelength as follows: UV-A, UV-B and UV-C radiation (180–280 nm) which is often used in water treatment systems.

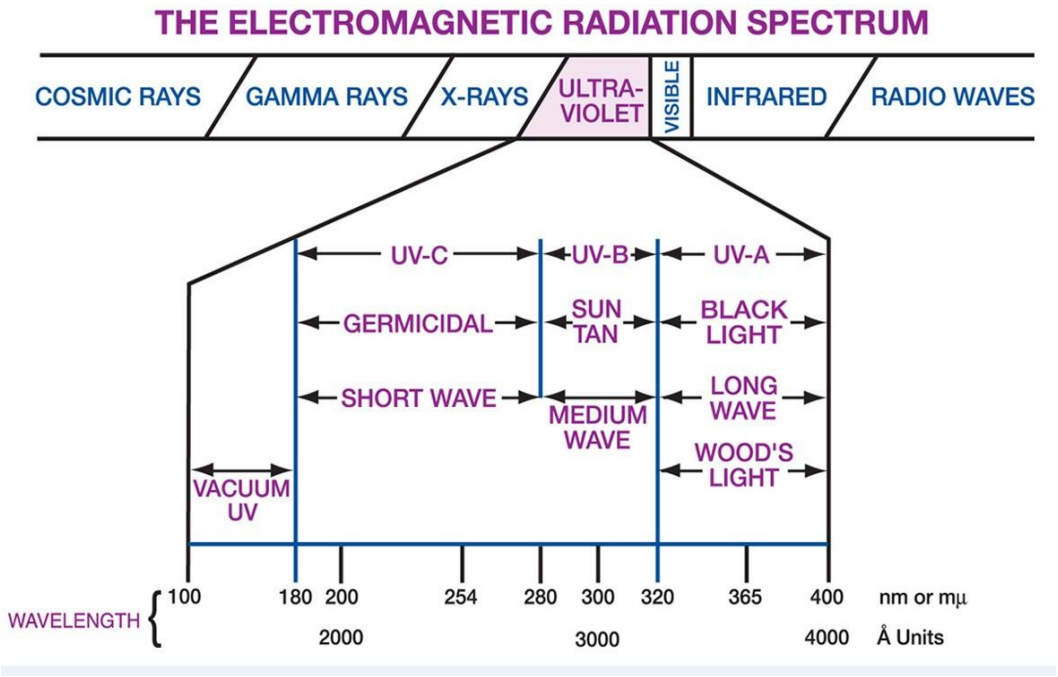

Figure 2-2 The UV spectrum (UV Resources, 2016)

The degradation mechanism can be direct by cleaving the bonds of the organic molecules or indirect by generating highly reactive $OH^{\bullet}$ radicals. The addition of hydrogen peroxide (H_2O_2) can enhance the formation rate of $OH^{\bullet}$, which is commonly combined with UV radiation as an effective AOPs. The effectiveness of these systems depends on the clarity of the water matrix; light scavengers can prevent UV light from penetrating to the organic contaminants and affects the whole light absorption efficiency. Full-scale UV systems are currently applied for drinking and wastewater systems, but the downsides of these systems are the significant energy input and the regular maintenance of the UV source for cleaning and replacement, which adds extra cost.

2.3.6 Fenton/photo-Fenton

Fenton/photo-Fenton processes decompose H_2O_2 in the presence of catalysing iron to oxidize wastewater contaminants and can be enhanced by the addition of UV irradiation. Fenton/photo-Fenton processes are considered effective techniques for most wastewater contaminants such as halogenated and non-halogenated organics, pesticides and herbicides (Andreozzi et al., 1999; Comninellis et al., 2008; Kavitha and Palanivelu, 2004; Perez et al., 2002). In Fenton processes, optimum efficiency can be achieved in the pH range of 2.5–3.0 (Ribeiro et al., 2015). Photo-Fenton is considered more efficient than the classical Fenton process due to the higher generation rate of hydroxyl radicals. The UV radiation accelerates the rate of degradation and lowers the catalyst need and less sludge volume is produced (Ribeiro et al., 2015). The downsides of these systems are the same as using H_2O_2 and UV and relate to the safety issues and economic challenges.

2.3.7 Adsorption: Activated Carbon (Granular and Powdered)

Activated carbon can be in the form of granular activated carbon (GAC) or powdered activated carbon (PAC) and both forms can be used to remove EDCs from drinking and wastewater systems (Chingombe et al., 2005; Comninellis et al., 2008; Joseph et al., 2013; Mohan et al., 2008). Activated carbon is used as a polishing treatment step for the removal of trace level contaminants. Most pollutants are removed by adsorption on the carbon's active surface by physical and chemical bonding. The adsorption characteristics such as adsorption capacity and kinetics can be highly influenced by the activated carbon pore size, distribution and contact time. In addition, water matrices such as temperature, pH, physicochemical properties of

contaminants of interest and contaminants load can affect the adsorption rate. GAC is used as a fixed-bed and the water is flowed through the carbon bed, while PAC is fed to the treatment process. The raw materials of activated carbon are inexpensive, but the energy input for manufacturing a high quality of activated carbon and regeneration of used activated carbon are considered quite expensive (Mohan and Pittman, 2007). In addition, the common problems of clogging lead to a higher pressure drop through the activated carbon bed and the fact that the contaminants are not degraded but adsorbed will generate a hazardous waste with added cost for handling and appropriate disposal methods.

2.4 Bubble Column Reactors

2.4.1 Introduction

Bubble column reactors are multiphase reactors used widely in industry for contacting liquid/liquid, liquid/solid, liquid/gas, or liquid/solid/gas phase and can be operated in packed bed or slurry mode (Deckwer and Schumpe, 1993; Weber, 2002). The wide use of bubble reactors in industry is due to the following advantages:

- Bubble column reactors are simple in construction and can be scaled-up with less occupation of space compared with agitated reactors.
- Lower maintenance cost due to the absence of moving parts compared to mechanical stirring reactors.
- Excellent thermal management due to the high liquid circulation rates that can be achieved.
- High mass transfer rate and effective interfacial area can be achieved.

- Bubble column reactors are considered an excellent choice for slurry chemical reactions because of less pressure drop when using solids without the development of plugging problems.
- Bubble column reactors are considered an excellent choice for slow reactions due to the high values of residence time that can be achieved.
- However, the main disadvantages of bubble column reactors are:
- Liquid phase backmixing can highly affect the performance of the bubble column reactor, which can be overcome by using packed or sectionalised bed columns.
- A length to diameter (L/D) ratio greater than 12 can lead to a lower specific interfacial area due to an increase in the rate of bubble coalescence (Steiner, 1987).

Bubble column reactors consist of vertically arranged cylindrical columns. The liquid can be in a co-current or counter-current flow. Bubble column reactor mixing is done by either gas sparging located at the bottom of the column or direct injection into the liquid flow from the top of bubble column. Gas distributors can take many kinds of different designs and be in various geometrical configurations, including ring type distributors, jet nozzles, porous plates, and perforated pipes, etc. (Kulkarni and Joshi, 2011). Different configurations of bubble column reactors can be seen in Figure 2-3. Bubble column reactors are characterized by their high-liquid content and a moderate phase boundary surface, which make them useful devices particularly in reaction where the gas-liquid reaction is slow in relation to the absorption rate that enable bubble column reactors to achieve high residence times. Also, the excellent thermal management and high mass transfer rates provide a variety of industrial applications, such as oxidation (Ochuma et al., 2007b; Weber, 2002; Winterbottom et al., 1997a), esterification (Alenezi et al., 2010b; Stacy

et al., 2014), cementation (El-Ashtoukhy and Abdel-Aziz, 2013), hydrogenation (Fishwick et al., 2007; Marwan and Winterbottom, 2003), fermentation (Chen et al., 2015; Sonego et al., 2014), heavy oil upgrading (Carbonell and Guirardello, 1997), the Fischer-Tropsch process and the production of synthetic fuels (Salehi et al., 2014; Vik et al., 2015). Bubble column reactors are simple in construction and easy to use, but their design and scale-up is considered to be very complex especially at industrial scales due to the complexity of their hydrodynamics, which will not only affect the overall design, but is a significant influence on factors such as selectivity and yield (Shah et al., 1982a).

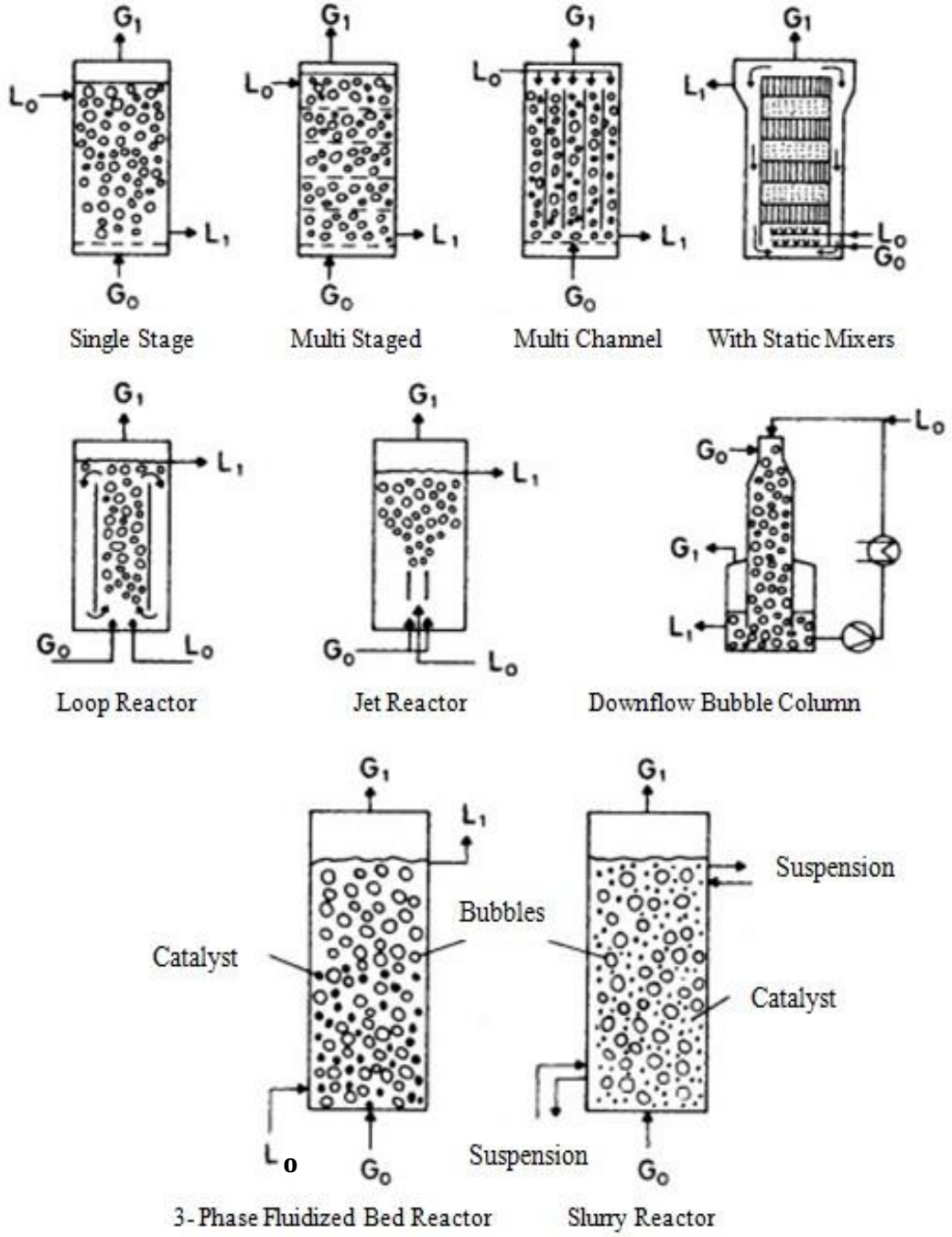

Figure 2-3 Bubble column reactors configuration. G_0, Gas inlet; G_1, Gas outlet; L_0, Liquid inlet; L_1, Liquid outlet (Shah et al., 1982a)

Design and scale-up of bubble column reactors takes into account an understanding of hydrodynamic, mass transfer and heat transfer characteristics, as well as, backmixing (Kantarci et al., 2005; Rollbusch et al., 2015). Research on bubble column reactor design and scale-up commonly focuses on flow regime characteristics (Li et al., 2014; Ruzicka et al., 2001; Thorat and Joshi, 2004; Ziegenhein et al., 2015), bubble characteristics (Li and Prakash, 2000; Mandal et al., 2005; Ojima et al., 2014), gas-hold up and interfacial area (Bouaifi et al., 2001; McClure et al., 2015; Wang et al., 2003) and mass and heat transfer studies (Behkish et al., 2002; Jhawar and Prakash, 2011; Lau et al., 2012).

2.4.2 Hydrodynamic Characteristics

2.4.2.1 Flow Characteristics

Flow characteristics can significantly affect bubble column reactor hydrodynamics and mixing properties. The flow regime is controlled mainly by the superficial gas velocity and the physical properties of the system and can be classified into three distinct regions (see Figure 2.4):

1. Homogeneous bubbly flow regime. This flow is obtained at superficial gas velocities less than 5 cm s^{-1} and is characterised by a small uniform bubble size due to the small interaction between bubbles and gentle mixing (Thorat & Joshi, 2004). Bubbles are well distributed across the entire cross-sectional area of the column with an absence of bubble coalescence or break-up process (Hyndman et al., 1997). Gas-hold up (εg) increases linearly with increasing superficial gas velocities (Kawagoe et al., 1976).
2. Heterogeneous churn-turbulent flow regime. This flow is obtained at superficial gas velocities greater than 5 cm s^{-1} and is characterised by unsteady flow patterns with a wide

variation in bubble sizes in column. The high turbulence between the gas phase and the liquid phase increases the coalescence and break-up process of the smaller sized bubbles leading to the formation of a larger bubble sizes in a rapid process. As a result, there are shorter residence times with this regime compared to homogeneous flow. Heterogeneous churn-turbulent flow regimes normally can be found in industrial-scale and large-diameter columns (Hyndman et al., 1997; Schumpe and Grund, 1986).

3. Slug flow. This flow is obtained at very high superficial gas velocities in small column diameters, in which larger bubbles are highly affected by the column walls, leading to the formation of bubble slugs. Slug flow regimes normally can be found in laboratory-scale.

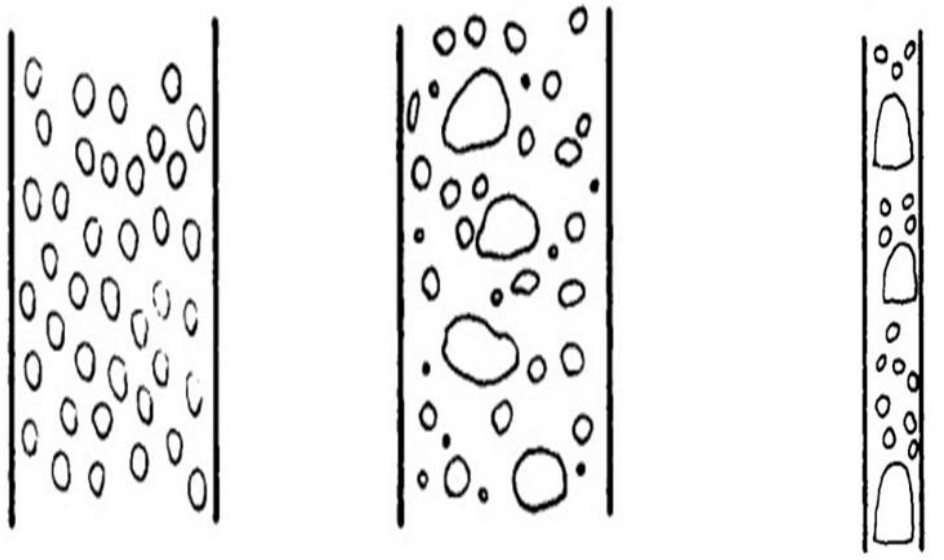

Bubbly Flow Churn Turbulent Slug Flow

Homogeneous Heterogeneous

Figure 2-4 Flow regimes in bubble columns reactors (Shah et al., 1982a)

Bubble column reactor design and scale-up strongly depends on the recognition of flow regime. The hydrodynamic behaviour of the flow regime becomes more unpredictable when transitions take place from homogeneous to churn-turbulent flow. Figure 2.5 shows a flow regime map as suggested by Shah showing the superficial gas velocity (U_G) and column diameter (D_T) between three distinct regions (Shah et al., 1982a). The grey region indicates transitional zone between the three distinct regions.

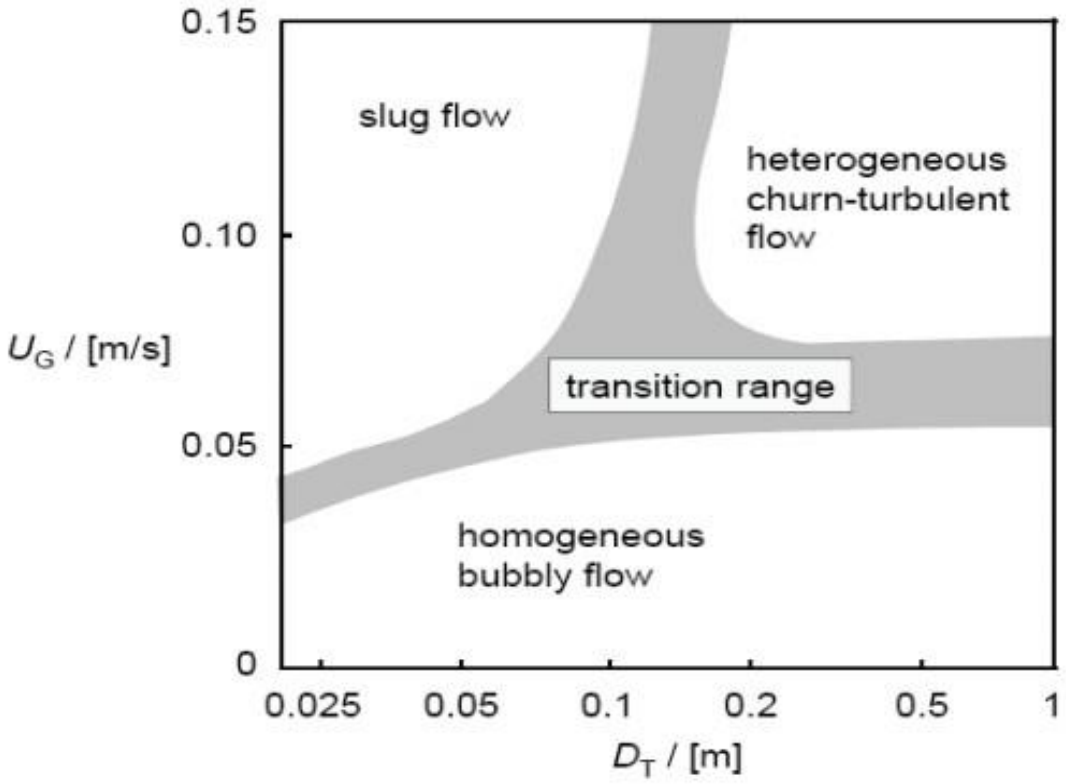

Figure 2-5 Flow regime map for air-water system at ambient pressure. Ug, superficial gas velocity; D_T, column diameter (Shah et al., 1982a)

2.4.2.2 Bubble Dynamics

Shah et al. (1982) states that the performance of bubble column reactors is highly affected by bubble dynamics, including bubble size, bubble rise velocity, bubble size distribution (BSD) and liquid and bubble velocity profiles. Determination methods used for bubble size vary due to their wide size distribution. In bubble columns particularly, in a heterogeneous churn-turbulent flow regime, (which is considered a challenging research area); the methodologies used include high speed cameras (video imaging techniques), light scattering, light reflection, Computer Automated Radioactive Particle Tracking (CARPT) and various optical and electrical probes (Lage and Esposito, 1999; Lau et al., 2013b; Mena et al., 2005; Rados et al., 2002). To avoid interference of the flow conditions with the methods used for determination of bubble size distribution, non-intrusive measurement techniques are preferred over intrusive methods (Lau et al., 2013a). However, one limitation of video imaging techniques, is that they are useful only in 2-D bubble columns. Also, imaging techniques can only be used with a transparent bubble column wall and liquid, low gas holdup, low temperature and low pressure. Beyond the column wall, bubble size determination relies on several assumptions, namely, that bubbles are identical and backed without voids in the bubble column and have a perfectly spherical shape. This does not represent the real situation due to the affect of different forces acting on bubbles including drag force, lift force, turbulent dispersion force, wall force and virtual mass that change according to the distance from the wall, liquid and gas jet velocities, pressure and temperature (Rzehak and Krepper, 2013). Thus, representing the actual 3-D dynamics in a bubble column is still a challenging problem and only practical in lab-scale columns. There are several reported studies on bubble size with different direction of flow: up-flow with gas distributors at the bottom of the bubble column (Akita and Yoshida, 1973; Parthasarathy and Ahmed, 1996), down-flow with gas

distributors at the bottom of the bubble column (Lu et al., 1996; Mandal et al., 2005) and down-flow with gas distributors at the top of the bubble column (Alenezi et al., 2010a; Boyes et al., 1991; Ochuma et al., 2007c; Winterbottom et al., 1995). Bubble size distributions vary along the distance from the gas distributor in the bubble column and with the different kinds of gas dispersion methods used. The evaluation of bubble size distributions has lead to the use and development of new models describing breakage and coalescence processes and the forces acting on bubbles (Colella et al., 1999).

Studies investigating the effect of superficial gas velocity on bubble size suggest that an increase in superficial gas velocity will lead to an increase in bubble size until a maximum bubble size is achieved at a certain superficial gas velocity (Fukuma et al., 1987; Li & Prakash, 2000; Saxena et al., 1990a). Larger bubble size was found to be concentrated in the column centre and a smaller size near the column walls. The importance of bubble size was found to highly affect the gas holdup values; smaller bubble size enhanced the gas holdup values more than larger bubble sizes (Li & Prakash, 2000). Studies have also shown an increase in superficial gas velocity will lead to an increase in rise velocity of large bubble size, whereas a decrease in rise velocity of smaller bubble size was observed (Prakash et al., 2001; Schumpe & Grund, 1986). Also, studies have reported that bubble size was increased with increasing liquid surface tension and liquid viscosity (Li and Prakash, 1997). Other researchers have reported that an increase in pressure or temperature resulted in a decrease in bubble size (Luo et al., 1999a; Schafer et al., 2002). Also, it was found that as foaming liquid concentrations increased, bubble size decreased (Veera et al., 2004). The impact of solids and solid concentration has been studied by many researchers; solids in bubble column reactors led to larger bubble sizes due to the increase in slurry concentration (Li & Prakash, 2000; Luo et al., 1999a).

2.4.2.3 Gas Holdup

Gas holdup (ε_g) is a dimensionless parameter defined as the gas volume fraction in a gas-liquid dispersion system (Deckwer, 1992). Gas holdup is considered to be one of the most important design parameters in bubble column reactors and affects all other design parameters (Li & Prakash, 2000; Luo et al., 1999a; Shah et al., 1982b). Gas holdup is used in the determination of residence times and interfacial area, which leads to the assessment of the mass transfer rate. Gas holdup can be estimated using different techniques such as volume expansion, as well as tomographic, hydrostatic pressure, ultrasonic, fibre optic or conductivity probes (Jin et al., 2007; Widyanto et al., 2006). Many factors affect gas holdup profiles in bubble column reactors, including superficial gas velocity and the physical properties of the system. Also, the liquid recirculation rate plays an important role in mass and heat transfer studies (Wu et al., 2001). Extensive studies of gas holdup correlations for bubble column are reported in the literature, the most studied is O_2/H_2O (Boyes et al., 1995b; Idogawa et al., 1986; Kemoun et al., 2001; Ochuma et al., 2007a; Therning and Rasmuson, 2001).

Superficial gas velocity, which can be defined as the gas volumetric flow rate divided by the cross sectional area of the column, has the highest influence on the gas holdup profiles (Shah et al., 1982b). It was found that gas holdup increases as the superficial gas velocity increases (Hyndman et al., 1997; Kara et al., 1982; Prakash et al., 2001). The physical properties of liquids used in bubble column reactors can affect bubble dynamics as discussed earlier in section 2.4.2.2. Higher liquid viscosity results in lower gas holdup due to an increase in the rise velocity of larger bubbles, while adding surfactants, electrolytes and other impurities led to an increase in gas holdup values (Bach and Pilhofer, 1977; Hikita et al., 1980; Li & Prakash, 1997; Sada et al., 1984).

A number of researchers conclude an increase in solid concentration or particle size leads to lower gas holdup (Koide et al., 1984; Li & Prakash, 2000; Sada et al., 1984). One study suggested that in slurry bubble column reactors, solid loading will not affect gas holdup at <5 vol. % and thus the reactors will still behave as solid-free bubble column reactors (Sada et al., 1984). Another study concludes that at high gas velocities (>0.1– 0.2 m s^{-1}), there will be a strong effect on gas holdup even at low solids loading in bubble column reactors (Kara et al., 1982).

The effect of pressure on gas holdup profiles has been investigated by many researchers. Studies show that as the pressure increases the gas holdup also increases (Luo et al., 1999a; Oyevaar et al., 1991; Therning & Rasmuson, 2001; Wilkinson et al., 1992). Another important operating condition parameter is temperature. There is disagreement in the literature about the effect of temperature on gas holdup profiles. One study reported that as the temperature increased the gas holdup was slightly decreased until reaching a constant value even with further increases in the temperature; this study was conducted in a small column diameter and the authors state that the temperature at larger diameters had no affect on gas holdup profiles (Deckwer et al., 1980). Another study concluded temperature only affected gas holdup in two-phase flow (Saxena et al., 1990a). Some studies have shown correlations with gas holdup at high elevated temperatures (Wilkinson and Vandierendonck, 1990; Zou et al., 1988).

Physical properties of bubble column reactors such as column diameter, column height and sparger type can affect gas holdup and have been extensively investigated. Some workers have reported that column diameter (>0.1– 0.15 m) has no effect on gas holdup profiles; this can be attributed to the wall effects (Deckwer et al., 1980; Shah et al., 1982b). Also, the effect of column height (>1–3 m) is negligible on gas holdup profiles where the aspect ratio of column height to diameter is larger than 5 (Luo et al., 1999b). Krishna et al, state that the gas holdup

decreases with an increase in the column diameter. The gas sparger can alter the bubble characteristics by changing bubble size, thus also affecting gas holdup profiles; smaller bubble sizes lead to higher gas holdup values (Bouaifi et al., 2001). The influence of sparger type will highly affect the gas holdup profiles (Luo et al., 1999a; Schumpe & Grund, 1986).

2.4.2.4 Interfacial Area

Gas-liquid interfacial area (a) is an important design parameter in bubble column reactors, a component of the volumetric mass transfer coefficient $k_L a$, used in the assessment of mass transfer rate (Matsuura and Fan, 1984; Shah et al., 1982a). Interfacial area can be affected by many factors such as bubble column geometry, operating conditions and the physical properties of the liquid phase used. Interfacial area can be calculated by physical or chemical methods. Calculation based on physical methods relates to the gas holdup and the Sauter mean bubble diameter (d_s, mean surface to volume diameter) and is described by Equation 2-1 (Patel et al., 1989).

$$a = \frac{6\,\varepsilon g}{d_s} \qquad 2\text{-}1$$

Equation 2.1 is based on the following assumptions:

- The spherical bubbles are perfect and have uniform size. This is an oversimplification especially with a high turbulent system, and is considered a rough assumption.
- The bubble matrix packs in a body-centred cubic arrangement.
- The absorption process is at steady state.

The chemical method of interfacial area estimation involves sulphite oxidation and CO_2 absorption into an alkali solution such as NaOH. Variation of area estimates between the physical and chemical methods can be more than 100 % (Schumpe and Deckwer, 1980).

An investigation of the effect of high pressure on interfacial area gave a similar result as the behaviour of gas holdup profiles: an increase in pressure up to 8 MPa in bubble column reactors led to an increase in both interfacial area and gas holdup, which was attributed to the change in regime transition as a result of superficial gas velocities (Oyevaar et al., 1991). Also, Oyevaar et al. found that the bubble rise velocities were lower due to the build-up of smaller bubbles under higher pressure. Another study reported that smaller the bubble sizes led to higher interfacial areas which enhanced the mass transfer rate (Han and Al-Dahhan, 2007).

2.4.3 Mass Transfer Characteristics

Mass transfer rate is considered to be one of the important factors in bubble column reactor design and scale-up and has been studied by many researchers due to its role in the chemical reactions taking place in a reactor (Deckwer & Schumpe, 1993). Mass transfer is mainly controlled by the volumetric mass transfer coefficient (k_La) with the assumption of a negligible effect of gas phase resistance on the mass transfer rate. The coefficient k_La can be manipulated by varying the gas-liquid interfacial area (Matsuura & Fan, 1984). The literature reports several other factors that affect k_La in bubble columns (Akita & Yoshida, 1973; Chilekar et al., 2010; Han & Al-Dahhan, 2007; Ozturk et al., 1987; Schumpe & Grund, 1986; Shah et al., 1982a; Sharma and Danckwer, 1970) and are discussed below.

Several studies have investigated the effects of operational parameters on the overall mass transfer rate and its impact on the performance of bubble column reactors. Flow regime can be highly affected by the superficial gas velocity as described earlier in Section 2.4.2.1. The volumetric mass transfer coefficient increased with an increase in superficial gas velocity, the same behaviour in gas holdup profiles (Behkish et al., 2002; Verma and Rai, 2003). Higher liquid recirculation rates led the bubble column reactor to be operated in a churn-turbulent regime, which was found to enhance the mass transfer rate (Deswart et al., 1996; Joshi and Sharma, 1979). Elevated pressure is another important factor, in particular in large-scale industrial applications, which normally operate at high pressure. The volumetric mass transfer coefficient was enhanced by increasing the working pressure, which can be attributed to higher values of gas holdup and smaller bubble size, leading to better values for the gas-liquid interfacial area (Han & Al-Dahhan, 2007; Kojima et al., 1997). Some studies reported that an increase in pressure will only enhance the mass transfer coefficient at a higher superficial gas velocity (Letzel et al., 1999; Wilkinson et al., 1994). Also, the presence of electrolytes in the bubble column was found to increase mass transfer processes due to smaller bubble size formation leading to increases in both the gas-liquid interfacial area and gas holdup (Baz-RodrÕguez et al., 2014; Muller and Davidson, 1995). The effect of higher liquid viscosity gives lowered values of volumetric mass transfer coefficients and these can be attributed to the lower gas-liquid interfacial area (Behkish et al., 2002; Fukuma et al., 1987; Kang et al., 1999). Also, increasing solids concentration was found to lower volumetric mass transfer coefficients due to the formation of smaller bubble size (Behkish et al., 2002; Koide et al., 1984; Vandu and Krishna, 2004).

2.4.4 Heat Transfer Characteristics

Thermal control can highly affect chemical reactions in bubble column reactors, especially factors such as selectivity and yield, which are important at industrial scales (Deckwer, 1992). In general, heat-control equipment such as coils or jackets in bubble column reactors is designed to minimize the interference with flow regimes, and depends on the process needed, whether heating (endothermic reactions) or cooling (exothermic reactions) (Kawase and Mooyoung, 1987; Sivaiah and Majumder, 2013). It was reported that bubble column reactors can achieve heat transfer 100 times faster than single phase flow (Deckwer, 1992). Bubble-reactor heat transfer coefficient studies have mainly studied the bed-to-wall heat transfer coefficient and immersed object-to-bed heat transfer coefficient (Chiu and Ziegler, 1985; Deckwer, 1980; Hikita et al., 1981; Kato et al., 1980; Li & Prakash, 1997; Saxena et al., 1992).

Heat transfer in bubble column reactors can be affected by operating conditions and geometry. Many researchers claim that superficial gas velocity, which is a critical factor in flow regimes, is the main factor affecting heat transfer rate in bubble columns (Jhawar and Prakash, 2007). An increase in superficial gas velocity leads to an increase in heat transfer rate, which can be attributed the turbulent flow developed in the bubble column; the heat transfer rate continues to increase until a full churn-turbulent flow takes place ($Ug \approx 0.15$ m s^{-1}), then the increase in heat transfer rate beyond that stage is slower as superficial gas velocity is increased (Jhawar & Prakash, 2007; Saxena and Patel, 1990; Wu et al., 2007). Liquid-phase properties such as viscosity were found to have the reverse effect on heat transfer rate; an increase in liquid viscosity led to a decrease in the heat transfer rate regardless of the fluid velocity and particle size, due to a decrease in turbulent flow (Chen et al., 2003; Kim et al., 1986; Kumar and Fan, 1994). Particle size and concentration is another important factor, especially in three-phase and

fluidized bed bubble column reactors (Deckwer et al., 1980; Li & Prakash, 2000; Saxena et al., 1990a). The heat transfer coefficient was found to increase with increasing particle size at low gas velocities (<5 cm s^{-1}) but beyond this velocity, particle sizes larger than 3.0 mm had no affect on heat transfer coefficient, which was attributed to the increase in bubble sizes and rise velocities (Deckwer et al., 1980). Some studies found, however, a weak dependence between the particle size and heat transfer coefficient (Li et al., 2003; Saxena et al., 1990b; Saxena et al., 1991b). The effects of elevated pressure on the heat transfer coefficient in bubble column reactors also shows conflicting results. Some researchers have found that heat transfer coefficient increases with increasing working pressure (Cho et al., 2002; Lin and Fan, 1999); while other researchers found an increase in working pressure led to a decrease in the heat transfer coefficient, attributable to a decrease in bubble sizes and liquid viscosity (Wu et al., 2007; Yang et al., 2000). Another study found no relation between higher working pressure and the heat transfer coefficient (Holcombe et al., 1983).

The heat transfer coefficient can be altered by the axial and radial location positions of the heat transfer probe in the bubble column reactor (Jhawar & Prakash, 2007; Saxena et al., 1992; Wu et al., 2007). The differences in heat transfer coefficient measurements can be estimated by the distance from the gas distributor in the axial position, while the heat transfer coefficient measurement in the radial position can be estimated by bubble populations (Saxena et al., 1990a). The heat transfer coefficient in the axial direction increases with the axial distance from the gas distributor until a fully bulk zone develops, and then the effect becomes insignificant (Li and Prakash, 2002; Saxena et al., 1992). In the radial direction, the maximum values of heat transfer coefficient can be found in the column centre and the lowest near the column wall (Li & Prakash, 1997; Li and Prakash, 2001; Wu et al., 2007). Also, in the radial direction, particle size and

column diameter do not affect the wall-region heat transfer coefficient. In fact, it was pointed out that the heat transfer coefficient is affected by slurry concentrations up to 30% vol, and beyond this concentration the effect is insignificant (Jhawar & Prakash, 2011; Li & Prakash, 2001).

The effect of column diameter on the heat transfer coefficient has also been studied; larger column diameters lead to an increase in heat transfer coefficient, due to the effect of the wall on the mixing process in bubble column reactors. It was found that beyond 0.3 m, the wall effect is negligible (Chen et al., 2003; Jhawar & Prakash, 2011; Saxena et al., 1990a). Also, increasing bed temperature was found to increase the heat transfer coefficient, which can be attributed to a reduction in liquid viscosity leading to an increase in flow turbulence (Saxena et al., 1991a).

2.4.5 Backmixing

Liquid backmixing is an important parameter for prediction of gas holdup. Backmixing is dependent on the structure of the chemical reaction network, the corresponding reaction rate parameters and the desired degree of chemical conversion. Liquid backmixing can be described in terms of axial dispersion coefficient (E). Fick's law of diffusion Equation 2-2 describes backmixing in axial dispersion as reported by (Levenspi, 1972).

$$\frac{\partial C}{\partial t} = E\frac{\partial^2 C}{\partial x^2} \quad \text{2-2}$$

where:

C = tracer concentration

t = time

x = axial coordinate

E = longitudinal or axial dispersion coefficient

Shah et al. (1978) state that axial dispersion coefficient (E) can be expressed in terms of Peclet Number (Pe) given in Equation 2-3, which can be used to differentiate between complete backmixing or dispersion (Pe → 0) and negligible backmixing plug flow (Pe → ∞). The L_c of the bubble column is equivalent to the column diameter, and in fixed-bed reactors the packing diameter (Sulidis, 1995):

$$Pe = \frac{uL_c}{E} \quad 2\text{-}3$$

where:

u = superficial velocity

L_c = characteristic length

Liquid backmixing in gas-liquid contactor is commonly obtained by residence time measurements (RTD), which can be determined by a tracer as a function of time from the injector to the respective phase. The tracer selection should be include the following requirements (Shah et al., 1978);

- The tracer must be miscible with similar physical properties to the fluid used.
- The tracer and the equipment used for tracer detection should be selected with minimal disturbance to the fluid phase used.
- To avoid a complicated RTD analysis, a non-reactive tracer should be selected.

2.5 Downflow Gas Contactor Reactor (DGCR)

2.5.1 Introduction

The Downflow Gas Contactor Reactor (DGCR) was developed from the Co-current Down flow Contactor Reactor (CDC). DGC reactors can be used as a multi-phase contacting (liquid, gas and solid) phase. DGC reactors consist of a single column made of glass or stainless steel as described by Boyes (Boyes et al., 1995a).They are operated in batch mode with recycle loop, and as slurry and fixed-bed catalytic reactors. It was originally developed by Boyes and Ellis (Boyes and Ellis, 1976); the overall performance and selectivity of the DGC are enhanced and improved compared to CSTR and other reactors (Akosman et al., 2004; Boyes et al., 1992a; Dursun and Akosman, 2006; Fishwick et al., 2007; Kulkarni et al., 2005). In addition, contact between phases can be employed for absorption, stripping to have a high conversion of petroleum feed stocks, and can also be used as an effective wastewater treatment for selected contaminates (Ochuma et al., 2007a; Ochuma et al., 2007b; Ochuma et al., 2007c; Winterbottom et al., 1997a). Vegetable oil hydrogenation of rapeseed oil and soybean oil was significantly improved using the DGC (Alenezi et al., 2009; Fishwick et al., 2007; Winterbottom et al., 1999; Winterbottom et al., 2000).

2.5.2 Hydrodynamic Characteristics

2.5.2.1 Flow Characteristics

The flow regime in DGC reactors has been studied by many researchers. Two distinct regions were observed using a 1m column, the first region (0.35 m) was described as a turbulent flow with average bubble size 1.5 mm in diameter, the second region (0.65 m) as a uniform bubble flow regime with average bubble size 3.0 mm in diameter for a CO_2/H_2O system and average bubble size 5.0 mm in diameter for an O_2/H_2O system (Evinc, 1982). Lu reported that four regions were observed using an O_2/H_2O system with a conical base adjustment: the first region was characterised by a highly turbulent region with continued redispersion of rising bubbles into small bubbles; the second region was less turbulent with an average bubble size of 5.0 mm in diameter; the third region was observed at the junction between the cylindrical and conical sections, where a swarm movement of small rising bubbles was observed; the last region was one of small bubbles in the conical section (Lu, 1988a). Another study using a packed-bed downflow gas column reactor observed two distinct regions, the unpacked and packed section, the bubble dispersion extending to the packed bed section (Khan, 1995). The effect on fluid properties was studied using different combinations of two- and three-phase systems. Two distinct sections were observed using O_2/H_2O and H_2/H_2O systems, and three distinct sections were observed using hydrogen/organic liquid and hydrogen/organic slurry systems (Zhang, 1997).

2.5.2.2 Bubble Dynamics

In DGC reactors, the bubble size can be determined by visual analysis in the vicinity of the column wall. Due to the good mixing and efficient dispersion, the bubble dispersion matrix is assumed to be consistently stable and uniform due to the larger bubbles being re-dispersed in the top of the column, controlling any disturbance in the balance of the forces acting on the bubbles such as buoyancy and drag forces (Alenezi, 2009; Ochuma, 2007; Zhang, 1997).

Many workers have found an increase in bubble size as a result of an increase in superficial gas velocity (Dursun & Akosman, 2006; Khan, 1995; Tilston, 1990). The effect of liquid properties such as viscosity and surface tension was demonstrated using different kind of solvents (pure water, glycerol and aqueous propanol) with oxygen; it was found that the average bubble size was in the range of 4–5 mm in coalescing systems and 0.5 mm in non-coalescing systems (Lu, 1988a). Also, the effect of adding electrolytes to the liquid led to an increase in the bubble size (Tilston, 1990).

2.5.2.3 Gas Hold-up and Interfacial Area

Gas hold-up (ε_g) is directly related to the interfacial area available. Many factors can influence gas hold-up values such as, superficial gas velocity, superficial liquid velocity, liquid physical properties and system geometry. Methods used in the estimation of gas hold-up values are mainly the expansion method, static shutdown method and the dead-leg method (Lu, 1988a; Sarmento, 1995; Tilston, 1990). A study observed the possibility of achieving gas hold-up values in a poor coalescent system comparable to those obtained with a good coalescent system by controlling the liquid and gas velocities. Gas hold-up values increased with an increase in the

superficial gas velocity and dispersion height but decreased with an increase of the liquid flow rate (Lu, 1988a). Gas hold-up values up to 50% were achieved in a trickle bed reactor (Sarmento, 1995). Lu observed the maximum values of gas holdup, where up to 60%, was achieved using an O_2/H_2O system (Lu, 1988a). In agreement with previous results, gas holdup was found to increase with increasing superficial gas velocity in air-aqueous glycerol systems (Akosman et al., 2004; Dursun & Akosman, 2006). Also, the addition of fines led to an increase in gas holdup in the trickle bed reactor, which was attributed to a reduction in stagnant zones and increase in pressure drop (Kulkarni et al., 2005). Varying the jet nozzle diameter was found to affect the gas hold-up values; an increase in jet nozzle diameter led to a decrease in gas hold-up values due to the formation of larger bubble sizes (Dursun & Akosman, 2006).

High values of interfacial area are typical of DGC reactors, usually in the range of 1000–6000 $m^2\ m^{-3}$, which can be attributed to the maximum residence time that can be achieved as a result of the near-suspension state of bubbles (Khan, 1995; Kulkarni et al., 2005; Lu, 1988a; Sarmento, 1995; Zhang, 1997). It was reported that the performance of the DGC compared to upflow bubble columns can be up to a two-fold increase in interfacial area and more stability at the same operating conditions (Kulkarni et al., 2005). Moreover, the interfacial area values in unpacked mode are larger than packed mode due to an increase in bubble size in the packed section (Sarmento, 1995).

2.5.3 Mass Transfer Characteristics

Mass transfer characteristics of DGC reactors have been studied by many researchers, due to its role in the chemical reactions taking place in the bubble column reactor (Akosman et al., 2004; Alenezi, 2009; Dursun & Akosman, 2006; Evinc, 1982; Khan, 1995; Lu, 1988a; Sarmento,

1995; Sulidis, 1995; Tilston, 1990; Zhang, 1997). The mass transfer coefficient (k_La) has been evaluated using a gas adsorption method into liquid (Boyes et al., 1992a; Boyes et al., 1995a; Lu, 1988a; Lu et al., 1996). A swirl flow introduced into DGC reactors increased the rate of mass transfer by 4 to 5 times; it was found that k_La values in the upper section increased with increasing superficial gas velocity, but the effect in the lower section was independent of the superficial gas velocity, which could be attributed to the difference in the bubble size in different sections along the DGC column height (Khan, 1995; Tilston, 1990). Therefore, k_La values decrease with increasing column height (Evinc, 1982). Lu found similar results for the relation of k_La values with dispersion height due the high turbulence and interfacial area in the upper section of The DGC (Lu, 1988a). The effect of packing design on k_La values was demonstrated by Sarmento (1995), who found that high voidage packings (Pall rings) gave better k_La values than low voidage packings (Raschig rings) due to the effect of rings shape on the balance between coalescence and break up process in DGC reactor. The k_La values with unpacking mode was higher than packing mode in DGC reactors (Sulidis, 1995). The resistance to the k_La parameter was negligible within DGC reactor, which indicated high values of mass transfer rate are occurring (Sharma, 1997).

2.5.4 Previous Studies of DGC Reactors

DGC reactors have been extensively studied at the University of Birmingham to investigate their hydrodynamic and mass transfer characteristics and to evaluate their performance as an effective chemical reactor in upgrading biodiesel and wastewater treatment processes. Examples of this research are summarized in the following table.

Table 2-3 Previous studies of DGC reactors at the University of Birmingham

Type of study	Reference
1. Mass transfer characteristics using the absorption of gases in a co-current downflow column.	(Evinc, 1982)
2. Mass transfer characteristics of a novel co-current downflow bubble column contactor for use as a three phase reactor.	(Lu, 1988a)
3. Triglyceride hydrogenation in a co-current downflow contactor using rapeseed oil.	(Raymahasay, 1989)
4. Mass transfer characteristics using the development of a swirlflow in DGCR.	(Tilston, 1990)
5. Mass transfer characteristics development of packed-bed co-current downflow.	(Chughtai, 1993)
6. Hydrodynamics and mass transfer characteristics of co-current downflow contactor operation in a fixed bed mode.	(Sarmento, 1995)
7. Photocatalytic oxidation of phenol in wastewater.	(Sulidis, 1995)
8. Selective hydrogenation of α,β-unsaturated aldehydes towards clean synthesis over noble metal catalysts in mass transfer efficient three-phase reactors.	(Zhang, 1997)
9. Selective hydrogenation of multifunctional organic reactants in three phase reactor	(Sharma, 1997)

Table 2-4 (continued)

Type of study	Reference
10. Photo - oxidation of pollutants in wastewater.	(Ochuma, 2007)
11. Biodiesel produced from different methods.	(Alenezi, 2009)

CHAPTER 3

3 EQUIPMENT AND METHODS

Chapter Overview

In this chapter, the experimental apparatus, materials and methods are presented. Section 3.1 describes the pilot–scale Down-flow Gas Contactor Reactor (DGCR) and the Solid Phase Extraction (SPE) experimental set-up with a detailed equipment list used in appendices 9.11. Some of the analytical instruments are necessary safety requirements for all people involved in the laboratories due to the high toxicity of the chemicals used. The liquid chromatography instrumentation experimental setup using HPLC-DAD and LC-TOF-MS are described in section 3.2. This is followed by gases, solvents and chemical regents used in section 3.3. The mass transfer studies described in sections 3.4 concerns the start-up and shut-down procedures, operating conditions and the design parameters for the DGCR. Degradation studies described in section 3.5 have the same procedure for the start-up and shut-down steps as the mass transfer studies with some further safety precautions required due to the high toxicity of the chemicals used. Section 3.6 illustrates the general analytical procedures used throughout in order to have satisfactory results at the ng L^{-1} level. Instrumental calibration is provided in section 3.7.

3.1 Experimental Apparatus

3.1.1 Downflow Gas Contactor Reactor (DGCR) Setup

The pilot–scale Downflow Gas Contactor Reactor (DGCR) system used in this study for screening its performance is a valuable and cost-effective waste-water treatment process. Its performance was screened for different water matrices dosed with selected female oestrogens. A photograph of the DGCR is shown in Figure 3.1, with a schematic diagram illustrated in Figure 3.2. The reactor consists of two different operating regions and both are made from standard QVF glassware. The top section was 0.5 m in length and 0.05 m i.d. and was used for gas/liquid mixing in the high turbulent region. The bottom section was 1.0 m in length and 0.10 m i.d. and was used for UV photolysis. Both sections were connected by a 0.10 m / 0.05 m i.d. QVF glassware reducer. The enlarged base was to prevent bubbles carrying over the flow of the liquid. All the glassware was sealed with standard fibre gaskets and all the piping systems were made from stainless steel. At each end of the reactor, a stainless steel plate was fitted and sealed with fibre gaskets. The stainless steel plate in the top section had a hole connected to the 12 mm i.d. inlet liquid line from the top side and was threaded from the bottom side allowing orifice units to be changed with different sizes (1-5 mm) as shown in Figure 3.3. This was necessary to study the effect of different liquid jet velocities on the mass transfer and degradation studies. A combined 6 mm i.d. pipeline, also was connected to the stainless steel plate in the top section from the top side, this included a vent valve and a pressure gauge to measure the column pressure. A thermocouple was also connected to the stainless steel plate in the top section from the top side to measure the column temperature. A T-piece was fitted to the 12 mm i.d. pipe in the top section to concurrently introduce the gas from the gas cylinder source to the fully flooded column. A detailed list of the DGCR equipment can be found in appendices 9.11.

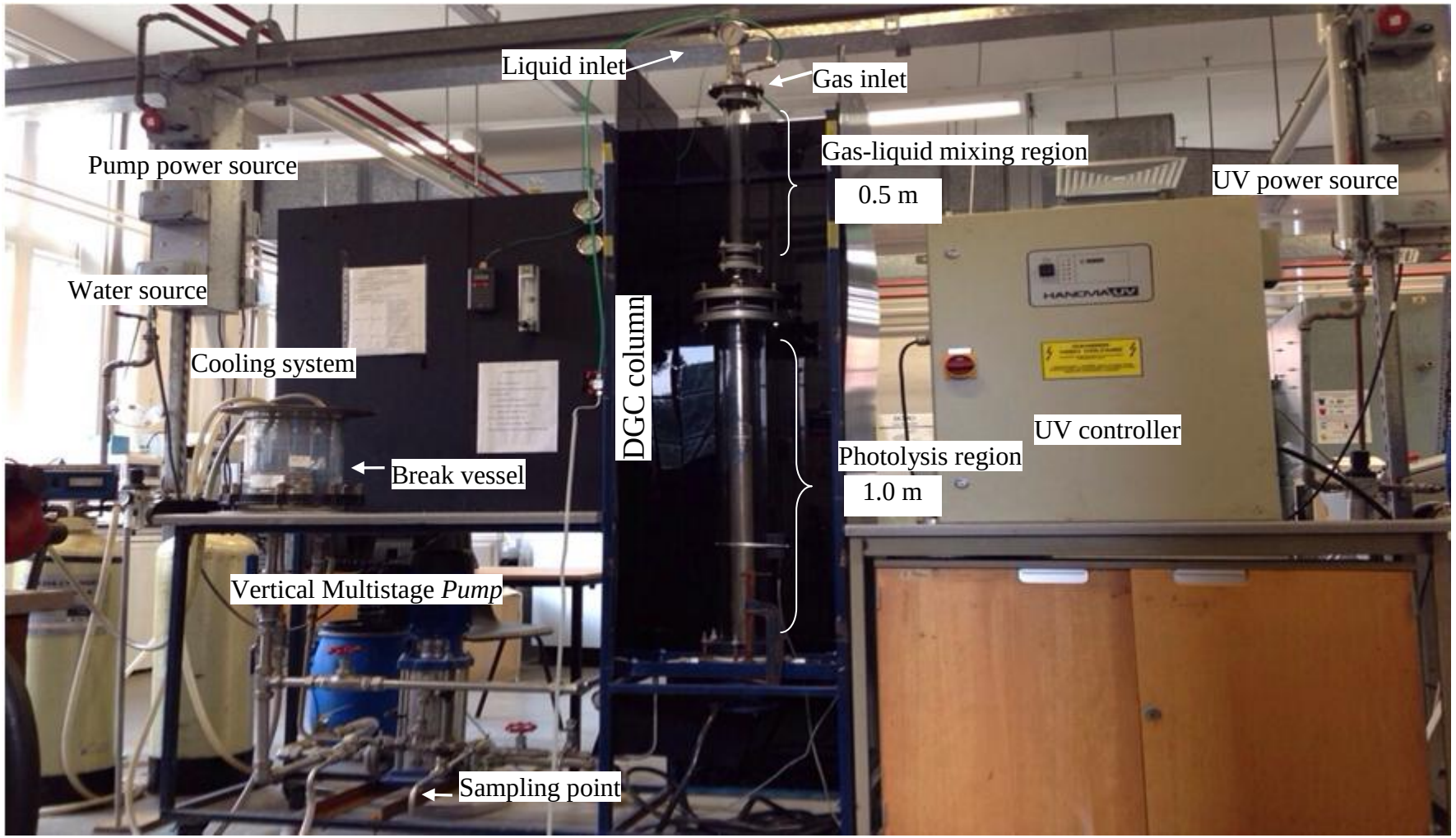

Figure 3-1 Image showing the Downflow Gas Contactor Reactor (DGCR)

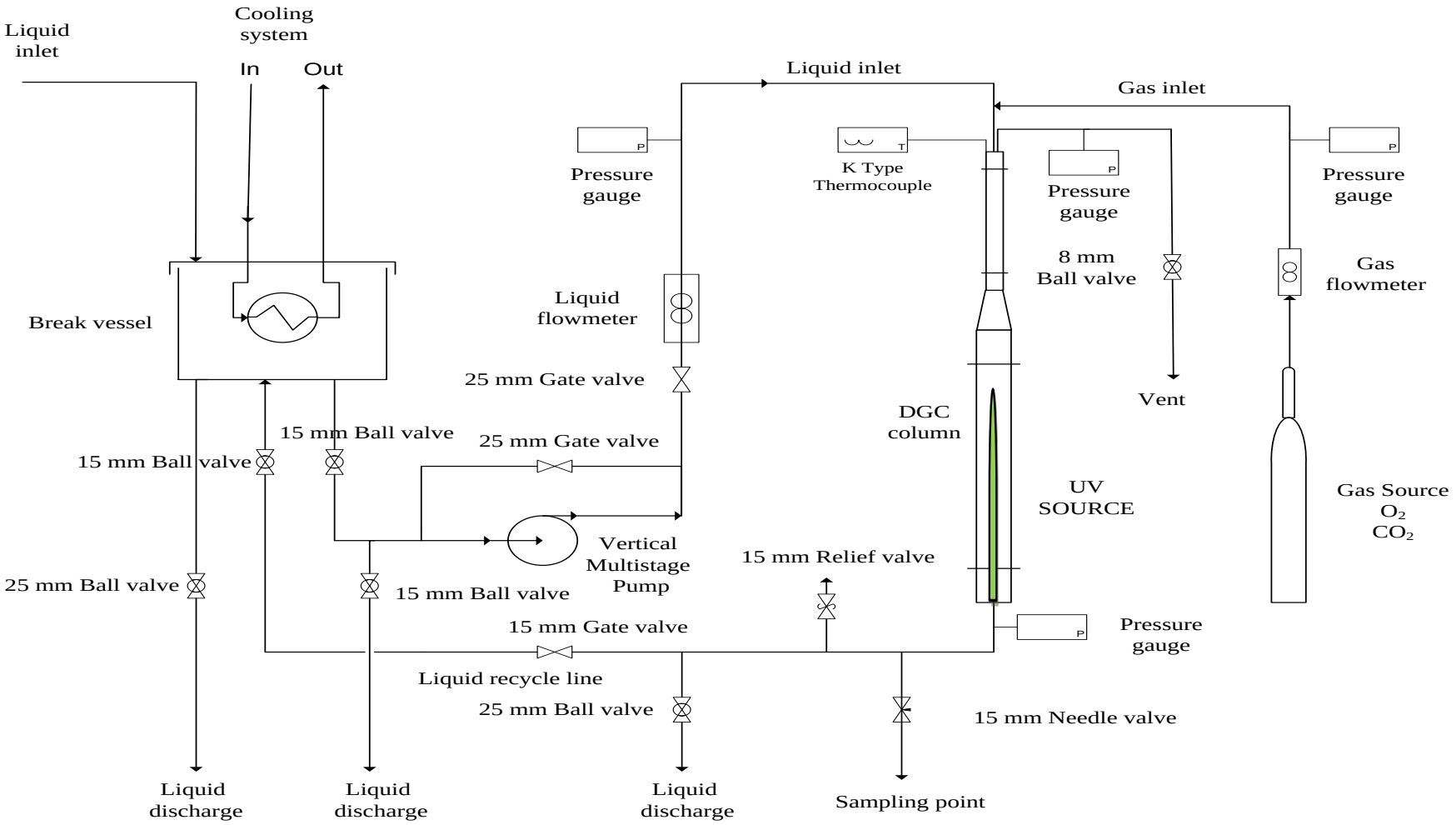

Figure 3-2 Schematic diagram of experimental apparatus used for the Downflow Gas Contactor Reactor (DGCR)

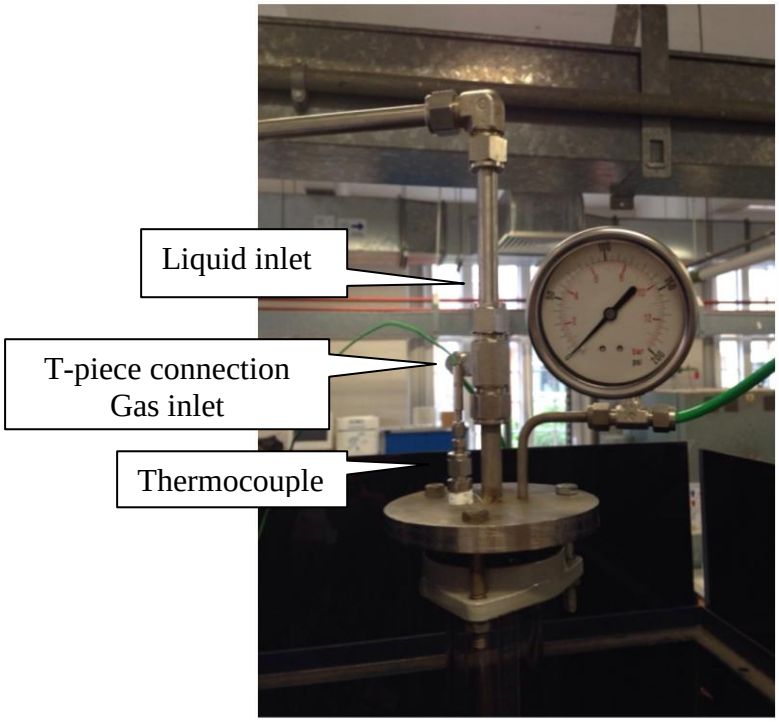

Figure 3-3 Image showing the inlet part located in centre of circular top plate of the Downflow Gas Contactor Reactor (DGCR)

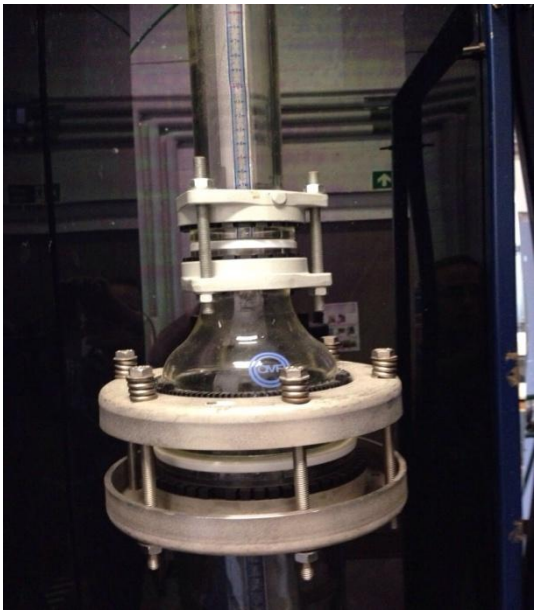

Figure 3-4 QVF glassware reducer

Figure 3-5 Glass reservoir (Break vessel): made from QVF glassware (0.015 – 0.018) m^3

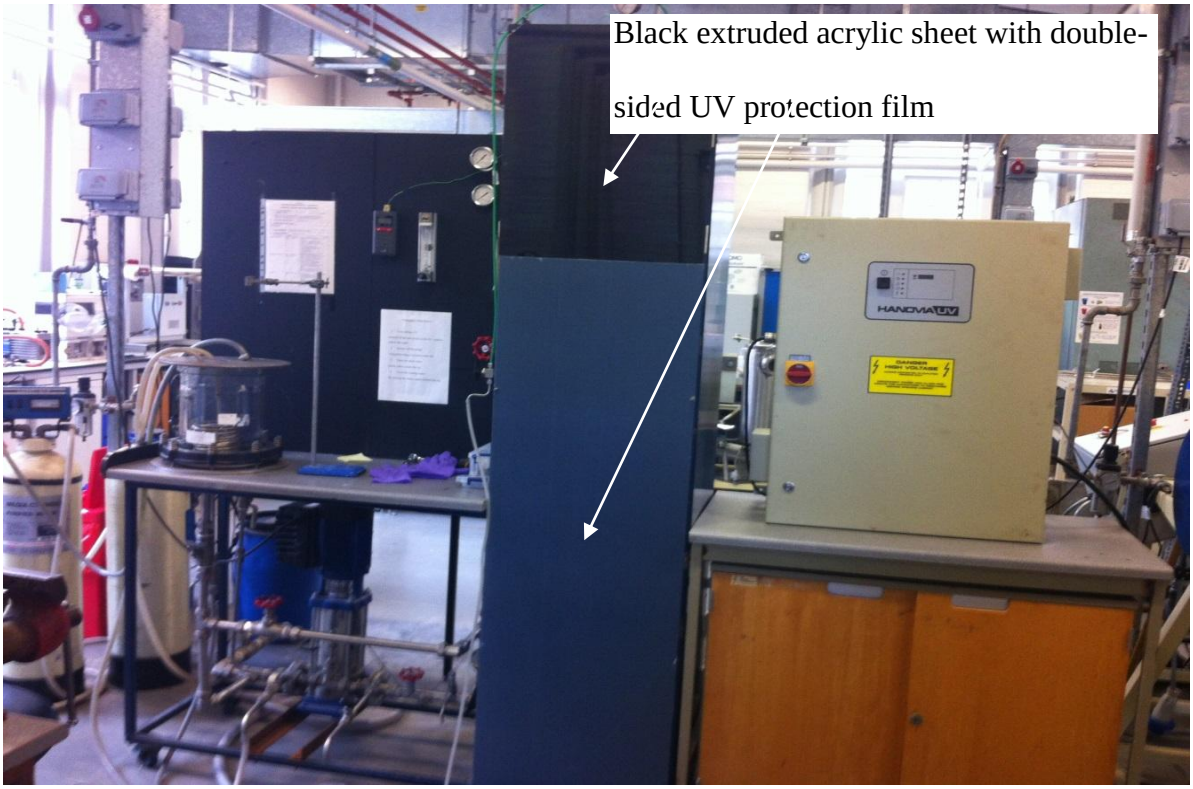

Figure 3-6 Black extruded acrylic sheet with double-sided UV protection window film

3.1.2 Analytical Instruments and Equipment

The following is a list and brief description of analytical instruments used.

- Waysafe 3 glove box for balances and general protection with a HEPA filter (99.999% efficient at 0.3 micron) as shown in Figure 3.7 was used for weighing hormones supplied by Solotec Scientific, UK.
- Analytical balance (accuracy 0.1 mg) supplied by Ohaus Adventurer Balances.
- Microbalance, MT-5, (accuracy 0.0008 mg) supplied by Mettler Toledo, UK
- SevenMulti pH meter, pH-range -2.000 to 19.999, accuracy ± 0.002 supplied by Mettler Toledo, UK and as shown in Figure 3.8.
- SG6 – SevenGo pro dissolved oxygen meter, accuracy ± 0.5% supplied by Mettler Toledo, UK as shown in Figure 3.9.

- Respirator 3M 7000 series full face mask supplied by Fisher Scientific, UK.
- Respirator 3M Particulate filters, 2000 series supplied by Fisher Scientific, UK.
- N-DEX gloves, class I medical with the specifications of EU Directive 89/686/EEC and the standard EN 374 supplied by Fisher Scientific, UK.
- Magnetic stirrer mini 1L supplied by Fisher Scientific, UK.
- Grant W28 Water bath (type ZA, SN: 039538008) supplied by Grant Instruments (Cambridge, UK) Ltd.
- Easy-Read thermometer (−10°C - +110°C, accuracy ±1.0°C, 1.5°C > 105°C) supplied by VWR International Ltd, UK.
- Magnetic stir bar octagonal PTFE encased 64mm x 9.5mm, Fisherbrand.
- Discovery comfort variable volume single channel pipette, 100-1000 ul HTL (Model HDM027) supplied by Appleton Woods Limited, UK.
- Discovery comfort variable volume single channel pipette, 20-200 ul (Model HDM025) supplied by Appleton Woods Limited, UK.
- Discovery comfort variable volume single channel pipette, 2-20 ul (Model HDM022) supplied by Appleton Woods Limited, UK.
- Dry bath / block heater supplied by Fisher Scientific, UK.
- Monmouth Scientific Circulaire 1400 non-ducted fume and particulate extraction cabinet supplied by Monmouth Scientific, UK.

Figure 3-7 Waysafe 3 glove box and Ohaus Adventurer analytical balance.

Figure 3-8 Mettler Toledo SevenMulti pH meter and Fisherbrand magnetic stirrer.

Figure 3-9 Mettler Toledo SG6 – SevenGo pro dissolved oxygen meter.

3.1.3 Solid Phase Extraction (SPE)

Sample preparation is an essential enrichment and purification step. It can significantly reduce interferences of sample matrices and increases the analytical performance, making the analytical results more accurate. The following items listed below can be seen in the SPE experimental set-up shown in Figure 3.10 and the SPE experimental set-up schematic diagram illustrated in Figure 3.11.

- Savant Instruments vacuum pump (Model VP 100 SN: 36057), Franklin electric motor
- Filter flask Buchner conical shape borosilicate glass with tubulature 5L Pyrex, (Fisher Scientific, UK).
- Narrow neck amber glass Winchester 1L bottles, (Fisher Scientific, UK).
- Pyrex measuring cylinders: $1x10^{-3}$ m^3 and $0.5x10^{-3}$ m^3, tolerance 5 mL, (Fisher Scientific, UK).
- Fisherbrand stopwatch with an ISO 17025 A2LA Traceable NIST cert battery included waterproof & shockproof, (Fisher Scientific, UK).
- Red Multi-Purpose Rubber Tubing 3/4" I.D x 1-1/2" o.d.
- Oasis HLB Glass Cartridge 5cc/200 mg LP, Waters (Hertfordshire, UK).
- Vacuum Manifold 20 port, Waters (Hertfordshire, UK).
- Rack, test tube 20 port, 16x100, Waters (Hertfordshire, UK).
- Teflon tubing, Waters (Hertfordshire, UK).
- Male/male Luer Fitting, Waters (Hertfordshire, UK).
- Adaptor, 5cc, Teflon, Waters (Hertfordshire, UK).
- Millex-GP, 0.22 µm, (Millipore, UK).
- Glass-fibre filters (GF/F, 0.7 µm pore size), Whatman (Whatman, UK).

– Certified screw top vial, 2 mL, amber, deactivated (silanized) supplied by Agilent Technologies, UK.

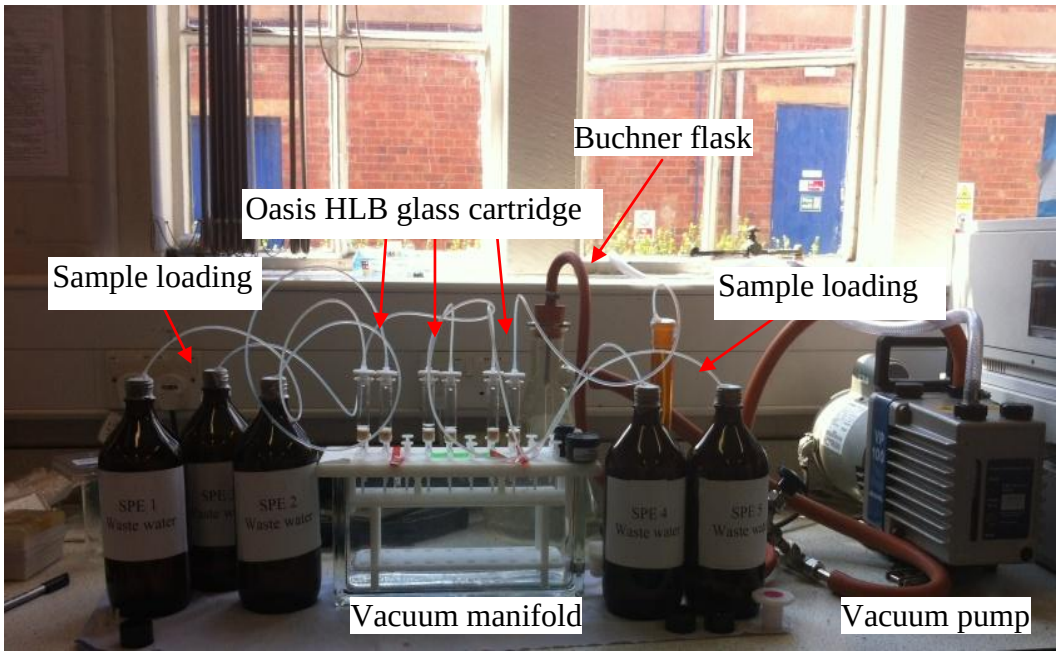

Figure 3-10 Image showing the SPE experimental set-up

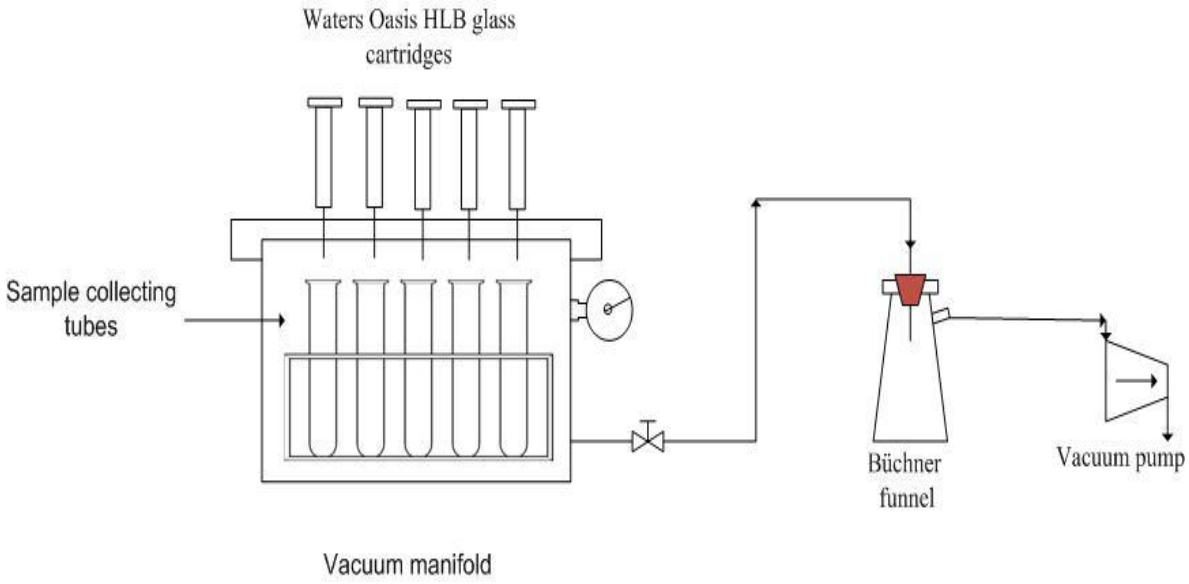

Figure 3-11 Schematic diagram of experimental set-up used for the SPE

3.2 Liquid Chromatography Instrumentation

Separations were performed using an Agilent HPLC system (Agilent Technologies, Germany). Agilent LC-MS Chemstation software was used to collect and analyse the data. Sample purity and identity confirmation were performed using Waters Micromass Time of Flight Mass Spectrometer (LC-TOF-MS) with Masslynx v4.1 software for collecting and analysing data using the facilities of the Chemistry Chromatography Laboratory in the University of Birmingham the following equipment were used:

- Agilent 1200 Series Vacuum Degasser (Model G1322A).
- Agilent 1200 Series Isocratic Pump (Model G1310A).
- Agilent 1100 Series Well-plate Sampler and Micro Well-plate Sampler (Model G1367A).
- Agilent 1200 Series Diode Array Detector (Model G1315D).
- Jones Chromatography Column Block Heater.
- Dell Dimension 5000 Series computer system with Agilent LC-MS Chemstation software.
- Kinetex 2.6 µm C18 100 Å, LC Column 75 x 4.6 mm was obtained from Phenomenex, UK.
- Security Guard ultra for column protection was obtained from Phenomenex, UK.

3.3 Experimental materials

3.3.1 Gases

The gases used are listed below in Table 3.1. The compressed air used in all experiments was supplied by the facilities of the School.

3.3.2 Solvents

The solvents used are listed below in Table 3.2. Distilled water used in all experiments was supplied by the facilities of the School. The deionised water used throughout the present study used the media cylinder purified water system was supplied by ELGA Process Water System, UK using tap water in G34 laboratory of the School and was connected directly to the DGCR.

3.3.3 Reagents

The chemical materials used are listed below in Table 3.3. All the chemicals used in the experiments were reagent grade or higher and were used as received, without any purification.

Table 3-1 A list of gases used.

Gases	Cas number	Purity	Supplier
Oxygen, O_2	7782-44-7	99.5%.	British Oxygen Company (BOC) UK
Nitrogen, N_2	7727-37-9	(Oxygen-Free), 99.9%.	British Oxygen Company (BOC) UK
Carbon Dioxide, CO_2	124-38-9	99.9%	British Oxygen Company (BOC) UK

Table 3-2 A list of solvents used.

Solvent	Cas number	Grade	Purity	Supplier
Acetonitrile	75-05-8	HPLC	≥ 99.9%	Sigma-Aldrich (Dorset, UK)
tert-Butyl methyl ether	1634-04-4	HPLC	≥ 99.8%	Sigma-Aldrich (Dorset, UK)
Water	7732-18-5	HPLC	-	Sigma-Aldrich (Dorset, UK)
Dichlorodimethylsilane	75-78-5	HPLC	≥ 99.5%	Sigma-Aldrich (Dorset, UK)
Methanol	67-56-1	HPLC	≥ 99.8%	Fisher Scientific, UK.
Toluene	108-88-3	HPLC	≥ 99.8%	Fisher Scientific, UK.

Table 3-3 A list of chemical reagents used.

Reagents	Cas number	Grade	Purity	Supplier
β-Estradiol, powder	50-28-2	AR	≥ 98%	Sigma-Aldrich (Dorset, UK)
α-Estradiol, powder	57-91-0	AR	≥ 98%	Sigma-Aldrich (Dorset, UK)
Estrone, powder	53-16-7	AR	≥ 99%	Sigma-Aldrich (Dorset, UK)
Progesterone, powder	57-83-0	AR	≥ 99%	Sigma-Aldrich (Dorset, UK)
Buffer solution pH 4 (phthalate)	-	-	-	Fisher Scientific, UK
Buffer solution pH 7 (phosphate)	-	-	-	Fisher Scientific, UK
Buffer solution pH 10 (borate)	-	-	-	Fisher Scientific, UK
Hydrogen peroxide solution	7722-84-1	ACS	30% (w/w)	Sigma-Aldrich (Dorset, UK)
Ammonium hydroxide solution	1336-21-6	ACS	28.0-30.0%	Sigma-Aldrich (Dorset, UK)
Sulfuric acid	7664-93-9	ACS	95.0-98.0%	Sigma-Aldrich (Dorset, UK)
Sodium hydroxide	1310-73-2	-	0.1 M NaOH	Sigma-Aldrich (Dorset, UK)

3.4 Mass transfer studies

3.4.1 Downflow Gas Contactor Reactor (DGCR)

All the mass transfer studies on the pilot scale DGCR (as shown in the schematic diagram illustrated in Figure 3.2), were conducted as batch modes with a recycle loop employing the absorption of oxygen into water as the model system. The effect of changing liquid flow rates, gas flow rates and different nozzle diameters on the overall performance of the DGCR were all examined.

3.4.1.1 Start-up Procedure for the DGCR

The following procedure was used for the DGCR mass transfer studies, the experimental apparatus listed throughout the current procedure can be found in schematic diagram of Figure 3.2:

1. The three ball valves (Liquid discharging lines) were fully closed.
2. The vent valve at the top section of the column was fully opened to allow the air inside the column to escape and the column achieves the condition of a fully flooded column.
3. The pump by-pass valve was fully opened.
4. The deionised water was fed to the DGCR. The water was prepared by a media cylinder purification system supplied by ELGA Process.
5. The liquid in the receiver was pumped into the DGCR unit through a Rotameter flow-meter into the top of the 50 mm diameter glass top section. The water flowed through the top section into the 100 mm diameter section.

6. The vent valve was closed when the fully flooded column was free from any air bubbles in the 50 mm top section.
7. A desired amount of water was continued to be added in the break vessel, while the water was kept circulating between the break vessel and the column until the desired total volume of water for the experimental work was attended. Normally the total volume in all experiments was 15 litres.
8. The DGCR was operated with a specific circulating rate up to 20 L min^{-1} by controlling the liquid flowmeter to give desired experimental condition.
9. The DGCR system temperature was allowed to reach a steady state due to the heat generated from the centrifugal pump and the heat removed by the cooling system.
10. Gas was introduced through a non-return valve into the liquid stream just before the inlet of the DGCR to create a high turbulence gas-liquid zone.
11. In all experiments, a gas pressure slightly higher than the liquid pressure was maintained in order to form the bubble dispersion phase.
12. The expansion of the bubble dispersion and the volume expansion of the liquid in the break vessel were measured by observing the changes in their levels simultaneously using transparent adhesive ruler (6.35 mm wide, 1mm grads, vertical) as reference scale attached to outside of the break vessel wall and the DGCR column wall.
13. Dissolved oxygen, column temperature and the bubble size also were recorded at the same time simultaneously throughout an experiment.

3.4.1.2 Shut-Down Procedure for the DGCR

The following procedure was used for shutting down the process:

1. The liquid supply to the column was shut off by switching off the centrifugal pump.
2. The liquid supply to the cooling system was shut off by closing the tap water valve.
3. The vent valve was opened.
4. The drainage valve was opened and the product was discharged to sewers (note, no chemicals used in mass transfer studies).

3.4.1.3 DGCR Maximum Operating Conditions

The maximum operating conditions that can be used in the DGCR are listed in Table 3.4. Due to the limitation of the rated pressure of the quartz tube, the UV system must be ≤7 bars and 80°C. All experiments therefore were conducted below that range as a safety precaution.

Table 3-4 DGCR maximum operating conditions

Parameters	Values
Liquid flow rate up to	20 L min^{-1}
Gas flow rate up to	1.0 L min^{-1}
Orifice diameter	2 – 5 mm
maximum temperature up to	10 – 60°C
DGCR system volume up to	18 L
Reactor pressure	1 barg

3.4.1.4 Dispersion-Initiating Velocity (u_i)

Dispersion – initiating velocity was defined as the minimum required velocity of the liquid flow to break up the small gas cushion at the top section of the DGCR at the start-up operation. This velocity was determined by keeping the liquid flow rate sufficiently low to maintain a small gas cushion. The liquid flow rate was increased gradually until a critical point was reached where the gas cushion was broken up. Achieving this was considered the start condition to disperse the gas in the liquid stream and to start the dispersion process. This step was repeated each time the nozzle diameter was changed.

3.4.1.5 Bubble Size

The bubble size can be determined by visual analysis (photographic method) of a bubble dispersion sample in the vicinity of the transparent column wall using scalafix tape attached to outside of the DGCR column wall as shown in Figure 3.12, the bubble dispersion sample then analysed using a particle size analyzer software to count the average value of the bubble dispersion sample. Due to the good mixing and efficient dispersion, the following assumptions for the calculations of bubble size were undertaken:

- Bubble dispersion matrix was considered consistently stable and uniform, due to the re-dispersed larger bubbles in top section of the DGCR column, this controlled any disturbance in the balance of the forces acting on the bubbles such as buoyancy and drag forces.
- All bubbles are spherical shape.
- The normal distribution of the bubbles size along the column are considered equivalent.

Figure 3-12 Bubble size measurements method by visual analysis in the vicinity of the column wall using reference tape (scale in mm) attached to outside of the DGCR column.

3.4.1.6 Gas Hold-up Measurements

Gas hold-up measurements carried throughout the study were conducted by the volume expansion method. Gas hold-up (ε_g) was defined as the fraction of the gas-phase volume (V_g) in the total gas-liquid dispersion volume (V_d) in a stable operating condition of the DGCR. Gas hold-up calculations were done by observing the changes of the liquid volume in the break vessel reservoir and the bubble matrix volume in the 0.5 m glass reactor using reference tape attached to outside wall of both the break vessel reservoir and the glass reactor. The derivation of the following expression can be found in detail in appendix 9.1

$$\varepsilon_g = \frac{V_g}{V_d} \quad (3\text{-}1)$$

$$V_d = V_g + V_L \quad (3\text{-}2)$$

Where:

V_d: Gas-liquid dispersion volume

V_g: Gas-phase volume in the dispersion

V_L: Liquid-phase volume in the dispersion

3.4.1.7 Gas-liquid interfacial areas

Gas-liquid interfacial area is considered one of the most important design parameters of gas-liquid contactor systems. Assuming a uniform bubble matrix, steady absorption process and bubbles are spherical shape and have the same size as suggested by previous studies (Lu, 1988a; Tilston, 1990) , of the bubbles in the gas-liquid dispersion will lead to the following expression (Sarmento, 1995):

$$a = 6\frac{\varepsilon_g}{d_b} \quad (3\text{-}3)$$

Where:

ε_g: Gas hold-up, dimensionless numbers

d_b: Bubble diameter, m

3.5 Degradation Studies

3.5.1 Start-Up Procedure for the DGC Reactor

The start-up procedure for the DGCR in the degradation studies is the same as described in section 3.4.1.1. In addition, the following steps were used due to the addition of chemicals added and sampling techniques:

1. Quality control samples were taken before adding the desired chemicals to the DGCR to ensure there were no traces of chemicals from the previous experiment.
2. The desired amounts of chemicals were added to the DGCR and the system was allowed to equilibrate for 30 minutes. This step ensured good mixing of the reactants inside the DGCR before starting the reaction.
3. Quality control samples were taken before starting the reaction to ensure the performance of the mixing process and to ascertain the actual concentration of chemicals in the DGCR.
4. A black extruded acrylic sheet with the clear window film (UV Protection) was installed to the DGCR (as seen in Figure 3.6) before starting the UV system as a safety precaution from UV emissions.
5. The UV system was started, the time noted and samples were taken from the sample point (as seen in Figure 3.1) at equal time intervals.
6. To evaluate the UV system in the absence of dissolved oxygen, DGCR was deoxygenated by pure nitrogen for 60 min before starting the experiments.
7. The pH of the DGCR solution was adjusted to evaluate the influence of different pH on the photodegradation process using 2 M NaOH and 2 M H_2SO_4.

8. The pH of the samples was adjusted to pH = 2 using 0.01 M solution of sulfuric acid before processing in the SPE.
9. The DGCR was operated as a batch mode with recycle, irradiation time of the degradation experiments of selected female steroid hormones were considered to be the total residence time of the reactants in the reaction zone which is shown in equation 3.4 and was described by previous study (Sulidis, 1995)

$$t_r = \frac{V_r}{V_S} \times t_o \qquad 3\text{-}4$$

Where:

t_r : Irradiation time, min

t_o: Reactor operating time, min

V_r: Reaction zone volume, L

V_s: Reactor total volume, L

3.5.2 Shut-Down Procedure for the DGC Reactor

The shut-down procedure for the DGCR in the degradation studies was the same as described in section 3.4.1.2 with the addition of the following step due to the presence of chemicals. All the waste and liquid samples were collected in a special container labelled with the appropriate hazardous information and were managed by the School.

3.5.3 Experiments Operating Conditions

The optimized operating conditions used in all experiments with the DGCR in the degradation studies to investigate the heterogeneous oxidation reactions of selected female steroid hormones, 17β-E2, 17α-E2, E1 and PG are listed in Table 3.5.

Table 3-5 DGCR experiments conditions

Parameters	Values
Liquid flow rate	10 L min^{-1}
Gas flow rate up to	0.0 -0.2 L min^{-1}
Orifice diameter	2 – 5 mm
Reaction temperature	30 – 45°C
Reaction zone volume	4 L
DGCR system volume	15 L
Reactor pressure	1 barg

3.6 General Analytical Procedure

In order to develop and validate analytical methods able to quantify accurately the selected female steroid hormones, 17β-Estradiol (17β-E2), 17α-Estradiol (17α-E2), Estrone (E1) and Progesterone (PG) in aqueous samples at the ng L^{-1} level and able to identify by-products resulting from the process, it is necessary to follow the following steps as shown in Figure 3.13:

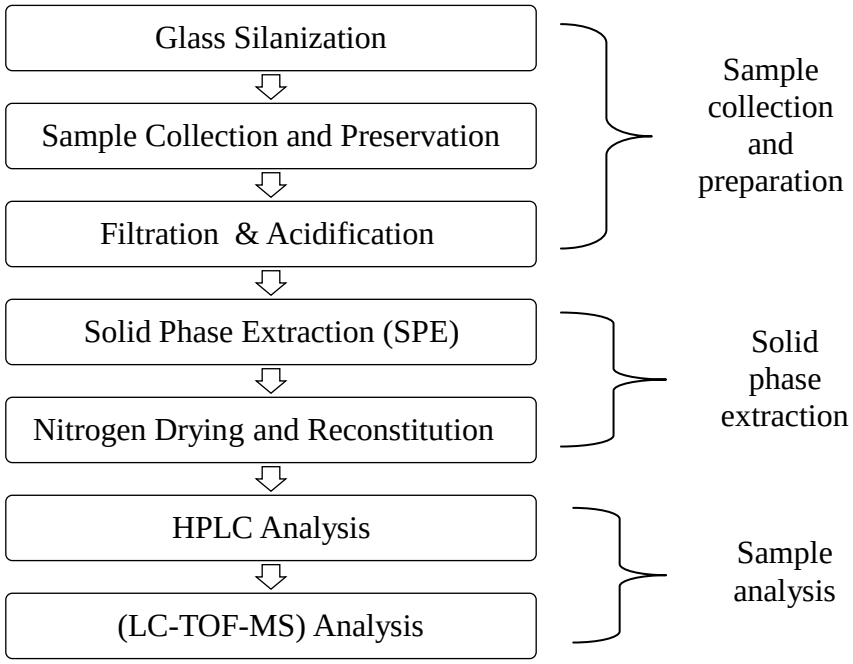

Figure 3-13 Overview of the analysis procedure

3.6.1 Standards Preparation and Stock Solutions

- Stock solutions of: 17β-estradiol (βE2), 17α- estradiol (αE2), estrone (E1) and progesterone were all prepared at 1 mg/mL by accurately weighed standard powders and dissolved in an HPLC grade methanol. They were kept at -18°C to prevent biodegradation and bacterial growth of the stock solution.
- A serial dilution with a concentration range of 1, 2, 5, 10, 20, 50, 100, 200, 500 and 1000 ng L^{-1} of reference hormone standards was used in all experimental work prepared from the stock solutions and calibration curves were generated (see appendices 9.8). Hormone standards were kept at -18°C to prevent biodegradation and bacterial growth.

3.6.2 Glass Silanization

Silanization is the first serious precautionary step that will increase the efficiency of an overall analytical method with regards to sensitivity and accuracy. To prevent any losses of the sample through adsorption to the sample container materials, all the glass used in the analytical procedure was silanized before use (Ahrer et al., 2001; Suri et al., 2012). All the glass used in the analytical procedure was silanized using 10% (v/v) dimethyldichlorosilane in toluene, then washing the glass twice with pure toluene and twice with pure methanol, followed by drying the glass at 160°C for three hours.

3.6.3 Sample collection and preservation

Hormones are typically present at the ng L^{-1} level in the environment with high octanol/water partition coefficients (logP) and low aqueous solubility. River water is considered more complex than mineral drinking water and ultra pure water due to interference from chemicals and contamination which can affect the efficiency of the entire analytical procedure. All samples were therefore filtered through a glass-fibre filter and the pH was adjusted immediately (pH=2) using 0.01 M solution of sulfuric acid as a sample preservative (Vanderford et al., 2003). Samples were stored at 4°C until extraction, and subsequently analysed within 24 hours of collection.

3.6.4 Solid Phase Extraction (SPE)

After collecting the samples from the DGCR with the adjusted pH, the samples were ready to be processed in the SPE. The SPE eliminated any chemical interference and allowed the analyte concentration to be reconstituted so that trace levels can be easily detected. SPE was performed offline using Oasis HLB cartridges as follows: condition with 3 mL of tert-butyl methyl ether (MTBE), rinse twice with 3 mL of methanol and rinse twice with 3 mL of ultrapure water. The sample volume was loaded at 1 to 5 mL min^{-1} flow rate in order to achieve the best recovery and avoid the loss of the targeted hormones (Wang et al., 2012). A wash step was performed to remove organic interferences with 3 mL of methanol/water (40/60, v/v) followed by re-equilibration by rinsing twice with 3 mL of ultrapure water.

A second wash step was performed (pH = 11) using 3 mL of methanol / 2% ammonium hydroxide in water (10/90, v/v) to remove non-organic interferences. Elution was achieved with 6 mL of tert-butyl methyl ether/methanol (90/10, v/v). Finally, eluents were evaporated to dryness under a gentle stream of N_2 and reconstituted in 1 mL of a mixture of acetonitrile/water (20/80, v/v).

3.6.5 Quality Control (QC) Procedure

- The first sample from the DGCR was neglected to ensure that the samples collected had been treated in DGCR and not trapped in the sampling point pipes. This is fundamental in retaining the sensitivity of the analytical method and the reliability of the results.
- All vials used in LC injections were amber, deactivated (silanized) materials and labelled and stored at -18°C prior to injection in the LC system.

- The first injection was a blank sample to check for possible sources of contamination in the chromatographic system.
- Blank samples were also used between injections and at the end of the injection run and to ensure nothing was carried over from previous injections in the routine analysis.
- Flushing the LC system with the mobile phase was carried out to remove any residue, to extend the column shelf-life and to maintain column performance and selectivity.

3.6.6 LC Analysis

Chromatographic separation was performed using a Kinetex 2.6 µm C18 100 Å, LC Column 75 x 4.6 mm. Separation was optimized by using acetonitrile/water with 12 minutes total run time per injection as follows: 3 minutes injection cycle time of acetonitrile/water (30/70, v/v), followed by 5 minutes gradient cycle time of acetonitrile/water (90/10, v/v) and finally re-equilibration cycle time for 4 minutes using acetonitrile/water (30/70, v/v); this is considered a necessary step to avoid baseline drift before the next injection. The flow rate of the mobile phase was 1 mL min^{-1} with a sample injection volume of 100 µL and 30°C column temperature. Compound detection was performed using LC-TOF-MS that used methanol/water (95/5) (v/v) with 0.1% formic acid carrier solvent in the electrospray ionisation and operated in the negative ion mode for β-estradiol, α-estradiol and estrone and the positive ion mode for progesterone (Table 3.6).

Table 3-6 The instrument detection conditions of the proposed method

Hormones	HPLC - DAD	LC-TOF-MS			
	Λ[a]	Electrospray ion	Cone voltage (V)	Desolvation temp. ℃	Source temp. ℃
17β-E2	200	ESI (-)	15	300	130
17α-E2	200	ESI (-)	15	300	130
E1	200	ESI (-)	15	300	130
PG	243	ESI (+)	15	300	130

a DAD Wavelength

3.6.7 Optimization of the Liquid Chromatography

The Kinetex core-shell technology columns enhanced the performance of the liquid chromatography analyses using a conventional 1100 Agilent HPLC system. The chromatograms obtained from the proposed analytical method show excellent separation for the selected estrogens in a short run time. In spite of using the maximum injection volume (100 μL), no column overloading problems such as fronting or rounded peaks were observed, however there was a need for 3 minute injection cycle time delay to avoid the overlap between injection and sample peaks. The similarity in molecular weight and the structure of the hormone compounds increase the difficulty of the separation. However, the use of a gradient step to give a total run time of 12 minutes resulted in an excellent separation for the targeted hormones. The DAD settings were optimized by selecting the optimum wavelength for each component. The maximum absorption was attained by monitoring several wavelengths at the same time, the

optimum wavelengths as described earlier (Table 3.6). The best wavelength with the maximum absorbance for β-estradiol, α-estradiol and estrone was 200 nm; whereas 243 nm was the best wavelength with the maximum absorbance for progesterone. Working with a UV wavelength of 200 nm will increase the sensitivity and the resolution, but it will also increase baseline drift and noise due to the solvent cut-off wavelengths. This was avoided by using the acetonitrile water gradient slope at 12% /min.

3.7 Instrumental calibration

3.7.1 Mettler Toledo SevenMulti pH meter calibration

Mettler Toledo SevenMulti pH meter was calibrated using Fisher Scientific buffers; pH 4 (phthalate), pH 7 (phosphate) and pH 10 (borate) using the calibration mode in pH meter and in accordance with calibration procedure supplied by the instrument manufacturer. The calibration procedure was made regularly each week with fresh buffers to ensure the reliability of the results.

3.7.2 Mettler Toledo SG6 – SevenGo pro dissolved oxygen meter calibration

The SG6 – SevenGo pro dissolved oxygen meter was calibrated with 100% water saturation with R^2 ≥96 % using the calibration mode in dissolved oxygen meter and in accordance with calibration procedure supplied by the instrument manufacturer. The calibration procedure was made regularly each week as recommended by the manufacture to ensure the reliability of the results.

3.7.3 Analytical balance calibration

Ohaus Adventurer analytical balance (accuracy 0.1 mg) and Mettler Toledo microbalance, MT-5 (accuracy 0.0008 mg) were calibrated by the facilities of the chemical engineering school.

3.7.4 DGC Reactor Pump Calibration

The pump of the continuous flow rig was controlled using the Platon flow-meter flow rate up to 22 $x10^{-3}$ m^3 min^{-1} with increment scale of $1x10^{-3}$ m^3 min^{-1} and ± 5% accuracy in the DGCR and was calibrated using tap water at room temperature. Pyrex measuring cylinder with total volumes of $1x10^{-3}$ m^3 and ± 5 mL accuracy together with a stop watch were used to measure the actual water collected compared to the liquid flow rates on the meter. The calibration results can be found in appendices 9.4.

3.7.5 Break Vessel Volume Calibration

Gas hold-up measurements were conducted by the volume expansion method as discussed in section 3.5.1.6. The break vessel was calibrated using tap water at room temperature by adding a known volume to the break vessel and comparing the calculated volume of the observation to the break vessel liquid height using transparent adhesive ruler (6.35 mm wide, 1 mm grads, vertical) as a reference scale attached to outside of the break vessel wall. The calibration results can be found in appendices 9.5

3.7.6 HPLC calibration

The HPLC was calibrated using the external standardization method. The selected hormones, 17β-estradiol (17β-E2), 17α-estradiol (17α-E2), estrone (E1) and progesterone (PG) were accurately prepared by weighing 1mg / ml in HPLC methanol grade and stored at -18°C. Fresh working solutions were prepared of exponential dilution (0, 1, 2, 5, 10, 20, 50, 100, 200, 500 and 1000 ng L^{-1}) in order to generate the calibration standard curves. The LC injections were made with the same volume from low to high concentrations to avoid carryover. The calibration curves and results for the selected hormones, 17β-E2, 17α-E2, E1 and PG can be in appendices 9.6

3.7.7 Thermocouple Calibration

The Digitron T200KC Thermometer was calibrated using Grant W28 water bath and the Mettler Toledo FG4 – FiveGo DO Temperature sensor (accuracy °C ± 0.3). The thermometer did not deviate more than +/- 0.5ºC.

3.7.8 DGC Reactor Pressure Gauges Calibrations

All pressure gauges were supplied as pre-calibrated and were checked periodically by the service available in the School of Bioscience.

CHAPTER 4

4 OPTIMIZATION AND VALIDATION FOR THE ANALYSIS OF SELECTED FEMALE STEROID HORMONES IN AQUEOUS SAMPLES AT THE NANOGRAM LEVEL

4.1 Results and Discussion

4.1.1 Analytical Method Validation

Analytical method performance was evaluated through Specificity, Repeatability, Recovery, Linearity, Range, Limit of Detection and Limit of Quantitation and are discussed in the following sections.

4.1.1.1 Specificity

Confirmation of the importance of optimizing separation is to the avoid co-elution of chemical compounds and to ensure peak purity. This step is considered even more important prior to starting quantitative calculations in order to establish the confidence of the analytical results. Specificity was evaluated by comparing the retention time (t_R) of the four analytes in spiked and non-spiked samples in ultra-pure, mineral drinking and river water matrices with the corresponding reference standards prepared from the stock solutions as discussed in section 3.6.1 and quantifying each analyte in the presence of the other analytes. The differences of the spectral similarity and threshold curves were compared using the Chemstation software in the DAD spectra acquiring during the peak elution in order to check

the analyte purity. Figure 4-1 shows the DAD spectrum for β-estradiol, while the spectra for 17α- estradiol, estrone and progesterone can be found in appendix (9.7). The ICH guideline recommends the evaluation of water matrix effects using real samples to evaluate the overall analysis method specificity (ICH et al., 2005). SPE was used to eliminate the interference from different water matrices and gave the observed excellent chromatographic separation of the four hormones in the different water matrices in short time. This enables the specificity to be evaluated for the proposed analytical method as supported by the chromatogram in ultra pure water (Figure 4-2). River water was used to confirm the peak identity and purity by LC-TOF-MS to overcome instances when there may be a lack of visible UV and there is a need to provide identity confirmation. Figure 4-3 shows the mass spectrum (MS) of β-estradiol in river water. Mass spectra for 17α- estradiol, estrone and progesterone can be found in appendix (9.8).

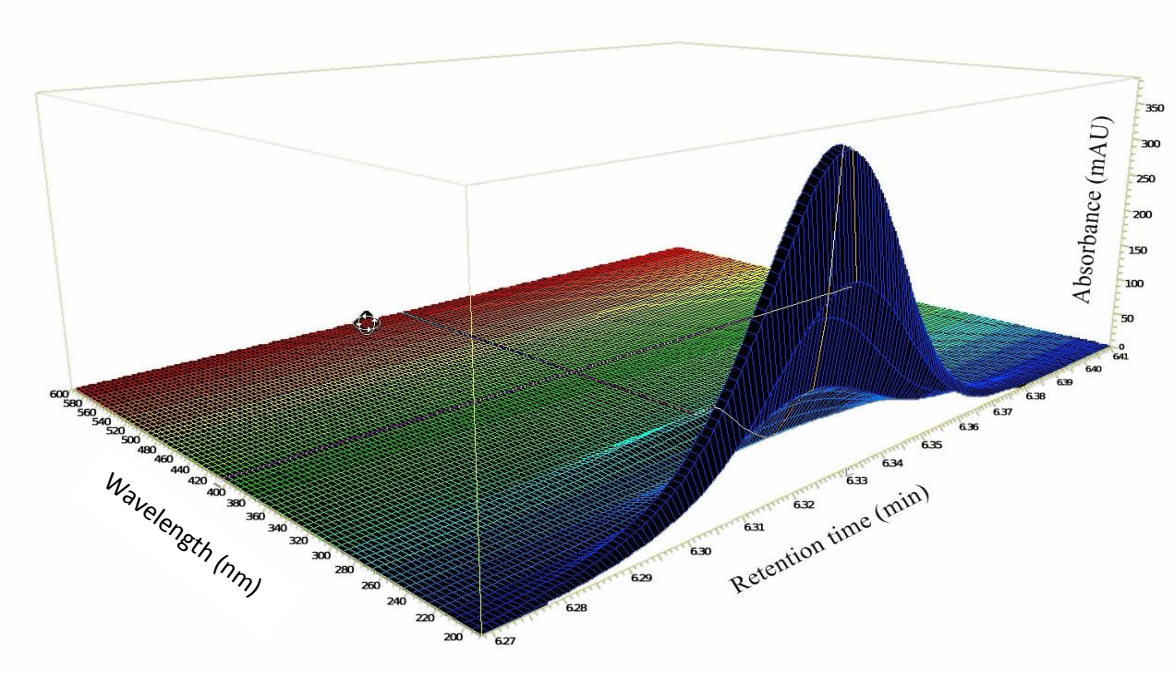

Figure 4-1 β-Estradiol DAD spectrum

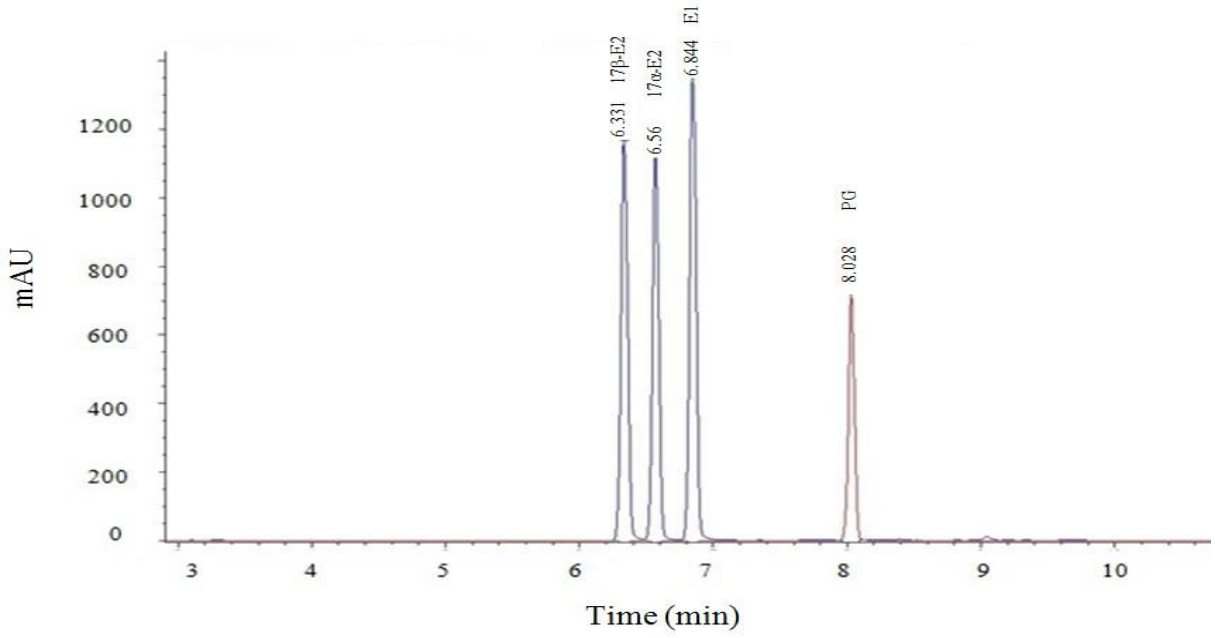

Figure 4-2 Chromatogram of standard solution of the four hormones at 1000 ng L^{-1} in ultra-pure water

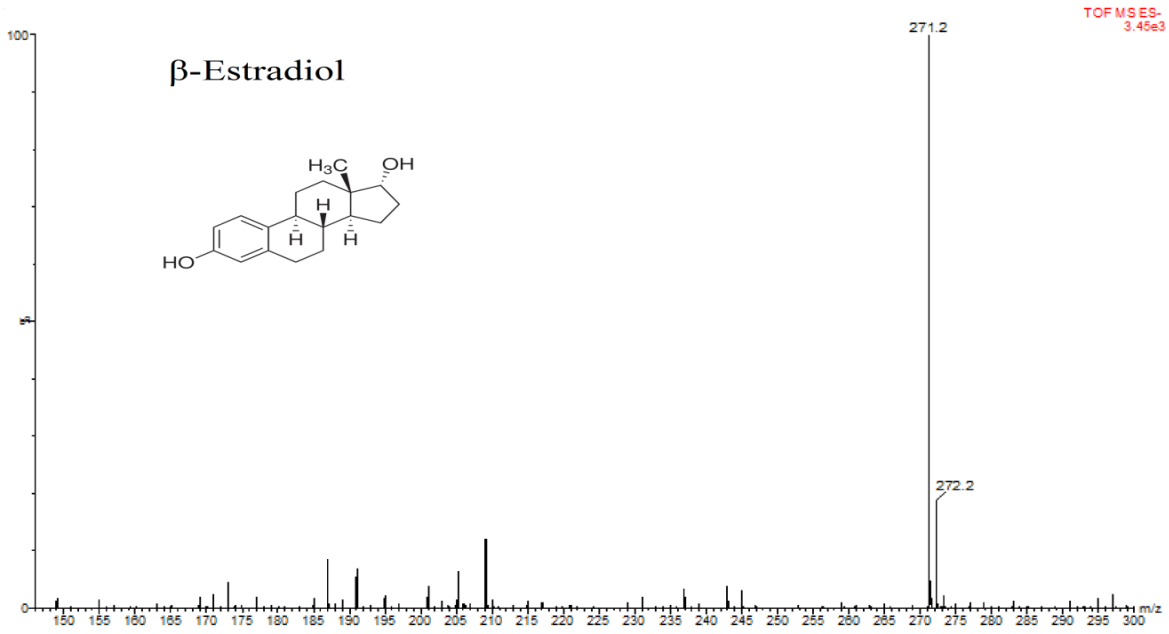

Figure 4-3 17β-estradiol LC-TOF-MS chromatogram in river water

4.1.1.2 Repeatability and Recovery

Repeatability of any analytical method relies on the generation of the same results in the same time and under identical conditions. The proposed method was successfully validated by comparing the retention time and the responses at different concentrations with different water matrices following the recommendation of the ICH guideline (ICH et al., 2005). Different water matrices spiked with 250 ng L^{-1} of hormone standards were used to check their effect on the retention time as shown in Figure 4.4. The results show that respective retention times of 6.3 ± 0.03 min, 6.54 ± 0.03 min, 6.82 ± 0.02 min and 8.00 ± 0.02 min for 17β-E2, 17α-E2, E1 and PG were established for the different water matrices. In the same way, Table 4.1 shows the effect of different water matrices on the overall recovery efficiency; all the samples were spiked with hormone standards in the range of (10-100 ng L^{-1}). This is of particular importance for the SPE process as the selectivity of the cartridges will be less when the sample is more contaminated due to the binding capacity and the ability to absorb the targeted solute of the SPE will be highly effected. Relative standard deviation (RSD) in Table 4.1 shows the results of six replicate injections for three different water matrices for the same sample volume of 1000 mL. The results show that RSDs are ≤ 9.13% which is quite satisfactory. Similar results for both low and high concentrations were obtained for ultrapure water, whereas for river and mineral water samples low concentration generally gave better recovery. The highest recovery was seen for ultrapure water at 98.7% and the lowest for river water at 88.2%. These results highlight the importance of chemical interference in sample recovery. The recovery of the spiked sample (C_s) with the reference standard (C_r) was compared using Eq. (4.1)

$$\% \text{ Recovery} = \frac{C_s(\text{ng L}^{-1})}{C_r(\text{ng L}^{-1})} \times 100 \qquad 4\text{-}1$$

Selecting the optimum sample volume is an important factor to avoid loss of the analytes during the solid phase extraction step due to breakthrough of the cartridge. Although SPE is time consuming, the analyte's solubility in water and the loading rate can lead to lower recoveries, and this was minimized by optimizing the SPE step for different water sample volumes (100 mL, 500 mL and 1000 mL). Table 4.2 gives the results obtained by spiking different water matrix volumes with 200 ng L^{-1} of hormone analyte in triplicate. The recovery loss increases with decreasing water volume. Using 100 mL of river water led to R% > 68.9 of progesterone, however with a 10 fold increase in water volume a R% > 91.6 was achieved. This behaviour was attributed to the solubility of the analytes in the water samples. The mineral drinking water and ultra-pure water exhibited similar behaviour of progesterone with R% > 84.9 and R% > 85.1 for the 100 mL respectively, whereas R% > 95.4 and R% > 95.2 for the 1000 mL respectively

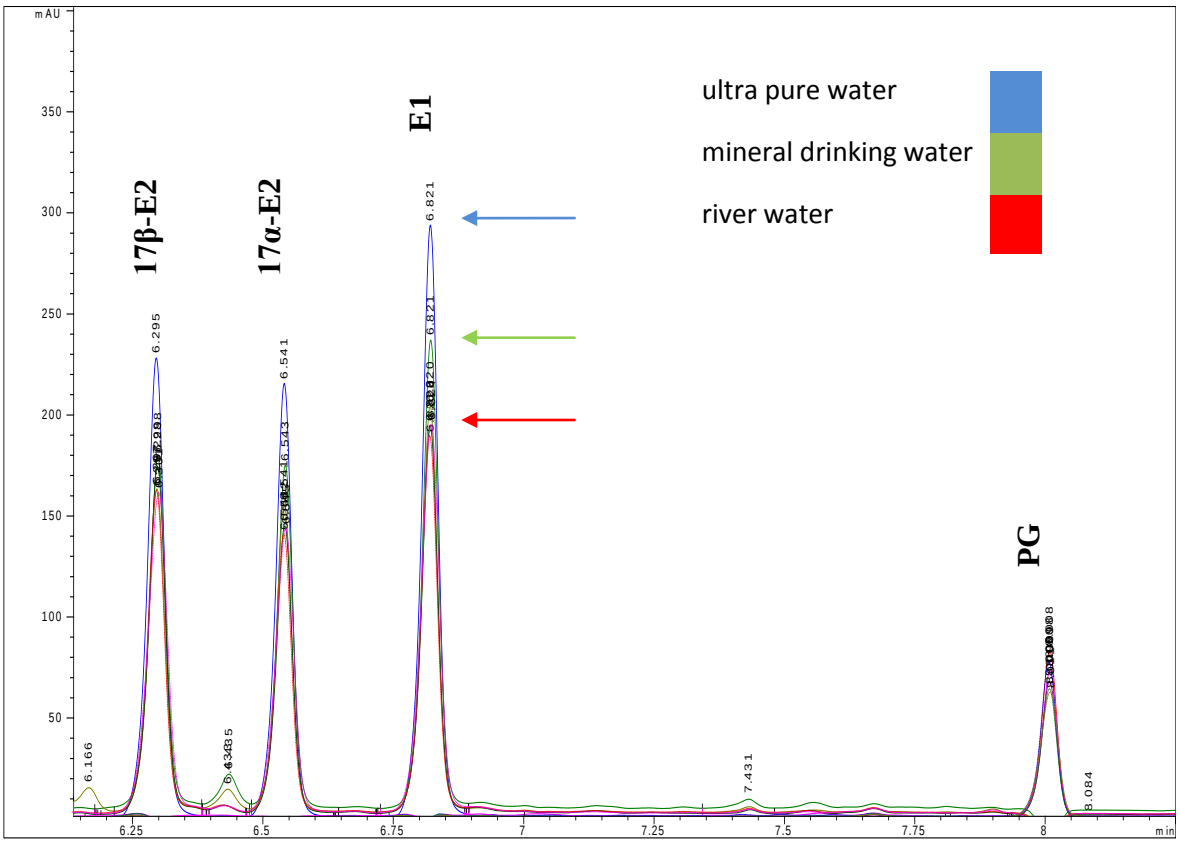

Figure 4-4 Chromatogram of different water matrices (ultra-pure water, mineral drinking water and river water) gave the same retention time spiked at 250 ng L^{-1}

Table 4-1 Average recovery (R %, n=6) and relative standard deviation (RSD, %) for four female hormones in river water, mineral drinking water and ultra-pure water (Milli-Q water) with 1000 mL sample volume.

Analyte	River water				Mineral drinking water				Ultrapure water			
	Spiking Conc. 40 ng L^{-1}		Spiking Conc. 100 ng L^{-1}		Spiking Conc. 20 ng L^{-1}		Spiking Conc. 60 ng L^{-1}		Spiking Conc. 10 ng L^{-1}		Spiking Conc. 50 ng L^{-1}	
	R%	RSD	R%	RSD	R%	RSD	R%	RSD	R%	RSD	R%	RSD
17β-E2	89.2	4.1	93.9	4.8	93.5	3.7	95.2	2.4	96.3	3.12	98.4	1.93
17α-E2	89.7	5.0	92.0	4.3	97.5	2.13	96.1	1.6	98.7	2.0	97.4	1.63
E1	91.9	6.4	93.1	3.6	96.9	3.36	98.6	2.15	97.7	1.0	98.0	1.27
PG	88.2	9.13	89.5	8.86	92.3	2.5	94.1	4.0	95.9	2.4	95.3	1.86

Table 4-2 The effect of different sample volumes spiked at 200 ng L–1 on the average recovery (R%, n=3) for four female hormones in river water, mineral drinking water and ultra-pure water (Milli-Q water).

Analyte	River water			Mineral drinking water			Ultrapure water		
	Sample 100 mL	Sample 500 mL	Sample 1000 mL	Sample 100 mL	Sample 500 mL	Sample 1000 mL	Sample 100 mL	Sample 500 mL	Sample 1000 mL
17β-E2	81.1	90.8	94.3	92.3	96.3	97.6	93.1	97.7	97.8
17α-E2	80.3	91.2	95.1	93.5	95.4	97.4	92.5	98.7	98.2
E1	82.4	90.0	94.8	93.9	95.7	98.8	91.3	96.4	97.7
PG	68.9	83.7	91.6	84.9	89.1	95.4	85.1	89.8	95.2

4.1.1.3 Linearity, Range, Limit of Detection and Limit of Quantification

An external standardization for each hormone with known purity was prepared by accurately weighing each one using a Mettler microbalance (MT-5, Mettler Toledo with 0.0008 mg standard deviation) in methanol to prepare stock solutions and storing at -18°C. A fresh standard solution was prepared for each hormone to make a calibration standard. Prior to analysis, solutions were injected from the lowest concentration to the highest concentration with the same injection volume (100 uL) to generate a calibration curve; a blank sample was injected between each injection. The evaluation of the linearity was tested using 10 concentration levels using linear-regression with 95% confidence level and compared with 5 concentration levels in ICH. Variation of retention time (t_R) of each analyte in different water matrices was almost negligible with ±0.040 minutes, and a satisfactory linearity in the range of 5-1000 ng L^{-1} with R^2 ≥ 0.9996 for each analyte (see appendix 9.6). LOD and LOQ were estimated by the response standard deviation (σ) and slope (S) using Eq. (4.2) and Eq. (4.3) respectively, and were verified by spiking with (1, 2, 5, 10, 20, 50, 100, 200, 500 and 1000 ng L^{-1}) with different water matrices (Table 4.3).

$$\text{LOD} = \frac{\mathbf{3.3} \times \boldsymbol{\sigma}}{\boldsymbol{S}} \quad \text{ng L}^{-1} \qquad \text{4-2}$$

$$\text{LOQ} = \frac{\mathbf{10} \times \boldsymbol{\sigma}}{\boldsymbol{S}} \quad \text{ng L}^{-1} \qquad \text{4-3}$$

Table 4-3 The instrumental performance of the proposed method (n = 7) in real matrices

Hormones	t_R min	LR (ng L^{-1})[a]	Slope	R^2	LOD (ng L^{-1}) [b]	LOQ (ng L^{-1}) [c]
17β-E2	6.30	5.0 - 1000	2.3680	1.0000	0.80	2.41
17α-E2	6.54	5.0 - 1000	2.0850	1.0000	1.05	3.17
E1	6.82	5.0 - 1000	3.9220	1.0000	0.93	2.82
PG	8.00	5.0 - 1000	0.3367	0.9999	3.97	12.02

[a] Linear range

[b] Limit of Detection

[c] Limit of Quantitation

4.2 Identification of Isomeric Products

The degradation of estrogens using advanced oxidation processes (AOPs) was investigated using the downflow gas contactor reactor (DGCR). AOPs were first defined by Glaze et al. in 1987 (Glaze et al., 1987). The process involves the production of highly reactive hydroxyl radicals ($^{\cdot}OH$) in a sufficient quantity to remove organic materials in wastewater by using oxidation in the presence of hydrogen peroxide (H_2O_2) and UV light as an energy source to have effective water purification. The mechanism of photo-degradation of E1 using UV/H_2O_2 process as shown in Eqs. (4-6):

$$H_2O_2 \xrightarrow{h\upsilon} 2OH^{\bullet} \quad 4\text{-}4$$

$$OH^{\bullet} + E1 \rightarrow \text{Intermediate} \quad 4\text{-}5$$

$$OH^{\bullet} + \text{Intermediate} \rightarrow CO_2 + H_2O \quad 4\text{-}6$$

The proposed analytical method was successfully capable of identifying unknowns resulting from the decomposition of E1 using the DGCR. In accordance with the experimental procedure in section (3.5.1), a sample was taken for HPLC analysis before starting the reaction (t = 0 minutes) as a quality control procedure to be ensure that the mixture was homogeneous; a typical spectrum is shown in Figure 4.5. After starting the DGCR, samples were taken every 2 minutes, which led to the discovery of an unknown peak, as shown in Figure 4.6 (t_R = 7.181 minutes). Fractionation and separation of the unknown was undertaken to allow further analysis and identification by LC/MS. The LC/MS confirmed the peak identity of the by-products from the photolysis reaction as an isomer of estrone by comparing its mass spectrometrum in the negative mode as shown in Figure 4.7 (t = 0 minutes) and Figure 4.8 (t = 2 minutes).

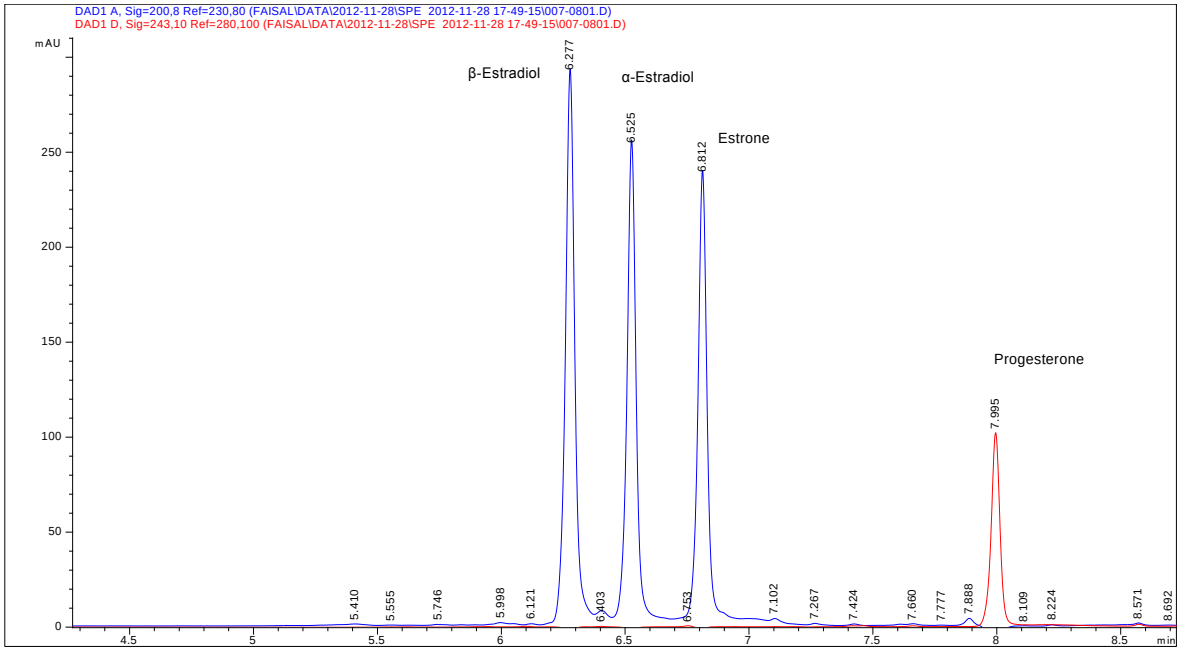

Figure 4-5 Chromatogram of ultra-pure water sample spiked with hormone standards at 300 ng L^{-1} in DGCR at (t = 0 minutes).

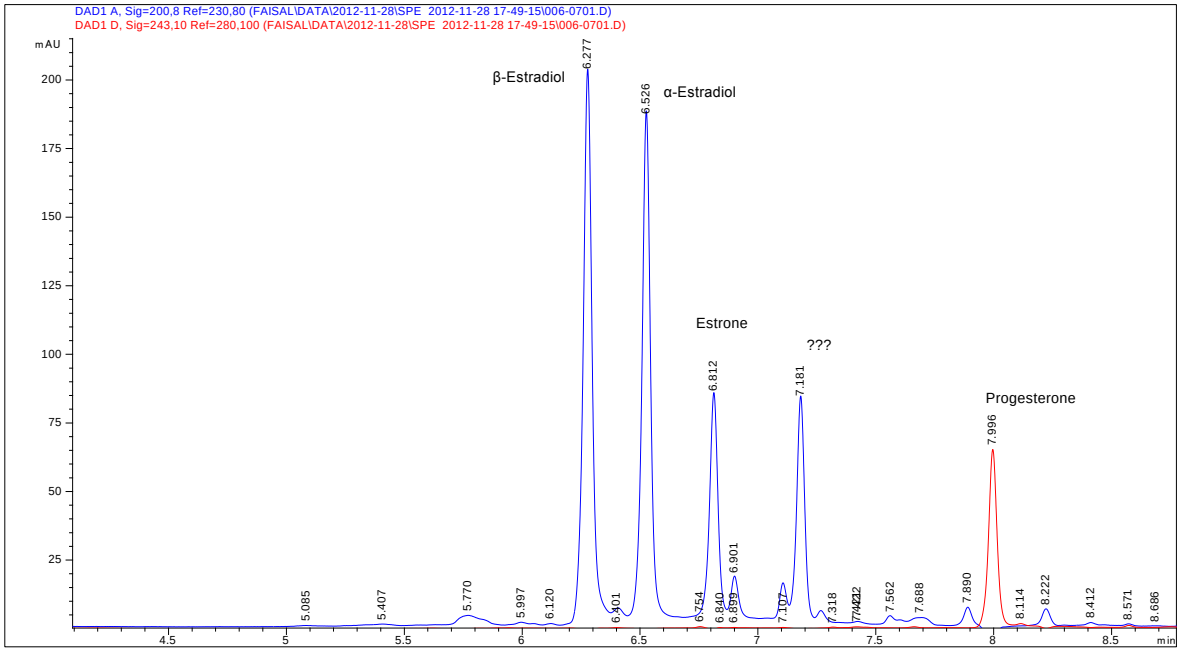

Figure 4-6 Chromatogram of ultra pure-water sample spiked with hormone standards at 300 ng L^{-1} in DGCR at (t = 2 minutes).

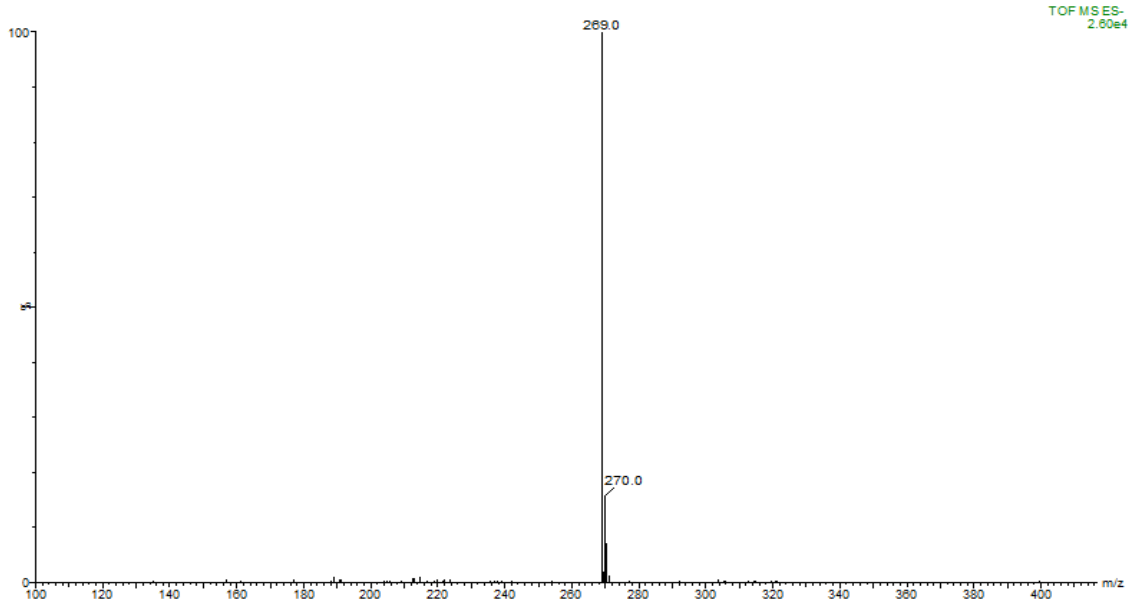

Figure 4-7 Estrone mass spectrometrum (t = 0 minutes)

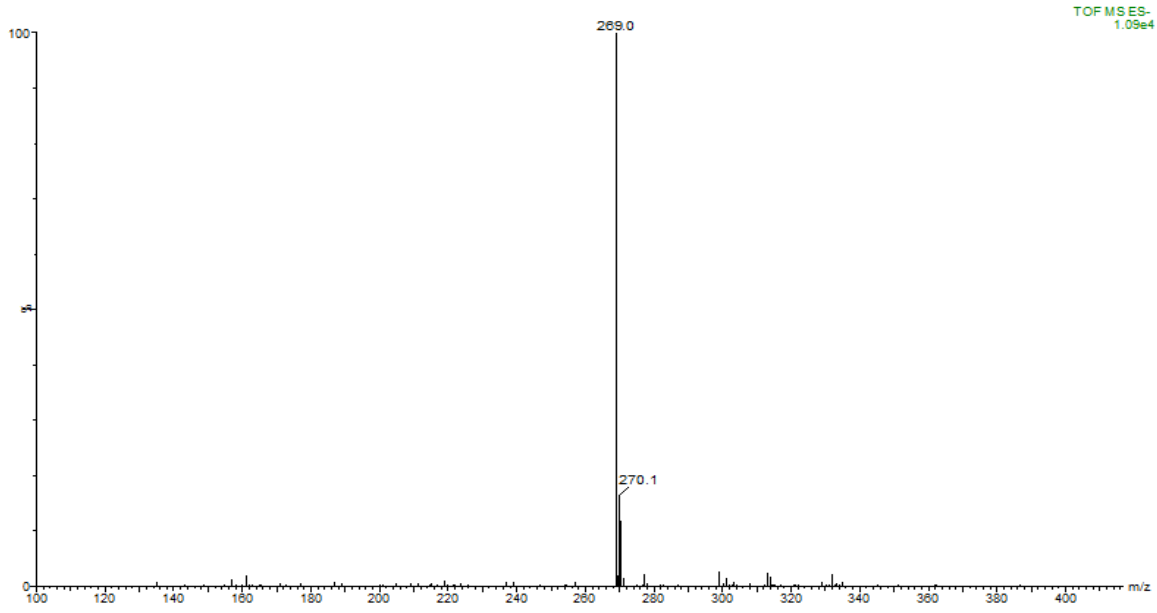

Figure 4-8 Estrone isomer mass spectrometrum (t = 2 minutes)

4.3 Conclusion

In this study, a fast, reliable and accurate analysis method was established for the detection of four selected female hormones at the ng L^{-1} level. Off-line analysis using an Oasis HLB SPE followed by HPLC-DAD for the quantification and identification of the compound was used. LC-TOF-MS was used for compound purity and identity confirmation. Optimization by SPE was a clean-up step which removed interfering species present in the water samples, (especially river water). Recoveries greater than 88.2%, a RDS less than 9.13% and respective LODs of 0.8, 1.05, 0.93 and 3.97 ng L^{-1} for 17β-E2, 17α-E2, E1 and PG were established for river water samples. Mineral water and ultrahigh purity water gave improved values. Detection down to the ng L^{-1} level for the selected hormones were effectively and satisfactorily achieved using conventional LC instruments with an excellent separation in short chromatographic time.

CHAPTER 5

5 HYDRODYNAMIC CHARACTERISTIC AND MASS TRANSFER STUDIES OF THE DOWNFLOW GAS CONTACTOR REACTOR (DGCR)

5.1 Results and Discussion

5.1.1 Hydrodynamic Characteristics

5.1.1.1 Flow Characteristics

The DGCR bubble dispersion characteristics depend on several factors: liquid and gas properties, gas input, liquid inlet velocity, liquid superficial velocity, and column geometrical design. The O_2/H_2O system was chosen in all experiments to be used subsequently in the photodegradation studies using the DGCR, due to the availability of the oxygen probes that facilitate the monitoring of the absorption process. Deionised water was used in all experiments to evaluate DGCR performance. The O_2/H_2O system was also used by many researchers to evaluate the hydrodynamic characteristics of the bubble column reactors (Boyes et al., 1992b; Degaleesan et al., 2001; Douek et al., 1997; Jena et al., 2009; Saxena and Rao, 1991; Shah et al., 1983). The injection of the gas phase in a fully flooded column led to the existence of four different zones due to the high turbulence at the jet nozzle, which led to the build-up of the gas-

liquid dispersion. Figure 5.1 demonstrates the four regions in the DGCR column. Oxygen was introduced through a simple T-piece connection to a fully flooded column with a turbulent jet stream to generate small bubbles; the small bubbles then coalesced to form larger bubbles with a continuous flow of gas stream, and this led to a stable bubble matrix with uniform bubble size and dispersion. The balance between the liquid velocity and the gas bubble rise velocity with the direct effect of the bubble size on the gas bubble rise velocity allowed the system to maintain a stable dispersion in the DGCR operation. The dispersion volume was controlled by controlling both the liquid jet velocity and the gas input.

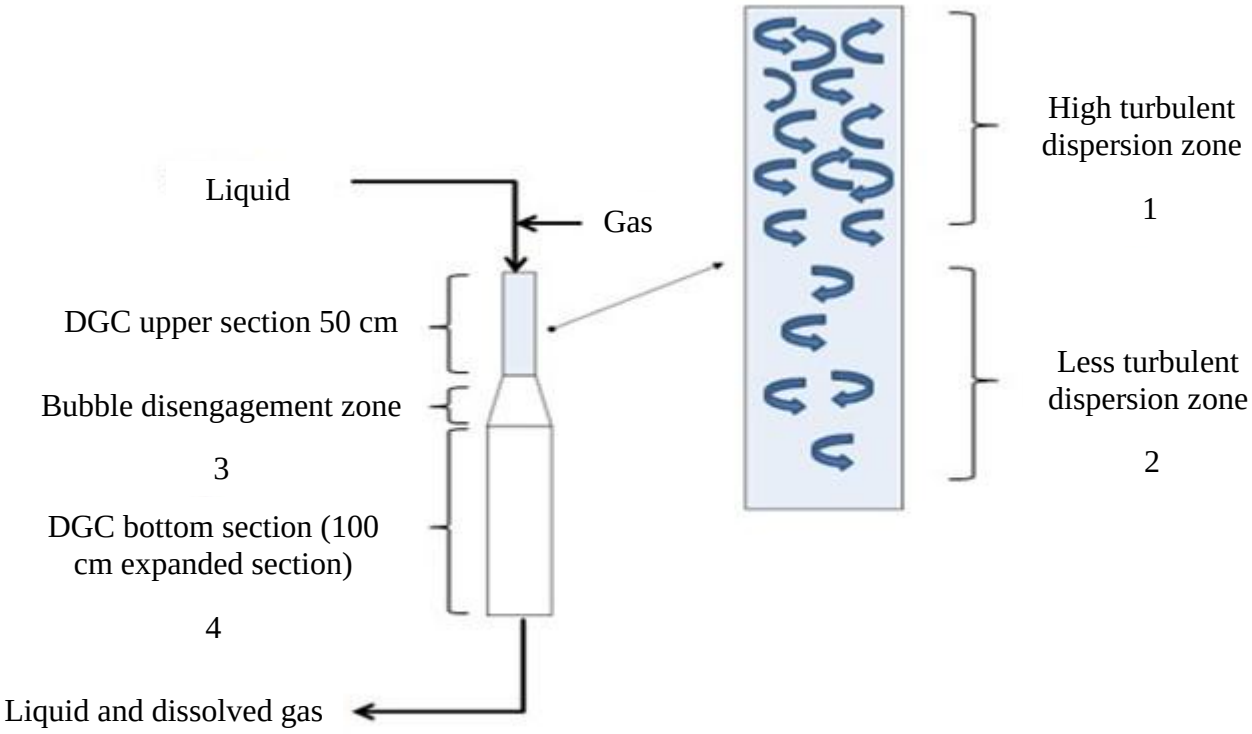

Figure 5-1 Schematic diagram of DGCR column

The flow regime for the O_2/H_2O system can be characterized by the following four regions;

1. The first region reflected a high-turbulent flow characterized with small bubble size (≤2 mm), a rapidly coalescing process, and a high-turbulent mixing zone with continuous and constant gas phase dispersion in the liquid phase. The efficient mixing zone (complete mixing) was present in the first 10 to 20 cm of the top section of the DGCR column with a cloud of very small bubbles (d_b = 1 to 2 mm) with back flow of both phases as shown in Figure 5.2a. This region was characterized with a relatively low mass transfer coefficient (k_La) and gas holdup (ε_g) due to the low interfacial area.
2. The second region reflected less turbulence with stable and uniform bubble dispersion occupying the whole cross-sectional area of the column; and this region could be considered a perfect bubbly flow, as shown in Figure 5.2b. The bubble diameter ranged (d_b = 3–5 mm) in a suspension state with a gas holdup value at its highest level (Lu, 1988b). This region can be extended to the bubble disengagement section with a large gas input to the system.
3. This was the bubble disengagement region. Tiny bubbles moved down to the expanded bottom section and returned to the bubble disengagement region intermittently in the 0.10 m / 0.05 m i.d. reducer section, as shown in Figure 5.2c.
4. This was a free zone region (expanded bottom). Small bubbles (d_b ≤1 mm) combined and then rose to the first region.

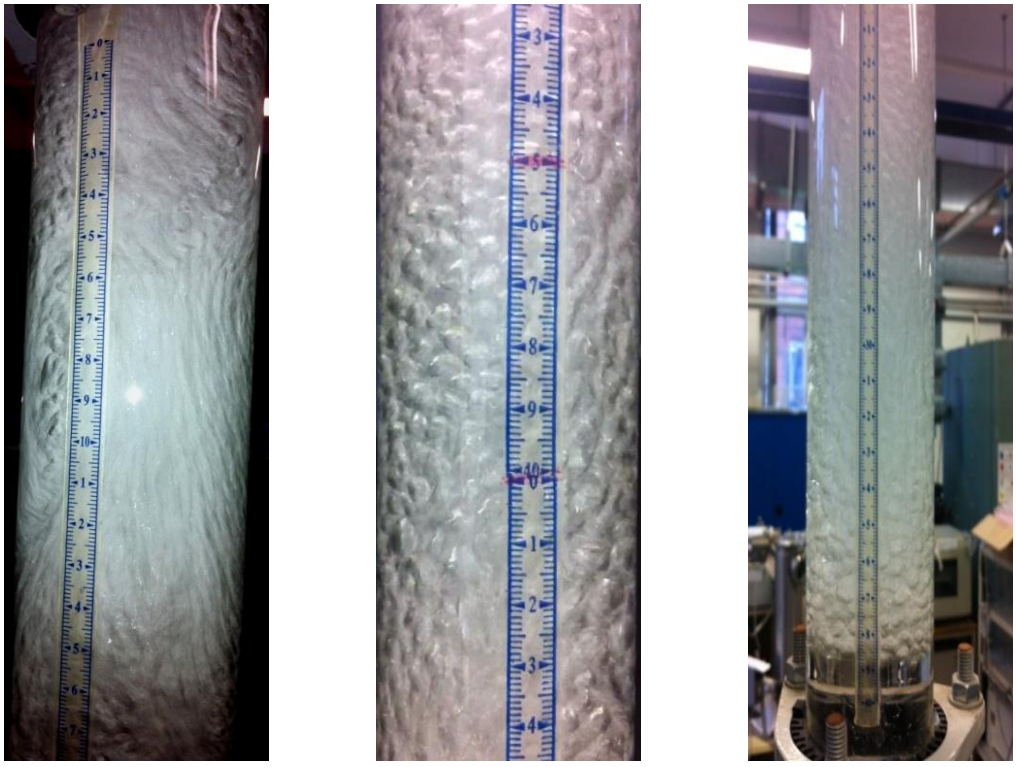

5-2a **5-2b** **5-2c**

Figure 5-2 Visualization of different flow regimes using the O_2/H_2O system in DGCR column (top section), high-turbulent mixing zone (5.2a), less turbulence with stable and uniform bubble dispersion zone (5.2b) and bubble disengagement zone (5.2c)

5.1.1.2 Minimum Inlet Liquid Velocity

The balance between bubble rise velocity and liquid downflow velocity is considered one of the most important operating parameters to maintain a stable operation of the DGCR and prevent the dispersion to collapse. As discussed in Section 5.1.1, unstable bubble dispersion occurred if the gas feed rate was higher than the inlet liquid velocity (bubble rise velocity was higher than the liquid downflow velocity). An expansion of the dispersion volume continued rapidly until the dispersion matrix collapsed and a gas pocket was formed at the top of the

column, as shown in Figure 5.3a, in order to prevent this phenomenon, inlet liquid velocity was increased slightly at start-up when the column was almost full with a small gas pocket. The inlet liquid velocity that was able to break the gas pocket was considered to be the minimum inlet liquid velocity to maintain the initiation of the dispersion process of the gas phase into the liquid phase at the top section of the DGCR, with a well-controlled stable dispersion process taking place. Unstable operation of the DGCR occurred when the liquid input was much higher than the gas input (liquid downflow velocity was larger than bubble rise velocity), and the dispersion process stopped expanding. The bubble coalesce process was highly affected with voids in the bubble matrix as seen in Figure 5.3b. It was found that each time the orifice size was changed, the minimum inlet liquid velocity needed to be changed; the smaller the orifice size used, a higher minimum inlet liquid flow rate was required due to the increase in the pressure drop across the orifice. It is considered a function of the column-to-orifice diameter ratio, as can be seen in Figure 5.4, and this finding is in accordance with Lu's observation (Lu, 1988b). It was also found that when using d_o = 1 mm, the dispersion process cannot be started, i.e., the oxygen cannot be introduced to the column due to the large pressure drop across the orifice even when the (minimum liquid flowrate) was used in the system. Figure 5.4 also shows that using orifices between (d_o = 2.0 – 4.0 mm) delivered the highest values of the superficial liquid velocity at the nozzle section in DGCR. This was necessary for higher shearing rates to alter bubble sizes which consequently altered the hydrodynamic and mass transfer characteristics of the DGCR.

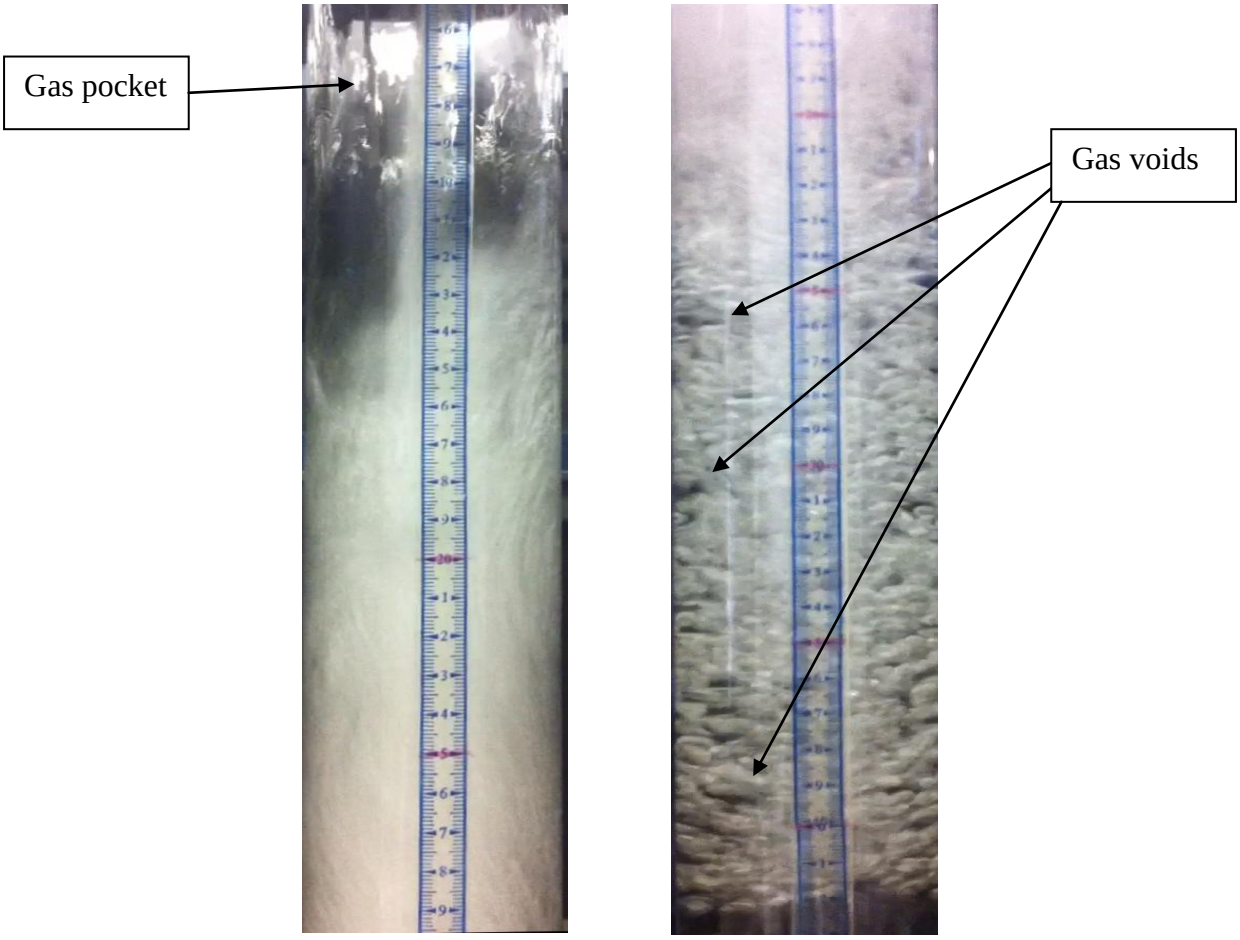

5-3a **5-3b**

Figure 5-3 Visualization of different unstable bubble dispersion processes at the top section of the DGCR column using the O_2/H_2O system, dispersion matrix collapsed with a gas pocket at the top section (5.3a), gas voids in the bubble matrix (5.3b)

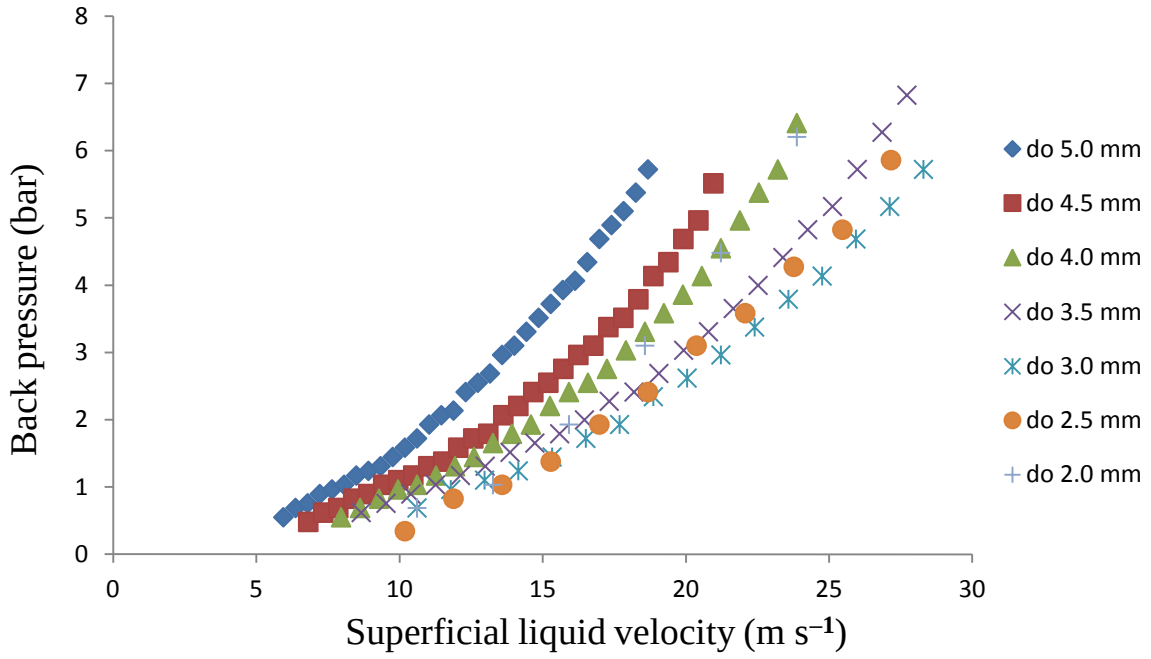

Figure 5-4 Effect of different jet nozzle orifices diameter on the back pressure at jet nozzle

5.1.1.3 Bubble Size

The ability to predict bubble size is considered one of the most important parameters in designing and scaling bubble column reactors with the knowledge of the liquid/gas/solid system characteristics (Boyes et al., 1991). The bubble dispersion in the DGCR was confirmed as non-homogeneous due to the formation of two distinct bubble size regions recognized as inlet and bulk regions as was observed by other researches (Evinc, 1982; Lu, 1988b). The average bubble size can be determined by visual analysis in the vicinity of the column wall (see Figure 3.12), which can be considered representative of the system for the experimental conditions tested. The high turbulence at the jet nozzle zone resulted in high values of the Reynolds number, as shown in Figure 5.5, which led to an efficient mixing in the entrance region as a result of injecting the

gas stream in to a high jet velocity of the liquid stream via a simple T-piece connection fitting as explained previously in Section 5.1.1. Additionally, the dispersion matrix occupied the whole volume of the DGCR column with a defined bubble boundary; it was delineated without bubble clustering and the bubbles were separated from each other by a thin layer of downflow liquid. Those conditions enabled the assumption that the bubble dispersion matrix was consistently considered stable and uniform due to the re-dispersion process of the larger bubbles by deforming and breaking in the top section of the DGCR column. Any disturbance, therefore in the balance of the forces acting on the bubbles, such as buoyancy and drag forces, will be controlled. Bubble size was controlled for the O_2/H_2O system by varying the liquid inlet and superficial velocities, gas input and different orifice sizes (d_o = 2 -5 mm) were used to change the jet velocity and their direct impact on the bubble size. The average bubble size was calculated using the visual method as discussed previously in Section 3.4.1.5, and the minimum number of bubbles was used in calculations was ≥ 250 per sample. The software used the assumption of a perfect spherical when analysing the bubbles using 2D images, which adds some error in the results due to the deformation in the shape of the bubble from the wall effect and the tendency of the bubbles in the DGCR to oblate spheroidal, especially at the bottom of the dispersion. This is a result of a prior stage of the break-up mechanism, which requires great attention in bubbles sampling, in particular for bubbles > 4 mm, which are easier to deform shape. It is found that uniform average bubble sizes of (d_b = 3-5 mm) were formed using the (d_o = 3-4 mm) orifice diameters, which gives the best optimized conditions, as shown in Figure 5.6. The 3.5 mm orifice diameter delivers the best kinetic jet power and the highest Reynolds number. This is important for achieving the best mixing rate in the first region (h_d = 20 cm) of the DGCR.

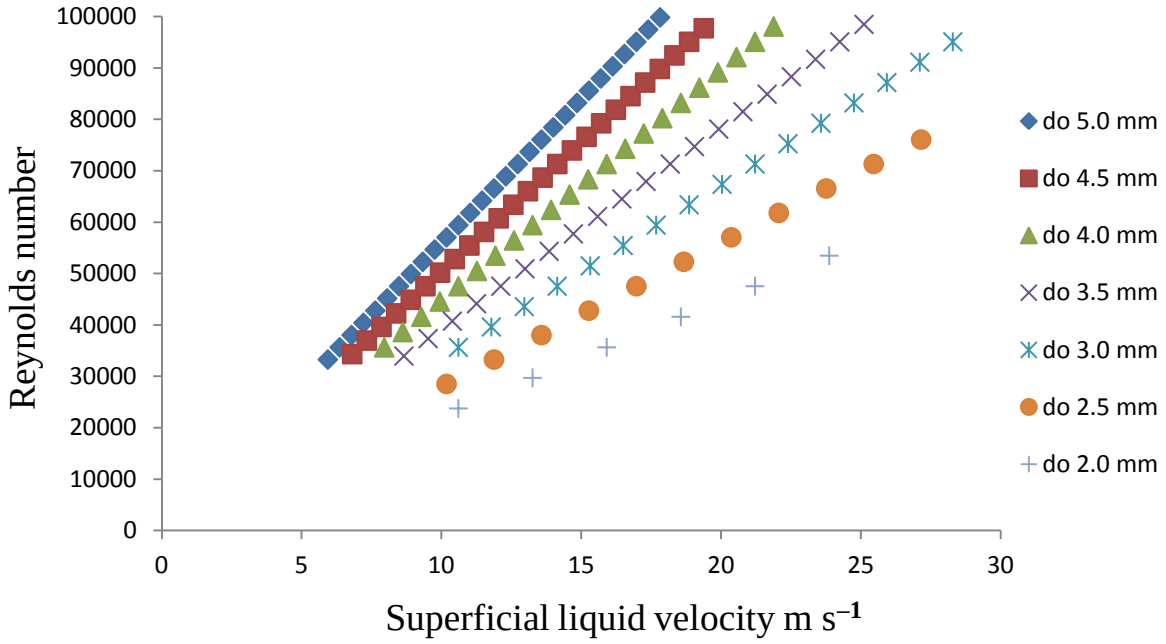

Figure 5-5 Effect of different nozzle orifices on liquid Reynolds Number in the DGCR (T = 25°C, Pcol = 1 barg)

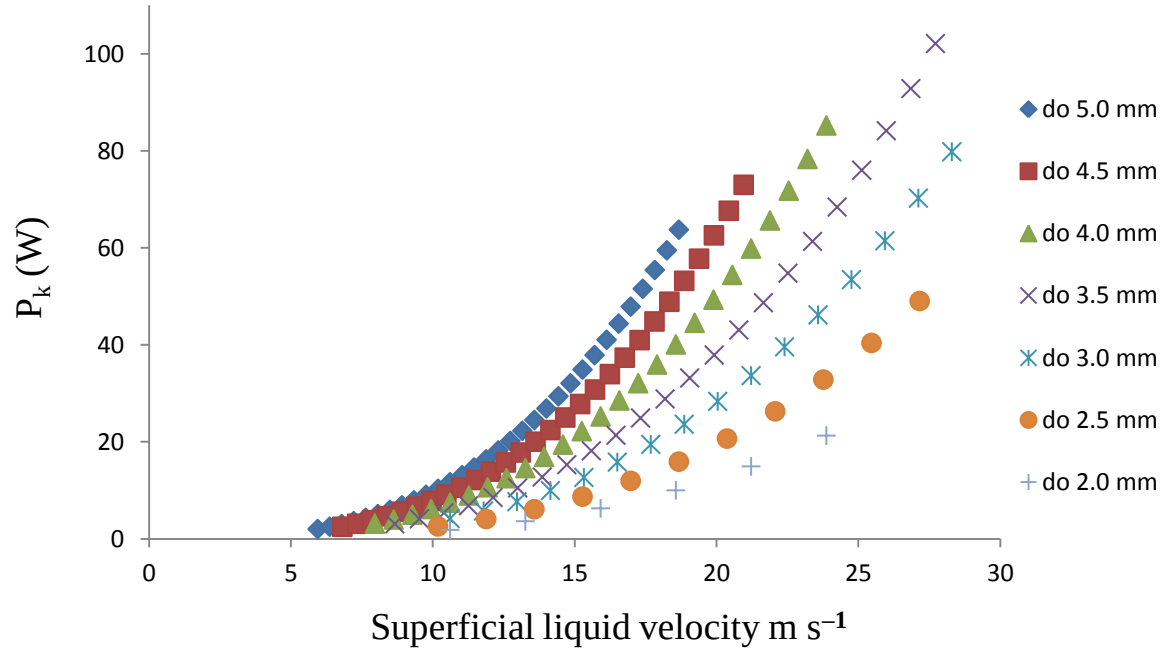

Figure 5-6 Effect of different nozzle orifices on the power input (P_k) in the DGCR (T = 25°C, P_{col} = 1 barg)

Kinetic jet power was calculated using equation 5.1 given by (Dutta and Raghavan, 1987; Tojo et al., 1982) and the Reynolds number was calculated using the standard form in equation 5.2.

$$P_k = \frac{\pi}{8} \rho L \, {d_o}^2 \, {V_j}^3 \qquad \text{(W)} \tag{5-1}$$

$$Re = \frac{d_n \, V_j}{\nu_L} \tag{5-2}$$

where:

P_k: kinetic jet power, Watt (W)

Re: Reynolds number, dimensionless quantity

ρ_L: liquid density, kg m^{-3}

d_o: orifice diameter, m

d_n: pipe diameter, m

V_j: liquid inlet velocity at nozzle, m s^{-1}

V_L: kinematic liquid viscosity, m^2 s^{-1}

The investigation of the effect of gas input flowrate (F_{O_2}) on the development of bubble dispersion in the DGCR showed that average bubble size was highly affected by the gas input (see Table 5.1), and that average bubble size increased with increasing gas input as bubble dispersion development was taking place in the DGCR. The result of different inlet velocities (V_j) on the average bubble size as the bubble dispersion developed was also examined, and the results indicated that inlet velocity has a slight effect on the average bubble size (see Table 5.2). The investigation of the effect of different liquid superficial velocities (U_L) on the average bubble

size showed that the average bubble size decreased with increasing superficial velocity as bubble dispersion development was taking place in the DGCR (see Table 5.3).

Table 5-1 Effect of oxygen input volumetric flowrate on the average bubble size (d_o = 3.5 mm, T = 25°C, P_{col} = 1 barg)

F_{O_2} (L min^{-1})	V_j (m s^{-1})	U_L (m s^{-1})	d_b (mm)	h_d (m)
0.1	13.86	0.07	3.0 ± 0.1	0.25
0.2	13.86	0.07	3.4 ± 0.1	0.30
0.3	13.86	0.07	4.0 ± 0.1	0.35
0.4	13.86	0.07	4.1 ± 0.1	0.40
0.5	13.86	0.07	4.4 ± 0.1	0.45
0.6	13.86	0.07	4.5 ± 0.1	0.50

Table 5-2 Effect of different inlet velocities on the average bubble size (T = 25°C, P_{col} = 1 barg)

F_{O_2} (L min^{-1})	V_j (m s^{-1})	U_L (m s^{-1})	d_b (mm)	h_d (m)
0.1	7.64	0.08	3.3 ± 0.1	0.25
0.2	9.43	0.08	3.3 ± 0.1	0.30
0.3	11.94	0.08	3.5 ± 0.1	0.35
0.4	15.59	0.08	3.4 ± 0.1	0.40
0.5	21.22	0.08	3.2 ± 0.1	0.45
0.6	30.56	0.08	3.2 ± 0.1	0.50

Table 5-3 Effect of different superficial velocities on the average bubble size (d_o = 3.5 mm, T = 25°C, P_{col} = 1 barg)

F_{O_2} (L min^{-1})	V_j (m s^{-1})	U_L (m s^{-1})	d_b (mm)	h_d (m)
0.1	12.13	0.06	3.7 ± 0.1	0.25
0.1	13.86	0.07	3.8 ± 0.1	0.30
0.1	15.59	0.08	3.6 ± 0.1	0.35
0.15	17.32	0.09	3.2 ± 0.1	0.40
0.15	19.92	0.10	3.0 ± 0.1	0.45
0.15	21.65	0.11	2.9 ± 0.1	0.50

5.1.1.4 Gas holdup (εg)

Gas holdup (ε_g), defined as the percentage by volume of gas in two or three phase dispersion, is one of the most important parameters in the DGCR since it is directly related to the interfacial area available, which leads to the assessment of the volumetric gas-liquid mass transfer coefficient (k_La). Many factors affecting gas hold-up values, such as liquid properties; orifice size, which is related to the change in jet velocity and its direct impact on the bubble size; column geometric design; and the gas input. It is possible to achieve high gas hold-up values up to 50-60 % in a strong coalescence system such as oxygen/water system (Lu, 1988b; Tilston, 1990). Gas holdup was highly affected by the dispersion height due to the direct effect of the gas input and liquid superficial velocity on the dispersion height. Gas holdup continued to increase until the bubble coalesce process of smaller size into larger size is occurred. Figure 5.7 shows

that the gas hold-up for the O_2/H_2O system was independent of the dispersion height until the interfacial area was stabilised and a bubble matrix started to form (h_d = 20 cm).

Figure 5-7 Beginning of a stable stage of the bubble matrix in DGCR column (h_d = 20 cm)

The effect of gas input on the gas hold-up can be related to the dispersion height, which can be considered as a secondary effect due to the dependency of the dispersion height on the gas input, liquid inlet and superficial velocities. At the selected conditions tested, the dispersion height increased as the gas input into the system increased (Figure 5.8); this observation does seem plausible. Also, it was found that dispersion height values increased as superficial velocity

increased for the selected liquid inlet velocity, and this can be assigned to the increased drag force acting on bubbles. Figure 5.9 shows that gas hold-up values started to increase as the dispersion height increased until gas hold-up achieve 50–55% and then started to fluctuate at this value, this observation gave an indication to the higher contact efficiency compared with the up-flow columns which was less than 2% (Fujie et al., 1980; Herbrechtsmeier et al., 1984; Ohkawa et al., 1987). This high value of gas hold-up indicates that DGCR can achieve the maximum residence time value (i.e., the gas phase residence time was equal to the contact time) due to the balance between bubble rise velocity and liquid downflow velocity, which led to the bubbles being in a suspension state in a well-defined volume of the DGCR column. It is also noted that the effect of increasing the liquid superficial velocity led to lower values of gas hold-up as a consequence of the increase in the drag force acting on the bubbles which affected the coalescing process.

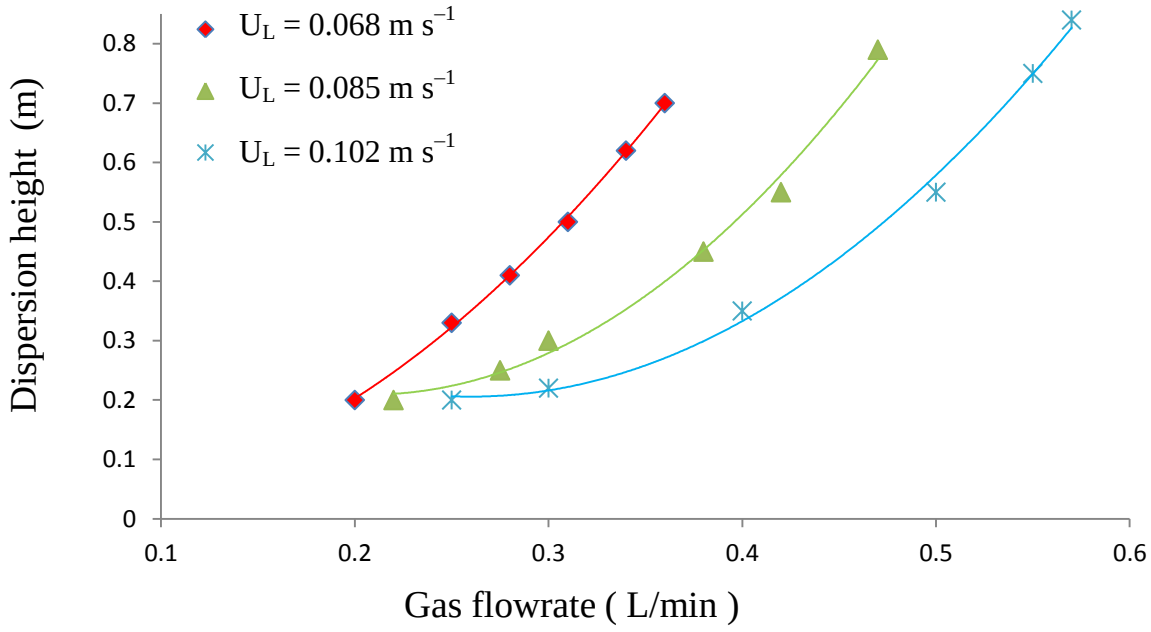

Figure 5-8 Effect of gas input with different liquid superficial velocity (U_L) on the dispersion height (V_j = 13.86 m s^{-1}, d_o = 3.5 mm, T = 25°C, P_{col} = 1 barg)

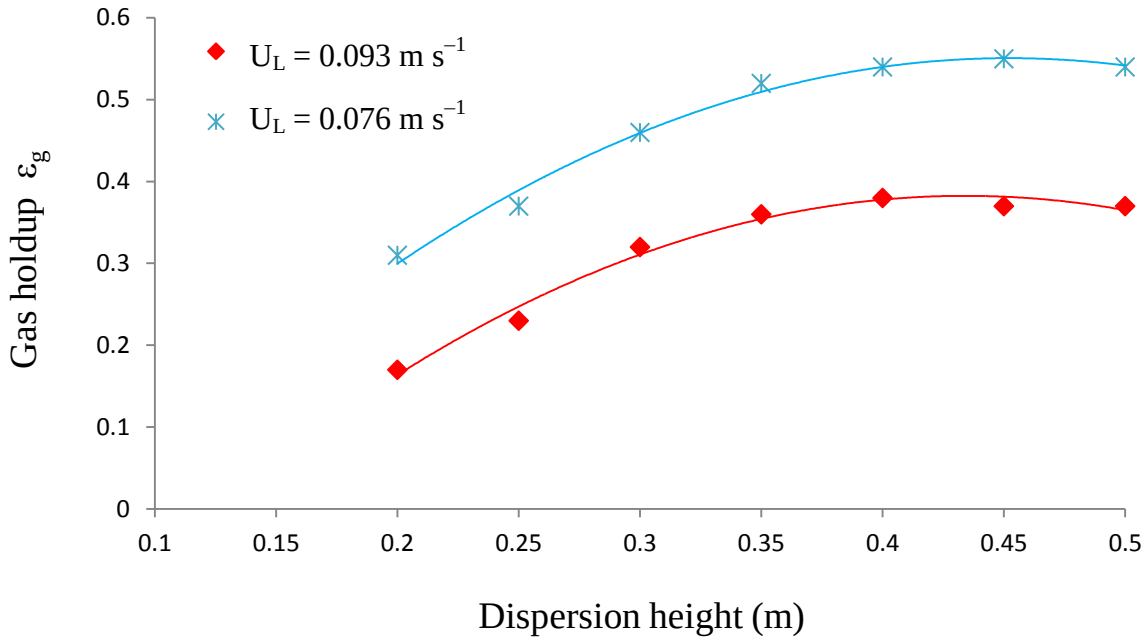

Figure 5-9 Effect of dispersion height with different liquid superficial velocity (U_L) on the gas hold-up (Vj = 15.6 m s^{-1}, do = 3.5 mm, T = 25°C, Pcol = 1 barg)

5.1.1.5 Gas-Liquid Interfacial Area (a)

Interfacial area (a) was calculated based on physical methods; it is related to the gas holdup and the Sauter mean diameter (mean surface to volume diameter), as shown previously in equation 3.3 and described by (Patel et al., 1989);

$$a = \frac{6\,\varepsilon_g}{d_s} \qquad 5\text{-}3$$

Equation 5.3 is based on the following assumptions:

- The spherical bubbles are perfect and have uniform size. This is an oversimplification especially with a high turbulent system, and is considered a rough assumption.
- The bubble matrix packs in a body-centred cubic arrangement.

- The absorption process is at steady state.

The results shown in Figure 5.10 and Figure 5.11, illustrate that the trends of interfacial area were similar to the gas hold-up behaviour, with the highest value for the interfacial area under the given operating parameters being 920 m^2 m^{-3}. Furthermore, it is found that increasing both gas input and dispersion height led to an increasing interfacial area value until a maximum value was reached at the same point where the gas hold-up was at its highest value. At higher values it then started to decrease. Increasing the liquid superficial velocity led to a decrease in the interfacial area values in a similar manner to the gas hold-up.

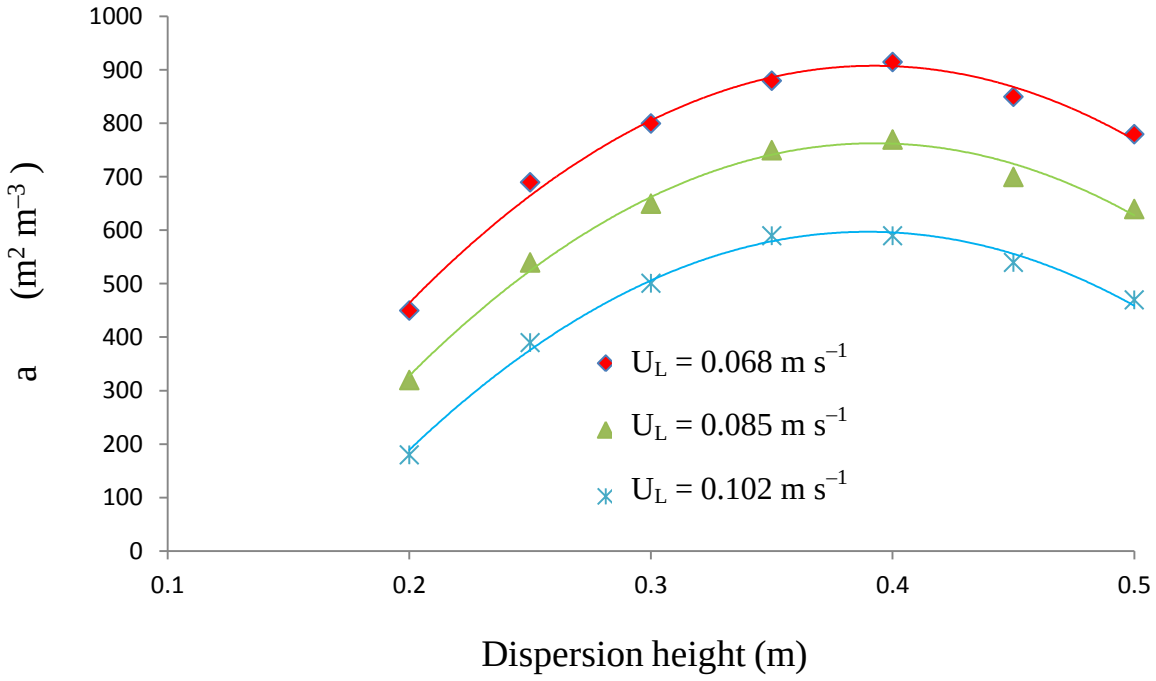

Figure 5-10 Effect of dispersion height with different liquid superficial velocity (U_L) on the specific interfacial area (V_{in} = 13.86 m s^{-1}, d_o = 3.5 mm, T = 25°C, P_{col} = 1 barg)

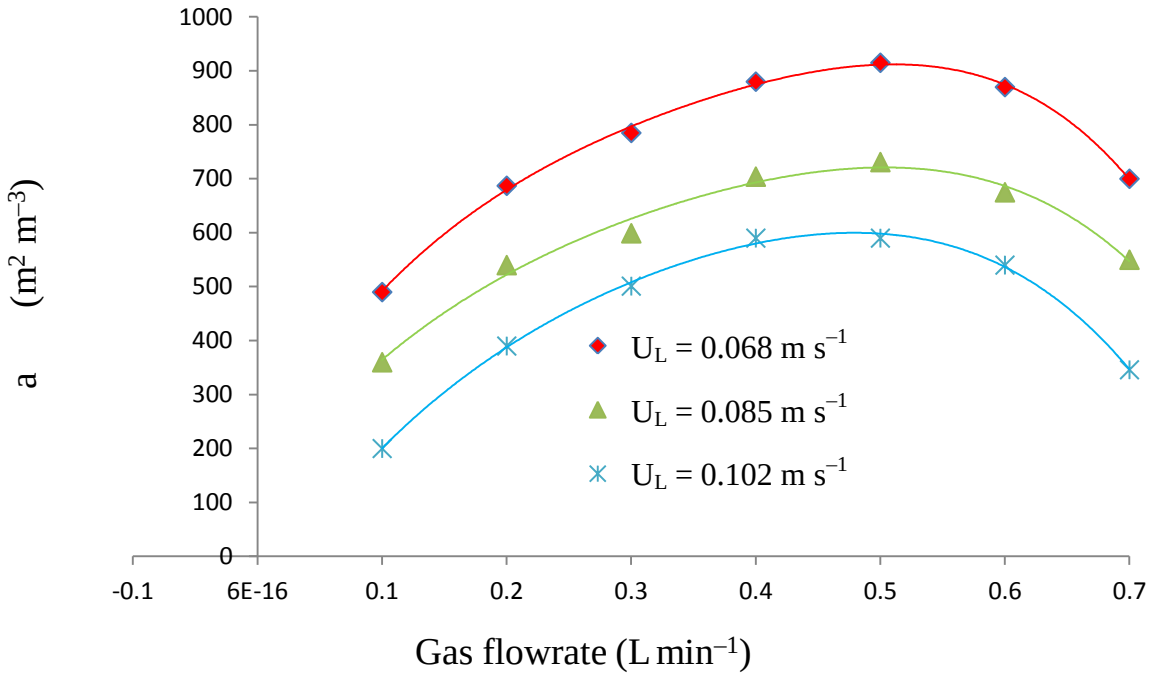

Figure 5-11 Effect of gas input with different liquid superficial velocity (U_L) on the specific interfacial area (V_{in} = 13.86 m s^{-1}, d_o = 3.5 mm, T = 25°C, P_{col} = 1 barg)

5.1.2 Gas Liquid Mass Transfer Characteristics

5.1.2.1 Dissolved Oxygen Profiles

The relationship between dissolved oxygen (DO) concentration profiles and the dispersion height for different liquid superficial velocities is shown in Figure 5.12. The results indicate that as the bubble matrix expanded; i.e., the axial dispersion height increased steadily, the DO concentration also increased, which means that more oxygen was dissolved by the time equilibrium state was reached. This observation does seem plausible; as more gas was fed into the column, the mass transfer process was developing and taking place from the gas phase to the

liquid phase. The dissolved oxygen rate also increased very fast in the first 30 cm in length of the DGCR column due to high turbulent mixing and the ability for the liquid phase to dissolve more oxygen. This indicated that the driving force in the top section was higher than the bottom section before the equilibrium stage was reached (h_d = 50-70 cm). The results also illustrate the effect of different liquid superficial velocity on the concentration profiles. As can be seen, DO concentration increased as the liquid superficial velocities increased for the conditions selected as a result of the drag force acting on the bubbles which means more gas is needed to be fed to the system.

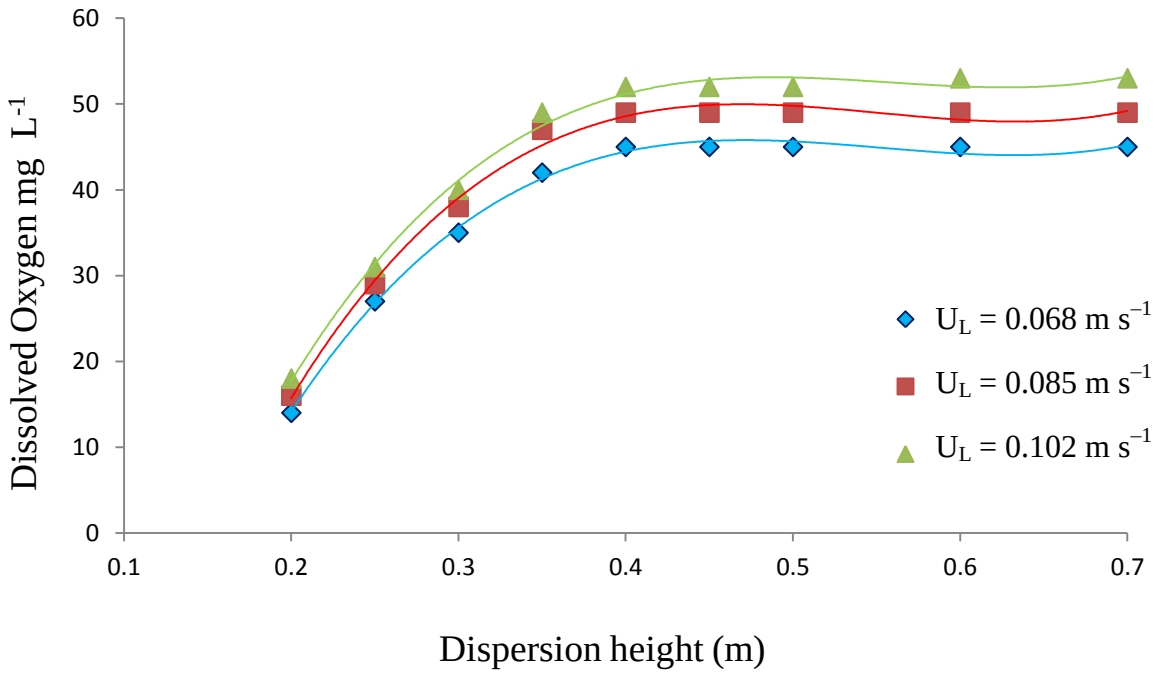

Figure 5-12 Effect of dispersion height with different liquid superficial velocity on the dissolved oxygen (d_o = 3.5 mm, T = 25°C, P_{col} = 1 barg)

5.1.2.2 Volumetric Gas-Liquid Mass Transfer Coefficient $K_L a$

The excellent performance of the DGCR in approaching gas/liquid equilibrium in a short time with 100% of gas utilization results in high values of the volumetric gas-liquid mass transfer coefficient ($K_L a$) (Alenezi et al., 2010a; Alenezi et al., 2010b; Boyes et al., 1992a; Boyes & Ellis, 1976; Ochuma et al., 2007a; Sulidis, 1995; Winterbottom et al., 1997a). The assumption for the mixing pattern along the DGCR column may produce unrealistic results. The first region considers a high-turbulent flow, and the second region is less turbulent with stable and uniform bubble dispersion, as discussed previously in Section 5.1.1. It is more reasonable to consider the first 20 cm to be ideal mixing (perfect mixing), and the plug flow reactor approach can be applied for h_d >20 cm as recommended by (Sarmento, 1995). The flow patterns of the DGCR were based on two models using the O_2/H_2O absorption system; both the plug flow model (equation 5.4) and the mixed flow model (complete mixing, equation 5.5) were described by (Sulidis, 1995).

Plug flow model

$$K_L a = \frac{F_L}{V_d} \ln\left(\frac{c^* - c_i}{c^* - c_o}\right) \quad \text{5-4}$$

Mix flow model

$$K_L a = \frac{F_L}{V_d} \ln\left(\frac{c_o - c_i}{c^* - c_o}\right) \quad \text{5-5}$$

Where:

$K_L a$: volumetric gas-liquid mass transfer coefficient, s^{-1}

F_L: liquid flowrate, m^3/s

V_d: gas-liquid dispersion volume, m

C^*: equilibrium concentration of gas in the liquid phase, mg L^{-1}

C_i: concentration of gas in liquid phase at dispersion inlet, mg L^{-1}

C_o: concentration of gas in liquid phase at dispersion outlet, mg L^{-1}

Figures 5.13 and 5.14 show the effect of the gas dispersion height with different liquid superficial velocity on the volumetric mass transfer coefficient for the O_2/H_2O system. The K_La value increased as the axial dispersion height increased steadily and was much improved by using higher liquid superficial velocities with a strong effect to the dissolved oxygen profiles, explained previously in Section 5.1.2.1. The figures also show that K_La values of the mixed flow model were higher than the plug flow model as a result of the logarithmic nature of the lumped concentration term in equation 5.4.

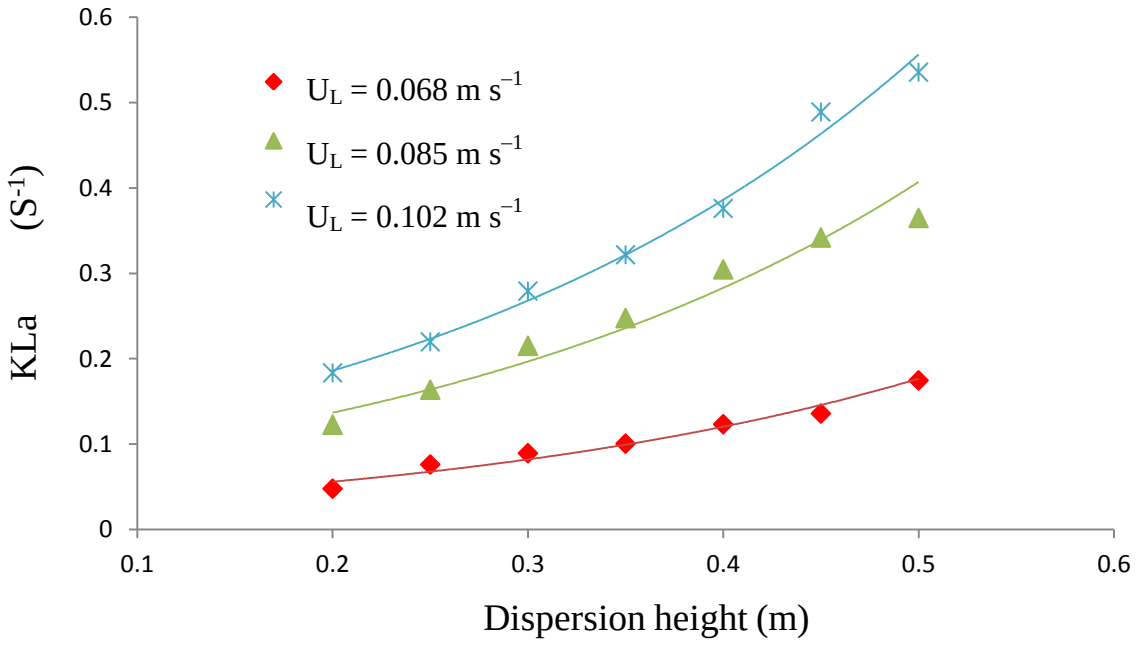

Figure 5-13 Effect of dispersion height with different liquid superficial velocity on the volumetric mass transfer coefficient (Mixed flow model, d_o = 3.5 mm, T = 25°C, P_{col} = 1 barg)

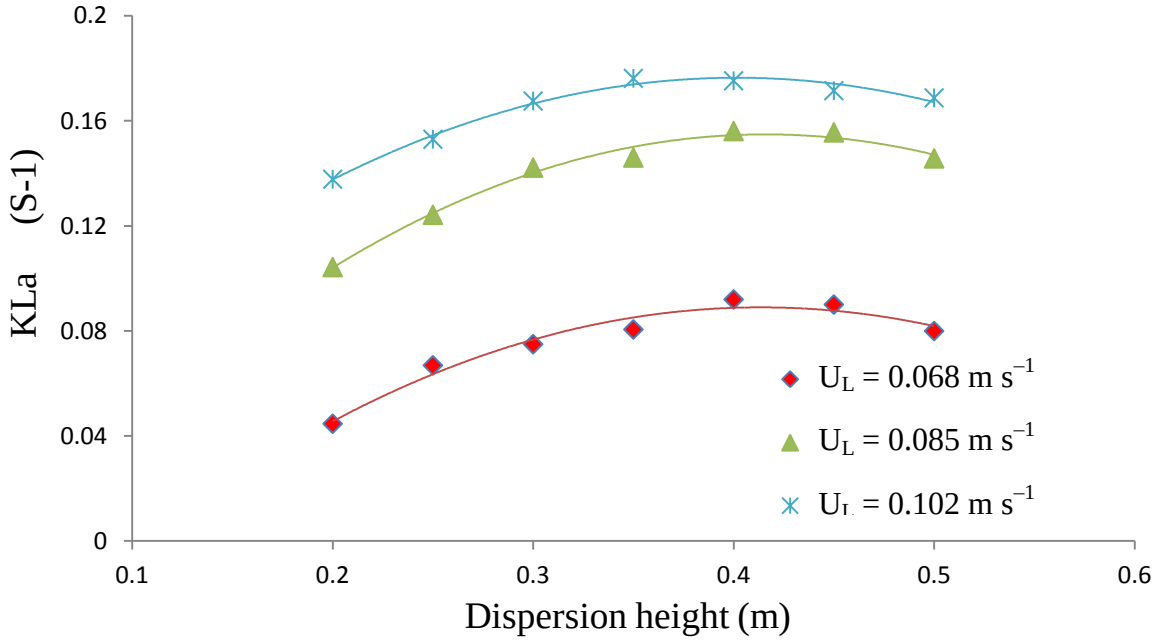

Figure 5-14 Effect of dispersion height with different liquid superficial velocity on the volumetric mass transfer coefficient (Plug flow model, d_o = 3.5 mm, T = 25°C, P_{col} = 1 barg)

5.2 Conclusion

Extensive experimental work examined the DGCR performance to evaluate its hydrodynamic and mass transfer characteristics in order to identify the optimum operating conditions required for the removal of the EDCs present in the water samples. It was found that using orifices between (d_o = 2.0–4.0 mm) delivered the highest values of the superficial liquid velocity at the nozzle section in DGCR. This was necessary for higher shearing rates to alter bubble sizes which consequently altered the hydrodynamic and mass transfer characteristics of the DGCR. Bubble size also was highly affected by the gas input, and the average bubble size increased with increasing gas input. On the contrary, average bubble size decreased with increasing superficial velocity as bubble dispersion development was taking place in the DGCR.

Gas hold-up values up to 50–60% were achieved and were highly affected by the dispersion height, which increased as more gas input and higher superficial velocity was present in the system. It was found that DGCR can achieve the maximum residence time value. It was also noted that the effect of increasing the liquid superficial velocity led to lower values of gas hold-up. The results illustrate that the trends of interfacial area were similar to those of gas hold-up behaviour. The highest value for the interfacial area under the given operating parameters was 920 m^2 m^{-3} compared with previous studies with 870 m^2 m^{-3} (Zhang, 1997) and 828 m^2 m^{-3} (Sarmento, 1995). Increasing both the gas input and dispersion height, led to the interfacial area value also being increased, whereas increasing the liquid superficial velocity led to the decrease in the interfacial area values with (a similar behaviour to the gas hold-up). Dissolved oxygen (DO) concentration increases with the increase of the axial dispersion height until an equilibrium state is reached at (h_d = 40–70 cm). DO concentration also increased as the liquid superficial velocity increased for the conditions selected. The results show that K_La value increased as the axial dispersion height increased steadily and was much improved by using higher liquid superficial velocities. It was found that K_La values for the mix flow model were higher than the plug flow model as a result of the logarithmic nature of the lumped concentration term in equation 5.4 and the assumption of the perfect mixing state in equation 5.5.

CHAPTER 6

6 ADVANCED OXIDATION AND DEGRADATION STUDIES OF SELECTED FEMALE STEROID HORMONES IN AQUEOUS SOLUTION

6.1 Results and Discussion

The following factors on the photodegradation and removal efficiency of selected female steroid hormones, 17β-E2, 17α-E2, E1 and PG in aqueous solution were studied and are described in detail. This included the effects of initial concentration, initial pH, different oxygen flowrate, initial H_2O_2 concentration and the effect of using different combination of wastewater treatment systems. Some preliminary experiments for each hormone were tested individually; the behaviour of using a mixture was similar and can be found in appendix 9.9. All degradation studies were conducted as a mixture of 17β-E2, 17α-E2, E1 and PG which was considered more cost and time effective, however for clarity the results are shown for each hormone separately.

Photodegradation and removal efficiency experiments were all conducted using deionised water. The impact for more complex matrices such as surface and wastewater can highly affect the process efficiency of the treatment methods used by the presence of more scavengers that will

consume the hydroxyl radicals and affect the irradiation intensity, which can lead to lower oxidation performance (Ribeiro et al., 2015).

The concentration of the selected model pollutants and the analytical method described previously in chapter 4 were used. The removal efficiency, which represents the change in concentration as a function of time and describes the degradation processes, is given by:

$$\text{Removal percent} = \frac{C_o - C}{C_o} \times 100 \qquad 6\text{-}1$$

Where:

C: concentrations at time t (min), ng L^{-1}

C_o: concentrations before treatment (t = 0), ng L^{-1}

Unless stated, all experiments were conducted under the following conditions by changing one variable while keeping other parameters constant; i.e. temperature, pressure (P_{col} = 1 bar), liquid flowrate (F_L = 10 L min^{-1}), initial concentration (10000 ng L^{-1} of each pollutant) and deionised water without pH adjustment (pH = 6.8). The optimum operating conditions of the DGCR required for the removal of the EDCs present in the water samples were used as discussed previously in chapter 5. Data points shown in the figures are experimental results with error bars representing the standard deviation (SD) of triplicate. UV dose were 0, 48000, 96000, 144000, 192000, 240000, 288000, 336000 and 384000 mJ cm^{-2} of irradiation time 0, 2, 4, 6, 8, 10, 12, 14, and 16 min, respectively. The change in concentration was described as a function of time instead of UV dose to be represented in the kinetic model proposed.

6.1.1 Degradation Kinetics Model

A simple pseudo-first order kinetic model was proposed to describe the degradation kinetics of 17β-E2, 17α-E2, E1 and PG using the DGCR with different experimental conditions as shown in Eq. 6-2. The model was fitted to the experimental results and was represented as dashed lines in the figures. The kinetic model linearity had an $R^2 \geq 99\%$, suggesting that the model was in good agreement with experimental data. This result is consistent with previous studies of photodegradation of steroid hormones (Frontistis et al., 2011; Liu and Liu, 2004; Zhang and Li, 2014; Zhang et al., 2007).

$$C^{cal} = C_o e^{-kt} \quad (6\text{-}2)$$

$$OF = Minimise \sum_{j=1}^{N} \left(\frac{[C]_j^{exp} - [C]_j^{calc}}{[C]_j^{exp}} \times 100 \right)^2 \quad (6\text{-}3)$$

Where:

C^{calc}: calculated concentrations at time t (min), ng L^{-1}

C_o: concentrations before treatment (t = 0), ng L^{-1}

C^{exp}: experimental concentrations at time t (min), ng L^{-1}

k: rate constant (min^{-1})

t: time (min)

N: number of experimental data points

Objective function (OF) given by Eq.6-3 represents the sum of the squares of percentage error between experimental concentrations and calculated concentrations (kinetic model), OF was minimised using the built-in solver function in Excel (Microsoft Office 2007) with acceptable constrain ($R^2 \geq 90$). The minimised average errors between experimental and calculated data were

found to be 5.65 ≤ for 17β-E2, 4.69 ≤ for 17α-E2, 6.61 ≤ for E1 and 7.77 ≤ for PG. Figure 6-1 shows the algorithm of parameter estimation for degradation kinetics model. The pseudo-first order kinetic rate constants (k, min^{-1}) values were estimated for the best possible representation of the experimental data.

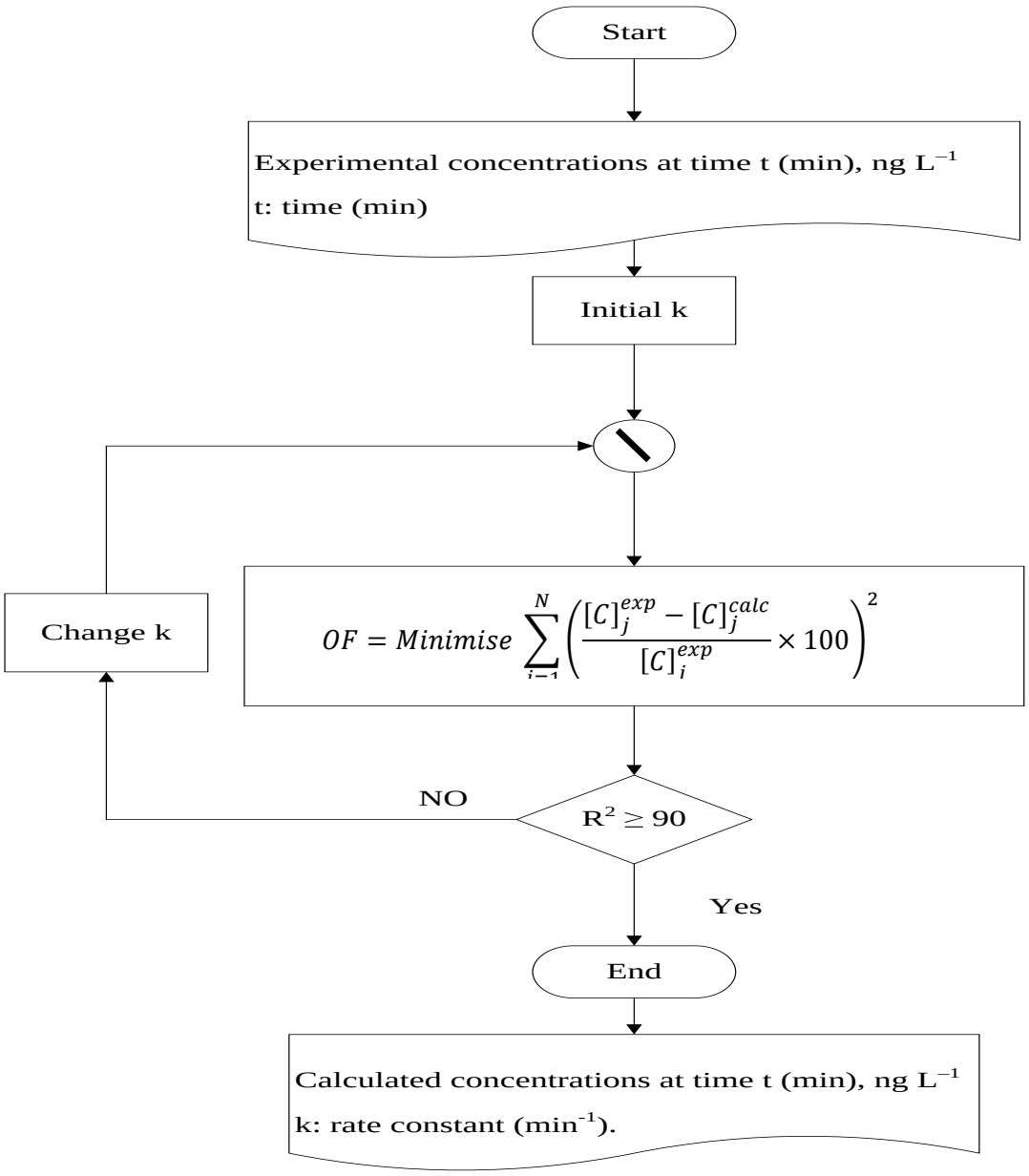

Figure 6-1 Flowchart of parameter estimation for degradation kinetics model

6.1.2 Effect of Initial Concentration

To evaluate the UV system in the absence of dissolved oxygen, DGCR was deoxygenated by pure nitrogen for 60 min before starting the experiments. To study the effect of initial concentration on the photodegradation process of model pollutant in aqueous solutions, various concentrations of 17β-E2, 17α-E2, E1 and PG at 1000, 5000 and 10000 ng L^{-1} were used. As shown in Figure 6.2, the photodegradation of 17β-E2 consist of two regions, fast degradation in the first 6 min of UV irradiation time followed by a slow degradation process. The removal efficiencies of 17β-E2 of initial concentration of 1000, 5000 and 10000 ng L^{-1} were 82.8%, 78.7% and 77.1%, respectively at t = 6 min. Simultaneously, 99.0%, 98.7 % and 97.9 %, respectively were achieved at the end of experiments (t = 16 min). The results also show that the effect of initial concentration has a dominant effect on the degradation rate; as the initial concentration increased the degradation rate decreased following the pseudo-first order reaction kinetics of equation 6.2. This trend can be explained by the decreased photon penetration generated by UV radiation absorbed by the organic molecules at higher initial concentrations, which increases the solutions resistance to UV radiation (Chowdhury et al., 2011; Liu & Liu, 2004; Zhang et al., 2010). Table 6.1 shows the results of the rate constants of 17β-E2 photodegradation and were 0.3830, 0.3455 and 0.2901 min^{-1} of initial concentration 1000, 5000 and 10000 ng L^{-1}, respectively, suggesting that UV power irradiation can be considered an effective treatment method for the degradation of the selected model pollutants.

Table 6-1 Pseudo-first order rate constant for the degradation of 17β-E2, 17α-E2, E1 and PG under different initial concentrations, $R^2 \geq 99\%$

Analyte			
	C_o ng L^{-1}		
	1000	5000	10000
	k min^{-1}		
17β-E2	0.3830	0.3455	0.2901
17α-E2	0.3219	0.2959	0.2822
E1	0.3363	0.3241	0.2972
PG	0.2344	0.2229	0.2108

The results shown in Figure 6.3 and Figure 6.4, illustrate that the behaviour of 17α-E2 and E1 removal efficiencies were similar to that of 17β-E2. The removal efficiencies of 17α-E2 increased rapidly in the first 6 min by approximately 81.9%, 78.7% and 77.1% of initial concentration of 1000, 5000 and 10000 ng L^{-1}, respectively. Simultaneously, the removal efficiencies of E1 increased rapidly in the first 6 min to approximately 83.4%, 81.9% and 78.5 % of initial concentrations of 1000, 5000 and 10000 ng L^{-1}, respectively. Again, increasing the initial concentration decreased the degradation rate following the pseudo-first order reaction kinetics of equation 6.2. As shown in Table 6.1, the rate constants of 17α-E2 photodegradation were 0.3219, 0.2959 and 0.2822 min^{-1} of initial concentration 1000, 5000 and 10000 ng L^{-1}, respectively. Whereas, the rate constants of E1 photodegradation were 0.3363, 0.3241 and 0.2972 min^{-1} for the same initial concentrations. At the end of experiments (t = 16 min), the removal of 17α-E2 was 98.9%, 98.3% and 97.9% of initial concentration 1000, 5000 and 10000 ng L^{-1},

respectively, whereas the removal of E1 was 99.2%, 99.0% and 98.3% for the 1000, 5000 and 10000 ng L^{-1}, respectively.

The results shown in Figure 6.5, illustrate that the trends in the PG degradation rate were slower than 17β-E2, 17α-E2 and E1. This result can be attributed to the optimum wavelength that can be absorbed for each component. The best wavelength with the maximum absorbance for 17β-E2, 17α-E2 and E1 was 200 nm; whereas 243 nm was the best wavelength with the maximum absorbance for PG as discussed previously in section 3.6.7. The removal efficiencies of PG increased rapidly in the first 6 min by approximately 71.1%, 69.4 and 67.1% for the 1000, 5000 and 10000 ng L^{-1} concentrations, respectively. Similarly, increasing the initial concentration decreased the degradation rate following the pseudo-first order reaction kinetics of equation 6.1. As can be seen in Table 6.1, the rate constants of PG photodegradation were 0.2344, 0.2229 and 0.2108 min^{-1} for the initial concentrations of 1000, 5000 and 10000 ng L^{-1}, respectively. At the end of experiments (t = 16 min), the removal of PG about 96.5%, 96% and 95% for the same concentrations.

DGCR is one of the most effective mass transfer devices, which can achieve high mass transfer efficiency, outstanding mixing and the enormously high interfacial area that aids chemical reaction and enables reaction to occur in very short irradiation times (Winterbottom et al., 1997b). Although removal efficiency was slightly improved when a UV/O_2 system was used, this can be attributed to the lower oxidation potential of O_2 (1.23 eV) compared with H_2O_2 (1.77 eV). In addition, a study comparison employing the use of pure oxygen with air using DGCR shows that the time needed for achieving total degradation was doubled using the H_2O_2/air system (Ochuma, 2007). This indicates the enhancement role of using O_2 and making the most of

the mass transfer efficiency using DGCR. Therefore, O_2 can improve reaction rates; higher O_2 flowrate can increase the rate of photodegradation and removal efficiency.

The complete photodegradation of 17β-E2, 17α-E2, E1 and PG by the absorption of UV radiation to the final products (CO_2, H_2O) can occur (Ahmed et al., 2009; Balcerski et al., 2007; Neamtu et al., 2002) , however for E1, intermediate was formed in the first 2 min which then break down to the final products CO_2, H_2O (See section 4.2). The photodegradation process can be represented by the following reactions:

17β-E2 $$C_{18}H_{24}O_2 + h\nu \rightarrow CO_2 + H_2O$$ 6-4

17α-E2 $$C_{18}H_{24}O_2 + h\nu \rightarrow CO_2 + H_2O$$ 6-5

E1 $$C_{18}H_{22}O_2 + h\nu \rightarrow \text{Intermediate}$$ 6-6

$$\text{Intermediate} + h\nu \rightarrow CO_2 + H_2O$$

PG $$C_{21}H_{30}O_2 + h\nu \rightarrow CO_2 + H_2O$$ 6-7

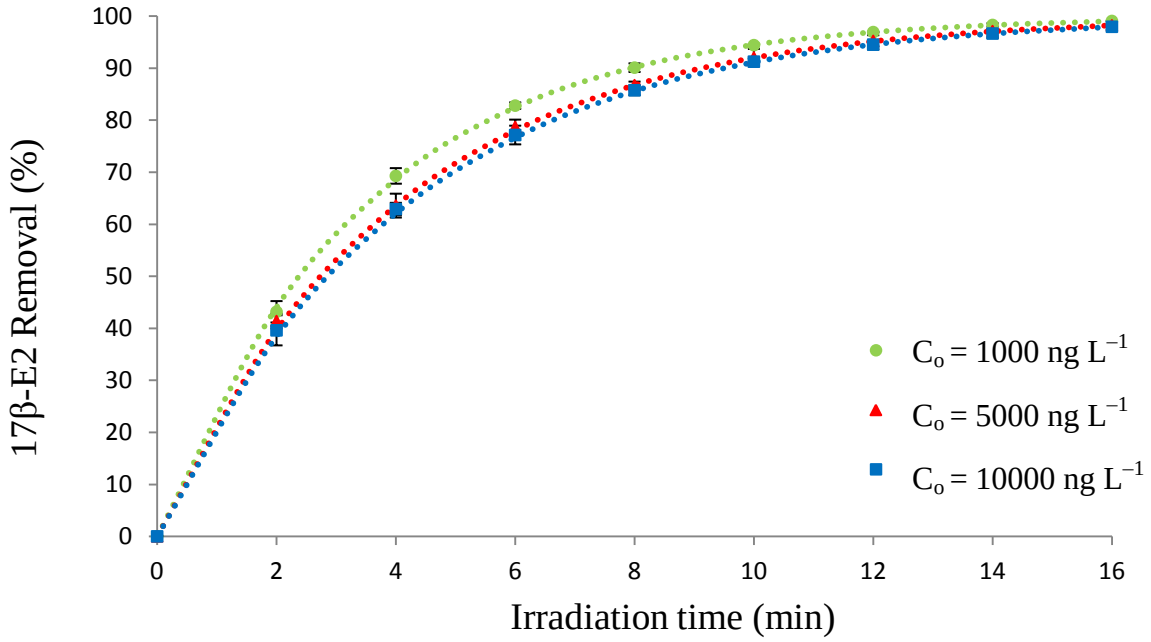

Figure 6-2 Effect of different starting concentration on 17β-E2 degradation, initial pH 6.8 and T = 35°C, data points are experimental results and the model is represented as dashed lines, (no oxidizing agents are used).

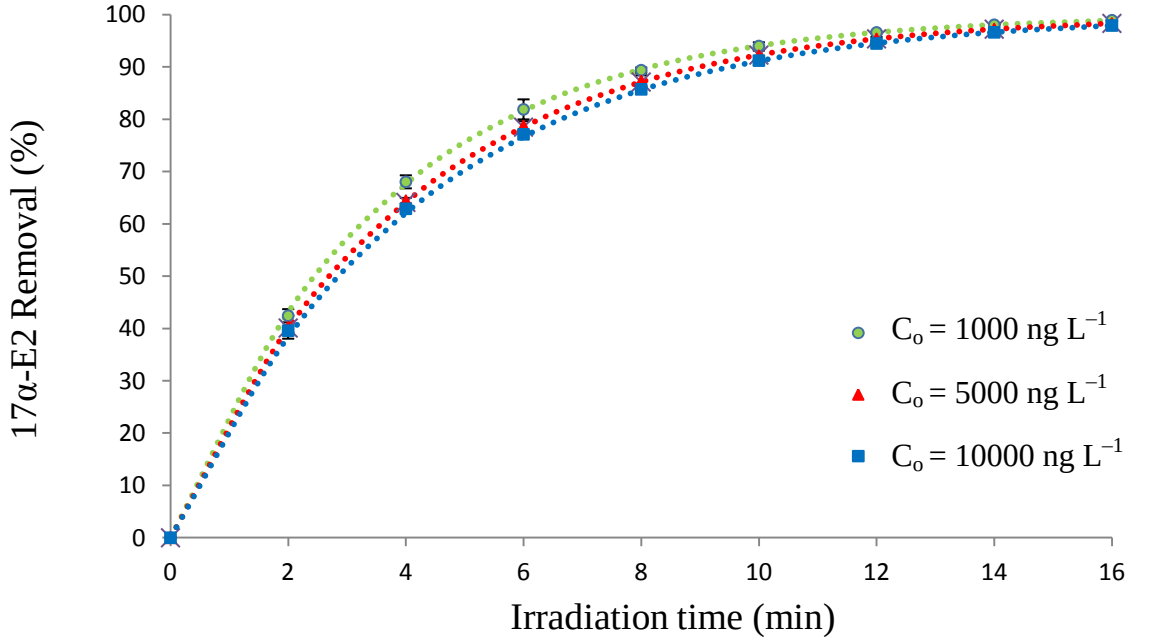

Figure 6-3 Effect of different starting concentration on 17 α-E2 degradation, initial pH 6.8 and T = 35°C, data points are experimental results and the model is represented as dashed lines, (no oxidizing agents are used).

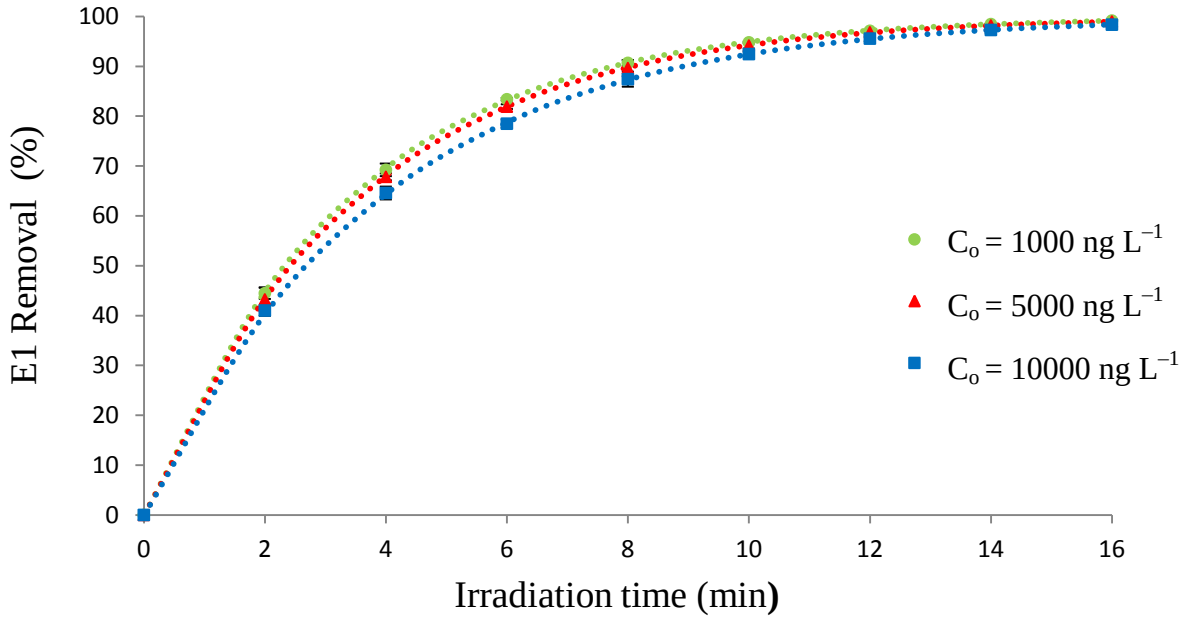

Figure 6-4 Effect of different starting concentration on E1 degradation, initial pH 6.8 and T = 35°C, data points are experimental results and the model is represented as dashed lines, (no oxidizing agents are used).

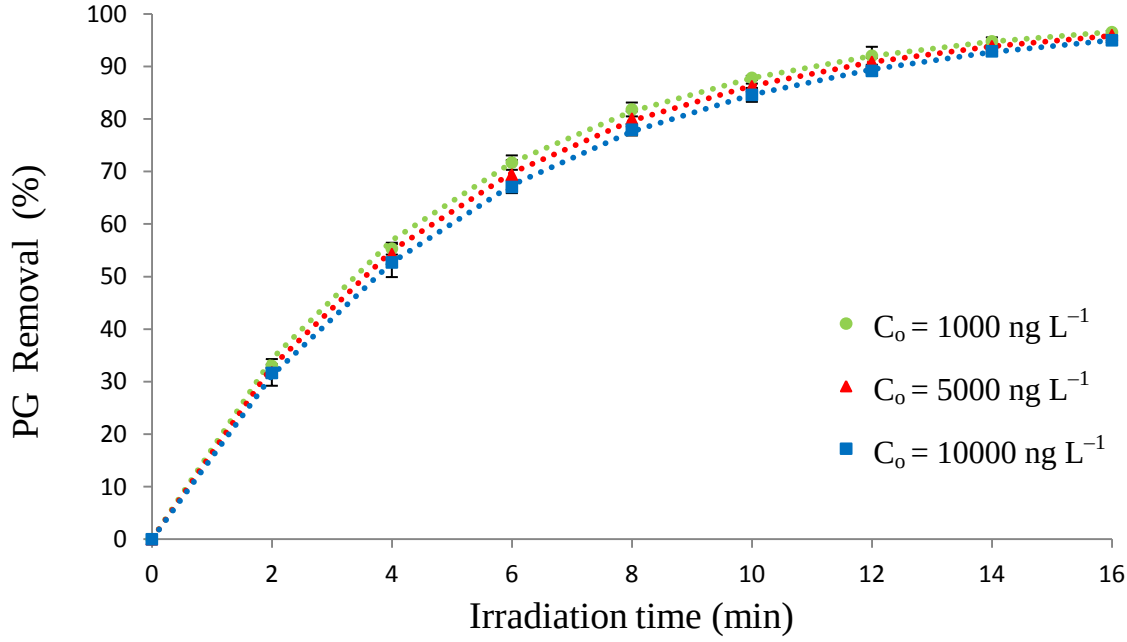

Figure 6-5 Effect of different starting concentration on PG degradation, initial pH 6.8 and T = 35°C, data points are experimental results and the model is represented as dashed lines, (no oxidizing agents are used).

6.1.3 Effect of Initial pH

The water pH is considered as one of the important factors to influence the photodegradation rate of EDCs in aqueous solutions. The effect of initial pH on the photodegradation rate of 17β-E2, 17α-E2, E1 and PG as model pollutants in aqueous solutions was carried out on a pH range of 3, 5, 6.8, 9 and 11. The pH of the DGCR solution was adjusted as described previously in section 3.5.1 using NaOH and H_2SO_4. Figure 6.6 illustrates the photodegradation of 17β-E2 at the selected pH range using the removal efficiency given by equation 6.1. The effect of UV irradiation (which is the main factor affecting the whole photodegradation process) in combination with pH adjustment had a significant impact on the photodegradation trend within the fast degradation region (<6 min) and in the ensuing a slow degradation process. Notably, the removal efficiency of 17β-E2 at a pH of 3, 5, 6.8, 9 and 11 were 67.0%, 80.7%, 87.8%, 53.4% and 46.2%, respectively at t = 6 min. Simultaneously, 94%, 98.7%, 99.7%, 87.1% and 82%, respectively were achieved at the end of experiments (t = 16 min). Table 6.2 shows the results of the rate constants of 17β-E2 photodegradation and were 0.1815, 0.2710, 0.3521, 0.1292 and 0.1062 min^{-1} at pH range 3, 5, 6.8, 9 and 11, respectively. The results verified that the optimum pH value was in the range of 5–7 and the lowest degradation rate was in the alkaline range, which implies that the removal efficiency has a pH dependency and can affect the formation of the hydroxyl radicals ($OH^{\bullet}$). The results shown in Figure 6.7 and Figure 6.8, illustrate that the behaviour of 17α-E2 and E1 removal efficiency were similar to that of the 17β-E2 degradation behaviour.

Table 6-2 Pseudo-first order rate constant for the degradation of 17β-E2, 17α-E2, E1 and PG under different pH, R2 ≥ 99%

Analyte	pH				
	3	5	6.8	9	11
	k min^{-1}				
17β-E2	0.1815	0.2710	0.3521	0.1292	0.1062
17α-E2	0.2196	0.3014	0.3824	0.1557	0.1147
E1	0.2320	0.3237	0.3929	0.1747	0.1557
PG	0.1619	0.2089	0.2625	0.1272	0.1062

The removal efficiency of 17α-E2 at a pH of 3, 5, 6.8, 9 and 11 were 73.6%, 82.23%, 89.77%, 60.38% and 49.39%, respectively at t = 6 min. Similarly, 97.01%, 99.21%, 99.78%, 91.72 and 84.22%, respectively was achieved at the end of experiments (t = 16 min). As shown in Table 6.2, the rate constants of 17α-E2 photodegradation were 0.2196, 0.3014, 0.3824, 0.1557 and 0.1147 min^{-1} over the pH range, respectively. While, the removal efficiency of E1 over the pH range was 75.45%, 84.88%, 90.63%, 64.61% and 61.23%, respectively at time (t = 6 min). Simultaneously, 97.56%, 99.32%, 99.82%, 93.89% and 91.82%, respectively at the end of experiments (t = 16 min). The rate constants of E1 photodegradation were 0.2320, 0.3237, 0.3929, 0.1747 and 0.1557 min^{-1} over the pH range, respectively.

The results shown in Figure 6.9, illustrate that the trends in the PG removal efficiency were less than 17β-E2, 17α-E2 and E1, and this result can be attributed to the optimum wavelength that can be absorbed for each component as discussed previously in section 3.6.7. The concentration of PG removal efficiency at a pH of 3, 5, 6.8, 9 and 11 were 62.87%, 71.41%,

79.33%, 54.04% and 48.76%, respectively at the time (t = 6 min). Similarly, 92.67%, 96.46%, 98.50%, 86.71% and 81.74%, respectively were achieved at the end of experiments (t = 16 min). The rate constants of PG photodegradation were 0.1619, 0.2089, 0.2625, 0.1272 and 0.1062 min^{-1} over the same pH range.

The results indicate that the photodegradation rate for 17β-E2, 17α-E2, E1 and PG were significantly dependent on the solution pH and was enhanced with increasing pH until the optimum efficiency removal was accomplished in a pH range of 5-7 as can be seen in Figure 6.10. The pH can strongly contribute to the formation of hydroxyl ions and the generation of hydroxyl radicals which react with the selected model pollutants. This statement can be explained with respect to the hydroxyl ions (OH^-) concentration in the presence of dissolved oxygen by the increase in the acidic media, which accelerated the generation of hydroxyl radicals ($OH^{\bullet}$) (Coleman et al., 2000; Liu et al., 2003; Zhang et al., 2007). As pH increases towards the alkaline range, H_2O_2 dissociation will increase and the formation of hydroperoxide anions (HO_2^-) will act as an efficient scavenger of $OH^{\bullet}$ radicals as shown by equation 6.8. Therefore, H_2O_2 becomes unstable, and loses its ability as a strong oxidizer and decomposes to oxygen and water as shown by equation 6.9. Similar results were also obtained by Horikoshi with the photo-degradation of 2,4-dichlorophenoxyacetic acid (2,4-D) in aqueous solution and Zhang who studied the removal of 6 EDCs including hormones from waste activated sludge (WAS) using UV/H_2O_2 (Horikoshi et al., 2004; Zhang & Li, 2014).

$$HO_2^- + OH^{\cdot} \rightarrow H_2O + O_2^- \cdot \qquad 6\text{-}8$$

$$2H_2O_2 \rightarrow O_2 + 2H_2O \qquad 6\text{-}9$$

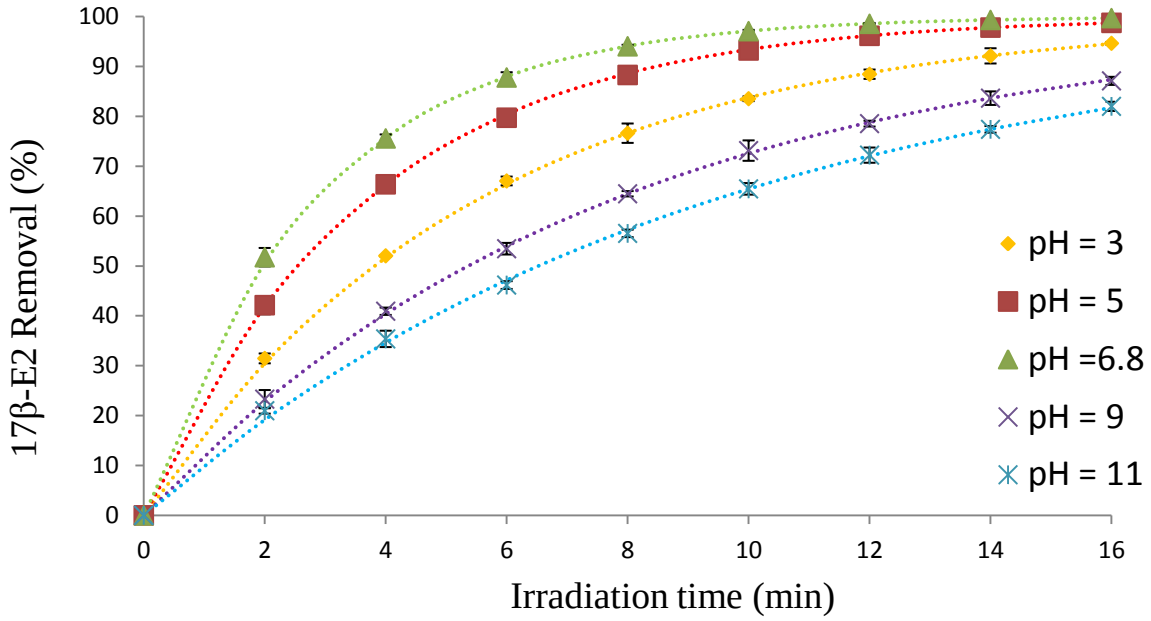

Figure 6-6 Effect of initial pH on 17β-E2 degradation, $[17\beta\text{-E2}]_o$ = 10000 ng L^{-1}, $[H_2O_2]_o$ = 2.5 mg L^{-1}, F_{O_2}= 0.1 L min^{-1} and T = 35°C, data points are experimental results and the model is represented as dashed lines.

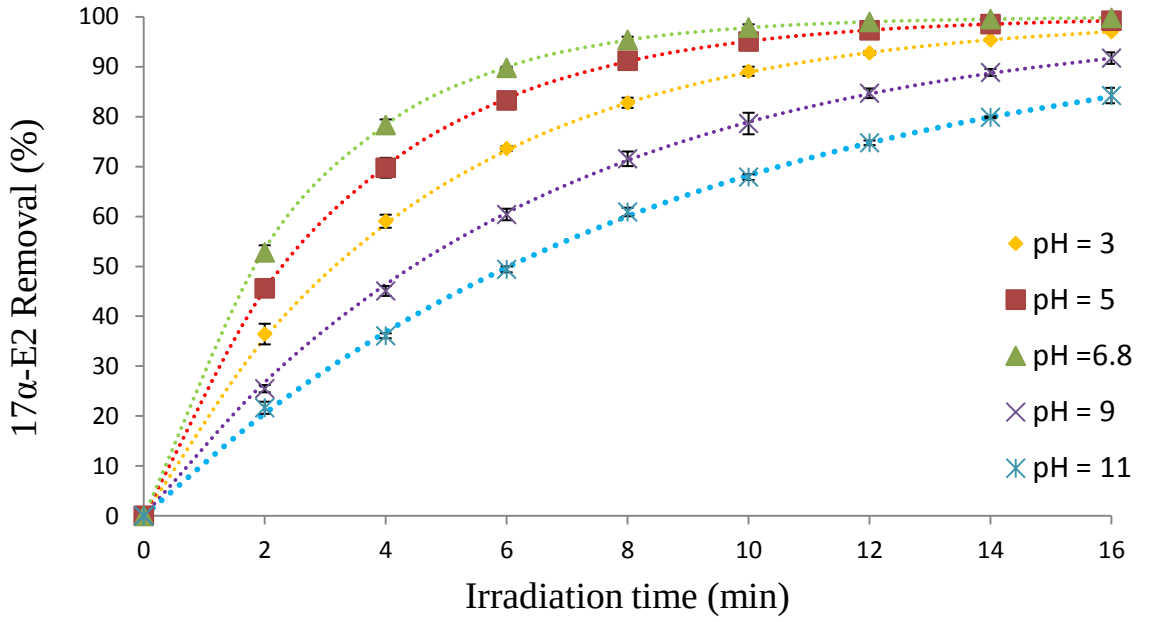

Figure 6-7 Effect of initial pH on 17α-E2 degradation, $[17\alpha\text{-E2}]_o$ = 10000 ng L^{-1}, $[H_2O_2]_o$ = 2.5 mg L^{-1}, F_{O_2}= 0.1 L min^{-1} and T = 35°C, data points are experimental results and the model is represented as dashed lines.

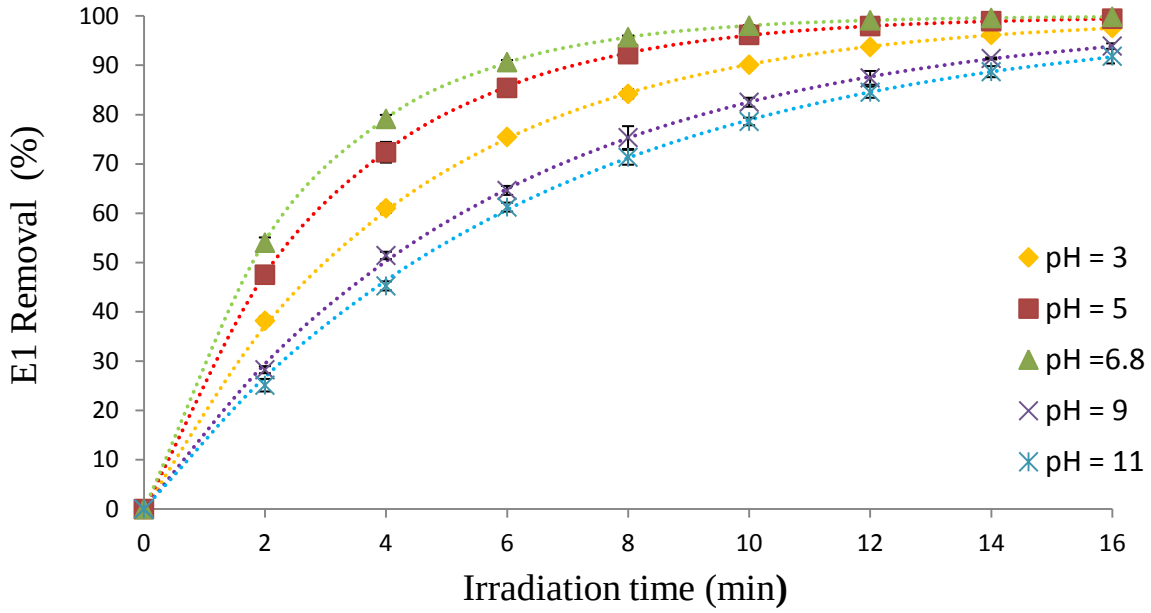

Figure 6-8 Effect of initial pH on E1 degradation, $[E1]_o$ = 10000 ng L^{-1}, $[H_2O_2]_o$ = 2.5 mg L^{-1}, F_{O_2}= 0.1 L min^{-1} and T = 35°C, data points are experimental results and the model is represented as dashed lines.

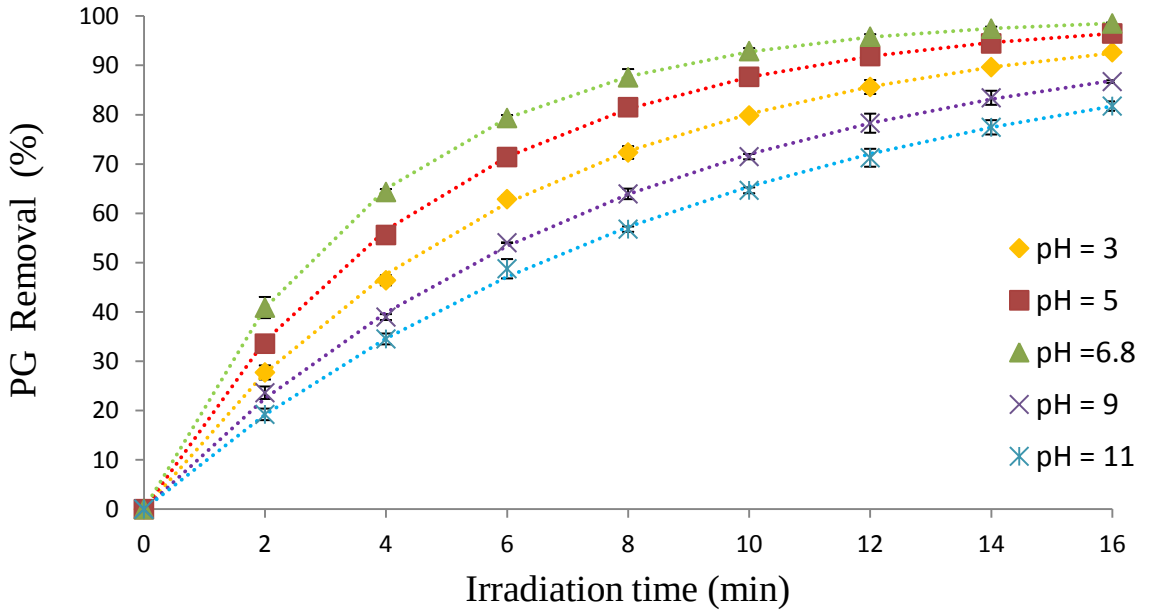

Figure 6-9 Effect of initial pH on PG degradation, $[PG]_o$ = 10000 ng L^{-1}, $[H_2O_2]_o$ = 2.5 mg L^{-1}, F_{O_2}= 0.1 L min^{-1} and T = 35°C, data points are experimental results and the model is represented as dashed lines.

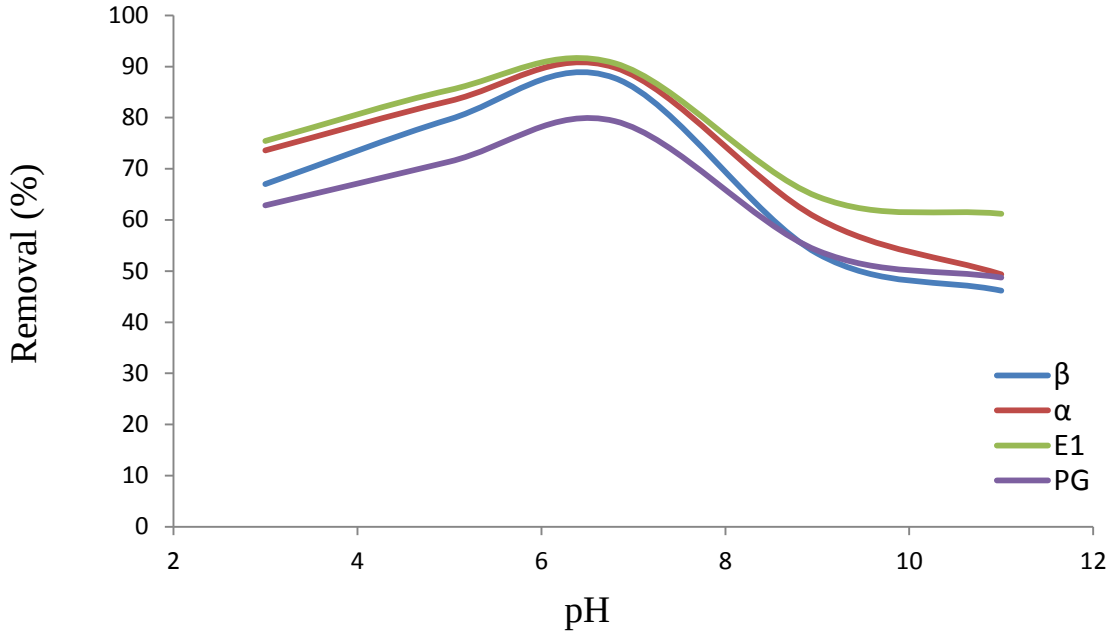

Figure 6-10 Effect of optimum pH values on the degradation behaviour of 17β-E2, 17α-E2, E1 and PG at t = 6 min, C_o = 10000 ng L^{-1}, $[H_2O_2]_o$ = 2.5 mg L^{-1}, F_{O_2} = 0.1 L min^{-1} and T = 35°C

6.1.4 Effect of Oxygen Flowrate

The excellent performance of the DGCR in approaching gas/liquid equilibrium in a short time with 100% of gas utilization results in high values of the volumetric gas-liquid mass transfer coefficient (K_La) as discussed previously in chapter 5. The ideal mixing in the first 20 cm of the DGCR, enhances the removal efficiency of the model pollutant in aqueous solution by maximizing the mass transfer between the oxidizing gas and water. The effect of O_2 flowrate on the photodegradation rate of 17β-E2, 17α-E2, E1 and PG as a model pollutant in aqueous solutions were carried out at different O_2 flowrates of 0, 0.05, 0.10, 0.15 and 0.2 L min^{-1}. Figure 6.11 illustrates the removal efficiency of 17β-E2 using equation 6.1. The role of UV irradiation has an effect on photodegradation behaviour with the same two distinct regions: fast degradation

in the first 6 min followed by a slow degradation process. It was observed that, the removal efficiencies with O_2 flowrate of 0, 0.05, 0.10, 0.15 and 0.2 L min^{-1} were 82.8%, 84.8%, 87.8%, 88.9% and 91.2%, respectively at time (t = 6 min). Similarly, 99.0%, 99.4%, 99.7%, 99.7% and 99.8%, respectively were obtained at the end of experiment (t = 16 min). Table 6.3 shows the results of the pseudo-first order rate constants of 17β-E2 and were 0.2901, 0.3140, 0.3521, 0.3665 and 0.4053 min^{-1} at O_2 flowrate of 0, 0.05, 0.10, 0.15 and 0.2 L min^{-1}, respectively. The same trend can be seen in figures 6.12, 6.13 and 6.14 for 17α-E2, E1 and PG, respectively. Figure 6.12 shows that the removal efficiencies of 17α-E2 for the O_2 flowrate range were 81.9%, 84.4%, 89.8%, 91.4% and 94.2, respectively at time (t = 6 min). Similarly, 98.9%, 99.3%, 99.8%, 99.8 and 100%, respectively were obtained at the end of the experiment (t = 16 min).

Table 6-3 Pseudo-first order rate constant for the degradation of 17β-E2, 17α-E2, E1 and PG under different O_2 flowrate, $R^2 \geq 99\%$

Analyte					
	O_2 L min^{-1}				
	0	0.05	0.10	0.15	0.20
	k min^{-1}				
17β-E2	0.2901	0.3140	0.3521	0.3665	0.4053
17α-E2	0.2822	0.3061	0.3824	0.4052	0.4745
E1	0.2972	0.3135	0.3929	0.4092	0.4540
PG	0.2108	0.2262	0.2625	0.2809	0.3228

Table 6.3 shows the pseudo-first order rate constants of 17α-E2 and were 0.2822, 0.3061, 0.3824, 0.4052 and 0.4745 min^{-1} at O_2 flowrates of 0, 0.05, 0.10, 0.15 and 0.2 L min^{-1}, respectively. The removal efficiencies of E1 as shown in Figure 6.13 at different O_2 flowrates of

0, 0.05, 0.10, 0.15 and 0.2 L min^{-1} were 83.4%, 85.3%, 90.6%, 91.6% and 93.4%, respectively at time (t = 6 min). Similarly, the removal efficiency was 99.2%, 99.3%, 99.8%, 99.9% and 100%, respectively at the end of experiment (t = 16 min). As shown in Table 6.3, the pseudo-first order rate constants of E1 were 0.2972, 03145, 0.3929, 0.4092 and 0.4540 min^{-1} for the O_2 flowrate range.

The results shown in Figure 6.14, illustrate that the trends in the PG removal efficiency were less than 17β-E2, 17α-E2 and E1, and this result can be attributed to the optimum wavelength that can be absorbed for each component as discussed previously in section 6.1.2. The removal efficiency of PG for the O_2 flowrates of 0, 0.05, 0.10, 0.15 and 0.2 L min^{-1} were 71.7%, 73.8%, 79.3%, 81.7% and 85.7%, respectively at time (t = 6 min). In a similar light, the removal efficiencies were 96.5%, 97.3%, 98.5%, 98.9% and 99.4%, respectively at the end of experiment (t = 16 min). As shown in Table 6.3, the pseudo-first order rate constants of PG were 0.2108, 0.2262, 0.2625, 0.2809 and 0.3228 min^{-1} for the respective O_2 flowrates.

These results indicate that removal efficiencies for 17β-E2, 17α-E2, E1 and PG were increased as more O_2 oxidizing gas was fed into the reactor which lead to an increase in the dissolved O_2 concentration, and more hydroxyl radicals were generated to oxide and reacted with the selected model pollutants. However, it was noted that the stability of the DGCR above 0.1 L min^{-1} of O_2 flowrate diminished. This was due to the fast saturation of the aqueous solution in the DGCR; this can lead to a fast expansion of the gas dispersion and the possibility of a gas pocket being formed in the upper section of the DGCR which led to dispersion collapse, as discussed previously in section 5.1.1.2. The optimum O_2 flowrate to give a stable operation (stable bubble matrix) is therefore $\leq$ 0.1 L min^{-1} for the selected water circulation rate.

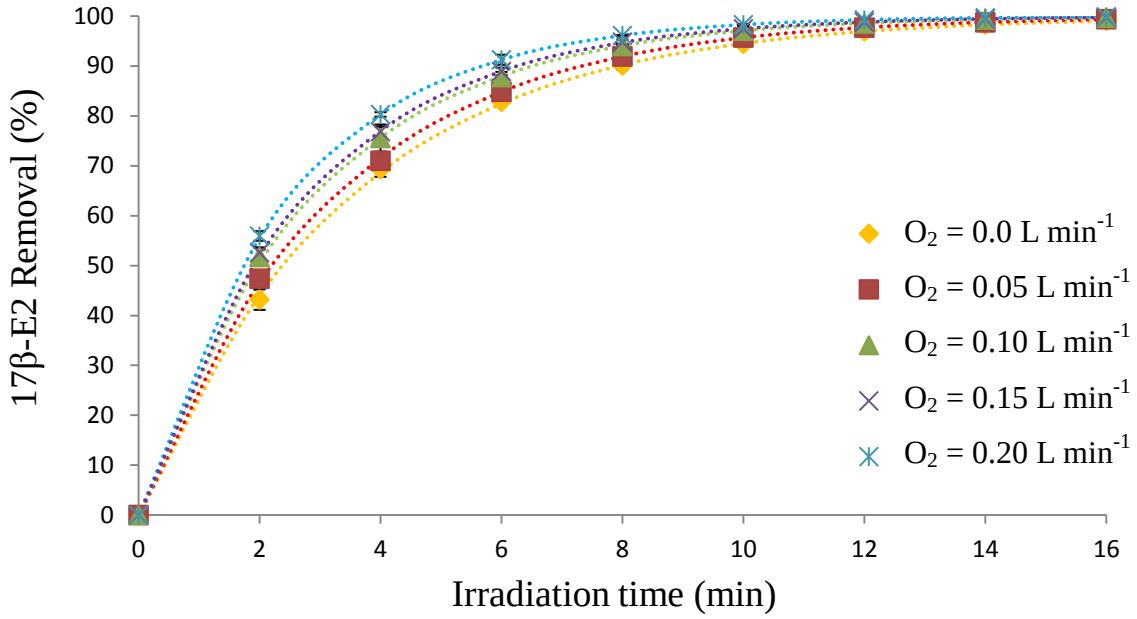

Figure 6-11 Effect of oxygen flowrate on 17β-E2 degradation, $[17\beta\text{-E2}]_o$ = 10000 ng L^{-1}, initial pH 6.8, $[H_2O_2]_o$ = 2.5 mg L^{-1} and T = 35°C, data points are experimental results and the model is represented as dashed lines.

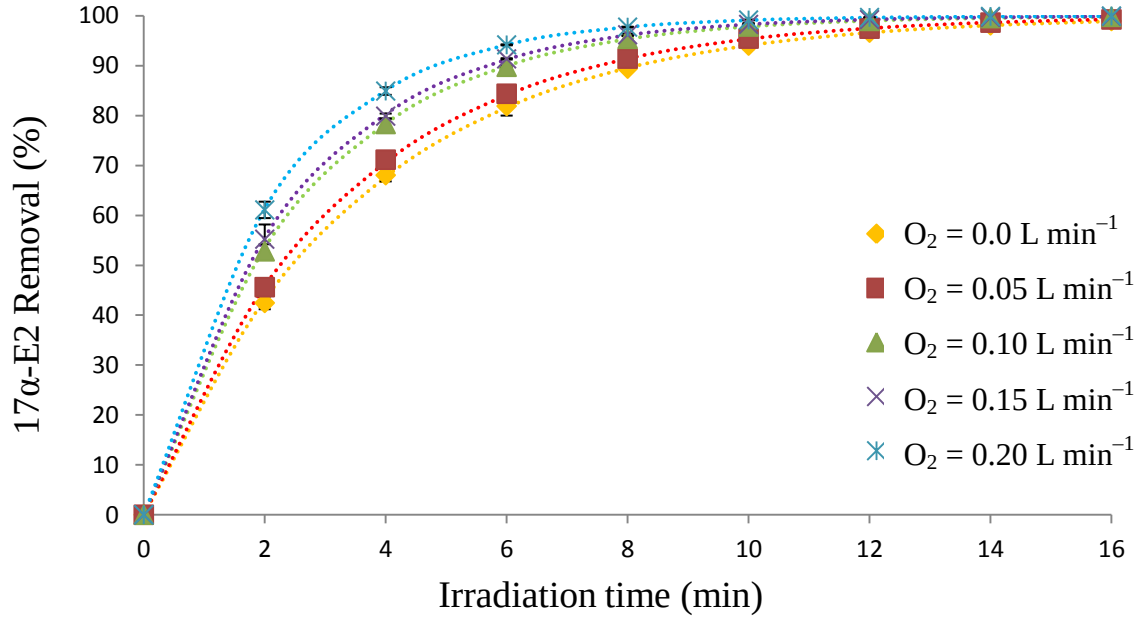

Figure 6-12 Effect of oxygen flowrate on 17β-E2 degradation, $[17\beta\text{-E2}]_o$ = 10000 ng L^{-1}, initial pH 6.8, $[H_2O_2]_o$ = 2.5 mg L^{-1} and T = 35°C, data points are experimental results and the model is represented as dashed lines..

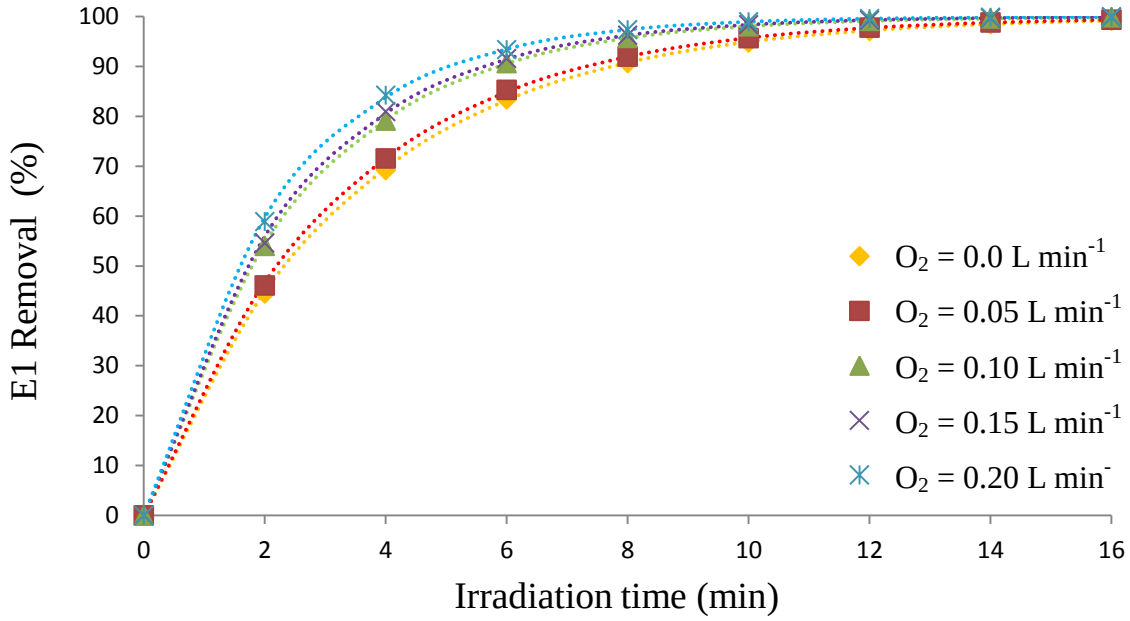

Figure 6-13 Effect of oxygen flowrate on E1 degradation, $[E1]_o$ = 10000 ng L^{-1}, initial pH 6.8, $[H_2O_2]_o$ = 2.5 mg L^{-1} and T = 35 °C, data points are experimental results and the model is represented as dashed lines.

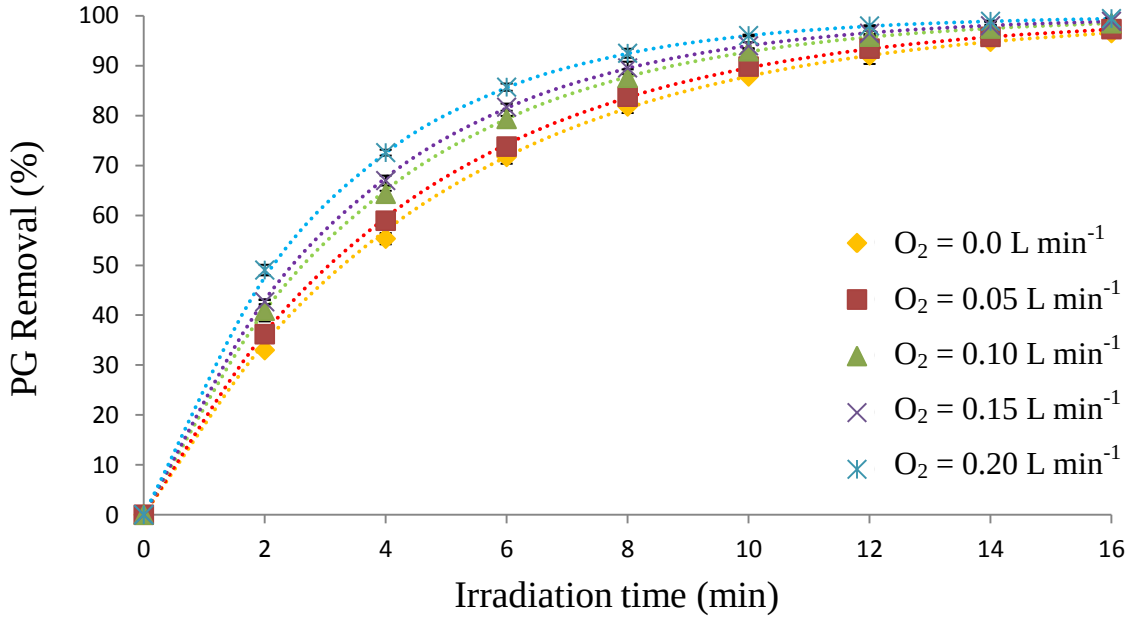

Figure 6-14 Effect of oxygen flowrate on PG degradation, $[PG]_o$ = 10000 ng L^{-1}, initial pH 6.8, $[H_2O_2]_o$ = 2.5 mg L^{-1} and T = 35°C, data points are experimental results and the model is represented as dashed lines.

6.1.5 Effect of H_2O_2 Dosage

Hydrogen peroxide with an oxidation potential of 1.77 eV, can enhance the photodegradation process of the selected model pollutant in aqueous solutions when it is combined with UV photolysis by generating hydroxyl ions (OH˙) which are considered very powerful oxidizers. The effect of different H_2O_2 concentrations on the photodegradation rate of 17β-E2, 17α-E2, E1 and PG as a model pollutant in aqueous solutions was carried out at 0, 2.5, 5, 10 and 20 mg L^{-1}. Figure 6.15 illustrate the removal efficiency of 17β-E2 determined from equation 6.1. It can be seen that the removal efficiencies with H_2O_2 concentrations of 0, 2.5, 5, 10 and 20 mg L^{-1} were 49.2%, 51.7%, 53.3%, 58.8% and 73.3%, respectively at time (t = 2 min). Similarly, 99.5%, 99.7%, and 100% was achieved with H_2O_2 concentrations of 0, 2.5, and 5 mg L^{-1} respectively at the end of experiment (t = 16 min). Total degradation was achieved at 14 and 10 minutes for 10 and 20 mg L^{-1} of H_2O_2 concentrations, respectively. Table 6.4 shows the results of the pseudo-first order rate constants of 17β-E2 and were 0.3299, 0.3521, 0.3697, 0.4522 and 0.6445 min^{-1} for H_2O_2 concentrations of 0, 2.5, 5, 10 and 20 mg L^{-1}, respectively.

The role of hydrogen peroxide in accelerating the photodegradation process is clear and very efficient keeping in mind that the high cost of using hydrogen peroxide (£10/L, ACS 30% (w/w), Sigma-Aldrich (Dorset, UK)) is considered economically unfeasible for larger scale wastewater treatment processes. Similar trends to 17β-E2 can be seen in figures 6.16, 6.17 and 6.18 for 17α-E2, E1 and PG, respectively. Figure 6.16 shows that the removal efficiencies of 17α-E2 with H_2O_2 concentrations of 0, 2.5, 5, 10 and 20 mg L^{-1} were 49.3%, 52.3%, 57.5%, 64.9% and 77.5%, respectively at time (t = 2 min). Similarly, 99.6%, 99.8%, and 100% was achieved with H_2O_2 concentrations of 0, 2.5, and 5 mg L^{-1} respectively at the end of experiment

(t = 16 min). Total degradation was achieved at 14 and 10 minutes for 10 and 20 mg L^{-1} of H_2O_2 concentrations used respectively.

Table 6-4 Pseudo-first order rate constant for the degradation of 17β-E2, 17α-E2, E1 and PG under different H_2O_2 concentrations, $R^2 \geq 99\%$

Analyte					
	H_2O_2 mg L^{-1}				
	0	2.5	5.0	10	20
	k min^{-1}				
17β-E2	0.3299	0.3521	0.3697	0.4522	0.6445
17α-E2	0.3473	0.3824	0.4178	0.5165	0.7393
E1	0.3540	0.3929	0.4645	0.7098	0.9948
PG	0.2480	0.2625	0.2814	0.3180	0.4275

As shown in Table 6.4, the pseudo-first order rate constants of 17α-E2 were 0.3473, 0.3824, 0.4178, 0.5165 and 0.7393 min^{-1} for H_2O_2 concentrations of 0, 2.5, 5, 10 and 20 mg L^{-1}, respectively. Figure 6.17 shows that the removal efficiency of E1 with H_2O_2 concentrations of 0, 2.5, 5, 10 and 20 mg L^{-1} were 50.7%, 54%, 61%, 76% and 86.8%, respectively at time (t = 2 min). Similarly, 99.7%, 99.8%, and 100% was achieved with H_2O_2 concentrations of 0, 2.5, and 5 mg L^{-1} respectively at the end of experiment (t = 16 min). Total degradation was achieved at 14 and 8 minutes for 10 and 20 mg L^{-1} of H_2O_2 concentrations, respectively. As shown in Table 6.4, the pseudo-first order rate constants of E1 were 0.3540, 0.3929, 0.4645, 0.7098 and 0.9948 min^{-1} with H_2O_2 concentrations of 0, 2.5, 5, 10 and 20 mg L^{-1}, respectively. Figure 6.18 shows that the removal efficiencies of PG for H_2O_2 concentrations of 0, 2.5, 5, 10 and 20 mg L^{-1} were 38.7%, 40.9%, 42.9%, 45.8% and 56.7%, respectively at time (t = 2 min). Similarly, 98.1%, 98.5%,

98.9%, 99.9% and 100% was achieved with H_2O_2 concentrations of 0, 2.5, 5, 10 and 20 mg L^{-1} respectively at the end of experiment (t = 16 min). The pseudo-first order rate constants of PG were 0.2480, 0.2625, 0.2814, 0.3180 and 0.4275 min^{-1} with H_2O_2 concentrations of 0, 2.5, 5, 10 and 20 mg L^{-1}, respectively.

The reactions can be explained by equations 6.10 and 6.11, where there were no detectable intermediates for 17β-E2, 17α-E2 and PG except for E1 as shown by equations 6.12 and 6.13 and were described earlier in section 4.2. This is due to the significant role of the powerful UV lamp (2 kW) which can be considered a very powerful photolysis source (Ochuma et al., 2007b).

$$H_2O_2 \xrightarrow{h\upsilon} 2OH^{\bullet} \quad \text{6-10}$$

$$OH^{\bullet} + (17\beta\text{-E2, } 17\alpha\text{-E2 and PG}) \rightarrow CO_2 + H_2O \quad \text{6-11}$$

$$OH^{\bullet} + E1 \rightarrow \text{Intermediate} \quad \text{6-12}$$

$$OH^{\bullet} + \text{Intermediate} \rightarrow CO_2 + H_2O \quad \text{6-13}$$

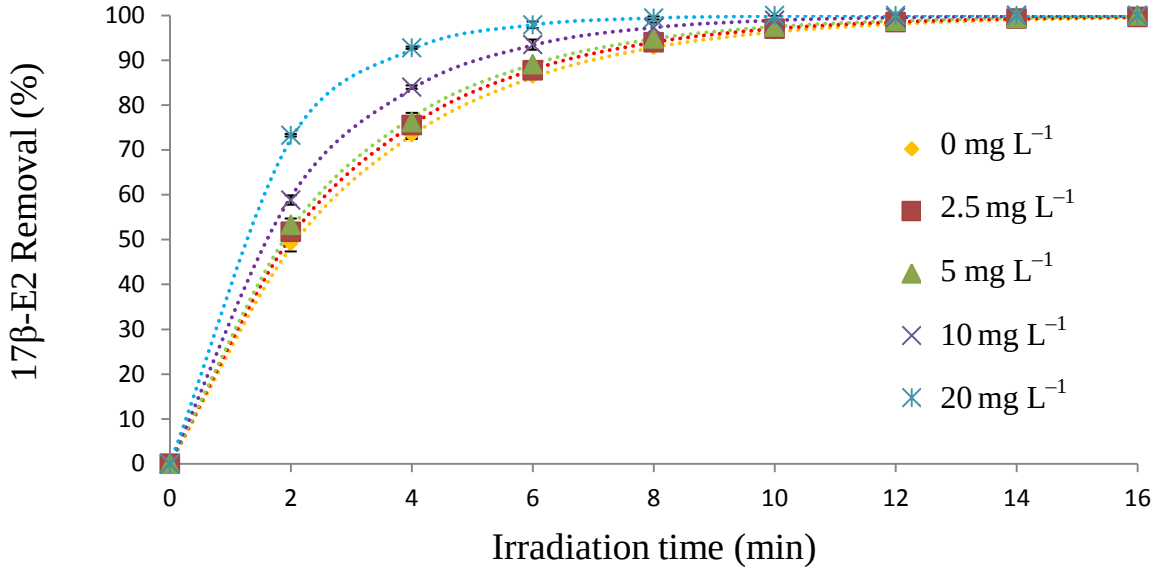

Figure 6-15 Effect of H_2O_2 dosage on 17β-E2 degradation, $[17\beta\text{-E2}]_o$ = 10000 ng L^{-1}, initial pH 6.8, F_{O_2}= 0.1 L min^{-1} and T = 35°C, data points are experimental results and the model is represented as dashed lines.

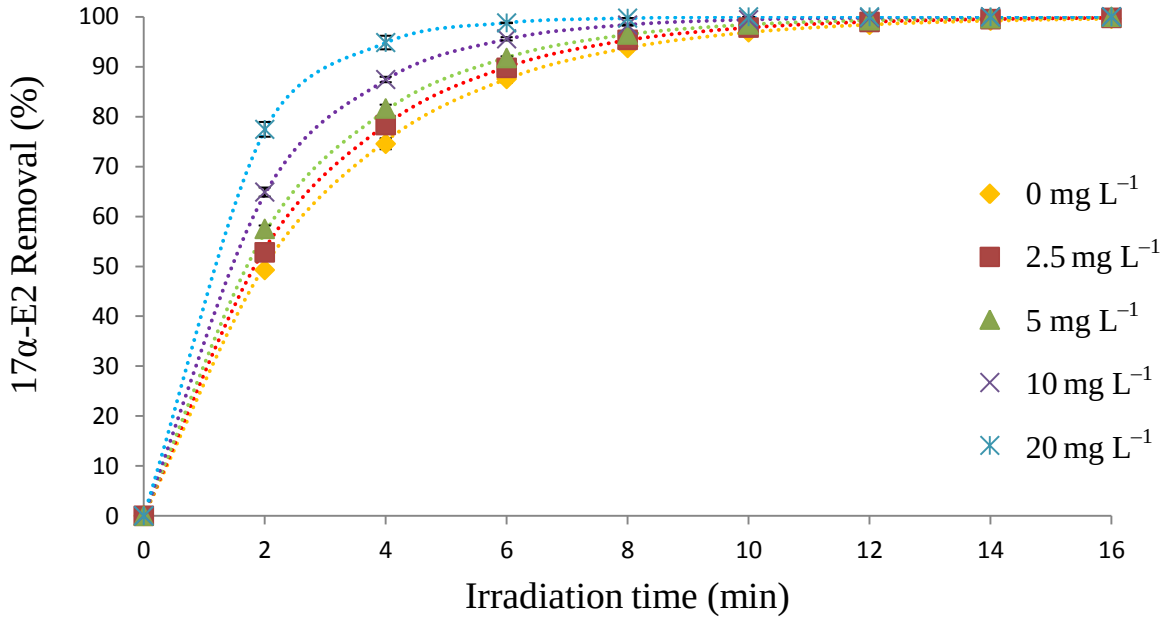

Figure 6-16 Effect of H_2O_2 dosage on 17α-E2 degradation, $[17\alpha\text{-E2}]_o$ = 10000 ng L^{-1}, initial pH 6.8, F_{O_2}= 0.1 L min^{-1} and T = 35°C, data points are experimental results and the model is represented as dashed lines.

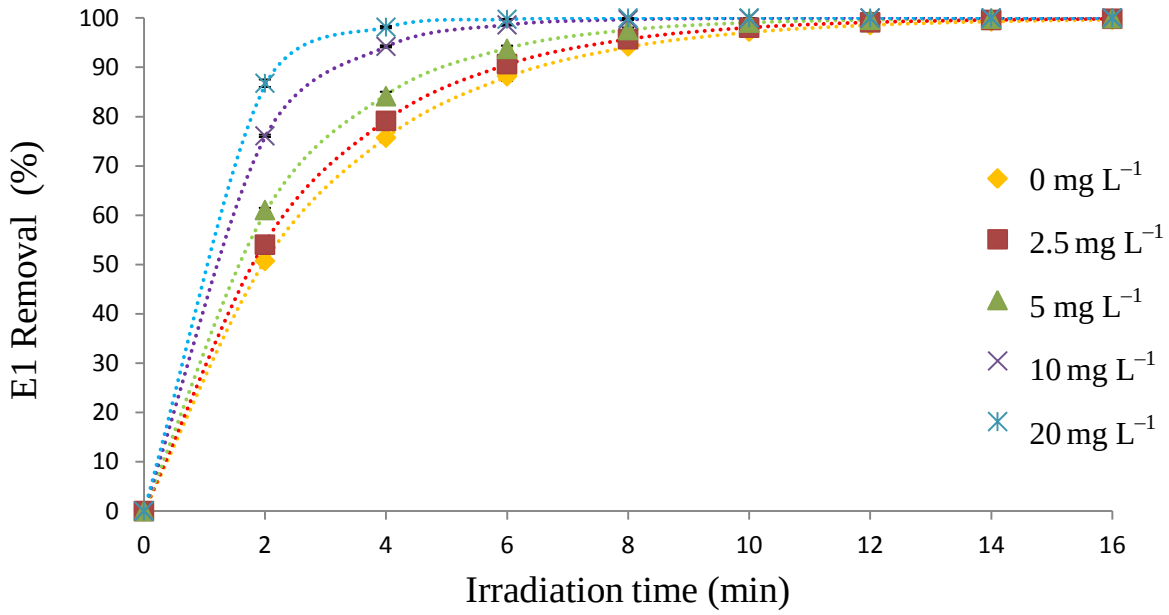

Figure 6-17 Effect of H_2O_2 dosage on E1 degradation, $[E1]_o$ = 10000 ng L^{-1}, initial pH 6.8, F_{O_2}= 0.1 L min^{-1} and T = 35°C, data points are experimental results and the model is represented as dashed lines.

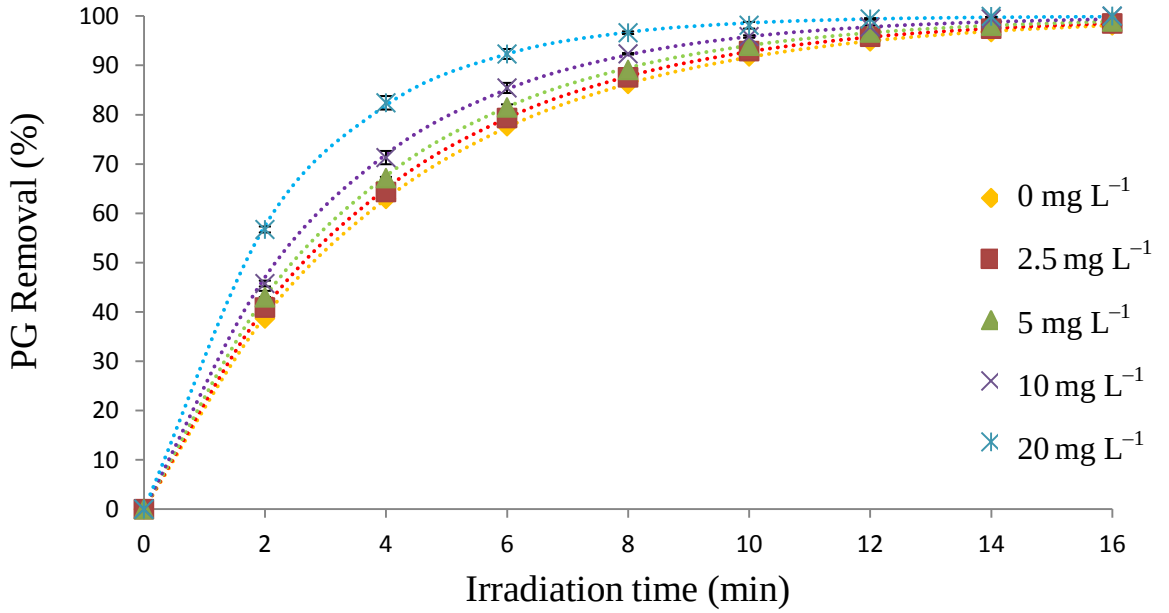

Figure 6-18 Effect of H_2O_2 dosage on PG degradation, $[PG]_o$ = 10000 ng L^{-1}, initial pH 6.8, F_{O_2}= 0.1 L min^{-1} and T = 35°C, data points are experimental results and the model is represented as dashed lines.

6.1.6 Effect of Different Combination of Treatment Systems on the Photodegradation Performance

The effect of using different combination of wastewater treatment systems using DGCR were explored to evaluate their photodegradation performance of the selected female steroid hormones, 17β-E2, 17α-E2, E1 and PG in aqueous solution to a safe and nontoxic end products such as CO_2 and H_2O. The set of experiments were O_2 and H_2O_2/O_2 with no UV irradiation (dark reaction oxidation) and three combinations of UV systems were UV only (photolysis), UV/O_2 and UV/O_2/H_2O_2 (photo-oxidation). Figure 6.19 illustrates the effects of different system combinations on the removal efficiencies of 17β-E2. The effect of O_2 was negligible with 1% removal efficiency at the end of experiment (t = 16 min), while using H_2O_2/O_2 removed 27% of the selected model pollutants at the end of experiment (t = 16 min), highlighting the role of the hydroxyl radical (OH˙) in the treatment method. The significant role of the UV irradiation (photolysis) on the removal efficiencies can be seen by 43.2%, 82.8% and 99% at 2, 6 and 16 min, respectively. These results suggest that the UV treatment method degraded the selected model pollutants. The use of UV/O_2 photo-oxidation illustrates the enhancement of O_2 with the power of UV irradiation on the removal efficiencies with 56.4%, 91.2% and 99.9% being obtained at 2, 6 and 16 min, respectively. The combination of UV/O_2/H_2O_2 enabled a total degradation of pollutants within 10 minutes. This clearly indicates the role of H_2O_2 in accelerating the oxidation rate of the selected model pollutants. Similar trends can be seen in figures 6.20, 6.21 and 6.22 for 17α-E2, E1 and PG, respectively. The effect of O_2 was negligible with 1% removal efficiency for 17α-E2, E1 and PG at the end of experiment (t = 16 min), while using H_2O_2/O_2 removed 27%, 28% and 26% for 17α-E2, E1 and PG, respectively at the end of

experiments (t = 16 min). UV photolysis for 17α-E2, E1 and PG showed the same trends of 17β-E2 with a slower degradation rate of PG due to the optimum wavelength that can be absorbed for each component as discussed earlier in section 6.1.2. It is clear that the role of the UV irradiation controls the degradation rate behaviour with 42.4%, 81.9% and 98.9% at 2, 6 and 16 min, respectively for 17α-E2. Similarly a degradation rate of 44.5%, 83.4% and 99.2% at 2, 6 and 16 min, respectively was observed for E1. While PG removal efficiencies were lower with 33%, 71.7% and 96.5% at 2, 6 and 16 min, respectively. The effect of UV/O_2 photo-oxidation on the removal efficiencies for 17α-E2, E1 and PG were 55%, 90% and 99.9% at 2, 6 and 16 min, respectively for 17α-E2. Degradation rates of 59.4%, 93.5% and 99.9% at 2, 6 and 16 min, respectively were observed for E1. PG removal efficiencies were lower with 49.6%, 86.1% and 99.5% at 2, 6 and 16 min, respectively. The combination of UV/O_2/H_2O_2 enabled total degradation to be achieved within 10 minutes for 17α-E2, total degradation achieved within 8 minutes for E1 and a total degradation achieved within 16 minutes for PG. The addition of O_2 and H_2O_2 clearly accelerate the photodegradation rate with total degradation of the targeted EDCs to the final products (CO_2, H_2O).

The half-life ($t_{½}$) of the first order-reaction can be estimated by isolating *t* from equation 6.2, which results in equation 6.14, and using the *k* values from Tables 6.1, 6.3 and 6.4. $t_{½}$ and 100% degradation values of the selected hormones are listed in Table 6.5.

$$t_{½} = \frac{\ln 2}{k} \qquad 6\text{-}14$$

Table 6-5 Summary of half-life ($t_{½}$) and total degradation of 17β-E2, 17α-E2, E1 and PG using different wastewater treatment systems in DGCR, C_o = 10000 ng L^{-1}, F_{O_2}= 0.1 L min^{-1} and $[H_2O_2]_o$ = 20 mg L^{-1}

Compound	UV		UV/O_2		$UV/O_2/H_2O_2$	
	$t_{½}$ min	100 % min	$t_{½}$ min	100 % min	$t_{½}$ min	100 % min
17β-E2	2.39	-	1.97	-	1.08	10
17α-E2	2.46	-	1.81	-	0.94	10
E1	2.33	-	1.76	-	0.70	8
PG	3.29	-	2.64	-	1.62	16

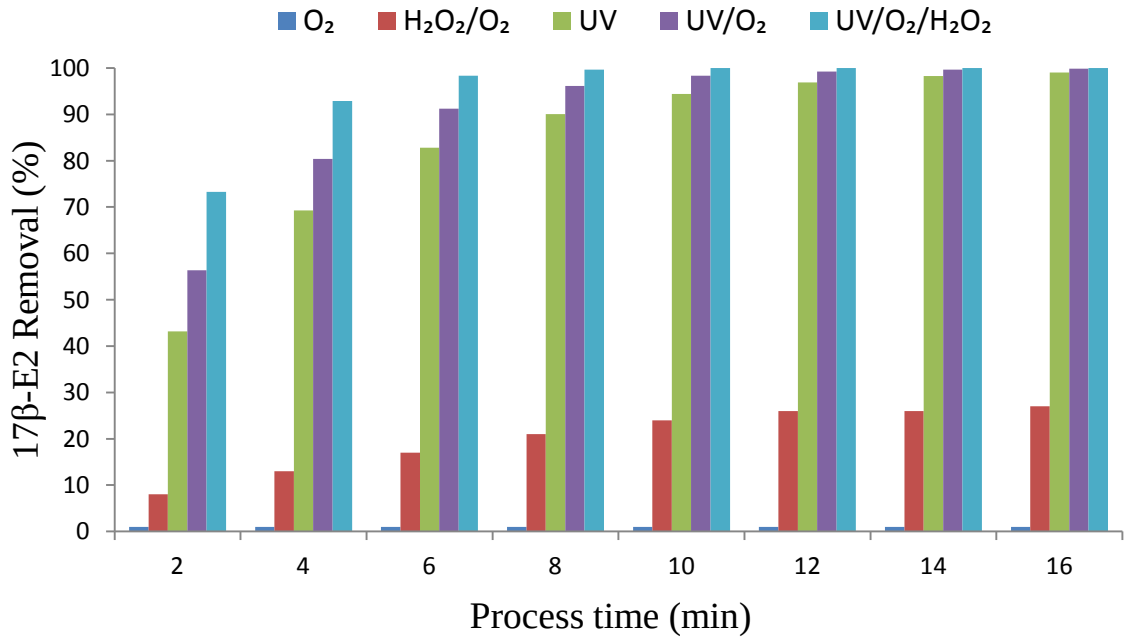

Figure 6-19 Effect of different wastewater treatment systems on 17β-E2 degradation, $[17β\text{-}E2]_o$ = 10000 ng L^{-1}, T = 35°C, F_{O_2}= 0.1 L min^{-1} and $[H_2O_2]_o$ = 20 mg L^{-1}.

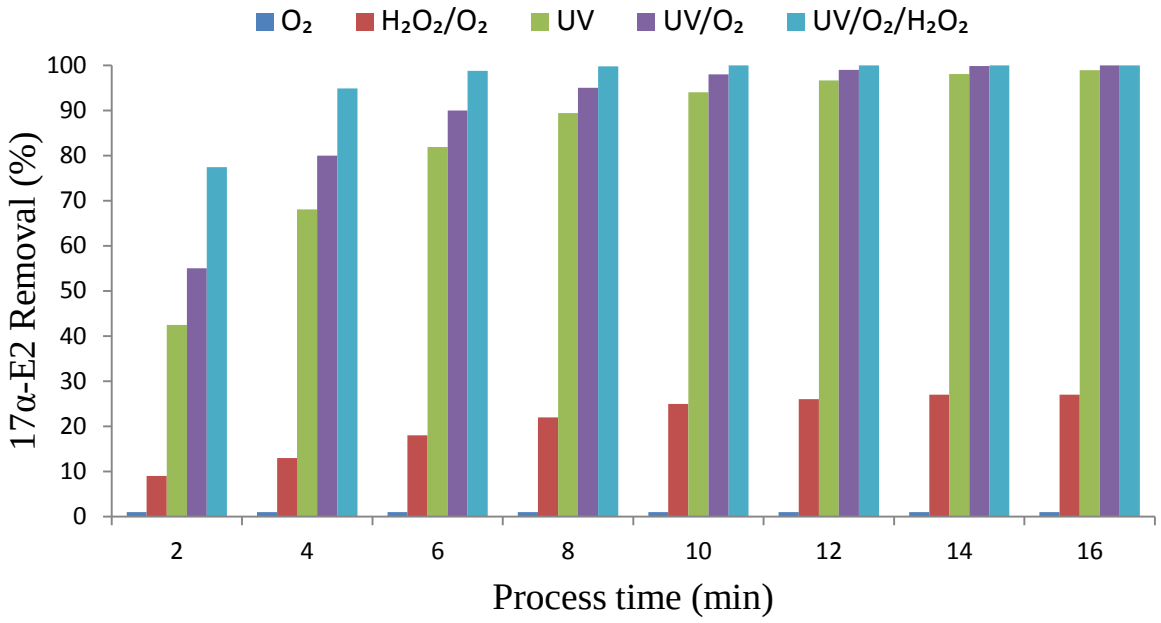

Figure 6-20 Effect of different wastewater treatment systems on 17α-E2 degradation, $[17\alpha\text{-E2}]_o$ = 10000 ng L^{-1}, T = 35°C, F_{O_2}= 0.1 L min^{-1} and $[H_2O_2]_o$ = 20 mg L^{-1}.

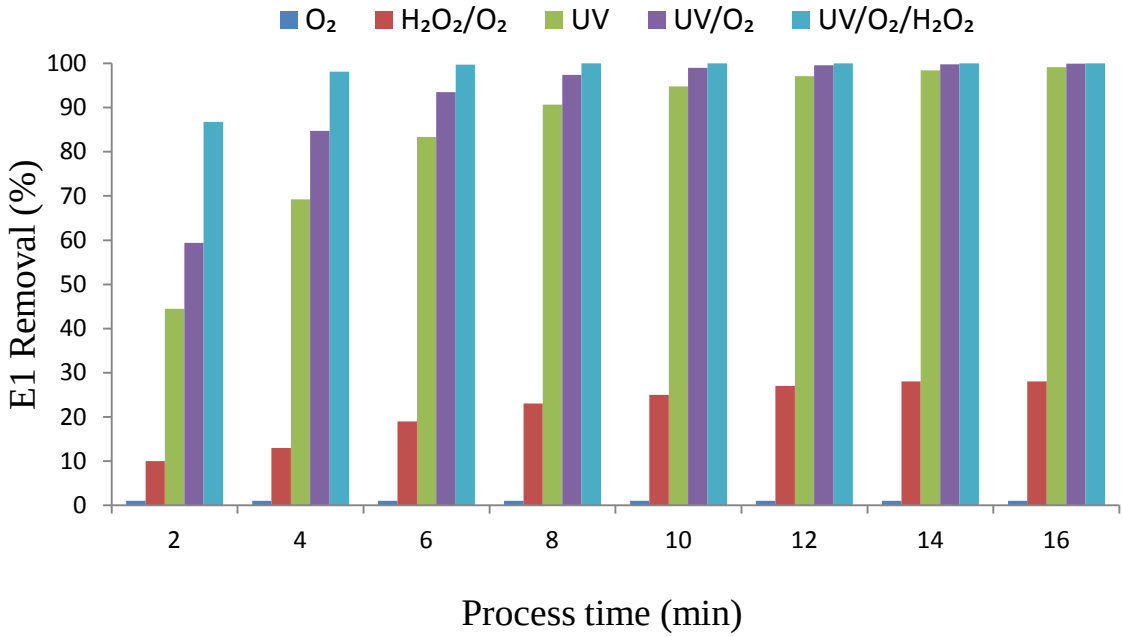

Figure 6-21 Effect of different wastewater treatment systems on E1 degradation, $[E1]_o$ = 10000 ng L^{-1}, T = 35°C, F_{O_2}= 0.1 L min^{-1} and $[H_2O_2]_o$ = 20 mg L^{-1}.

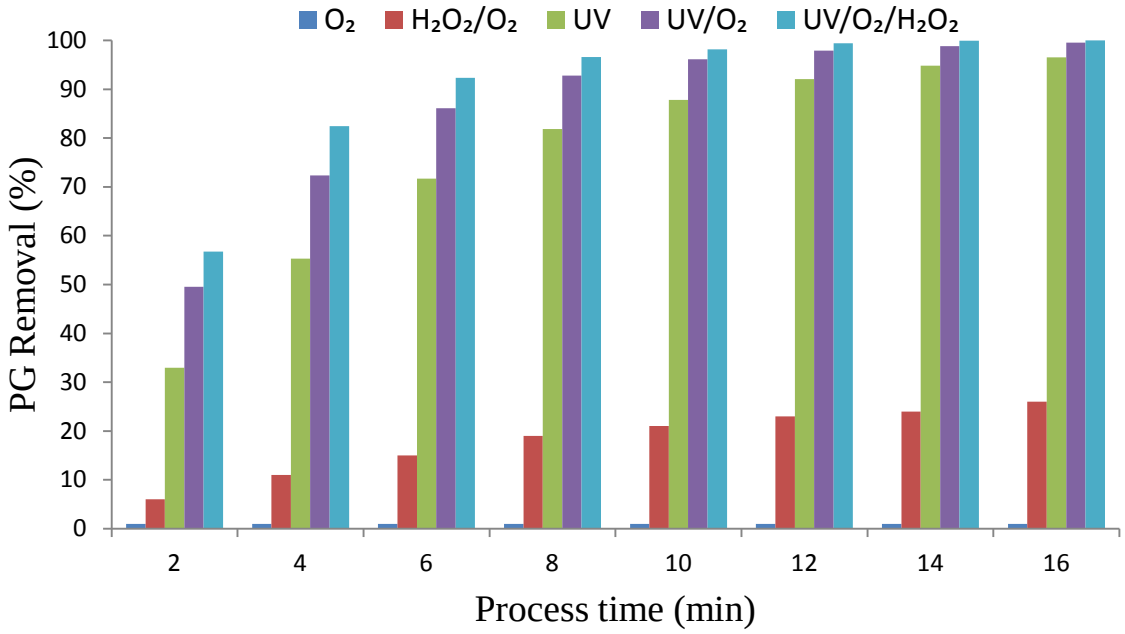

Figure 6-22 Effect of different wastewater treatment systems on PG degradation, $[PG]_o$ = 10000 ng L^{-1}, T = 35°C, F_{O_2} = 0.1 L min^{-1} and $[H_2O_2]_o$ = 20 mg L^{-1}.

Different wastewater treatment systems employed for the total degradation of 17β-E2, 17α-E2, E1 and PG using DGCR lead to different cost estimation. Both UV irradiation and O_2 are used on a continual basis, while H_2O_2 was added at the start of the experiments. UV irradiation is considered essential and indispensable for a total degradation of the selected hormones that were discussed previously; UV irradiation shows that the effect of this form of irradiation is the main factor affecting the whole degradation process. The price of electricity in the UK currently (2015) averages around 13.9 pence per kW, all prices include VAT (GOV.UK, 2015). The pump operating cost (0.2567 pence per min) was added to all cost calculations. The total time of the experiment is 16 min using the 2 kW UV lamp; therefore, the cost of using UV irradiation is approximately 3.47 – 4 pence per run. Figure 6.23 shows that UV irradiation has the highest cost compared with O_2 and H_2O_2, which were used to enhance the degradation rate. Although the

increased cost of UV irradiation from the unpredicted prices of the electricity can arise annually and is related to the fuel prices, using lower energy UV lamps with satisfactory results would lower the overall total cost of the wastewater treatment method. Moreover, the continuous development of more efficient UV lamps with shorter wave length can have a positive influence on the total cost of the method used. Also, the use of solar energy can also be applied as a source of radiation, but it will extend the treatment time (Han et al., 2012). The cost of H_2O_2 (30% (w/w) solution) is approximately 4.8 pence per ml (Sigma-Aldrich, 2016), and the cost of O_2 (99.5%, BOC) is approximately 0.000252 pence per ml. Both are used to enhance the photodegradation rate, which will add additional cost as can be seen in Figure 6.23; however, this will have a positive influence on the total cost by reducing the time required to achieve satisfactory results.

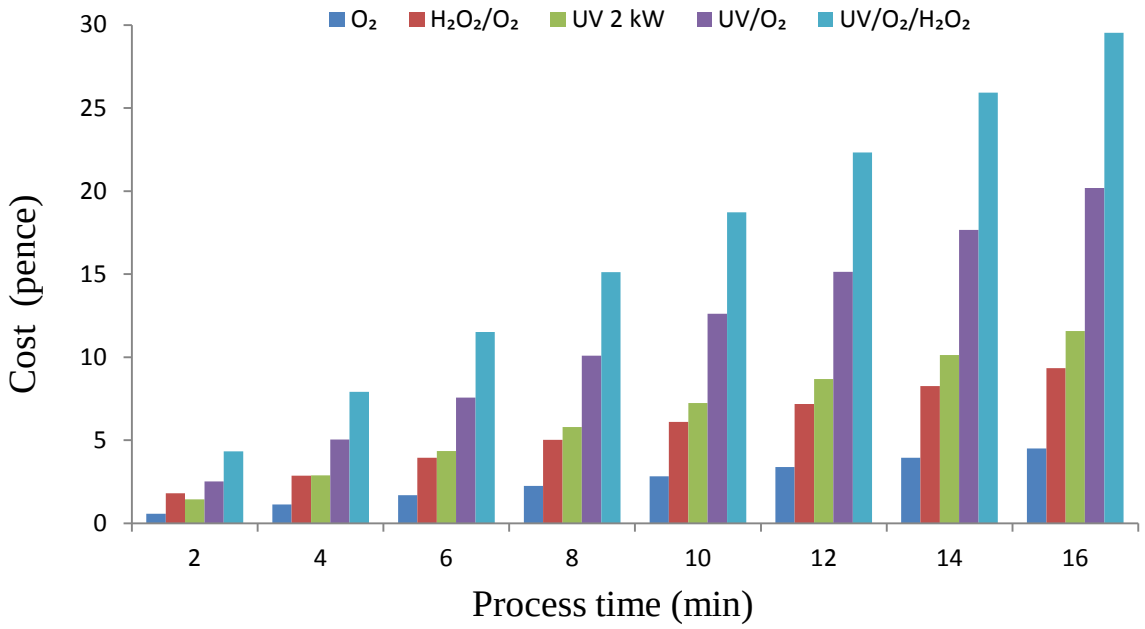

Figure 6-23 Cost comparison per pence of different wastewater treatment systems of 17β-E2, 17α-E2, E1 and PG using DGCR, F_{O_2} = 0.1 L min^{-1} and $[H_2O_2]_o$ = 20 mg L^{-1}.

6.2 Conclusion

The results of the degradation and removal efficiencies of the selected female steroid hormones, 17β-E2, 17α-E2, E1 and PG in aqueous solutions using the DGCR demonstrated that it can be considered a promising advance oxidation process (AOPs) capable of total degradation in a short amount of time compared to a previous studies such as; degradation of 2,4,6-trichlorophenol (2,4,6-TCP) using the DGCR with 100% conversion in 180 min (Ochuma et al., 2007b). Also, the degradation of E1 and E2 has been achieved in 60 min using UV-photo-reactors (Zhang et al., 2007). In addition, a study of the degradation of 17-ethinylestradiol (EE2) and levonorgestrel (LNG) using a photocatalytic treatment was performed within 40 min (Nasuhoglu et al., 2012). The photodegradation process fit well with pseudo-first order kinetics with $R^2 \geq 99\%$. The investigations with UV irradiation (photolysis) show that the effect of UV irradiation is the main factor affecting the whole degradation process and its significant impact on the degradation trend over the two regions; fast degradation in the first 6 min followed by a slow degradation process. The results also show that the initial concentration has a dominant effect on the degradation rate, as the initial concentration increased the degradation rate decreased. E1 has the fastest degradation rate while PG was the slowest and 17β-E2 and 17α-E2 were similar in photodegradation behaviour, this result can be attributed to the optimum wavelength that can be absorbed for each component (see section 6.1.2). The results indicate that the photodegradation rate was significantly dependent on the solution pH and was enhanced with increasing pH until the optimum efficiency removal was achieved in a pH range of 5-7. The pH can strongly contribute to the formation of hydroxyl ions and hydroxyl radicals and the worst performance was in the alkaline range. The maximum residence time that was achieved with a stable

dispersion process in the perfectly mixed zone of the DGCR (first 20 cm) maximizes the oxidation process when the oxidizing agents (H_2O_2, O_2) were used, the removal efficiencies with an O_2 flowrate of 0.1 L min^{-1} were 87.8%, 89.8%, 90.6%, and 79.3% for 17β-E2, 17α-E2, E1 and PG, respectively at time t = 6 min. A total degradation was achieved using 20 mg L^{-1} of H_2O_2 for 17β-E2 and 17α-E, at 10 min, E1 at 8 min and PG at 16 min. These results clearly indicate that adding these oxidizing agents to the DGCR enhanced and accelerated the photodegradation process. UV irradiation is considered the highest cost in the treatment method used and it is essential and indispensable to the total degradation of the selected hormones compared with O_2 and H_2O_2, which were used to enhance the degradation rate. The use of these oxidizers adds additional cost, but will have a positive influence on the total cost by reducing the time needed for satisfactory results.

CHAPTER 7

7 CONCLUSIONS AND RECOMMENDATIONS

7.1 Conclusions

The experimental results in this thesis, demonstrated the suitability and potential of the Downflow Gas Contactor Reactor (DGCR) as an effective advanced oxidation process (AOP) towards the removal of endocrine disrupting compounds (EDCs). The high performance of the DGCR gave total degradation of the selected female steroid hormones, 17β-estradiol (17β-E2), 17α-estradiol (17α-E2), Estrone (E1) and progesterone (PG) in a short amount of time. To achieve this target, two steps were necessary before starting the degradation studies; development of a new analysis method for the detection of four selected female hormones at the ng L^{-1} level and the optimization of the DGCR hydrodynamics and evaluation of the mass transfer for optimum operating conditions.

7.1.1 Optimization and Validation for the Analysis of Selected Female Steroid Hormones in Aqueous Samples at the Nanogram Level

- A fast, reliable and accurate analysis method was established and validated for the detection of four selected female hormones at the ng L^{-1} level using HPLC-DAD for the quantification and identification, while LC-TOF-MS was used for compound purity and identity confirmation.

- The analysis method achieved an excellent separation in short chromatographic time using conventional LC instruments with detection down to the ng L^{-1} level of the selected hormones, especially the separation of 17β-E2 and 17α-E2. Also, the separation of E1 and its isomer was possible, which is a challenge in LC development methods.
- Off-line solid phase extraction (SPE) using an Oasis HLB with RSDs ≤ 9.13%, which are quite satisfactory.
- The highest recovery of EDCs was achieved for ultrapure water at 98.7% and the lowest for river water at 88.2%. These results highlight the importance of chemical interference in sample recovery. This result is consistent with previous studies (Al-Odaini et al., 2010; Al-Qaim et al., 2014; Tan et al., 2015).
- The recovery loss increases with decreasing water volume. This behaviour was attributed to the solubility of the analytes in the water samples.
- LODs of 0.8, 1.05, 0.93 and 3.97 ng L^{-1} were established for 17β-E2, 17α-E2, E1 and PG respectively, for river water matrix samples. While, mineral water and ultra high purity water gave improved values compared to river water.
- LC-TOF-MS was used to confirm the peak identity of the by-products from the photolysis reaction as an isomer of E1.

7.1.2 Hydrodynamic Characteristics and Mass Transfer Studies of the Downflow Gas Contactor Reactor (DGCR)

- The first region (10–20 cm) reflected a high-turbulent flow characterized with small bubble size (≤2 mm), a rapidly coalescing process, and a high-turbulent mixing zone with continuous and constant gas phase dispersed in the liquid phase.
- The second region reflected less turbulence with stable and uniform bubble dispersion occupying the whole cross-sectional area of the column; this region could be considered a bubbly flow.
- A maximum residence time value could be achieved for the oxygen/water system due to the balance between the liquid velocity and the gas bubble rise velocity maintaining a stable dispersion.
- Orifices between (d_o = 2.0–4.0 mm) delivered the highest values of the superficial liquid velocity at the nozzle section in DGCR. This was necessary for higher shearing rates to alter bubble sizes which consequently altered the hydrodynamic and mass transfer characteristics of the DGCR.
- Bubble size was highly affected by the gas input, and the average bubble size increased with increasing gas input. On the contrary, the average bubble size decreased with increasing superficial velocity as a result of bubble dispersion development in the DGCR.
- Gas hold-up values of up to 50–60% were achieved and were highly affected by the dispersion height. Gas hold-up increased when there was more gas input with higher superficial velocity in the system.
- Increasing the liquid superficial velocity led to lower values of gas hold-up.

- The results show that the trends of interfacial area were similar to those of gas hold-up behaviour. The highest value for the interfacial area under the operating parameters was 920 m^2 m^{-3}.
- Increasing both the gas input and dispersion height, led to the interfacial area value also being increased, whereas increasing the liquid superficial velocity led to the decrease in the interfacial area values (a similar behaviour to the gas hold-up).
- Dissolved oxygen (DO) concentration increases with the increase of the axial dispersion height until an equilibrium state is reached at (h_d = 40–70 cm). DO concentration also increased as the liquid superficial velocity increased for the conditions selected.
- The results show that K_La values increased as the axial dispersion height increased steadily and was much improved by using higher liquid superficial velocities.
- The flow patterns of the DGCR for the O_2/H_2O absorption system were based on two models; plug flow reactor (PFR) and the continuous stirred tank reactor (CSTR, complete mixing). It was found that K_La values of the CSTR model were higher than the PFR model.

7.1.3 Advanced Oxidation and Degradation Studies of Selected Female Steroid Hormones in Aqueous Samples

- The photodegradation process of 17β-E2, 17α-E2, E1 and PG fit well with a pseudo-first order kinetic model with a $R^2 \geq 99\%$.
- Investigations with UV irradiation (photolysis) showed that the effect of UV irradiation is the controlling factor affecting the photodegradation process; it has significant impact on

the photodegradation trend for the fast degradation region in <6 min which was then followed by a slow degradation process.

- Initial concentration has an important effect on the degradation rate, as the initial concentration increased the degradation rate decreased. E1 has the fastest degradation rate while PG was the slowest, while the 17β-E2 and 17α-E2 were similar in photodegradation behaviour.
- The degradation rate was significantly dependent on the solution pH and was enhanced with increasing pH until the optimum efficiency removal was accomplished in a pH range of 5–7. The pH can strongly contribute to the formation of hydroxyl ions and hydroxyl radicals and the lowest were in the alkaline range.
- The removal efficiency was enhanced with the addition of O_2 and H_2O_2. Total degradation was achieved using 20 mg L^{-1} of H_2O_2 for 17β-E2 and 17α-E in 10 min, for E1 in 8 min and for PG in 16 min. These results clearly indicate that adding these oxidizing agents to the DGCR enhanced and accelerated the photodegradation process.
- UV irradiation considered the highest cost in the treatment method used which is essential and indispensable to the total degradation of the selected hormones compared to O_2 and H_2O_2 which they were used to enhance the degradation rate, the use of these oxidizers add additional cost, but will have a positive influence on the total cost by reducing the time needed for satisfactory results.

7.2 Recommendations for Future Work

There are number of areas that could have been explored in this work, but due to the financial, equipment and time constraints they were not carried out within the present work. However, the following recommendations are proposed:

- The effect of high and low temperatures on the hydrodynamic and mass transfer properties of the DGCR. Solubility of oxygen in water is a function of temperature, solubility increases at low temperature and decreases at high temperature which has a direct impact on the bubble dispersion development in the DGCR. The DGCR temperature was controlled using tap water with a simple cooling coil inside the break vessel to maintain constant temperature during the experiments; the DGCR needs a major upgrade with a temperature controller unit and a cooling jacket surrounding the DGC column.
- The effect of elevated pressure on the hydrodynamic and mass transfer properties of the DGCR. The solubility of gases increases as the partial pressure of the gas increases, this relationship is described by Henry's law.

$$C = kP \qquad 7\text{-}1$$

Where:

C is the concentration of dissolved gas at equilibrium, mg L^{-1}.

P is the partial pressure of the gas, atm.

k is the Henry's law constant.

Due to the limitation of the rated pressure of the quartz tube in DGCR, the UV system must be ≤7 bars and 80°C. All experiments therefore were conducted below that range as a safety

precaution. In addition, elevated pressure can significantly impact the flow patterns inside DGCR, the reason can be attributed to the interfacial forces acting on bubbles.

- The effect of more complex wastewater matrices such as sewage-treatment works (STW), surface and supply water, landfill water and industrial effluents.
- . The photodegradation process can be highly affected due to the interference of compounds that act as a scavenging and radiation scattering (Souza et al., 2014).
- An improved understanding of the bubble properties, including bubble velocity, size and interfacial area measurements in bubble columns to predict the flow behaviour, such as using Computer Automated Radioactive Particle Tracking (CARPT).
- The effect of lower power UV radiation such as 1 kW, 500 W and 100 W on the degradation behaviour of selected EDCs in real samples; reducing energy consumption with acceptable results will lead to a more cost-effective treatment method, which is considered a research area worthy of exploration.
- The effect of different oxidizing gases on the degradation studies of EDCs in aqueous samples is worthy of exploration, such as ozone (O_3), which is one of the common gases used in wastewater treatment and is considered a strong oxidizing agent that can be decomposed rapidly within minutes of addition and enhance the generation of hydroxyl radicals.
- The effect of more complex matrices of EDCs, such as male hormones, pharmaceuticals and pesticides on the degradation studies in model and real water samples. The more complex the matrix, the more difficult the separation and extraction steps is required due to the differences in physical and chemical properties of each analyte.

CHAPTER 8

8 REFERENCES

Adeleye, A. S., Conway, J. R., Garner, K. et al (2016) Engineered nanomaterials for water treatment and remediation: Costs, benefits, and applicability. **Chemical Engineering Journal,** 286 640-662

Ahmed, B., Mohamed, H., Limem, E. et al (2009) Degradation and Mineralization of Organic Pollutants Contained in Actual Pulp and Paper Mill Wastewaters by a UV/H_2O_2 Process. **Industrial & Engineering Chemistry Research,** 48 (7): 3370-3379

Ahrer, W., Scherwenk, E. and Buchberger, W. (2001) Determination of drug residues in water by the combination of liquid chromatography or capillary electrophoresis with electrospray mass spectrometry. **Journal of Chromatography A,** 910 (1): 69-78

Akita, K. and Yoshida, F. (1973) Gas Holdup and Volumetric Mass-Transfer Coefficient in Bubble Columns - Effects of Liquid Properties. **Industrial & Engineering Chemistry Process Design and Development,** 12 (1): 76-80

Akosman, C., Orhan, R. and Dursun, G. (2004) Effects of liquid property on gas holdup and mass transfer in co-current downflow contacting column. **Chemical Engineering and Processing,** 43 (4): 503-509

Al-Odaini, N. A., Zakaria, M. P., Yaziz, M. I. et al (2010) Multi-residue analytical method for human pharmaceuticals and synthetic hormones in river water and sewage effluents by solid-phase extraction and liquid chromatography-tandem mass spectrometry. **Journal of Chromatography A,** 1217 (44): 6791-6806

Al-Qaim, F. F., Abdullah, M. P., Othman, M. R. et al (2014) Multi-residue analytical methodology-based liquid chromatography-time-of-flight-mass spectrometry for the analysis of pharmaceutical residues in surface water and effluents from sewage treatment plants and hospitals. **Journal of Chromatography A,** 1345 139-153

Alenezi, R. (2009) **Biodiesel Production from Different Methods, PhD Thesis, University of Birmingham.**

Alenezi, R., Baig, M., Wang, J. et al (2010a) Continuous Flow Hydrolysis of Sunflower Oil for Biodiesel. **Energy Sources Part A-Recovery Utilization and Environmental Effects,** 32 (5): 460-468

Alenezi, R., Leeke, G. A., Santos, R. C. D. et al (2009) Hydrolysis kinetics of sunflower oil under subcritical water conditions. **Chemical Engineering Research & Design,** 87 (6A): 867-873

Alenezi, R., Leeke, G. A., Winterbottom, J. M. et al (2010b) Esterification kinetics of free fatty acids with supercritical methanol for biodiesel production. **Energy Conversion and Management,** 51 (5): 1055-1059

Alzaga, R., Ryan, R. W., Taylor-Worth, K. et al (2007) A generic approach for the determination of residues of alkylating agents in active pharmaceutical ingredients by in situ derivatization-headspace-gas chromatography-mass spectrometry. **Journal of Pharmaceutical and Biomedical Analysis,** 45 (3): 472-479

Andreozzi, R., Caprio, V., Insola, A. et al (1999) Advanced oxidation processes (AOP) for water purification and recovery. **Catalysis Today,** 53 (1): 51-59

Asghar, A., Abdul Raman, A. A. and Wan Daud, W. M. A. (2015) Advanced oxidation processes for in-situ production of hydrogen peroxide/hydroxyl radical for textile wastewater treatment: a review. **Journal of Cleaner Production,** 87 826-838

Azzouz, A. and Ballesteros, E. (2014) Trace analysis of endocrine disrupting compounds in environmental water samples by use of solid-phase extraction and gas chromatography with mass spectrometry detection. **Journal of Chromatography A,** 1360 (0): 248-257

Bach, H. F. and Pilhofer, T. (1977) Influence of Various Material and Operating Parameters on Relative Gas Content of Bubble-Columns. **Chemie Ingenieur Technik,** 49 (5): p. 435

Balcerski, W., Ryu, S. Y. and Hoffmann, M. R. (2007) Visible-light photoactivity of nitrogen-doped TiO2: Photo-oxidation of HCO2H to CO_2 and H_2O. **Journal of Physical Chemistry C,** 111 (42): 15357-15362

Bang, D. Y., Kyung, M., Kim, M. J. et al (2012) Human Risk Assessment of Endocrine-Disrupting Chemicals Derived from Plastic Food Containers. **Comprehensive Reviews in Food Science and Food Safety,** 11 (5): 453-470

Baz-RodrÕguez, S. A., Botello-Alvarez, J. Ñ. E., Estrada-Baltazar, A. et al (2014) Effect of electrolytes in aqueous solutions on oxygen transfer in gas–liquid bubble columns. **Chemical Engineering Research and Design,** 92 (11): 2352-2360

Behkish, A., Men, Z. W., Inga, J. R. et al (2002) Mass transfer characteristics in a large-scale slurry bubble column reactor with organic liquid mixtures. **Chemical Engineering Science,** 57 (16): 3307-3324

Belfroid, A. C., van Drunen, M., Beek, M. A. et al (1998) Relative risks of transformation products of pesticides for aquatic ecosystems. **Science of the Total Environment,** 222 (3): 167-183

Beltran, J., Serrano, E., Lopez, F. et al (2006) Comparison of two quantitative GC-MS methods for analysis of tomato aroma based on purge-and-trap and on solid-phase microextraction. **Analytical and Bioanalytical Chemistry,** 385 (7): 1255-1264

Benijts, T., Dams, R., Lambert, W. et al (2004) Countering matrix effects in environmental liquid chromatography-electrospray ionization tandem mass spectrometry water analysis for endocrine disrupting chemicals. **Journal of Chromatography A,** 1029 (1-2): 153-159

Birnbaum, L. S. and Staskal, D. F. (2004) Brominated flame retardants: Cause for concern? **Environmental Health Perspectives,** 112 (1): 9-17

Blackburn, M. A. and Waldock, M. J. (1995) Concentrations of Alkylphenols in Rivers and Estuaries in England and Wales. **Water Research,** 29 (7): 1623-1629

Bouaifi, M., Hebrard, G., Bastoul, D. et al (2001) A comparative study of gas hold-up, bubble size, interfacial area and mass transfer coefficients in stirred gas-liquid reactors and bubble columns. **Chemical Engineering and Processing,** 40 (2): 97-111

Boyes, A. P., Chughtai, A., Lu, X. X. et al (1992a) The Cocurrent Downflow Contactor (CDC) Reactor - Chemically Enhanced Mass-Transfer and Reaction Studies for Slurry and Fixed-Bed Catalytic-Hydrogenation. **Chemical Engineering Science,** 47 (13-14): 3729-3736

Boyes, A. P., Chughtai, A., Lu, X. X. et al (1992b) The Cocurrent Downflow Contactor (CDC) Reactor - Chemically Enhanced Mass-Transfer and Reaction Studies for Slurry and Fixed-Bed Catalytic-Hydrogenation. **Chemical Engineering Science,** 47 (13-14): 3729-3736

Boyes, A. P., Chugtai, A., Khan, Z. et al (1995a) The Cocurrent Downflow Contactor (CDC) As A Fixed-Bed and Slurry Reactor for Catalytic-Hydrogenation. **Journal of Chemical Technology and Biotechnology,** 64 (1): 55-65

Boyes, A. P. & Ellis, S. R. M. (1976), **Gas Liquid Contacting. Patent. 1,596,738. U.K.**

Boyes, A. P., Lu, X. X., Raymahasay, S. et al (1991) The Cocurrent Downflow Contactor (CDC) - Mass-Transfer and Reaction Characteristics in Unpacked and Packed-Bed Operation. **Chemical Engineering Research & Design,** 69 (3): 200-202

Boyes, A. P., Raymahasay, S., Sulidis, A. T. et al (1995b) Oxidation of Aqueous Organic Pollutants in Industrial Waste Water by Heterogeneous Photocatalysis Using A Cocurrent Downflow Bubble Column Contactor (CDC). **Water Pollution Iii: Modelling, Measuring and Prediction,** 313-320

Caldwell, D. J., Mastrocco, F., Nowak, E. et al (2010) An Assessment of Potential Exposure and Risk from Estrogens in Drinking Water. **Environmental Health Perspectives,** 118 (3): 338-344

Caliman, F. A. and Gavrilescu, M. (2009) Pharmaceuticals, Personal Care Products and Endocrine Disrupting Agents in the Environment - A Review. **Clean-Soil Air Water,** 37 (4-5): 277-303

Campos, J. C., Borges, R. M. H., Oliveira, A. M. et al (2002) Oilfield wastewater treatment by combined microfiltration and biological processes. **Water Research,** 36 (1): 95-104

Carabias-Martinez, R., Rodriguez-Gonzalo, E., Paniagua-Marcos, P. H. et al (2000) Analysis of pesticide residues in matrices with high lipid contents by membrane separation coupled on-line to a high-performance liquid chromatography system. **Journal of Chromatography A,** 869 (1-2): 427-439

Carabias-Martinez, R., Rodriguez-Gonzalo, E., Revilla-Ruiz, P. et al (2005) Pressurized liquid extraction in the analysis of food and biological samples. **Journal of Chromatography A,** 1089 (1-2): 1-17

Carbonell, M. M. and Guirardello, R. (1997) Modelling of a slurry bubble column reactor applied to the hydroconversion of heavy oils. **Chemical Engineering Science,** 52 (21Γ_ô22): 4179-4185

Cervera, M., I, Beltran, J., Lopez, F. et al (2011) Determination of volatile organic compounds in water by head space-solid-phase microextraction gas chromatography coupled to tandem mass spectrometry with triple quadrupole analyzer. **Analytica Chimica Acta,** 704 (1-2): 87-97

Chang, H., Wu, S. M., Hu, J. Y. et al (2008) Trace analysis of androgens and progestogens in environmental waters by ultra-performance liquid chromatography-electrospray tandem mass spectrometry. **Journal of Chromatography A,** 1195 (1-2): 44-51

Chen, J., Gomez, J. A., Hoffner, K. et al (2015) Metabolic modeling of synthesis gas fermentation in bubble column reactors. **Biotechnology for Biofuels,** 8

Chen, W., Hasegawa, T., Tsutsumi, A. et al (2003) Generalized dynamic modeling of local heat transfer in bubble columns. **Chemical Engineering Journal,** 96 (1-3): 37-44

Chilekar, V. P., van der Schaaf, J., Kuster, B. F. et al (2010) Influence of Elevated Pressure and Particle Lyophobicity on Hydrodynamics and Gas-Liquid Mass Transfer in Slurry Bubble Columns. **Aiche Journal,** 56 (3): 584-596

Chimchirian, R. F., Suri, R. P. S. and Fu, H. X. (2007) Free synthetic and natural estrogen hormones in influent and effluent of three municipal wastewater treatment plants. **Water Environment Research,** 79 (9): 969-974

Chingombe, P., Saha, B. and Wakeman, R. J. (2005) Surface modification and characterisation of a coal-based activated carbon. **Carbon,** 43 (15): 3132-3143

Chiu, T. M. and Ziegler, E. N. (1985) Liquid Holdup and Heat-Transfer Coefficient in Liquid-Solid and 3-Phase Fluidized-Beds. **Aiche Journal,** 31 (9): 1504-1509

Cho, Y. J., Woo, K. J., Kang, Y. et al (2002) Dynamic characteristics of heat transfer coefficient in pressurized bubble columns with viscous liquid medium. **Chemical Engineering and Processing,** 41 (8): 699-706

Chowdhury, R. R., Charpentier, P. A. and Ray, M. B. (2011) Photodegradation of 17 beta-estradiol in aquatic solution under solar irradiation: Kinetics and influencing water parameters. **Journal of Photochemistry and Photobiology A-Chemistry,** 219 (1): 67-75

Chughtai, A. (1993) **The Development of Packed-Bed Co Current Downflow. Contactor Reactor. PhD thesis University of Birmingham.**

Colborn, T. & Clement, C. (1992) "Chemically-induced Alterations in Sexual and Functional Development: The Wildlife/human Connection. Princeton Scientific Pub. Co., Princeton, NJ.". In.

Colella, D., Vinci, D., Bagatin, R. et al (1999) A study on coalescence and breakage mechanisms in three different bubble columns. **Chemical Engineering Science,** 54 (21): 4767-4777

Coleman, H. M., Eggins, B. R., Byrne, J. A. et al (2000) Photocatalytic degradation of 17-__-oestradiol on immobilised TiO2. **Applied Catalysis B: Environmental,** 24 (1): p. L1-L5

Collier, A. C. (2007) Pharmaceutical contaminants in potable water: Potential concerns for pregnant women and children. **Ecohealth,** 4 (2): 164-171

Commission of the European Communities. European Workshop on the Impact of Endocrine Disrupters on Human Health and Wildlife, Weybridge, UK, 2-4 December 1996, Commission of the European Communities, EUR 17549 Brussels, 1997, 126 pages. 1997.
Ref Type: Generic

Comninellis, C. (1994) Electrocatalysis in the Electrochemical Conversion/Combustion of Organic Pollutants for Waste-Water Treatment. **Electrochimica Acta,** 39 (11-12): 1857-1862

Comninellis, C., Kapalka, A., Malato, S. et al (2008) Advanced oxidation processes for water treatment: advances and trends for R&D. **Journal of Chemical Technology and Biotechnology,** 83 (6): 769-776

Conn, K. E., Barber, L. B., Brown, G. K. et al (2006) Occurrence and fate of organic contaminants during onsite wastewater treatment. **Environmental Science & Technology,** 40 (23): 7358-7366

Courant, F., Antignac, J. P., Maume, D. et al (2007) Determination of naturally occurring oestrogens and androgens in retail samples of milk and eggs. **Food Additives and Contaminants,** 24 (12): 1358-1366

Cui, C. W., Ji, S. L. and Ren, H. Y. (2006) Determination of steroid estrogens in wastewater treatment plant of a controceptives producing factory. **Environmental Monitoring and Assessment,** 121 (1-3): 409-419

Damstra, T. (2002) Potential effects of certain persistent organic pollutants and endocrine disrupting chemicals on the health of children. **Journal of Toxicology-Clinical Toxicology,** 40 (4): 457-465

de Alda, M. J. L. and Barcelo, D. (2000) Determination of steroid sex hormones and related synthetic compounds considered as endocrine disrupters in water by liquid chromatography-diode array detection-mass spectrometry. **Journal of Chromatography A,** 892 (1-2): 391-406

de Alda, M. J. L. and Barcelo, D. (2001) Use of solid-phase extraction in various of its modalities for sample preparation in the determination of estrogens and progestogens in sediment and water. **Journal of Chromatography A,** 938 (1-2): 145-153

Deckwer, W. D. (1980) On the Mechanism of Heat-Transfer in Bubble Column Reactors. **Chemical Engineering Science,** 35 (6): 1341-1346

Deckwer, W. D. (1992) **Bubble Column Reactions, John Wiley & Sons Ltd.**

Deckwer, W. D., Louisi, Y., Zaidi, A. et al (1980) Hydrodynamic Properties of the Fischer-Tropsch Slurry Process. **Industrial & Engineering Chemistry Process Design and Development,** 19 (4): 699-708

Deckwer, W. D. and Schumpe, A. (1993) Improved Tools for Bubble Column Reactor Design and Scale-Up. **Chemical Engineering Science,** 48 (5): 889-911

Degaleesan, S., Dudukovic, M. and Pan, Y. (2001) Experimental study of gas-induced liquid-flow structures in bubble columns. **Aiche Journal,** 47 (9): 1913-1931

Desbrow, C., Routledge, E. J., Brighty, G. C. et al (1998) Identification of estrogenic chemicals in STW effluent. 1. Chemical fractionation and in vitro biological screening. **Environmental Science & Technology,** 32 (11): 1549-1558

Deswart, J. W. A., vanVliet, R. E. and Krishna, R. (1996) Size, structure and dynamics of "large" bubbles in a two-dimensional slurry bubble column. **Chemical Engineering Science,** 51 (20): 4619-4629

Diamanti-Kandarakis, E., Bourguignon, J. P., Giudice, L. C. et al (2009) Endocrine-Disrupting Chemicals: An Endocrine Society Scientific Statement. **Endocrine Reviews,** 30 (4): 293-342

Diaz-Cruz, M. S., de Alda, M. J. L., Lopez, R. et al (2003) Determination of estrogens and progestogens by mass spectrometric techniques (GC/MS, LC/MS and LC/MS/MS). **Journal of Mass Spectrometry,** 38 (9): 917-923

Douek, R. S., Hewitt, G. F. and Livingston, A. G. (1997) Hydrodynamics of vertical co-current gas-liquid-solid flows. **Chemical Engineering Science,** 52 (23): 4357-4372

Dursun, G. and Akosman, C. (2006) Gas-liquid interfacial area and mass transfer coefficient in a co-current down flow contacting column. **Journal of Chemical Technology and Biotechnology,** 81 (12): 1859-1865

Dutta, N. N. and Raghavan, K. V. (1987) Mass-Transfer and Hydrodynamic Characteristics of Loop Reactors with Downflow Liquid Jet Ejector. **Chemical Engineering Journal and the Biochemical Engineering Journal,** 36 (2): 111-121

Dzieweczynski, T. L. and Hebert, O. L. (2013) The Effects of Short-Term Exposure to an Endocrine Disrupter on Behavioral Consistency in Male Juvenile and Adult Siamese Fighting Fish. **Archives of Environmental Contamination and Toxicology,** 64 (2): 316-326

EDSTAC (1998), **Endocrine Disruptor and Testing Advisory Committee** .

El-Ashtoukhy, E. S. Z. and Abdel-Aziz, M. H. (2013) Removal of copper from aqueous solutions by cementation in a bubble column reactor fitted with horizontal screens. **International Journal of Mineral Processing,** 121 (0): 65-69

EPA (2010), **Treating Contaminants of Emerging Concern, U.S. Environmental Protection Agency, EPA-820-R-10-002** .

Esplugas, S., Bila, D. M., Krause, L. G. T. et al (2007) Ozonation and advanced oxidation technologies to remove endocrine disrupting chemicals (EDCs) and pharmaceuticals and personal care products (PPCPs) in water effluents. **Journal of Hazardous Materials,** 149 (3): 631-642

EUROSTAT (2015), **Production of environmentally harmful chemicals, by environmental impact class** .

Evinc, F. Absorption of gases in a co current downflow column. M.Sc. thesis, University of Birmingham, U.K. 1982.
Ref Type: Generic

Fan, Y., Zhang, M., Da, S. L. et al (2005) Determination of endocrine disruptors in environmental waters using poly(acrylamide-vinylpyridine) monolithic capillary for in-tube solid-phase microextraction coupled to high-performance liquid chromatography with fluorescence detection. **Analyst,** 130 (7): 1065-1069

Fang, X., Wang, J., Zhou, H. et al (2009) Microwave-assisted extraction with water for fast extraction and simultaneous RP-HPLC determination of phenolic acids in Radix Salviae Miltiorrhizae. **Journal of Separation Science,** 32 (14): 2455-2461

Ferrer, I. and Thurman, E. M. (2012) Analysis of 100 pharmaceuticals and their degradates in water samples by liquid chromatography/quadrupole time-of-flight mass spectrometry. **Journal of Chromatography A,** 1259 148-157

Filby, A. L., Shears, J. A., Drage, B. E. et al (2010) Effects of Advanced Treatments of Wastewater Effluents on Estrogenic and Reproductive Health Impacts in Fish. **Environmental Science & Technology,** 44 (11): 4348-4354

Filby, A. L., Neuparth, T., Thorpe, K. L. et al (2007) Health impacts of estrogens in the environment, considering complex mixture effects. **Environmental Health Perspectives,** 115 (12): 1704-1710

Fishwick, R. P., Natividad, R., Kulkarni, R. et al (2007) Selective hydrogenation reactions: A comparative study of monolith CDC, stirred tank and trickle bed reactors. **Catalysis Today,** 128 (1-2): 108-114

Frontistis, Z., Xekoukoulotakis, N. P., Hapeshi, E. et al (2011) Fast degradation of estrogen hormones in environmental matrices by photo-Fenton oxidation under simulated solar radiation. **Chemical Engineering Journal,** 178 175-182

Fu, F. and Wang, Q. (2011) Removal of heavy metal ions from wastewaters: A review. **Journal of Environmental Management,** 92 (3): 407-418

Fujie, K., Takaine, M., Kubota, H. et al (1980) Flow and Oxygen-Transfer in Cocurrent Gas-Liquid Downflow. **Journal of Chemical Engineering of Japan,** 13 (3): 188-193

Fukuma, M., Muroyama, K. and Yasunishi, A. (1987) Properties of Bubble Swarm in A Slurry Bubble Column. **Journal of Chemical Engineering of Japan,** 20 (1): 28-33

Gabet, V., Miege, C., Bados, P. et al (2007) Analysis of estrogens in environmental matrices. **Trac-Trends in Analytical Chemistry,** 26 (11): 1113-1131

Gabriel, C., Gabriel, S., Grant, E. H. et al (1998) Dielectric parameters relevant to microwave dielectric heating. **Chemical Society Reviews,** 27 (3): 213-223

Gadipelly, C., Perez-Gonzalez, A., Yadav, G. D. et al (2014) Pharmaceutical Industry Wastewater: Review of the Technologies for Water Treatment and Reuse. **Industrial & Engineering Chemistry Research,** 53 (29): 11571-11592

Geary, P. M. (2005) Effluent tracing and the transport of contaminants from a domestic septic system. **Water Science and Technology,** 51 (10): 283-290

Giergielewicz-Mozajska, H., Dabrowski, L. and Namiesnik, J. (2001) Accelerated Solvent Extraction (ASE) in the analysis of environmental solid samples - Some aspects of theory and practice. **Critical Reviews in Analytical Chemistry,** 31 (3): 149-165

Glaze, W. H., Kang, J. W. and Chapin, D. H. (1987) The Chemistry of Water-Treatment Processes Involving Ozone, Hydrogen-Peroxide and Ultraviolet-Radiation. **Ozone-Science & Engineering,** 9 (4): 335-352

Gore, A. C. e. al. (2014), **Introduction to Endocrine Disrupting Chemicals (EDCs) - A Guide for Public Interest Organizations and Policy-makers. Endocrine Society.** **http://www.endocrine.org/~/media/endosociety/Files/Advocacy%20and%20Outreach/Important%20Documents/Introduction%20to%20Endocrine%20Disrupting%20Chemicals.pdf** .

GOV.UK (2015), **GOV.UK,** **https://www.gov.uk/government/uploads/system/uploads/attachment_data/file/416987/table_224.xls** .

Grey, D., Garrick, D., Blackmore, D. et al (2013) Water security in one blue planet: twenty-first century policy challenges for science. **Philosophical Transactions of the Royal Society A-Mathematical Physical and Engineering Sciences,** 371 (2002):

Guedes-Alonso, R., Sosa-Ferrera, Z. and Santana-Rodriguez, J. J. (2015) An on-line solid phase extraction method coupled with UHPLC-MS/MS for the determination of steroid hormone compounds in treated water samples from waste water treatment plants. **Analytical Methods,** 7 (14): 5996-6005

Gunatilake, S. R., Craver, S., Kwon, J. W. et al (2013) Analysis of Estrogens in Wastewater Using Solid-Phase Extraction, QuEChERS Cleanup, and Liquid Chromatography/Tandem Mass Spectrometry. **Journal of Aoac International,** 96 (6): 1440-1447

Guo, F., Liu, Q., Qu, G. b. et al (2013) Simultaneous determination of five estrogens and four androgens in water samples by online solid-phase extraction coupled with high-performance liquid chromatography-tandem mass spectrometry. **Journal of Chromatography A,** 1281 9-18

Haigh, S. D. (1996) A review of the interaction of surfactants with organic contaminants in soil. **Science of the Total Environment,** 185 (1-3): 161-170

Hale, R. C., La Guardia, M. J., Harvey, E. P. et al (2001) Polybrominated diphenyl ether flame retardants in virginia freshwater fishes (USA). **Environmental Science & Technology,** 35 (23): 4585-4591

Han, L. and Al-Dahhan, M. H. (2007) Gas-liquid mass transfer in a high pressure bubble column reactor with different sparger designs. **Chemical Engineering Science,** 62 (1-2): 131-139

Hartmann, S., Lacorn, M. and Steinhart, H. (1998) Natural occurrence of steroid hormones in food. **Food Chemistry,** 62 (1): 7-20

Hauser, R. and Calafat, A. M. (2005) Phthalates and human health. **Occupational and environmental medicine,** 62 (11): 806-818

Herbrechtsmeier, P., Schafer, H. and Steiner, R. (1984) Influence of Operating Parameters on the Phase Interface in Bubble Column Downflow Reactors. **Chemie Ingenieur Technik,** 56 (5): 402-403

Hernando, M., Rodriguez, A., Vaquero, J. et al (2011) Environmental Risk Assessment of Emerging Pollutants in Water: Approaches Under Horizontal and Vertical EU Legislation. **Critical Reviews in Environmental Science and Technology,** 41 (7): 699-731

Hikita, H., Asai, S., Kikukawa, H. et al (1981) Heat-Transfer Coefficient in Bubble-Columns. **Industrial & Engineering Chemistry Process Design and Development,** 20 (3): 540-545

Hikita, H., Asai, S., Tanigawa, K. et al (1980) Gas Hold-Up in Bubble-Columns. **Chemical Engineering Journal and the Biochemical Engineering Journal,** 20 (1): 59-67

Holcombe, N. T., Smith, D. N., Knickle, H. N. et al (1983) Thermal Dispersion and Heat-Transfer in Non-Isothermal Bubble-Columns. **Chemical Engineering Communications,** 21 (1-3): 135-150

Horikoshi, S., Hidaka, H. and Serpone, N. (2004) Environmental remediation by an integrated microwave/UV illumination technique - VI. A simple modified domestic microwave oven integrating an electrodeless UV-Vis lamp to photodegrade environmental pollutants in aqueous media. **Journal of Photochemistry and Photobiology A-Chemistry,** 161 (2-3): 221-225

Huang, C. H. and Sedlak, D. L. (2001) Analysis of estrogenic hormones in municipal wastewater effluent and surface water using enzyme-linked immunosorbent assay and gas chromatography/tandem mass spectrometry. **Environmental Toxicology and Chemistry,** 20 (1): 133-139

Hyndman, C. L., Larachi, F. and Guy, C. (1997) Understanding gas-phase hydrodynamics in bubble columns: A convective model based on kinetic theory. **Chemical Engineering Science,** 52 (1): 63-77

International Conference on Harmonization of Technical Requirements for Registration of Pharmaceuticals for Human Use, ICH Harmonized Tripartite Guideline, Validation of Analytical Procedures. (2005ICH, International Conference on Harmonization of Technical Requirements for Registration of Pharmaceuticals for Human Use, http: www.ich.org/products/guidelines/quality/quality-single/article/validation-of-analytical-procedures-text-and-methodology.html .

Idogawa, K., Ikeda, K., Fukuda, T. et al (1986) Effect of Pressure on Bubble Formation Through A Single Round Nozzle. **Kagaku Kogaku Ronbunshu,** 12 (1): 107-109

Ikonomou, M. G., Cai, S. S., Fernandez, M. P. et al (2008) Ultra-trace analysis of multiple endocrine-disrupting chemicals in municipal and bleached kraft mill effluents using gas chromatography-high-resolution mass spectrometry. **Environmental Toxicology and Chemistry,** 27 (2): 243-251

Isobe, T., Shiraishi, H., Yasuda, M. et al (2003) Determination of estrogens and their conjugates in water using solid-phase extraction followed by liquid chromatography-tandem mass spectrometry. **Journal of Chromatography A,** 984 (2): 195-202

Ivankovic, T. and Hrenovic, J. (2010) Surfactants in the Environment. **Arhiv Za Higijenu Rada I Toksikologiju-Archives of Industrial Hygiene and Toxicology,** 61 (1): 95-110

Jena, H. M., Roy, G. K. and Meikap, B. C. (2009) Hydrodynamics of a gas-liquid-solid fluidized bed with hollow cylindrical particles. **Chemical Engineering and Processing,** 48 (1): 279-287

Jhawar, A. and Prakash, A. (2007) Analysis of local heat transfer and hydrodynamics in a bubble column using fast response probes. **Chemical Engineering Science,** 62 (24): 7274-7281

Jhawar, A. and Prakash, A. (2011) Influence of bubble column diameter on local heat transfer and related hydrodynamics. **Chemical Engineering Research & Design,** 89 (10A): 1996-2002

Jiang, J. Q., Zhou, Z. and Sharma, V. K. (2013) Occurrence, transportation, monitoring and treatment of emerging micro-pollutants in waste water - A review from global views. **Microchemical Journal,** 110 292-300

Jin, H., Yang, S., Wang, M. et al (2007) Measurement of gas holdup profiles in a gas liquid cocurrent bubble column using electrical resistance tomography. **Flow Measurement and Instrumentation,** 18 (5-6): 191-196

Joseph, L., Boateng, L. K., Flora, J. R., V et al (2013) Removal of bisphenol A and 17 alpha-ethinyl estradiol by combined coagulation and adsorption using carbon nanomaterials and powdered activated carbon. **Separation and Purification Technology,** 107 37-47

Joshi, J. B. and Sharma, M. M. (1979) Circulation Cell Model for Bubble-Columns. **Transactions of the Institution of Chemical Engineers,** 57 (4): 244-251

Kagliwal, L. D., Patil, S. C., Pol, A. S. et al (2011) Separation of bioactives from seabuckthorn seeds by supercritical carbon dioxide extraction methodology through solubility parameter approach. **Separation and Purification Technology,** 80 (3): 533-540

Kang, Y., Cho, Y. J., Woo, K. J. et al (1999) Diagnosis of bubble distribution and mass transfer in bubble columns with viscous liquid medium. **Chemical Engineering Science,** 54 (21): 4887-4893

Kantarci, N., Borak, F. and Ulgen, K. O. (2005) Bubble column reactors. **Process Biochemistry,** 40 (7): 2263-2283

Kara, S., Kelkar, B. G., Shah, Y. T. et al (1982) Hydrodynamics and Axial Mixing in A 3-Phase Bubble Column. **Industrial & Engineering Chemistry Process Design and Development,** 21 (4): 584-594

Kartinen, E. O. and Martin, C. J. (1995) An overview of arsenic removal processes. **Desalination,** 103 (1-2): 79-88

Kato, Y., Kago, T., Uchida, K. et al (1980) Wall-Bed Heat-Transfer Characteristics of 3-Phase Packed and Fluidized-Bed. **Kagaku Kogaku Ronbunshu,** 6 (6): 579-584

Kavitha, V. and Palanivelu, K. (2004) The role of ferrous ion in Fenton and photo-Fenton processes for the degradation of phenol. **Chemosphere,** 55 (9): 1235-1243

Kavlock, R. J., Daston, G. P., DeRosa, C. et al (1996) Research needs for the risk assessment of health and environmental effects of endocrine disruptors: A report of the US EPA-sponsored workshop. **Environmental Health Perspectives,** 104 715-740

Kawagoe, K., Inoue, T., Nakao, K. et al (1976) Flow-Pattern and Gas-Holdup Conditions in Gas-Sparged Contactors. **International Chemical Engineering,** 16 (1): 176-183

Kawase, Y. and Mooyoung, M. (1987) Heat-Transfer in Bubble Column Reactors with Newtonian and Non-Newtonian Fluids. **Chemical Engineering Research & Design,** 65 (2): 121-126

Kemoun, A., Ong, B. C., Gupta, P. et al (2001) Gas holdup in bubble columns at elevated pressure via computed tomography. **International Journal of Multiphase Flow,** 27 (5): 929-946

Khan, Z. (1995) **Catalytic Hydrogenation in a Cocurrent Downflow Contactor Reactor, PhD Thesis, University of Birmingham.**

Kim, I. and Tanaka, H. (2009) Photodegradation characteristics of PPCPs in water with UV treatment. **Environment International,** 35 (5): 793-802

Kim, S. D., Kang, Y. and Kwon, H. K. (1986) Heat-Transfer Characteristics in 2-Phase and 3-Phase Slurry-Fluidized Beds. **Aiche Journal,** 32 (8): 1397-1400

Koide, K., Takazawa, A., Komura, M. et al (1984) Gas Holdup and Volumetric Liquid-Phase Mass-Transfer Coefficient in Solid-Suspended Bubble-Columns. **Journal of Chemical Engineering of Japan,** 17 (5): 459-466

Kojima, H., Sawai, J. and Suzuki, H. (1997) Effect of pressure on volumetric mass transfer coefficient and gas holdup in bubble column. **Chemical Engineering Science,** 52 (21-22): 4111-4116

Kolpin, D. W., Furlong, E. T., Meyer, M. T. et al (2002) Pharmaceuticals, hormones, and other organic wastewater contaminants in US streams, 1999-2000: A national reconnaissance. **Environmental Science & Technology,** 36 (6): 1202-1211

Kotronarou, A., Mills, G. and Hoffmann, M. R. (1992) Decomposition of Parathion in Aqueous-Solution by Ultrasonic Irradiation. **Environmental Science & Technology,** 26 (7): 1460-1462

Kuch, H. M. and Ballschmiter, K. (2001) Determination of endocrine-disrupting phenolic compounds and estrogens in surface and drinking water by HRGC-(NCI)-MS in the picogram per liter range. **Environmental Science & Technology,** 35 (15): 3201-3206

Kulkarni, A. V. and Joshi, J. B. (2011) Design and selection of sparger for bubble column reactor. Part II: Optimum sparger type and design. **Chemical Engineering Research & Design,** 89 (10A): 1986-1995

Kulkarni, R., Natividad, R., Wood, J. et al (2005) A comparative study of residence time distribution and selectivity in a monolith CDC reactor and a trickle bed reactor. **Catalysis Today,** 105 (3-4): 455-463

Kumar, S. and Fan, L. S. (1994) Heat-Transfer Characteristics in Viscous Gas-Liquid and Gas-Liquid-Solid Systems. **Aiche Journal,** 40 (5): 745-755

Kuster, M., Azevedo, D., Lopez de Alda, M. et al (2009) Analysis of phytoestrogens, progestogens and estrogens in environmental waters from Rio de Janeiro (Brazil). **Environment International,** 35 (7): 997-1003

Lagana, A., Bacaloni, A., De Leva, I. et al (2004) Analytical methodologies for determining the occurrence of endocrine disrupting chemicals in sewage treatment plants and natural waters. **Analytica Chimica Acta,** 501 (1): 79-88

Lage, P. L. C. and Esposito, R. O. (1999) Experimental determination of bubble size distributions in bubble columns: prediction of mean bubble diameter and gas hold up. **Powder Technology,** 101 (2): 142-150

Lai, K. M., Johnson, K. L., Scrimshaw, M. D. et al (2000) Binding of waterborne steroid estrogens to solid phases in river and estuarine systems. **Environmental Science & Technology,** 34 (18): 3890-3894

Lau, R., Lee, P. H. V. and Chen, T. (2012) Mass transfer studies in shallow bubble column reactors. **Chemical Engineering and Processing,** 62 18-25

Lau, Y., Deen, N. and Kuipers, J. (2013a) Development of an image measurement technique for size distribution in dense bubbly flows. **Chemical Engineering Science,** 94 20-29

Lau, Y. M., Sujatha, K. T., Gaeini, M. et al (2013b) Experimental study of the bubble size distribution in a pseudo-2D bubble column. **Chemical Engineering Science,** 98 203-211

Letzel, H. M., Schouten, J. C., Krishna, R. et al (1999) Gas holdup and mass transfer in bubble column reactors operated at elevated pressure. **Chemical Engineering Science,** 54 (13-14): 2237-2246

Levenspi, O. (1972) **Chemical Reaction Engineering, 2nd Edition, John Wiley & Sons Inc.**

Li, H. and Prakash, A. (1997) Heat transfer and hydrodynamics in a three-phase slurry bubble column. **Industrial & Engineering Chemistry Research,** 36 (11): 4688-4694

Li, H. and Prakash, A. (2000) Influence of slurry concentrations on bubble population and their rise velocities in a three-phase slurry bubble column. **Powder Technology,** 113 (1-2): 158-167

Li, H. and Prakash, A. (2001) Survey of heat transfer mechanisms in a slurry bubble column. **Canadian Journal of Chemical Engineering,** 79 (5): 717-725

Li, H. and Prakash, A. (2002) Analysis of flow patterns in bubble and slurry bubble columns based on local heat transfer measurements. **Chemical Engineering Journal,** 86 (3): 269-276

Li, H., Prakash, A., Margaritis, A. et al (2003) Effects of micron-sized particles on hydrodynamics and local heat transfer in a slurry bubble column. **Powder Technology,** 133 (1-3): 171-184

Li, W., Zhong, W., Jin, B. et al (2014) Flow patterns and transitions in a rectangular three-phase bubble column. **Powder Technology,** 260 (0): 27-35

Lidstrom, P., Tierney, J., Wathey, B. et al (2001) Microwave assisted organic synthesis - a review. **Tetrahedron,** 57 (45): 9225-9283

Lin, T. J. and Fan, L. S. (1999) Heat transfer and bubble characteristics from a nozzle in high-pressure bubble columns. **Chemical Engineering Science,** 54 (21): 4853-4859

Lishman, L., Smyth, S. A., Sarafin, K. et al (2006) Occurrence and reductions of pharmaceuticals and personal care products and estrogens by municipal wastewater treatment plants in Ontario, Canada. **Science of the Total Environment,** 367 (2-3): 544-558

Liu, B. and Liu, X. L. (2004) Direct photolysis of estrogens in aqueous solutions. **Science of the Total Environment,** 320 (2-3): 269-274

Liu, F. H. and Jiang, Y. (2007) Room temperature ionic liquid as matrix medium for the determination of residual solvents in pharmaceuticals by static headspace gas chromatography. **Journal of Chromatography A,** 1167 (1): 116-119

Liu, J., Wang, R., Huang, B. et al (2012) Biological effects and bioaccumulation of steroidal and phenolic endocrine disrupting chemicals in high-back crucian carp exposed to wastewater treatment plant effluents. **Environmental Pollution,** 162 325-331

Liu, X. L., Wu, F. and Deng, N. S. (2003) Photo degradation of 17 alpha-ethynylestradiol in aqueous solution exposed to a high-pressure mercury lamp (250 W). **Environmental Pollution,** 126 (3): 393-398

Lord, H. L., Rajabi, M., Safari, S. et al (2006) Development of immunoaffinity solid phase microextraction probes for analysis of sub ng/mL concentrations of 7-aminoflunitrazepam in urine. **Journal of Pharmaceutical and Biomedical Analysis,** 40 (3): 769-780

Lu, X. X. (1988a) **A study of the characteristics of a novel co current downflow bubble column contactor for use as a three phase reactor. PhD. thesis. University of Birmingham, UK.**

Lu, X. X. (1988b), **A study of the characteristics of a novel co current downflow bubble column contactor for use as a three phase reactor. PhD. thesis. University of Birmingham, UK.**

Lu, X. X., Boyes, A. P. and Winterbottom, J. M. (1996) Study of mass transfer characteristics of a cocurrent downflow bubble column reactor using hydrogenation of itaconic acid. **Chemical Engineering Science,** 51 (11): 2715-2720

Luo, X. K., Lee, D. J., Lau, R. et al (1999a) Maximum stable bubble size and gas holdup in high-pressure slurry bubble columns. **Aiche Journal,** 45 (4): 665-680

Luo, X. K., Lee, D. J., Lau, R. et al (1999b) Maximum stable bubble size and gas holdup in high-pressure slurry bubble columns. **Aiche Journal,** 45 (4): 665-680

Malekinejad, H., Scherpenisse, P. and Bergwerff, A. A. (2006) Naturally occurring estrogens in processed milk and in raw milk (from gestated cows). **Journal of Agricultural and Food Chemistry,** 54 (26): 9785-9791

Malik, P. K. and Saha, S. K. (2003) Oxidation of direct dyes with hydrogen peroxide using ferrous ion as catalyst. **Separation and Purification Technology,** 31 (3): 241-250

Mandal, A., Kundu, G. and Mukherjee, D. (2005) A comparative study of gas holdup, bubble size distribution and interfacial area in a downflow bubble column. **Chemical Engineering Research & Design,** 83 (A4): 423-428

Martinez-Huitle, C. A. and Ferro, S. (2006) Electrochemical oxidation of organic pollutants for the wastewater treatment: direct and indirect processes. **Chemical Society Reviews,** 35 (12): 1324-1340

Marwan, H. and Winterbottom, J. M. (2003) Operating characteristics and performance of a monolithic downflow bubble column reactor in selective hydrogenation of butyne-1,4-diol. **Chemical Engineering & Technology,** 26 (9): 996-1002

Matsuura, A. and Fan, L. S. (1984) Distribution of Bubble Properties in A Gas-Liquid-Solid Fluidized-Bed. **Aiche Journal,** 30 (6): 894-903

McClure, D. D., Lee, A. C., Kavanagh, J. M. et al (2015) Impact of Surfactant Addition on Oxygen Mass Transfer in a Bubble Column. **Chemical Engineering & Technology,** 38 (1): 44-52

Melo, S. M. and Brito, N. M. (2014) Analysis and Occurrence of Endocrine Disruptors in Brazilian Water by HPLC-Fluorescence Detection. **Water Air and Soil Pollution,** 225 (1):

Mena, P. C., Pons, M. N., Teixeira, J. A. et al (2005) Using image analysis in the study of multiphase gas absorption. **Chemical Engineering Science,** 60 (18): 5144-5150

Mendes, R. L., Nobre, B. P., Cardoso, M. T. et al (2003) Supercritical carbon dioxide extraction of compounds with pharmaceutical importance from microalgae. **Inorganica Chimica Acta,** 356 328-334

Miege, C., Bados, P., Brosse, C. et al (2009) Method validation for the analysis of estrogens (including conjugated compounds) in aqueous matrices. **Trac-Trends in Analytical Chemistry,** 28 (2): 237-244

Minioti, K. S., Sakellariou, C. F. and Thomaidis, N. S. (2007) Determination of 13 synthetic food colorants in water-soluble foods by reversed-phase high-performance liquid chromatography coupled with diode-array detector. **Analytica Chimica Acta,** 583 (1): 103-110

Mohan, D. and Pittman, C. U. (2007) Arsenic removal from water/wastewater using adsorbents - A critical review. **Journal of Hazardous Materials,** 142 (1-2): 1-53

Mohan, D., Singh, K. R. and Singh, V. K. (2008) Wastewater treatment using low cost activated carbons derived from agricultural byproducts - A case study. **Journal of Hazardous Materials,** 152 (3): 1045-1053

Mol, H. G. J., Sunarto, S. and Steijger, O. M. (2000) Determination of endocrine disruptors in water after derivatization with N-methyl-N-(tert.-butyldimethyltrifluoroacetamide) using gas chromatography with mass spectrometric detection. **Journal of Chromatography A,** 879 (1): 97-112

Moreno-Gonzalez, R., Campillo, J., Garcia, V. et al (2013) Seasonal input of regulated and emerging organic pollutants through surface watercourses to a Mediterranean coastal lagoon. **Chemosphere,** 92 (3): 247-257

Muller, F. L. and Davidson, J. F. (1995) On the Effects of Surfactants on Mass-Transfer to Viscous-Liquids in Bubble-Columns. **Chemical Engineering Research & Design,** 73 (A3): 291-296

Nagel, S. C. and Bromfield, J. J. (2013) Bisphenol A: A Model Endocrine Disrupting Chemical With a New Potential Mechanism of Action. **Endocrinology,** 154 (6): 1962-1964

Nasuhoglu, D., Berk, D. and Yargeau, V. (2012) Photocatalytic removal of 17 alpha-ethinylestradiol (EE2) and levonorgestrel (LNG) from contraceptive pill manufacturing plant wastewater under UVC radiation. **Chemical Engineering Journal,** 185 52-60

Neamtu, M., Siminiceanu, I., Yediler, A. et al (2002) Kinetics of decolorization and mineralization of reactive azo dyes in aqueous solution by the UV/H2O2 oxidation. **Dyes and Pigments,** 53 (2): 93-99

Nieto, A., Borrull, F., Pocurull, E. et al (2008) Determination of natural and synthetic estrogens and their conjugates in sewage sludge by pressurized liquid extraction and liquid chromatography-tandem mass spectrometry. **Journal of Chromatography A,** 1213 (2): 224-230

Nieto, A., Borrull, F., Pocurull, E. et al (2010) Pressurized liquid extraction: A useful technique to extract pharmaceuticals and personal-care products from sewage sludge. **Trac-Trends in Analytical Chemistry,** 29 (7): 752-764

Ochuma, I. J. (2007) **Photo - oxidation of Pollutants in Wastewater, PhD Thesis, University of Birmingham.**

Ochuma, I. J., Fishwick, R. P., Wood, J. et al (2007a) Optimisation of degradation conditions of 1,8-diazabicyclo[5.4.0]undec-7-ene in water and reaction kinetics analysis using a cocurrent downflow contactor photocatalytic reactor. **Applied Catalysis B-Environmental,** 73 (3-4): 259-268

Ochuma, I. J., Fishwick, R. P., Wood, J. et al (2007b) Photocatalytic oxidation of 2,4,6-trichlorophenol in water using a cocurrent downflow contactor reactor (CDCR). **Journal of Hazardous Materials,** 144 (3): 627-633

Ochuma, I. J., Osibo, O. O., Fishwick, R. P. et al (2007c) Three-phase photocatalysis using suspended titania and titania supported on a reticulated foam monolith for water purification. **Catalysis Today,** 128 (1-2): 100-107

Ohkawa, A., Kawai, Y., Kusabiraki, D. et al (1987) Bubble-Size, Interfacial Area and Volumetric Liquid-Phase Mass-Transfer Coefficient in Downflow Bubble-Columns with Gas Entrainment by A Liquid Jet. **Journal of Chemical Engineering of Japan,** 20 (1): 99-101

Ojima, S., Hayashi, K. and Tomiyama, A. (2014) Effects of hydrophilic particles on bubbly flow in slurry bubble column. **International Journal of Multiphase Flow,** 58 (0): 154-167

Oyevaar, M. H., Bos, R. and Westerterp, K. R. (1991) Interfacial-Areas and Gas Hold-Ups in Gas-Liquid Contactors at Elevated Pressures from 0.1 to 8.0 Mpa. **Chemical Engineering Science,** 46 (5-6): 1217-1231

Ozturk, S. S., Schumpe, A. and Deckwer, W. D. (1987) Organic Liquids in A Bubble Column - Holdups and Mass-Transfer Coefficients. **Aiche Journal,** 33 (9): 1473-1480

Parthasarathy, R. and Ahmed, N. (1996) Size distribution of bubbles generated by fine-pore spargers. **Journal of Chemical Engineering of Japan,** 29 (6): 1030-1034

Patel, S. A., Daly, J. G. and Bukur, D. B. (1989) Holdup and Interfacial Area Measurements Using Dynamic Gas Disengagement. **Aiche Journal,** 35 (6): 931-942

Perez, M., Torrades, F., Domenech, X. et al (2002) Fenton and photo-Fenton oxidation of textile effluents. **Water Research,** 36 (11): 2703-2710

Poelmans, S., De Wasch, K., Noppe, H. et al (2005) Endogenous occurrence of some anabolic steroids in swine matrices. **Food Additives and Contaminants,** 22 (9): 808-815

Poole, C. F. (2003) New trends in solid-phase extraction. **Trac-Trends in Analytical Chemistry,** 22 (6): 362-373

Prakash, A., Margaritis, A., Li, H. et al (2001) Hydrodynamics and local heat transfer measurements in a bubble column with suspension of yeast. **Biochemical Engineering Journal,** 9 (2): 155-163

Quintana, J. B., Carpinteiro, J., Rodriguez, I. et al (2004) Determination of natural and synthetic estrogens in water by gas chromatography with mass spectrometric detection. **Journal of Chromatography A,** 1024 (1-2): 177-185

Quintero, J. C., Moreira, M. T., Feijoo, G. et al (2005) Anaerobic degradation of hexachlorocyclohexane isomers in liquid and soil slurry systems. **Chemosphere,** 61 (4): 528-536

Rados, N., Kemoun, A., Shaikh, A., Al-Dahhan, M. H., & Dudukovic, M. P. (2002) "Implementation of Radioactive Particle Tracking and Tomography in Flow Visualization of High Pressure Slurry Bubble Column Reactors, Oral Presentation, 4th Symposium on High Pressure Technology and Chemical Engineering, Venice, Italy". In.

Raymahasay, S. (1989), **Report on Triglyceride Hydrogenation in a Cocurrent Downflow Contactor, SERC Report, School of Chemical Engineering, University of Birmingham** .

Regal, P., Nebot, C., Vazquez, B. I. et al (2010) Determination of naturally occurring progestogens in bovine milk as their oxime derivatives using high performance liquid chromatography-electrospray ionization-tandem mass spectrometry. **Journal of the Science of Food and Agriculture,** 90 (10): 1621-1627

Ribeiro, A. R., Nunes, O. C., Pereira, M. F. R. et al (2015) An overview on the advanced oxidation processes applied for the treatment of water pollutants defined in the recently launched Directive 2013/39/EU. **Environment International,** 75 33-51

Rocha, M. J., Cruzeiro, C., Reis, M. et al (2013) Determination of seventeen endocrine disruptor compounds and their spatial and seasonal distribution in Ria Formosa Lagoon (Portugal). **Environmental Monitoring and Assessment,** 185 (10): 8215-8226

Rodriguez-Rojo, S., Visentin, A., Maestri, D. et al (2012) Assisted extraction of rosemary antioxidants with green solvents. **Journal of Food Engineering,** 109 (1): 98-103

Rollbusch, P., Bothe, M., Becker, M. et al (2015) Bubble columns operated under industrially relevant conditions - Current understanding of design parameters. **Chemical Engineering Science,** 126 660-678

Rosal, R., Rodriguez, A., Antonio Perdigon-Melon, J. et al (2010) Occurrence of emerging pollutants in urban wastewater and their removal through biological treatment followed by ozonation. **Water Research,** 44 (2): 578-588

Rosenfeld, C. S. (2015) Bisphenol A and phthalate endocrine disruption of parental and social behaviors. **Frontiers in Neuroscience,** 9

Rosenfeldt, E. J. and Linden, K. G. (2004) Degradation of endocrine disrupting chemicals bisphenol A, ethinyl estradiol, and estradiol during UV photolysis and advanced oxidation processes. **Environmental Science & Technology,** 38 (20): 5476-5483

Rosenfeldt, E. J., Chen, P. J., Kullman, S. et al (2007) Destruction of estrogenic activity in water using UV advanced oxidation. **Science of the Total Environment,** 377 (1): 105-113

Rudel, R. A., Melly, S. J., Geno, P. W. et al (1998) Identification of alkylphenols and other estrogenic phenolic compounds in wastewater, septage, and groundwater on Cape Cod, Massachusetts. **Environmental Science & Technology,** 32 (7): 861-869

Ruzicka, M. C., Drahos, J., Fialova, M. et al (2001) Effect of bubble column dimensions on flow regime transition. **Chemical Engineering Science,** 56 (21-22): 6117-6124

Rzehak, R. and Krepper, E. (2013) Bubble-induced turbulence: Comparison of CFD models. **Nuclear Engineering and Design,** 258 57-65

Sada, E., Katoh, S., Yoshii, H. et al (1984) Performance of the Gas Bubble Column in Molten-Salt Systems. **Industrial & Engineering Chemistry Process Design and Development,** 23 (1): 151-154

Salehi, K., Jokar, S. M., Shariati, J. et al (2014) Enhancement of CO conversion in a novel slurry bubble column reactor for methanol synthesis. **Journal of Natural Gas Science and Engineering,** 21 170-183

Sarmento, S. M. (1995) **A Systemic Investigation of the Hydrodynamic and Mass Transfer Characteristics of the Co-current Downflow Contactor Operation in Fixed Bed Mode, PhD Thesis, University of Birmingham.**

Savall, A. (1995) Electrochemical Treatment of Industrial Organic Effluents. **Chimia,** 49 (1-2): 23-27

Saxena, S. C. and Patel, B. B. (1990) Heat-Transfer and Hydrodynamic Investigations in A Baffled Bubble Column - Air Water Glass Bead System. **Chemical Engineering Communications,** 98 65-88

Saxena, S. C. and Rao, N. S. (1991) Heat-Transfer and Gas Holdup in A 2-Phase Bubble Column - Air-Water System - Review and New Data. **Experimental Thermal and Fluid Science,** 4 (2): 139-151

Saxena, S. C., Rao, N. S. and Saxena, A. C. (1990a) Heat-Transfer and Gas-Holdup Studies in A Bubble Column - Air-Water-Glass Bead System. **Chemical Engineering Communications,** 96 31-55

Saxena, S. C., Rao, N. S. and Saxena, A. C. (1990b) Heat-Transfer from A Cylindrical Probe Immersed in A 3-Phase Slurry Bubble Column. **Chemical Engineering Journal and the Biochemical Engineering Journal,** 44 (3): 141-156

Saxena, S. C., Rao, N. S. and Saxena, A. C. (1992) Heat-Transfer and Gas Holdup Studies in A Bubble Column - Air Water Sand System. **Canadian Journal of Chemical Engineering,** 70 (1): 33-41

Saxena, S. C., Rao, N. S. and Yousuf, M. (1991a) Heat-Transfer and Hydrodynamic Investigations Conducted in A Bubble Column with Powders of Small Particles and A Viscous-Liquid. **Chemical Engineering Journal and the Biochemical Engineering Journal,** 47 (2): 91-103

Saxena, S. C., Rao, N. S. and Yousuf, M. (1991b) Hydrodynamic and Heat-Transfer Investigations Conducted in A Bubble Column with Fine Powders and A Viscous-Liquid. **Powder Technology,** 67 (3): 265-275

Scandura, J. E. and Sobsey, M. D. (1997) Viral and bacterial contamination of groundwater from on-site sewage treatment systems. **Water Science and Technology,** 35 (11-12): 141-146

Schafer, R., Merten, C. and Eigenberger, G. (2002) Bubble size distributions in a bubble column reactor under industrial conditions. **Experimental Thermal and Fluid Science,** 26 (6-7): 595-604

Schubert, S., Peter, A., Schoenenberger, R. et al (2014) Transient exposure to environmental estrogen affects embryonic development of brown trout (Salmo trutta fario). **Aquatic Toxicology,** 157 141-149

Schulz, K., Dressler, J., Sohnius, E. M. et al (2007) Determination of volatile constituents in spirits using headspace trap technology. **Journal of Chromatography A,** 1145 (1-2): 204-209

Schumpe, A. and Deckwer, W. D. (1980) Analysis of Chemical Methods for Determination of Interfacial-Areas in Gas-In-Liquid Dispersions with Nonuniform Bubble Sizes. **Chemical Engineering Science,** 35 (10): 2221-2233

Schumpe, A. and Grund, G. (1986) The Gas Disengagement Technique for Studying Gas Holdup Structure in Bubble-Columns. **Canadian Journal of Chemical Engineering,** 64 (6): 891-896

Serikawa, R. M., Isaka, M., Su, Q. et al (2000) Wet electrolytic oxidation of organic pollutants in wastewater treatment. **Journal of Applied Electrochemistry,** 30 (7): 875-883

Serodio, P. and Nogueira, J. (2006) Considerations on ultra-trace analysis of phthalates in drinking water. **Water Research,** 40 (13): 2572-2582

Shah, Y. T., Kelkar, B. G., Godbole, S. P. et al (1982a) Design Parameters Estimations for Bubble Column Reactors. **Aiche Journal,** 28 (3): 353-379

Shah, Y. T., Kelkar, B. G., Godbole, S. P. et al (1982b) Design Parameters Estimations for Bubble Column Reactors. **Aiche Journal,** 28 (3): 353-379

Shah, Y. T., Kulkarni, A. A., Wieland, J. H. et al (1983) Gas Holdup in 2-Phase and 3-Phase Downflow Bubble-Columns. **Chemical Engineering Journal and the Biochemical Engineering Journal,** 26 (2): 95-104

Shah, Y. T., Stiegel, G. J. and Sharma, M. M. (1978) Backmixing in Gas-Liquid Reactors. **Aiche Journal,** 24 (3): 369-400

Sharma, M. M. and Danckwer, P. V. (1970) Chemical Methods of Measuring Interfacial Area and Mass Transfer Coefficients in 2-Fluid Systems. **British Chemical Engineering,** 15 (4): p. 522-&

Sharma, S. (1997) **Selective Hydrogenation of Multifunctional Organic Reactants in Three Phase Reactor, PhD Thesis, University of Birmingham .**

Shi, B., Li, G., Wang, D. et al (2007) Removal of direct dyes by coagulation: The performance of preformed polymeric aluminum species. **Journal of Hazardous Materials,** 143 (1-2): 567-574

Sigma-Aldrich (2016), **http://www.sigmaaldrich.com/** .

Sivaiah, M. and Majumder, S. K. (2013) Mass Transfer and Mixing in an Ejector-Induced Downflow Slurry Bubble Column. **Industrial & Engineering Chemistry Research,** 52 (35): 12661-12671

Smith, R. M. (2002) Extractions with superheated water. **Journal of Chromatography A,** 975 (1): 31-46

Snyder, S., Wert, E., Lei, H., Westerhoff, P., & Yoon, Y. (2007), **Removal of EDCs and Pharmaceuticals in Drinking and Reuse Treatment Processes, Denver, CO: American Water Works Research Foundation (AwwaRF)** .

Socas-Rodriguez, B., Asensio-Ramos, M., Hernandez-Borges, J. et al (2013) Chromatographic analysis of natural and synthetic estrogens in milk and dairy products. **Trac-Trends in Analytical Chemistry,** 44 58-77

Somenath Mitra (2003) **Sample Preparation Techniques in Analytical Chemistry. John Wiley & Sons, Inc.**

Sonego, J. L. S., Lemos, D. A., Rodriguez, G. Y. et al (2014) Extractive Batch Fermentation with CO_2 Stripping for Ethanol Production in a Bubble Column Bioreactor: Experimental and Modeling. **Energy & Fuels,** 28 (12): 7552-7559

Souza, B. S., Dantas, R. F., Cruz, A. et al (2014) Photochemical oxidation of municipal secondary effluents at low H_2O_2 dosage: Study of hydroxyl radical scavenging and process performance. **Chemical Engineering Journal,** 237 268-276

Srivastava, N. and Majumder, C. (2008) Novel biofiltration methods for the treatment of heavy metals from industrial wastewater. **Journal of Hazardous Materials,** 151 (1): 1-8

Stacy, C. J., Melick, C. A. and Cairncross, R. A. (2014) Esterification of free fatty acids to fatty acid alkyl esters in a bubble column reactor for use as biodiesel. **Fuel Processing Technology,** 124 (0): 70-77

Stanford, B. D. and Weinberg, H. S. (2010) Evaluation of On-Site Wastewater Treatment Technology to Remove Estrogens, Nonylphenols, and Estrogenic Activity from Wastewater. **Environmental Science & Technology,** 44 (8): 2994-3001

Stavrakakis, C., Colin, R., Hequet, V. et al (2008) Analysis of endocrine disrupting compounds in wastewater and drinking water treatment plants at the nanogram per litre level. **Environmental Technology,** 29 (3): 279-286

Steiner, R. (1987) Operating Characteristics of Special Bubble Column Reactors. **Chemical Engineering and Processing,** 21 (1): 1-8

Sulidis, A. T. (1995) **Application of the Cocurrent Downflow Bubble Column Contactor (CDC) for Use as a Photocatalytic Reactor and Assorted Mass Transfer Studies, PhD Thesis, University of Birmingham.**

Sun, M. and Temelli, F. (2006) Supercritical carbon dioxide extraction of carotenoids from carrot using canola oil as a continuous co-solvent. **Journal of Supercritical Fluids,** 37 (3): 397-408

Suri, R. P. S., Singh, T. S. and Chimchirian, R. F. (2012) Effect of process conditions on the analysis of free and conjugated estrogen hormones by solid-phase extraction-gas chromatography/mass spectrometry (SPE-GC/MS). **Environmental Monitoring and Assessment,** 184 (3): 1657-1669

Tan, E. S. S., Bin Ho, Y., Zakaria, M. P. et al (2015) Simultaneous extraction and determination of pharmaceuticals and personal care products (PPCPs) in river water and sewage by solid-phase extraction and liquid chromatography-tandem mass spectrometry. **International Journal of Environmental Analytical Chemistry,** 95 (9): 816-832

Tan, S. N., Yong, J. W. H., Teo, C. C. et al (2011) Determination of metabolites in Uncaria sinensis by HPLC and GC-MS after green solvent microwave-assisted extraction. **Talanta,** 83 (3): 891-898

Teo, C. C., Chong, W. P. K. and Ho, Y. S. (2013) Development and application of microwave-assisted extraction technique in biological sample preparation for small molecule analysis. **Metabolomics,** 9 (5): 1109-1128

Teo, C. C., Tan, S. N., Yong, J. W. H. et al (2008) Evaluation of the extraction efficiency of thermally labile bioactive compounds in Gastrodia elata Blume by pressurized hot water extraction and microwave-assisted extraction. **Journal of Chromatography A,** 1182 (1): 34-40

Ternes, T. A., Stumpf, M., Mueller, J. et al (1999) Behavior and occurrence of estrogens in municipal sewage treatment plants - I. Investigations in Germany, Canada and Brazil. **Science of the Total Environment,** 225 (1-2): 81-90

Therning, P. and Rasmuson, A. (2001) Liquid dispersion, gas holdup and frictional pressure drop in a packed bubble column at elevated pressures. **Chemical Engineering Journal,** 81 (1-3): 331-335

Thorat, B. N. and Joshi, J. B. (2004) Regime transition in bubble columns: experimental and predictions. **Experimental Thermal and Fluid Science,** 28 (5): 423-430

Tilston, M. W. (1990) **The Development of a Swirlflow CDC, PhD Thesis, University of Birmingham.**

Tojo, K., Naruko, N. and Miyanami, K. (1982) Oxygen-Transfer and Liquid-Mixing Characteristics of Plunging Jet Reactors. **Chemical Engineering Journal and the Biochemical Engineering Journal,** 25 (1): 107-109

Tolgyesi, A., Verebey, Z., Sharma, V. K. et al (2010) Simultaneous determination of corticosteroids, androgens, and progesterone in river water by liquid chromatography-tandem mass spectrometry. **Chemosphere,** 78 (8): 972-979

van Wezel, A. P. and van Vlaardingen, P. (2004) Environmental risk limits for antifouling substances. **Aquatic Toxicology,** 66 (4): 427-444

Vanderford, B. J., Pearson, R. A., Rexing, D. J. et al (2003) Analysis of endocrine disruptors, pharmaceuticals, and personal care products in water using liquid chromatography/tandem mass spectrometry. **Analytical Chemistry,** 75 (22): 6265-6274

Vandu, C. O. and Krishna, R. (2004) Volumetric mass transfer coefficients in slurry bubble columns operating in the churn-turbulent flow regime. **Chemical Engineering and Processing,** 43 (8): 987-995

Vas, G. and Vekey, K. (2004) Solid-phase microextraction: a powerful sample preparation tool prior to mass spectrometric analysis. **Journal of Mass Spectrometry,** 39 (3): 233-254

Veera, U. P., Kataria, K. L. and Joshi, J. B. (2004) Effect of superficial gas velocity on gas hold-up profiles in foaming liquids in bubble column reactors. **Chemical Engineering Journal,** 99 (1): 53-58

Vega-Morales, T., Sosa-Ferrera, Z. and Santana-Rodriguez, J. (2012) Development and optimisation of an on-line solid phase extraction coupled to ultra-high-performance liquid chromatography-tandem mass spectrometry methodology for the simultaneous determination of endocrine disrupting compounds in wastewater samples. **Journal of Chromatography A,** 1230 66-76

Verma, A. K. and Rai, S. (2003) Studies on surface to bulk ionic mass transfer in bubble column. **Chemical Engineering Journal,** 94 (1): 67-72

Viglino, L., Aboulfadl, K., Mahvelat, A. D. et al (2008) On-line solid phase extraction and liquid chromatography/tandem mass spectrometry to quantify pharmaceuticals, pesticides and some metabolites in wastewaters, drinking, and surface waters. **Journal of Environmental Monitoring,** 10 (4): 482-489

Vik, C. B., Solsvik, J., Hillestad, M. et al (2015) Modeling of a Slurry Bubble Column Reactor for the Production of Biofuels via the Fischer-Tropsch Synthesis. **Chemical Engineering & Technology,** 38 (4): 690-700

Vince, F., Aoustin, E., Breant, P. et al (2008) LCA tool for the environmental evaluation of potable water production. **Desalination,** 220 (1-3): 37-56

Wang, H. X., Zhou, Y. and Jiang, Q. W. (2012) Simultaneous screening of estrogens, progestogens, and phenols and their metabolites in potable water and river water by ultra-performance liquid chromatography coupled with quadrupole time-of-flight mass spectrometry. **Microchemical Journal,** 100 83-94

Wang, J., Cheng, C. S. and Yang, Y. L. (2015) Determination of Estrogens in Milk Samples by Magnetic-Solid-Phase Extraction Technique Coupled With High-Performance Liquid Chromatography. **Journal of Food Science,** 80 (12): p. C2655-C2661

Wang, S., Arimatsu, Y., Koumatsu, K. et al (2003) Gas holdup, liquid circulating velocity and mass transfer properties in a mini-scale external loop airlift bubble column. **Chemical Engineering Science,** 58 (15): 3353-3360

Weber, M. (2002) Large bubble columns for the oxidation of cumene in phenol processes. **Chemical Engineering & Technology,** 25 (5): 553-558

Wert, E. C., Rosario-Ortiz, F. L. and Snyder, S. A. (2009) Effect of ozone exposure on the oxidation of trace organic contaminants in wastewater. **Water Research,** 43 (4): 1005-1014

WHO (2012), **Pharmaceuticals in Drinking-Water, World Health Organization** .

Widyanto, M. R., Utomo, M. B., Kawamoto, K. et al (2006) Local gas holdup measurement of a bubble column using SONIA-ultrasonic non-invasive method. **Sensors and Actuators A-Physical,** 126 (2): 447-454

Wilkinson, P. M., Haringa, H. and Vandierendonck, L. L. (1994) Mass-Transfer and Bubble-Size in A Bubble-Column Under Pressure. **Chemical Engineering Science,** 49 (9): 1417-1427

Wilkinson, P. M., Spek, A. P. and Vandierendonck, L. L. (1992) Design Parameters Estimation for Scale-Up of High-Pressure Bubble-Columns. **Aiche Journal,** 38 (4): 544-554

Wilkinson, P. M. and Vandierendonck, L. L. (1990) Studies on Gas Holdup in A Bubble Column Operated at Elevated-Temperatures. **Industrial & Engineering Chemistry Research,** 29 (5): 927-928

Winterbottom, J. M., Boyes, A. P., Raymahasay, S. et al (1995) **The use of a mass transfer efficient bubble column reactor for process intensification in selective three phase catalytic hydrogenations.**

Winterbottom, J. M., Khan, Z., Boyes, A. P. et al (1997a) Photocatalyzed oxidation of phenol in water using a cocurrent downflow contactor reactor (CDCR). **Environmental Progress,** 16 (2): 125-131

Winterbottom, J. M., Khan, Z., Boyes, A. P. et al (1997b) **The photocatalysed oxidation of phenol in waste water using advanced oxidation processes in a mass transfer efficient bubble column reactor.**

Winterbottom, J. M., Khan, Z., Boyes, A. P. et al (1999) Catalytic hydrogenation in a packed bed bubble column reactor. **Catalysis Today,** 48 (1-4): 221-228

Winterbottom, J. M., Khan, Z., Raymahasay, S. et al (2000) A comparison of triglyceride oil hydrogenation in a downflow bubble column using slurry and fixed bed catalysts. **Journal of Chemical Technology and Biotechnology,** 75 (11): 1015-1025

Wu, C., Al-Dahhan, M. H. and Prakash, A. (2007) Heat transfer coefficients in a high-pressure bubble column. **Chemical Engineering Science,** 62 (1-2): 140-147

Wu, Y. X., Ong, B. C. and Al-Dahhan, M. H. (2001) Predictions of radial gas holdup profiles in bubble column reactors. **Chemical Engineering Science,** 56 (3): 1207-1210

Xie, W., Han, C., Zheng, Z. et al (2011) Determination of Gibberellin A3 residue in fruit samples by liquid chromatography-tandem mass spectrometry. **Food Chemistry,** 127 (2): 890-892

Yang, G. Q., Luo, X., Lau, R. et al (2000) Heat-transfer characteristics in slurry bubble columns at elevated pressures and temperatures. **Industrial & Engineering Chemistry Research,** 39 (7): 2568-2577

Ying, G. G. (2006) Fate, behavior and effects of surfactants and their degradation products in the environment. **Environment International,** 32 (3): 417-431

Zhang, A. and Li, Y. (2014) Removal of phenolic endocrine disrupting compounds from waste activated sludge using UV, H_2O_2, and UV/H_2O_2 oxidation processes: Effects of reaction conditions and sludge matrix. **Science of the Total Environment,** 493 (0): 307-323

Zhang, L. (1997) **Selective Hydrogenation of Alpha, Beta-Unsaturated AldehydesTowards Clean Synthesis over Noble Metal Catalysts in Mass Transfer Efficient Three Phase Reactors, Ph.D. Thesis, University of Birmingham.**

Zhang, Y., Zhou, J. L. and Ning, B. (2007) Photodegradation of estrone and 17 beta-estradiol in water. **Water Research,** 41 (1): 19-26

Zhang, Z. H., Feng, Y. J., Liu, Y. et al (2010) Kinetic degradation model and estrogenicity changes of EE2 (17 alpha-ethinylestradiol) in aqueous solution by UV and UV/H_2O_2 technology. **Journal of Hazardous Materials,** 181 (1-3): 1127-1133

Ziegenhein, T., Rzehak, R. and Lucas, D. (2015) Transient simulation for large scale flow in bubble columns. **Chemical Engineering Science,** 122 (0): 1-13

Zou, R. J., Jiang, X. Z., Li, B. Z. et al (1988) Studies on Gas Holdup in A Bubble Column Operated at Elevated-Temperatures. **Industrial & Engineering Chemistry Research,** 27 (10): 1910-1916

Zou, Y., Li, Y. H., Jin, H. et al (2012) Determination of estrogens in human urine by high-performance liquid chromatography/diode array detection with ultrasound-assisted cloud-point extraction. **Analytical Biochemistry,** 421 (2): 378-384

Zuehlke, S., Duennbier, U. and Heberer, T. (2005) Determination of estrogenic steroids in surface water and wastewater by liquid chromatography-electrospray tandem mass spectrometry. **Journal of Separation Science,** 28 (1): 52-58

CHAPTER 9

9 APPENDICES

9.1 Hydrodynamic Characteristic and Mass Transfer Studies

9.1.1 Gas Hold-up

Mass balance calculations over DGCR were based on steady-state operation and 100% gas utilization assumption, the following mathematical development (Sarmento, 1995). Mass balance of gas-liquid dispersion given by:

$$m_d = m_L + m_g \quad \text{Equation 9-1}$$

$$\rho_d V_d = \rho_L V_L + \rho_g V_g \quad \text{Equation 9-2}$$

The gas-liquid dispersion density ($\boldsymbol{\rho_d}$) in two-phase system can be expressed in term of:

$$\rho_d = \varepsilon_g \rho_g + (1 - \varepsilon_g)\rho_L \quad \text{Equation 9-3}$$

In oxygen-water system $\rho_L >>> \rho_g$, thus equation 9.3 can be approximated to

$$\rho_d \cong (1 - \varepsilon_g)\rho_L \quad \text{Equation 9-4}$$

Using equations 9.2 and 9.4 led to:

$$(1 - \varepsilon_g)\rho_L V_d = \rho_L V_L + \rho_g V_g \quad \text{Equation 9-5}$$

Rearrange equation 9.5 by dividing on ρ_L with $\frac{\rho_g}{\rho_L} \cong 0$ resulting the following expression

$$(1 - \varepsilon_g)\rho_L V_d = V_L \quad \text{Equation 9-6}$$

$$\varepsilon_g = 1 - \frac{V_L}{V_d} \quad \text{Equation 9-7}$$

Where $\mathbf{V_d = V_g + V_L}$

$$\varepsilon_g = \frac{V_g}{V_d} \quad \text{Equation 9-8}$$

Where:

V_d: Gas-liquid dispersion volume

V_g: Gas-phase volume in the dispersion

V_L: Liquid-phase volume in the dispersion

ρ_d: Density of dispersion

ρ_g: Density of gas-phase

ρ_L: Density of liquid-phase

ε_g: Gas hold-up, dimensionless numbers

9.1.2 Gas Liquid Mass Transfer Characteristics

Plug flow model $$K_L a = \frac{F_L}{V_d} \ln\left(\frac{c^* - c_i}{c^* - c_o}\right) \quad 9\text{-}9$$

Mix flow model $$K_L a = \frac{F_L}{V_d} \ln\left(\frac{c_o - c_i}{c^* - c_o}\right) \quad 9\text{-}10$$

Where:

$K_L a$: volumetric gas-liquid mass transfer coefficient, s^{-1}

F_L: liquid flowrate, m^3/s

V_d: gas-liquid dispersion volume, m

C^*: equilibrium concentration of gas in the liquid phase, mg L^{-1}

C_i: concentration of gas in liquid phase at dispersion inlet, mg L^{-1}

C_o: concentration of gas in liquid phase at dispersion outlet, mg L^{-1}

9.2 Sample Calculation

1- Solubility of Oxygen in Water at 1 atm (X_{O_2})

$$\text{Ln } X_{O_2} = -66.735 + \frac{87.475}{\frac{T}{100}} + 24.453 \ln \frac{T}{100} \qquad 9\text{-}11$$

2- Henrys Low Coefficient (H)

$$H = \frac{P_{O_2}}{X_{O_2}} = \frac{1}{X_{O_2}} \qquad 9\text{-}12$$

where:

T = temperature (K)

X_{O_2} = oxygen mole fraction in water

P_{O_2} = oxygen partial pressure, atm

3- Inlet Oxygen Concentration

$$C_{in} = \frac{32}{18}\ 1.0\ \times 10^6 P_{O_2} X_{O_2} \qquad 9\text{-}13$$

where: $P_{O_2} = 1 - P_{N_2}$

4- Oxygen Equilibrium Concentration at Operation Pressure

Using equation 9.11 and $P_{O_2} = \frac{P_{col} + 14.7}{14.7} - P_{N_2}$

$$C^* = 1.778 \times 10^6 + (\frac{P_{col} + 14.7}{14.7} - 0.79)\, X_{O_2} \qquad 9\text{-}14$$

where: C^* = Oxygen Equilibrium Concentration mg L^{-1}

Sample calculation

System: H_2O/O_2

F_L = 8 L min^{-1} = 0.000133 m^3 s^{-1}

$^{V}_{d}$ = 2 cm = 0.02 m

d_b = 5 mm = 0.005 m

V_{in} = 13.86 m s^{-1}

d_o = 3.5 mm = 0.0035 m

T = 25°C (298.15 K)

P_{col} = 14 psig

Using equation 9.11	Ln X_{O_2} = -10.667 Hence, X_{O_2} = 2.33 x 10^{-5}
Using equation 9.13	C_i = 8.702059
Using equation 9.14	C* = 42.53462056
Using equation 9.9	K_La (PFR) = 0.0920 s^{-1}
Using equation 9.10	K_La (Mix) = 0.1233 s^{-1}

9.3 HANOVIA UV System Specifications

Table 9-1 HANOVIA UV system specifications

HANOVIA UV system	Ultra-Violet water treatment unit	
Part number	C004274-001	
Model number	UVV 20	
Serial number	040401	
Arc tube number	130015-2002	
Quartz tube number	320004-072s	
Rated pressure	700 KPa, 105 psi, 7 bar	
Rated temperature	80°C	
Input rating	Supply voltage	240 VOLTS
	Rated current	10.5 AMPS
Lamp rating	Voltage	610 VOLTS
	Current	4.0 AMPS
	Power	2.0 KWATTS

9.4 DGC Reactor Pump Calibration

The pump of the continuous flow rig has been calibrated by using a stop watch and measuring cylinder as shown in Figure 9-1.

Rotameter setting (L min^{-1})	0	3	6	9	12	15	18
Measured flowrate (L min^{-1})	0	2.29	5.38	8.41	11.54	14.71	17.81

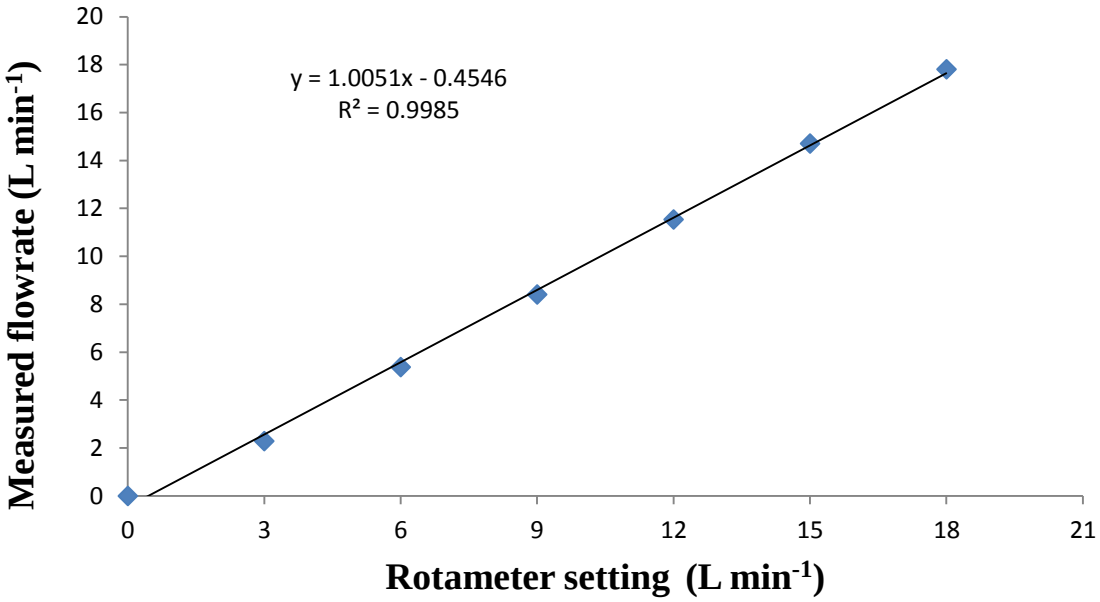

Figure 9-1 Calibration of DGCR Pump

9.5 Break Vessel Volume Calibration

Volume added L	Height in cm
0.1	0.3
0.2	0.65
0.3	1
0.4	1.3
0.5	1.6
0.6	1.9
0.7	2.25
0.8	2.55
0.9	2.9
1	3.2
1.1	3.5
1.2	3.85
1.3	4.15
1.4	4.5
1.5	4.8
1.6	5.1
1.7	5.5
1.8	5.7
1.9	6.1
2	6.4

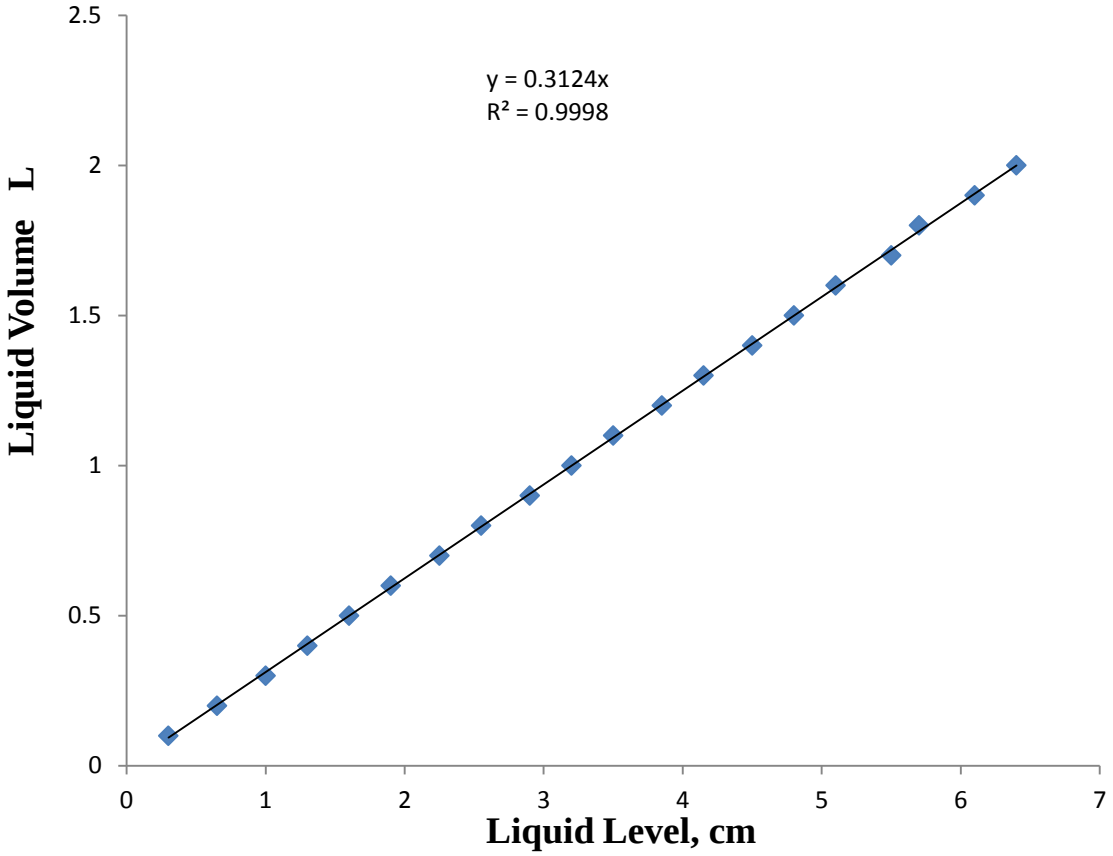

Figure 9-2 Calibration of DGCR charging vessel

9.6 Steroid Hormones Standard calibrations

9.6.1 Calibration of β-Estradiol standard

Conc. ng L^{-1}	β-Estradiol
1	2.4
2	4.3
5	11.2
20	46
50	117
100	238
200	473
500	1180
1000	2369

SUMMARY OUTPUT

Regression Statistics	
Multiple R	0.9999982
R Square	0.9999964
Adjusted R Square	0.999996
Standard Error	1.536838
Observations	10

ANOVA

	df	*SS*	*MS*	*F*	*Significance F*
Regression	1	5308758	5308758.474	2247692	4.388E-23
Residual	8	18.89497	2.361870992		
Total	9	5308777			

	Coefficients	*Standard Error*	*t Stat*	*P-value*
Intercept	-0.726628	0.570201	-1.274336767	0.23831
X Variable 1	2.3682025	0.00158	1499.230461	4.4E-23

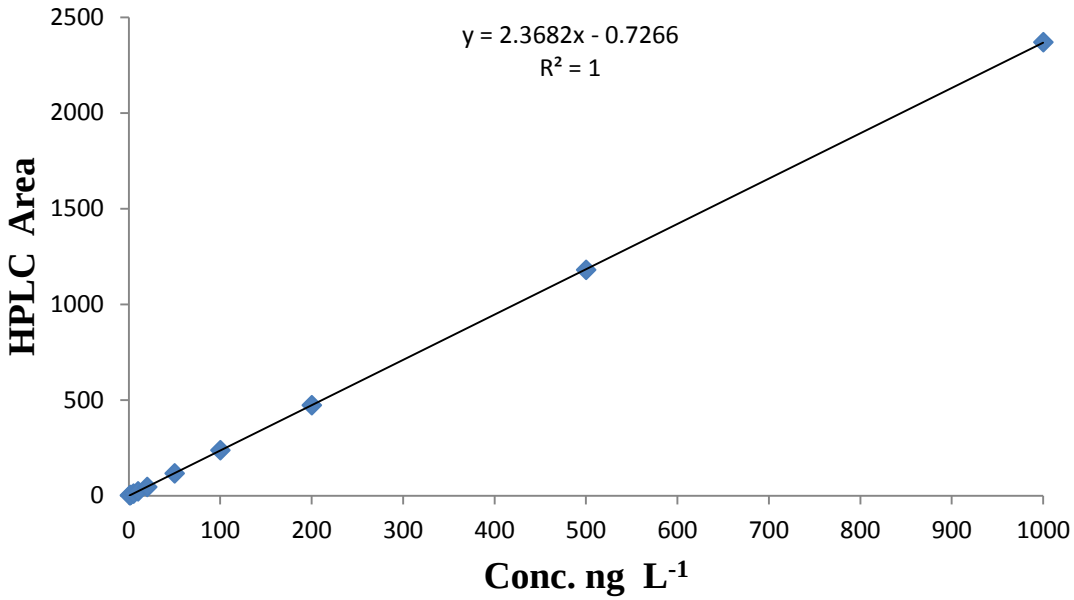

Figure 9-3 Calibration of 17β-Estradiol external standard

9.6.2 Calibration of α- Estradiol standard

Conc. ng L^{-1}	α- estradiol
1	2.1
2	4.3
5	10.3
10	21.5
20	42.8
50	103
100	211
200	417
500	1039
1000	2087

SUMMARY OUTPUT

Regression Statistics	
Multiple R	0.999996907
R Square	0.999993813
Adjusted R Square	0.99999304
Standard Error	1.78406081
Observations	10

ANOVA

	df	*SS*	*MS*	*F*	*Significance F*
Regression	1	4115722.22	4115722	1293084	4.006E-22
Residual	8	25.4629838	3.182873		
Total	9	4115747.68			

	Coefficients	*Standard Error*	*t Stat*	*P-value*
Intercept	0.116362433	0.66192565	0.175794	0.8648242
X Variable 1	2.085188758	0.00183372	1137.139	4.006E-22

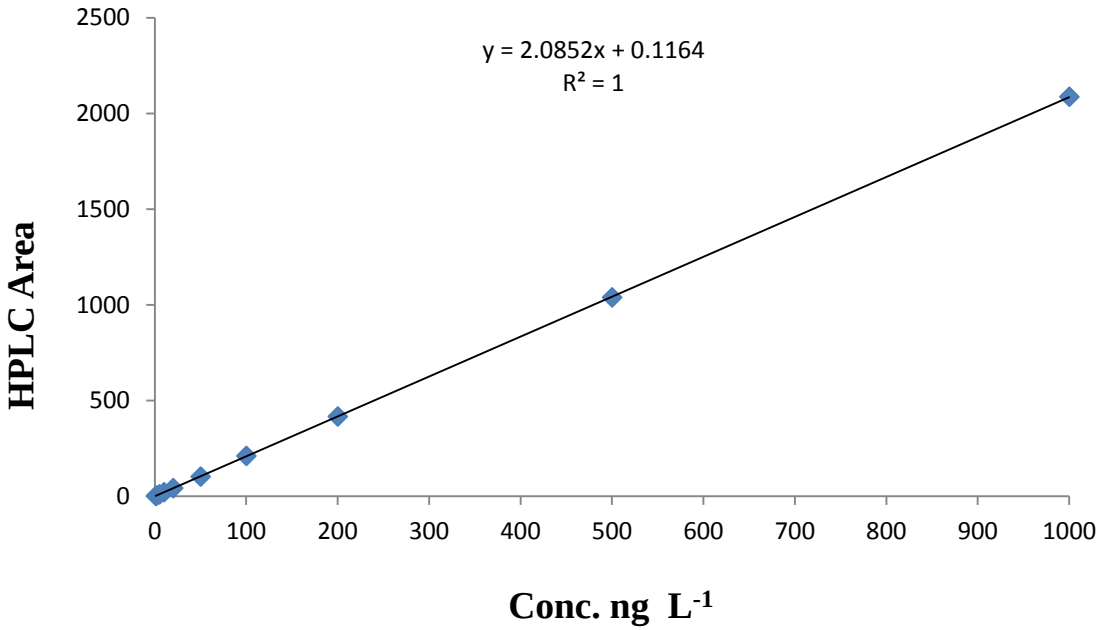

Figure 9-4 Calibration of 17α-Estradiol external standard

9.6.3 Calibration of Estrone standard

Conc. ng L^{-1}	Estrone
1	3.9
2	8
5	20.7
10	40
20	80
50	197
100	397
200	785
500	1969
1000	3920

SUMMARY OUTPUT

Regression Statistics	
Multiple R	0.999998
R Square	0.999995
Adjusted R Square	0.999994
Standard Error	2.983281
Observations	10

ANOVA

	df	*SS*	*MS*	*F*	*Significance F*
Regression	1	14557910.06	14557910.06	1635726.021	1.56447E-22
Residual	8	71.199748	8.8999685		
Total	9	14557981.26			

	Coefficients	*Standard Error*	*t Stat*	*P-value*
Intercept	1.64731	1.106862794	1.488269785	0.175000458
X Variable 1	3.921677	0.003066314	1278.955051	1.56447E-22

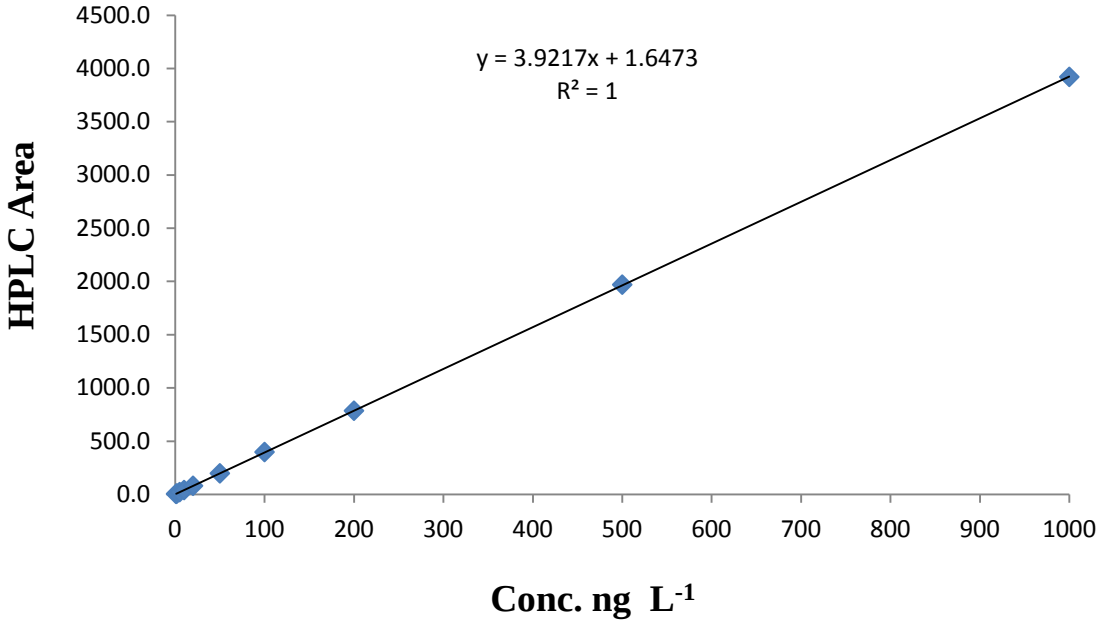

Figure 9-5 Calibration of Estrone standard

9.6.4 Calibration of Progesterone standard

Conc. ng L^{-1}	Progesterone
1	0.3
2	0.7
5	1.8
10	3.5
20	6.7
50	18.2
100	34.2
200	68.0
500	166.0
1000	338.0

SUMMARY OUTPUT

Regression Statistics	
Multiple R	0.999955684
R Square	0.99991137
Adjusted R Square	0.999900292
Standard Error	1.090547865
Observations	10

ANOVA

	df	*SS*	*MS*	*F*	*Significance F*
Regression	1	107340.1526	107340.1526	90255.30642	1.68729E-17
Residual	8	9.51435716	1.189294645		
Total	9	107349.667			

	Coefficients	*Standard Error*	*t Stat*	*P-value*	*Lower 95%*
Intercept	0.168807961	0.40461715	0.417204168	0.687499938	-0.764240858
X Variable 1	0.33674678	0.001120901	300.4252094	1.68729E-17	0.334161979

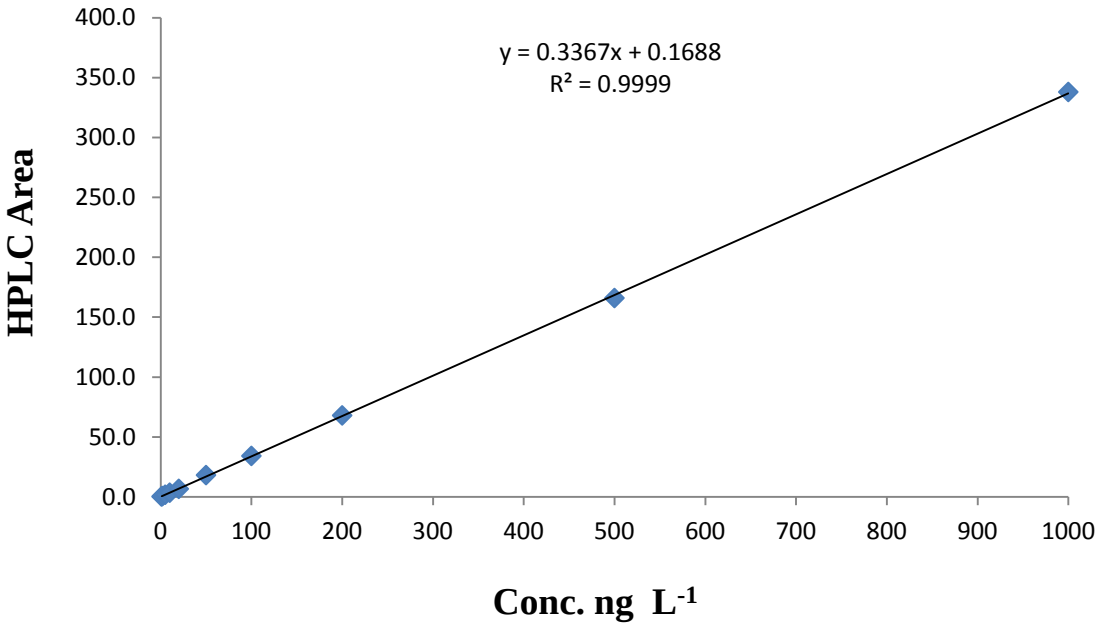

Figure 9-6 Calibration of Progesterone standard

9.7 Steroid Hormones DAD Spectrums

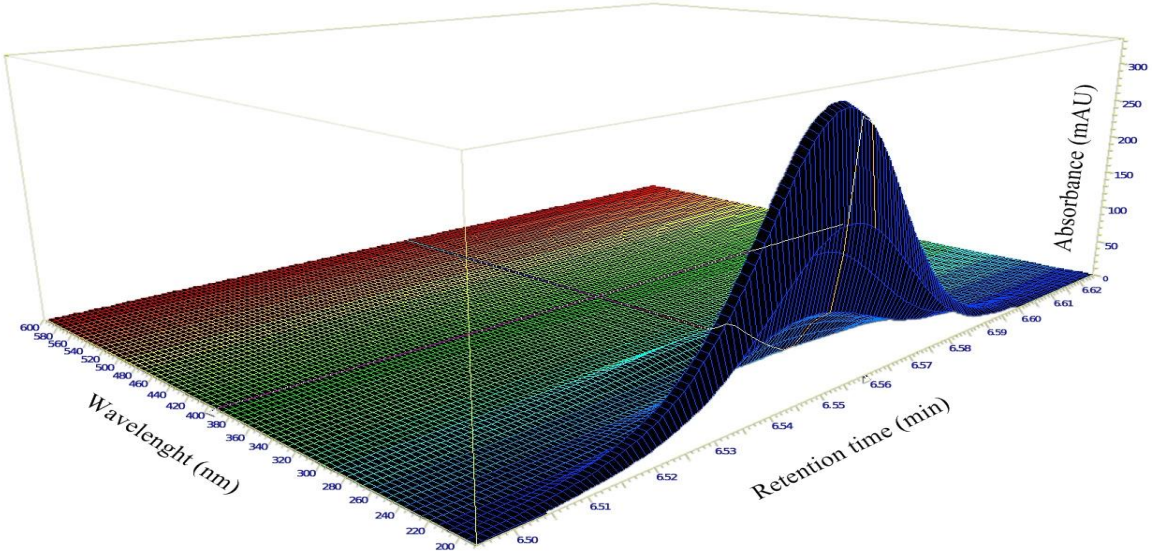

Figure 9-7 17α- estradiol DAD spectrum

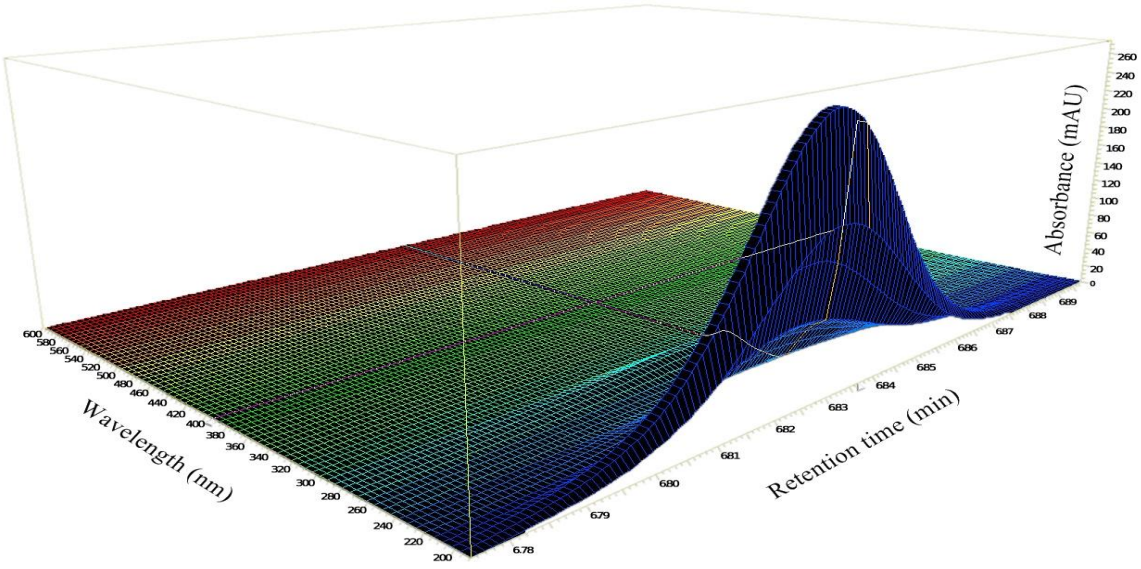

Figure 9-8 Estrone DAD spectrum

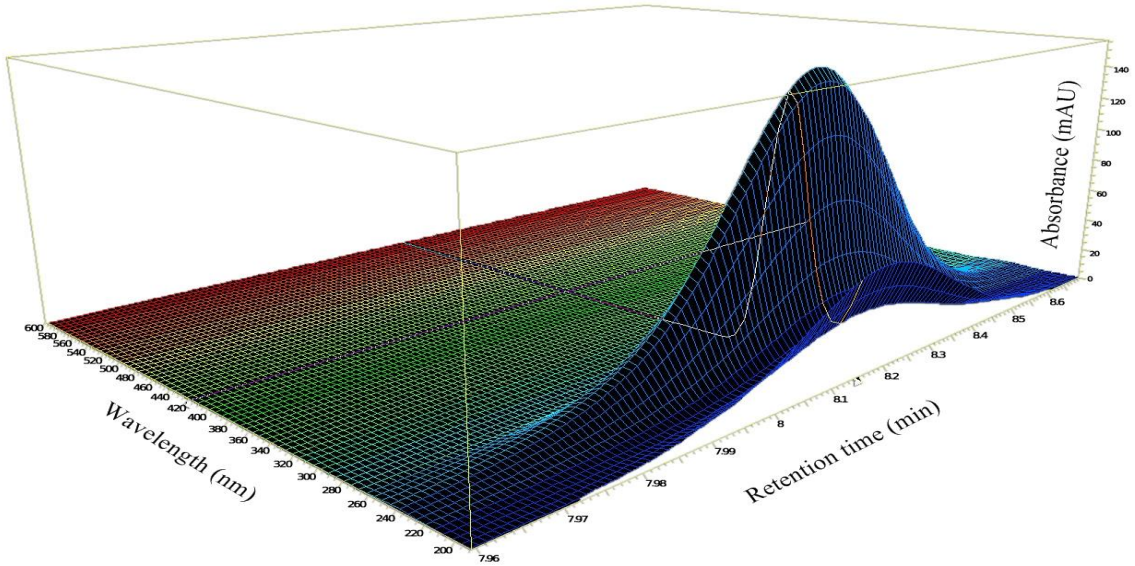

Figure 9-9 Progesterone DAD spectrum

9.8 Steroid Hormones LC/TOF-MS Chromatograms

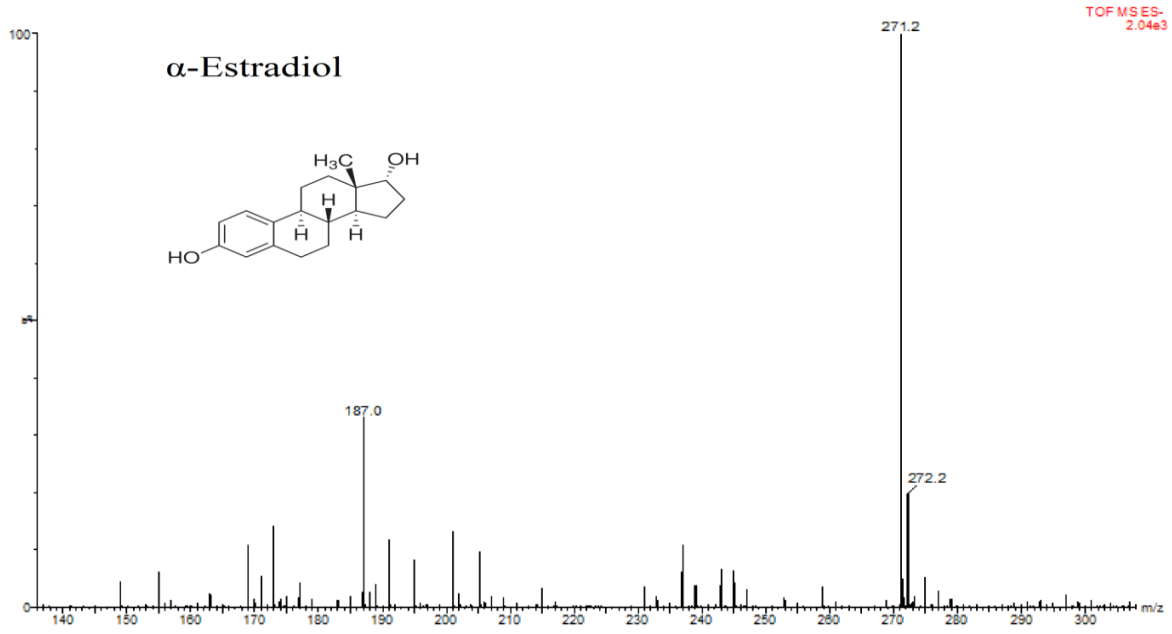

Figure 9-10 17α- estradiol LC/TOF-MS chromatogram in river water

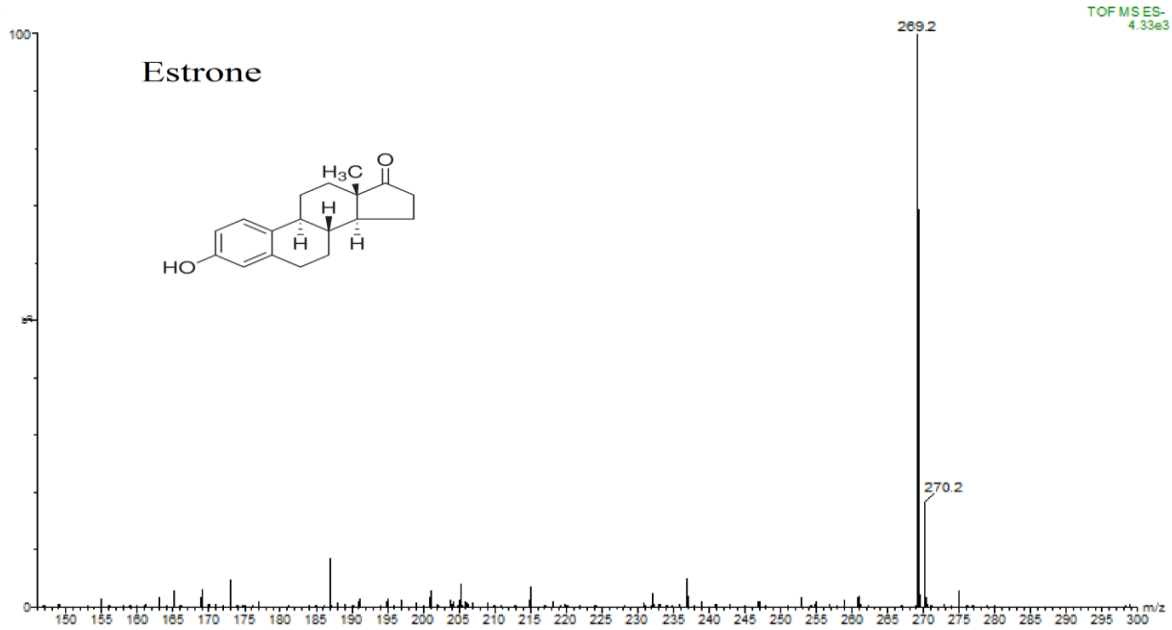

Figure 9-11 Estrone LC/TOF-MS chromatogram in river water

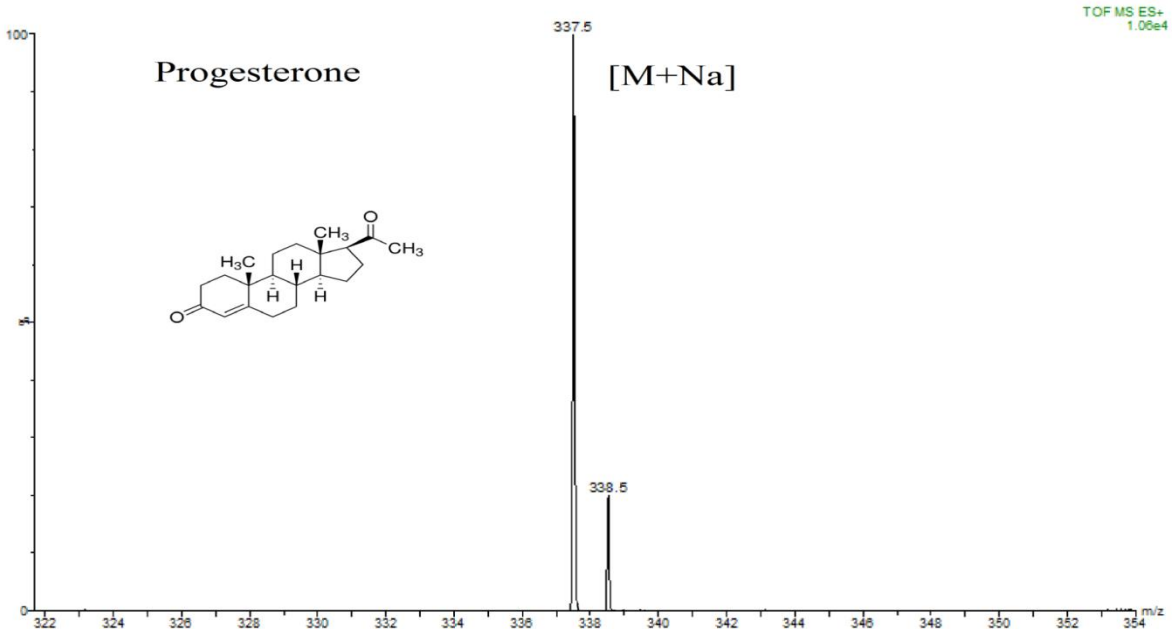

Figure 9-12 Progesterone LC/TOF-MS chromatogram in river water

9.9 Preliminary Experiments for Each Hormone Tested Individually

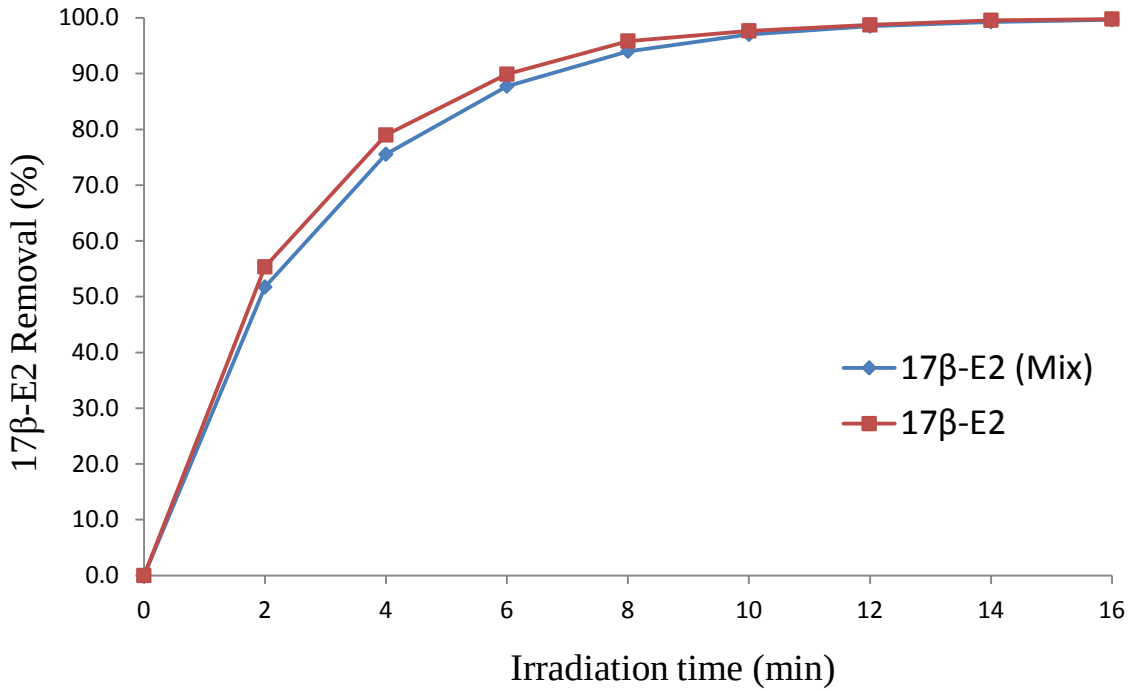

Figure 9-13 Degradation of 17β-E2 in a mixture of hormones and individual, initial pH 6.8, $[17\beta\text{-E2}]_o$ = 10000 ng L^{-1}, $[H_2O_2]_o$ = 2.5 mg L^{-1}, F_{O_2}= 0.1 L min^{-1} and T = 35°C.

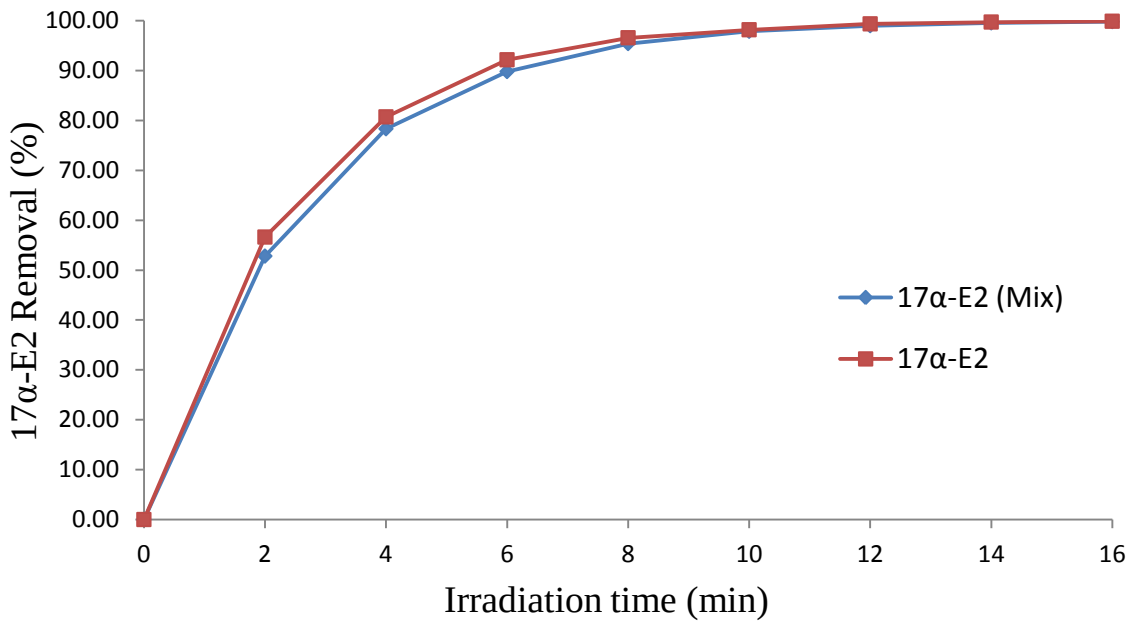

Figure 9-14 Degradation of 17α-E2 in a mixture of hormones and individual, initial pH 6.8, $[17\beta\text{-E2}]_o$ = 10000 ng L^{-1}, $[H_2O_2]_o$ = 2.5 mg L^{-1}, F_{O_2}= 0.1 L min^{-1} and T = 35°C.

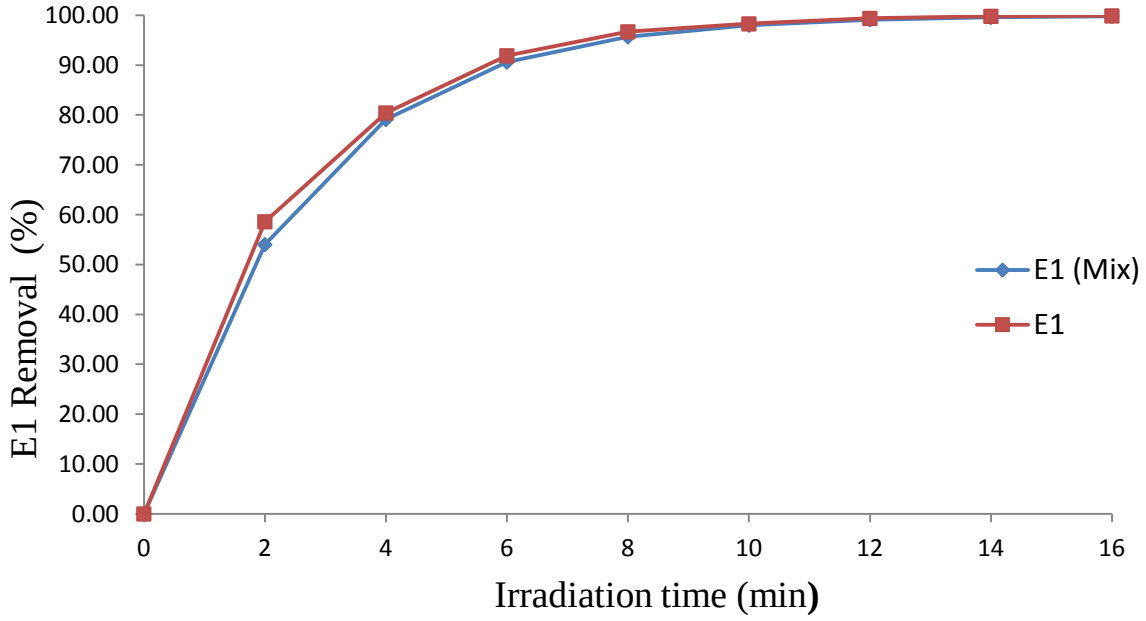

Figure 9-15 Degradation of E1 in a mixture of hormones and individual, initial pH 6.8, $[17\beta\text{-E2}]_o$ = 10000 ng L^{-1}, $[H_2O_2]_o$ = 2.5 mg L^{-1}, F_{O_2}= 0.1 L min^{-1} and T = 35°C.

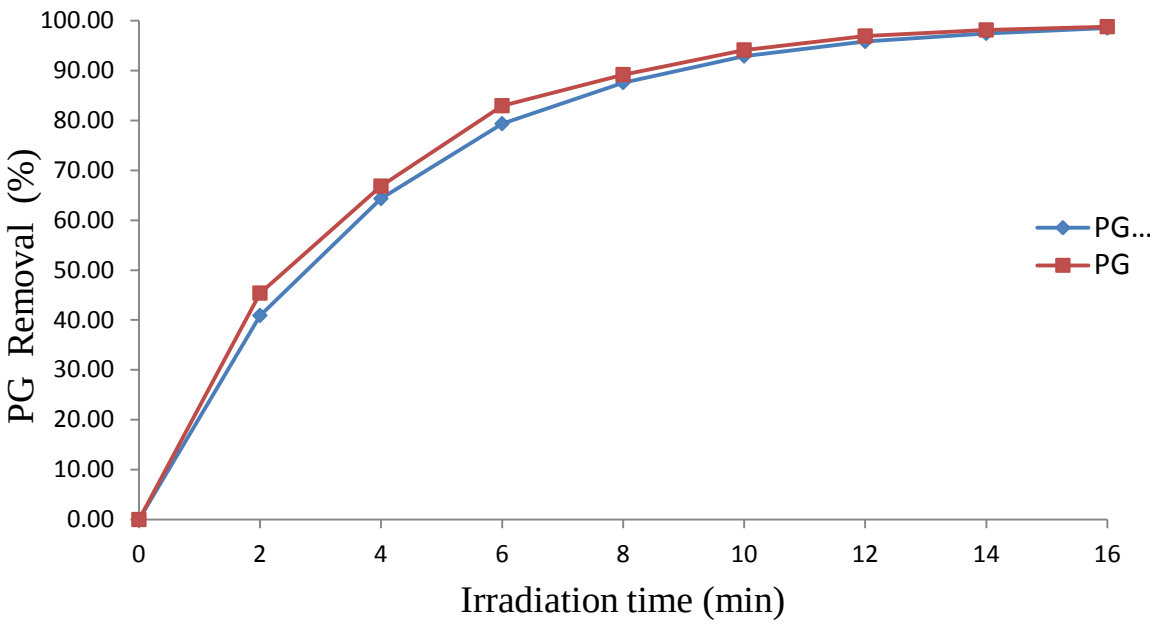

Figure 9-16 Degradation of PG in a mixture of hormones and individual, initial pH 6.8, $[17\beta\text{-E2}]_o$ = 10000 ng L^{-1}, $[H_2O_2]_o$ = 2.5 mg L^{-1}, F_{O_2}= 0.1 L min^{-1} and T = 35°C.

9.10 Schematic Diagrams of DGC Reactor

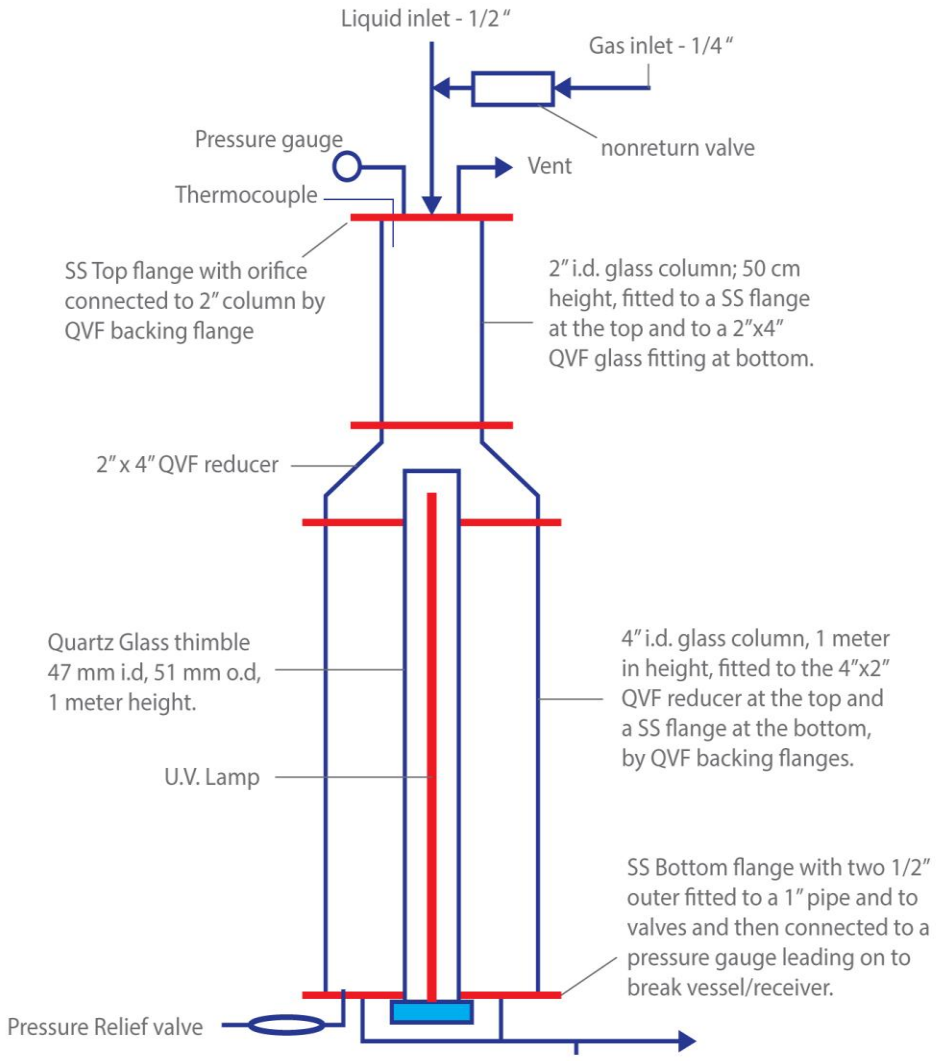

Figure 9-17 Over all view of DGC reactor

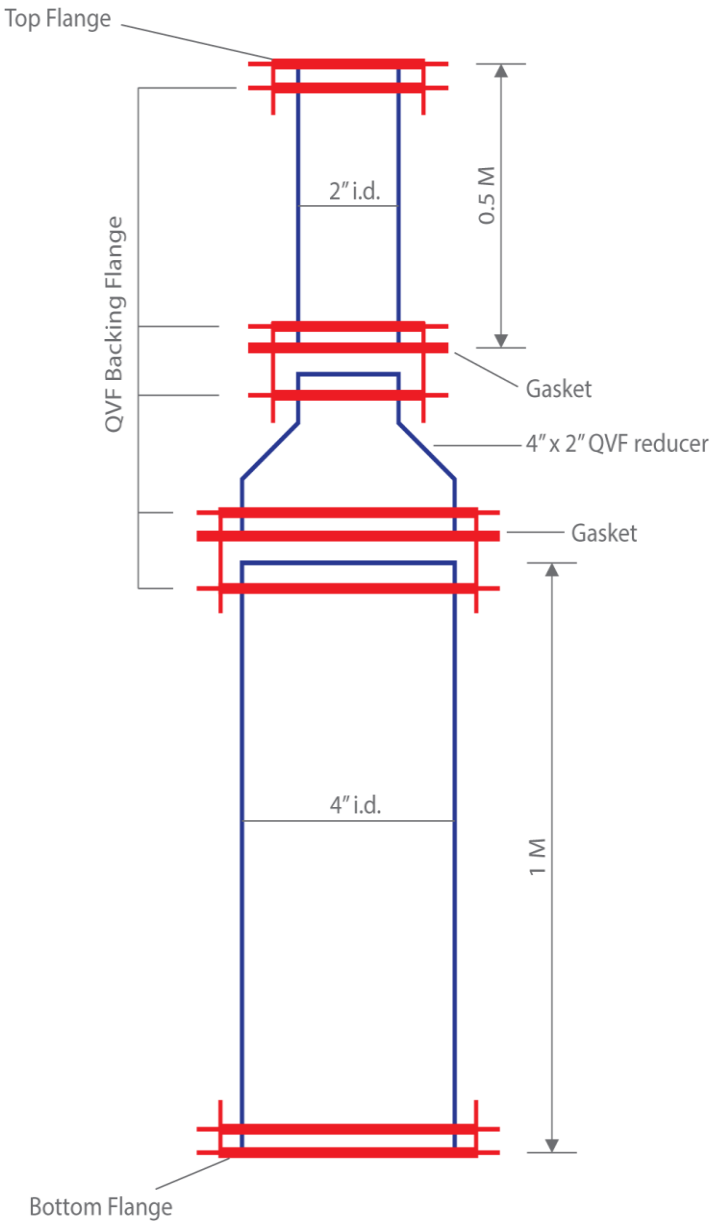

Figure 9-18 DGC Main Reactor

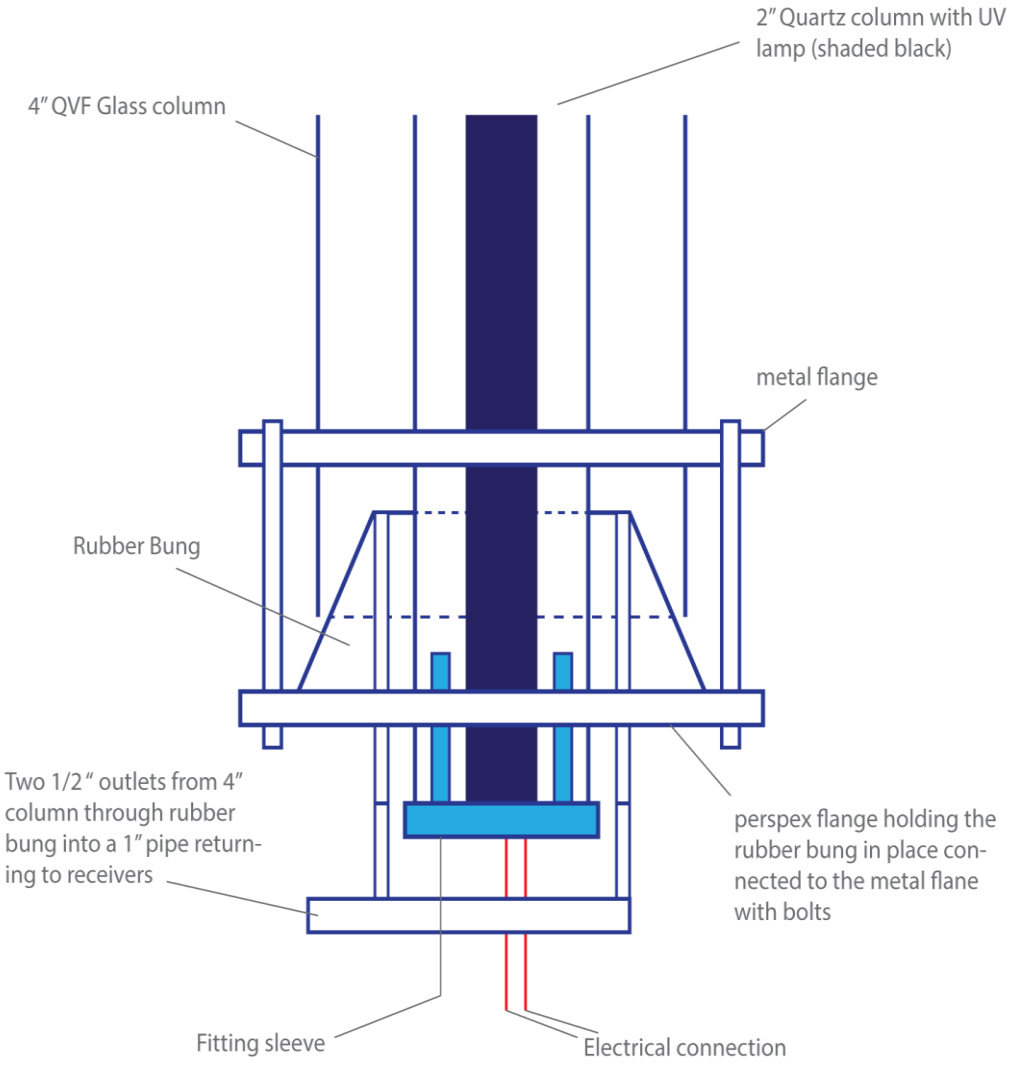

Figure 9-19 DGC rector bottom flange design in detailed

9.11 Equipment List

9.11.1 Downflow Gas Contactor Reactor (DGCR)

The downflow gas contactor reactor consisted of the following parts:

- Lowara vertical multistage pump with AISI 304 steel impellers 1.1 kW *(*Model No.SV208F11T).
- Glass column reactor (gas-liquid mixing region – top section): made from QVF glassware, 0.5 m length and 0.05 m i.d.
- Glass column reactor (photolysis region – bottom section): made from QVF glassware, 1.0 m length and 0.10 m i.d.
- 0.10 / 0.05 m i.d. QVF glassware reducer as shown in Figure 3.4.
- Glass reservoir (break vessel): made from QVF glassware, 0.199 m i.d. as shown in Figure 3.5.
- Digitron T200KC Thermometer, -200°C to 1350°C comes with a type K thermocouple
- Orifice units: diameter of 2-5 $x10^{-3}$ m stainless steel.
- 2 X 25 mm stainless steel threaded end ball valve supplied by GCE Fluid Power, UK.
- 2 X 25 mm stainless steel threaded end gate valve supplied by GCE Fluid Power, UK.
- 3 X 15 mm stainless steel threaded end ball valve supplied by GCE Fluid Power, UK.
- 15 mm stainless steel threaded end needle valve supplied by GCE Fluid Power, UK.
- 1 X 15 mm stainless steel threaded end gate valve supplied by GCE Fluid Power, UK.
- 1 X 15 mm stainless steel relief valve supplied by Swagelok, UK.
- 1X 8 mm stainless steel threaded end trunnion ball valves supplied by Swagelok, UK.

- 4 X 63 mm glycerine filled pressure gauges ranging from 0-14 bar with accuracy of 1.6%.
- 25 mm stainless steel pipe connections.
- 15 mm stainless steel pipe connections.
- 10 mm stainless steel pipe connections.
- 8 mm stainless steel pipe connections.
- Liquid flow meter: Platon PG - EAU series rotameter with maximum flow rate up to 22 $x10^{-3}$ m^3/min with increment scale of $1x10^{-3}$ m^3/min and ± 5% accuracy.
- Gas flow meter: Platon Rotameter. NG flow ranges – 100 mm scale with maximum flow rate of $11x\ 10^{-4}$ m^3/min with increment scale of $5\ x\ 10^{-5}$ m^3/min and ± 1.25% accuracy.
- Plastic hose connections: Griflex reinforced flexible hose with o.d. of $1.26\ x10^{-2}$ m.
- Black extruded acrylic (UV protection) supplied by Amari Plastics Plc, UK, as shown in Figure 3.6.
- Clear window film (UV protection) supplied by Omega Window Films, UK
- MILLIPORE Milli-RO 6 water system supplied by Millipore (UK.) Limited.
- Ultraviolet water treatment unit (2 kW UV lamp tube), supplied by Hanovia UV, UK.

9.11.2 Solid Phase Extraction (SPE)

- Savant Instruments vacuum pump (Model VP 100 SN: 36057), Franklin electric motor
- Filter flask Buchner conical shape borosilicate glass with tubulature 5L Pyrex, (Fisher Scientific, UK).
- Narrow neck amber glass Winchester 1L bottles, (Fisher Scientific, UK).

- Pyrex measuring cylinders: $1x10^{-3}$ m^3 and $0.5x10^{-3}$ m^3, tolerance 5 mL, (Fisher Scientific, UK).
- Fisherbrand stopwatch with an ISO 17025 A2LA Traceable NIST cert battery included waterproof & shockproof, (Fisher Scientific, UK).
- Red Multi-Purpose Rubber Tubing 3/4" I.D x 1-1/2" o.d.
- Oasis HLB Glass Cartridge 5cc/200 mg LP, Waters (Hertfordshire, UK).
- Vacuum Manifold 20 port, Waters (Hertfordshire, UK).
- Rack, test tube 20 port, 16x100, Waters (Hertfordshire, UK).
- Teflon tubing, Waters (Hertfordshire, UK).
- Male/male Luer Fitting, Waters (Hertfordshire, UK).
- Adaptor, 5cc, Teflon, Waters (Hertfordshire, UK).
- Millex-GP, 0.22 µm, (Millipore, UK).
- Glass-fibre filters (GF/F, 0.7 µm pore size), Whatman (Whatman, UK).
- Certified screw top vial, 2 mL, amber, deactivated (silanized) supplied by Agilent Technologies, UK.